DEVELOPMENT AND EVALUATION OF PICEATANNOL-L-ARGININE FLEXI-LIPOSOMES AGAINST MICROBIAL BIOFILMS FOR THE TREATMENT OF DENTAL CARIES

Thesis Submitted for the Award of the Degree of

DOCTOR OF PHILOSOPHY

in

(Pharmaceutics)

By

Palwinder Kaur

Registration Number: 41800832

Supervised By

Dr. Manish Vyas (17410)

Department of Pharmaceutical Sciences

(Professor)

Lovely Professional University, Phagwara, Punjab

Co-Supervised by

Dr. Surajpal Verma

Department of Pharmaceutical Sciences

(Assistant Professor)

Delhi University of Pharmaceutical Sciences and Research, Delhi

LOVELY PROFESSIONAL UNIVERSITY

PUNJAB-2024

DECLARATION

I, hereby declared that the presented work in the thesis entitled "Development and Evaluation of Piceatannol-l-Arginine Flexi-liposomes against Microbial Biofilms for the Treatment of Dental Caries" in fulfilment of degree of **Doctor of Philosophy (Ph. D.)** is outcome of research work carried out by me under the supervision of Dr. Manish Vyas, working as Professor, in the Department of Pharmaceutical Sciences, of Lovely Professional University, Punjab, India. In keeping with general practice of reporting scientific observations, due acknowledgements have been made whenever work described here has been based on findings of other investigator. This work has not been submitted in part or full to any other University or Institute for the award of any degree.

(Signature of Scholar)

Name of the scholar: Palwinder Kaur

Registration No.: 41800832

Department/School: Department of Pharmaceutical Sciences

Lovely Professional University,

Punjab, India

CERTIFICATE

This is to certify that the work reported in the Ph. D. thesis entitled "Development and Evaluation of Piceatannol-l-Arginine Flexi-liposomes against Microbial Biofilms for the Treatment of Dental Caries" submitted in fulfillment of the requirement for the award of degree of **Doctor of Philosophy (Ph.D.)** in the Department of Pharmaceutical Sciences, is a research work carried out by Palwinder kaur, 41800832, is bonafide record of his/her original work carried out under my supervision and that no part of thesis has been submitted for any other degree, diploma or equivalent course.

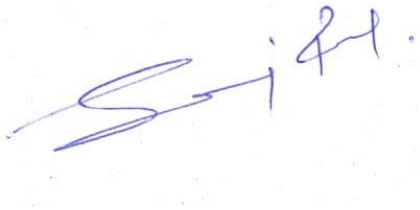

(Signature of Supervisor)

Dr. Manish Vyas (17410)

Professor

Department of Pharmaceutical Sciences,

Lovely Professional University, Phagwara.

(Signature of Co-Supervisor)

Dr. Surajpal Verma

Assistant Professor

Department of Pharmaceutical Sciences,

Delhi University of Pharmaceutical Sciences and Research, Delhi.

Acknowledgment

As I count my blessings in the culminating moment of this arduous yet immensely fulfilling academic journey, I am profoundly grateful to the Almighty, whose boundless energy and presence have infused every moment, every effort, and every result in the course of this research journey. It is through this divine grace that I have found the strength, inspiration, and guidance to embark on this scholarly endeavour.

I take this privilege to extend my gratitude to our Chancellor Dr. Ashok Kumar Mittal and Prochancellor Mrs. Rashmi Mittal, Lovely Professional University, for providing all the facilities during my Ph.D. research work.

I am highly grateful to Prof. (Dr.) Monica Gulati, Dean, and Head of School of Pharmaceutical Sciences, Lovely Professional University, Phagwara, Punjab, India, for her support and constant encouragement to carry out this research work and for providing an environment for learning in the faculty and school at large.

I owe an immeasurable debt of thanks to my esteemed supervisor, Dr. Manish Vyas, whose wisdom has illuminated my academic path. Your mentorship and tireless dedication to my growth, have been nothing short of transformative. Your belief in my potential has served as a wellspring of motivation, pushing me to reach further and strive for excellence.

To my co-supervisor, Dr. Surajpal Verma, I extend my heartfelt gratitude for your profound expertise and invaluable contributions to this work. Your insights and collaborative spirit have refined and elevated this thesis to its fullest potential. Your guidance has been a compass, steering me towards academic achievement.

I wanted to take a moment to express my deepest gratitude for the unwavering support and vision provided by Dr. Sandeep Sharma. You are truly inspiring and your enthusiasm sparks the light in those who are working with you. Your clarity of thought, your steadfast belief in our abilities, and the guidance you've offered have been nothing short of extraordinary. It's through your vision that we've been able to navigate through challenges and steer toward our shared goal. Your dedication and determination have been a driving force, reminding me that with you by my side, no aspiration is too lofty.

Together, we make an incredible team, and I am continually inspired by your insight and tenacity.

I wanted to take a moment to express my deepest gratitude to my husband for providing the vision and unwavering support in our pursuit of this degree. Your unwavering belief in my abilities, ceaseless encouragement, and boundless love have been the driving force behind every stride I have taken. Your sacrifices, both seen and unseen, and unflagging support have fortified me in times of doubt and propelled me towards success.

And of course my dear friends Sandeep and Gagan, you are the stars that have lit up the darkest nights of this journey. Your unwavering support, your shared laughter, and your empathetic understanding have been the balm to my weary soul. Each of you has been a source of strength and camaraderie, reminding me of the power of friendship in navigating life's challenges.

Furthermore, I extend my thanks to my seniors and collegues, administrative staff, technical support teams, and fellow researchers whose collective efforts create the fertile ground upon which academic pursuits can thrive.

Lastly, but by no means least, I extend my gratitude to all those whose names may not grace these pages but whose influence is woven into the fabric of this work. Your presence, however brief or understated, has left an indelible mark.

This Ph.D. journey has been a tapestry of shared experiences, lessons, and growth. It stands as a testament to the power of human connection, support, and belief in one another. As this chapter draws to a close, I carry with me the collective energy, wisdom, and love of each of you.

Palwinder Kaur

List of Abbreviations

%	Percentage
%EE	Percentage entrapment efficiency
%RSD	Percentage relative standard deviation
°C	Degree Celcius
µg	Micro gram
µl	Micro liter
A. naeslundii	*Actinomyces naeslundii*
ADS	arginine deiminase system
AMP	Antimicrobial peptides
ANOVA	Analysis of variance
API	Active pharmaceutical ingredient
AUC	Area under curve
CAA's	Critical analytical attributes
Caco-2	Epithelial intestinal cells
CCD	Central composite design
C_{max}	Maximum concentration
CQA	Critical quality attribute
DDW	distilled demineralized water
DMEM	Dulbecco's Modified Eagle's Medium
DoE	Design of Experiment
DSC	Differential scanning colorimetry
EA	Edge activator
EE	Entrapment efficiency
FESEM	Field emission scanning electron microscopy
FTIR	Fourier transform Infrared Spectra
GRAS	Generally regarded as safe
Gtf	glycosyltransferase
HETP	Height equivalent to theoretical plate
HLB	Hydrophilic lipophilic balance
HPLC	High-performance liquid chromatography
HQC	Higher quality control

hrs	hours
IC_{50}	Inhibitory Concentration 50
ICH	International council of harmonization
L-Arg	L-Arginine
LOD	Limit of detection
LOQ	Limit of quantification
LQC	Lower quality control
mg	Milligram
ml	Milli liter
MQC	Middle quality control
MRT	Mean resident time
MTT	3-(4,5-dimethylthiazol-2-yl)-2,5 diphenyltetrazolium bromide
mV	Milli-volt
nm	Nano meter
OFG	Optimized Flexi-liposomal Gel
OPA	Ortho phosphoric acid
PC	Phosphatidylcholine
PDI	Polydispersity index
PIC	Piceatannol
PRPs	Proline-rich glycoproteins
R.B.F	Round bottom flask
rpm	Rotations per minute
RSD	Relative standard deviation
S. gordonii	*Streptococcus gordonii*
S. mutans	*Streptococcus mutans*
S. oralis,	*Streptococcus oralis*
S. salivarius	*Streptococcus salivarius*
S. sanguinis	*Streptococcus sanguinis*
SDC	Sodium deoxycholate
sec	Seconds
SM	*Streptococcus mutans*
$t_{1/2}$	Half life

Tm	transition temperature
UV	Ultraviolet
v/v	Volume/volume
w/v	Weight/volume
w/w	Weight/weight
ZP	Zeta potential
μM	Micromole

Table of Contents

List of Tables

List of Figures

Abstract

The present work focuses on developing a topical formulation for the treatment of dental caries. This gel-based formulation is composed of suspended flexible liposomes with entrapped PIC and L-Arg in them. The study revolves around the rationale of using a combination of an antibiofilm agent (PIC) along a supplement (L-Arg) for the oral microbes. As the oral microbiome is composed of both cariogenic and noncariogenic microbes, the formulation rationally attempts to promote the noncariogenic microbes of the oral cavity, which thus acts as competition to cariogenic microbes. This strategy used an anti-biofilm agent, which works to prevent the adhesion of pathogenic microbial colonies, to prevent biofilm formation. This agent thus works to decrease the virulent nature of cariogenic microbes. L-Arg acts as a food supplement for the growth of noncariogenic microbes, which will provide competition to pathogenic microbes.

The formulation development was done with preformulation studies to rationally select the excipients based on their physical and chemical compatibility. Later, for the development of formulation selection of 'Edge activator' (span 60 and SDC) was done by evaluating their effect on the entrapment efficiency. SDC was found to have more entrapment efficiency for both PIC and L-Arg. The formulation was optimized using Central composite design using two level two factorial design. The average of vesicle size, PDI, and zeta potential were observed to be 194.7 nm, 0.216, and -36.1 mV. The average entrapment efficiency was found to be 35 % and 56.3 % for L-Arg and PIC respectively. The dissolution study of the final optimized gel was conducted using the dialysis bag method. The percentage release was found to be 86.19 ± 0.45% for PIC after 48 hrs. The release analysis predicted a higher correlation of R^2 with the Korsemayer-peppas model for PIC. The value of the slope comes out to be 0.2427 which confirmed that release is fickian in nature. The formulation was further investigated for accelerated studies at 25°C±2°C/60% RH ± 5% RH for 6 months. The 6-month stability data showed the p-value of the 't'-test ($p>0.05$) 0.42, 0.21, 0.10, 0.11 for vesicle size, zeta potential, entrapment efficiency for L-Arg, and entrapment efficiency for PIC respectively. The data for drug release was also compared statistically with model independence analysis. The f2 (similarity value) for fresh formulation and aged formulation (at 6 months) was found to be 53.28 for PIC. As these values come out to be above 50, it indicated that the drug release profile of PIC after keeping at 25°C ± 2°C/60% RH ± 5% RH for 6 months showed a similar release as that of the fresh formulation.

To identify the toxicity profile of the developed formulation, a cytocompatibility assay was conducted on fibroblast cells. The toxicity profile was identified at various dilutions and IC_{50} Value was calculated to be 15.488 µM of PIC. To check the efficacy of the formulation, clinical investigation was performed on pooled human saliva. The study showed the treatment group was able to maintain the pH of saliva above the potential demineralization zone for up to 24 hrs. The change in pH of saliva between the control and treatment groups was compared using student t-test. These changes are significant as the p-value of the 't'-test for pH at 24 hrs was found to be 0.027 ($p<0.05$). The change in the exopolysaccharides

amount in the saliva was calculated in the form of carbon content. The results showed that carbon content for treatment showed a significantly reduced value of percentage carbon content (28.08 %) after 24 hrs of treatment in comparison to the control group (59.03 %). The statistical analysis concluded a significant difference between the treatment and control group after 24 hrs and its p-value comes out to be 0.006 ($p<0.05$). This confirmed the therapeutic efficacy of the developed gel formulation of flexi-liposomes of PIC and L-Arg which showed a 52.3 % reduction in carbon content after 24 hrs when compared to control.

1 Introduction

1.1 Dental caries

Dental caries is a disease related to localized demineralization of the inorganic portion of the enamel part of teeth irreversibly (Chen & Wang, 2011). The causes for the development of dental caries on the calcified tissues of the teeth can be attributed to factors ranging from oral unhygienic conditions, oral microbiota, diet (high intake of sugar), the anatomy of teeth, and salivary flows (Kaur, Vyas, & Verma, 2022) (Aida et al., 2018). Etiological factors are very much evident to support the significant involvement of the interaction of developed microbial biofilm on tooth structure (Pitts et al., 2017). To date, anti-caries treatment involves mainly anti-microbial drugs as the main causative microbe is found to be *Streptococcus mutans* (*S. mutans*). *S. mutans* is an acidogenic microorganism that feeds on dietary sugar and produces acid with the help of exoenzyme glucosyltransferases in the oral cavity, along with its byproducts are thought to be the primary causative agents for dental caries (Shanmugam, Masthan, Balachander, Jimson, & Sarangarajan, 2013). The development of *S. mutans* biofilm on the dental enamel causes a net loss of minerals from the enamel. It happens because of prolonged reduced pH in the local microenvironment in the vicinity of enamel due to the metabolism of dietary sugar by *S. mutans* (Aida et al., 2018).

1.2 Prevalence of disease

The global prevalence of dental caries is affecting public health at large as it is the main cause of tooth loss among all age groups (Veiga et al., 2016). Human teeth are a high-valued part of a person's personality and thus have aesthetic value. Apart from it, teeth are meant for mastication, help in speech, and smiling, and affect the quality of life (Pitts et al., 2017) (Mathur & Dhillon, 2018). A meta-analysis conducted by researchers (Janakiram, Antony, Joseph, & Ramanarayanan, 2018) includes the prevalence index of dental caries in India. Global Oral Health Data confirms the prevalence of dental caries, varying from 49% to 83% across different countries. In India, Northern India: 75%, Southern India: 48%, Eastern India: 59%, and Western India: 55% prevalence is reported (WHO, 2022) (Jain et al., 2023). This study concluded the prevalence of the disease starts from 5 years of age and both males and females are contributing equally to its occurrence. In the United States, 90% of adults have dental caries. Dental caries are often not self-limiting and without proper care, caries can progress until the tooth is destroyed (Chen & Wang, 2011). There

are approximately 1 million cases of patients with oral infection reported to be hospitalized in 2016 with 9,00,000 cases of dental caries (Rukavina & Vanić, 2016).

In general, over the last 6 decades, the prevalence has invariably remained between 58% to 78% in India (Ingle, Dubey, Kaur, & Gupta, 2014). The prevalence in urban areas is a little less than in rural areas but broadly the prevalence can be concluded as the same in both cases. Another cross-sectional study in India shows that 78.9% of WHO reported DMFT (Decayed, missing, filled teeth index) (Hiremath et al., 2016). Another study claims it to be between 27% to 64% in children at the age of 12 years (Mathur & Dhillon, 2018).

Particularly in children, early childhood caries (ECC) can become prevalent causing swelling, pain, and discomfort. Caries preventive measures and good oral hygiene are essential even starting at a very early age (Mathur & Dhillon, 2018).

1.3 Therapeutic interventions used till now

Table 1. 1 Therapeutic class used till now (Chen & Wang, 2011) (Kabra, 2012)

Sr. No.	Therapeutic class	Drugs
1	Antimicrobial peptides	Meta-phenylene ethynylene and a peptide derived from milk casein
2	Chemo-prophylactic agents	Penicillin and vancomycin, chlorhexidine, Triclosan
3	Vaccines	GTFs and glucan-binding proteins
4	Sugar substitutes	Xylitol, Sorbitol
5	Probiotics and Replacement Therapy	Probiotics or release of antimicrobial peptides
6	Remineralizing approach	Fluoride, Dicalcium phosphate anhydrous
7	Casein Phospho-peptides	Casein phosphoproteins present in milk

Most of the therapeutic interventions used till now belong to anti-microbial compounds, which tend to kill the pathogenic microorganisms in the oral cavity. Although the demineralization of tooth enamel can not be reversed, many researchers are still finding a remineralizing approach as a method to treat caries. In general, preventive approaches, wherein the cause to stop the demineralization is targeted as it is more effective and also helps in protecting the aesthetic appearance of a person.

1.4 Role of PIC as an anti-biofilm agent

Biofilms occur on the surface of teeth through the accumulation of various pathogens and the formation of colonies of microorganisms. They have a special character to adhere to one another through receptors (Shanmugam et al., 2013) and become easily drug-resistant. These biofilms have complex and heterogenous structures and the composition of the biofilm depends on the type of microorganism, and the exchange of nutrients with its surface properties (Rukavina & Vanić, 2016) Due to the heterogeneous nature of biofilms, the development of drug resistance is easy, which is why dental caries caused by biofilms are difficult to target and treat.

Piceatannol (3, 3', 4'5-Tetrahydroxystilbene) is a stilbene derivative and analogue of resveratrol (a polyphenolic compound), obtained from the seeds of *Euphorbia lagascae*. It was reported to have antioxidant and anti-inflammatory effects. Studies revealed that piceatannol has an anti-biofilm effect with a 52 μM IC_{50} value and more selectivity than its precursor resveratrol. Piceatannol is known to have glucosyltransferase inhibitory action thus preventing biofilm formation. *S. mutans* viability does not get affected by piceatannol (J. D. B. Featherstone & Chaffee, 2018) .

The anticaries activity of PIC was evaluated against oral bacteria pathogens like *Streptococcus mutans*, *Pseudomonas aeruginosa*, *Staphylococcus aureus,* and *Escherichia coli*. The minimum inhibitory concentration of piceatannol was observed to be in the range of 0.025 – 0.3 mg/ml (Osamudiamen, Oluremi, Oderinlo, & Aiyelaagbe, 2020).

1.5 Role of L-Arg as substrate for cario-protective microbes

L-Arginine, on the other hand, is a basic amino acid that acts through the arginine deiminase system (ADS) of certain oral bacteria to produce alkaline metabolites. Thus, raises the pH of the oral cavity, thereby protecting the host from dental caries (Chakraborty & Burne, 2017). The report suggests that the presence of other commensal bacteria (*S. sanguinis)* in the oral cavity provides competition to *S. mutans*. These commensals are alkali-producing microbes and have proved beneficial in preventing caries by increasing the local pH (Chakraborty & Burne, 2017). L-Arginine metabolism produces ammonia thus neutralizing biofilm pH. L-Arginine thus provides ecological benefits to oral microbiota to prevent caries (Roupe, Yáñez, Teng, & Davies, 2006).

1.6 Flexi-liposomes as a drug delivery approach

Flexi-liposomes are also termed transferosomes', deformable liposomes, or Nano-Elastic vesicles in literature (Kaur et al., 2023). The activity is aided with the help of an Edge activator (EA) in addition to conventional liposomes. The resultant liposomes thus develop the ability to deform and reform, thus also termed transferosomes.

It is a novel drug delivery approach to dental caries where their ultra-deformable character is primarily used for better penetration mainly through pores of the biofilm. Since these vesicles can penetrate a pore size 10 times smaller than its own, The present work focuses on developing Piceatannol-L-Arginine flexi-liposomes in combination, which can penetrate the biofilms present above the surface of teeth.

Piceatannol and L-Arginine are selected to achieve the desired biofilm dispersal as they will make *S. mutans* less virulent. L-Arginine will serve as a substrate for carioprotective microbes. Collectively this combination will promote the growth of carioprotective microbes and will help bring a state of symbiosis from the dysbiosis of microbes in the oral cavity. The present study will target the societal problem and the intended to give industrial benefit by developing a formulation having a potential benefit to the market.

2 Review of literature

2.1 Dental Caries

Dental caries is a disruptive dynamic process where microbes, dietary supplies and salivary secretions, and many other factors play a role (Hajishengallis et al., 2018). The progression of the disease occurs when a pathogenic microbe usually *S. mutans* gets access to the oral cavity. *S. mutans* along with a carbohydrate-rich diet produce weak organic acid, lowering the pH in the vicinity of the enamel, causing the corrosion of dental enamel. It is an irreversible disease and can cause cavitation of the teeth. If left untreated can cause severe systemic infections. It has a high risk of recurrence even after sufficient pharmacological treatments (Shanmugam et al., 2013).

2.1.1 Pathogenesis

The proposed genesis of the disease is attributed to vertical or horizontal transmission of *S. mutans* from either caregiver or the environment respectively. *S. mutans* produces insoluble exopolysaccharides like glucans and to some extent fructans. These insoluble exopolysaccharides are produced when exoenzymes (glucosyltransferases) present in *S. mutans* consume dietary sugar. As metabolic products organic acids get generated. *S. mutans* releases these exoenzymes in the local microenvironment and these bind with the glycoproteins of the pellicle of teeth. Consumption of sugar by these active exoenzymes produces insoluble glucans. This extracellular matrix of biofilm holds microbial cells together (Hajishengallis et al., 2018).

These insoluble glucans cause the increased binding of micro-organisms to one another. As a result of this, the microbes start becoming closely associated together, also the attachment of glucosyltransferases to their surface converts them to glucan producers. This local accumulation of microorganisms produces a diffusion-limiting matrix (Fig 2. 1).

Further, *S. mutans* is an acidogenic microorganism as it produces organic acids. This acidic microenvironment causes other microbes to increase their glucosyltransferase gene expression. This leads to increased production of insoluble glucan by various microbes, increasing acidic stress locally.

Development of the disease depends upon intrinsic factors of the patient like salivary antibodies (IgA, IgG). Antibodies can destroy invading *S. mutans* and related pathogenic microbe by enzyme interference, opsonization, or by complement system activation

In dietary sugar, sucrose is a critical mediator which produces acid locally. The presence of sucrose potentiates the pathogenesis of the disease. *S. mutans* also have a special ability to develop cariogenic biofilm in the presence of sucrose.

The presence of non-mutans streptococci, for instance, *actinomyces, lactobacilli, bifidobacteria,* and *Scardovia* species, have also been verified as agents which produce acid in the vicinity of teeth, ultimately promoting the pathogenesis of the disease.

On the other hand, alkali-producing microbes that produce ammonia, such as *S. gordonii* and *S. sanguinis* organisms by using salivary substrates such as L-Arg via the arginine deiminase system (ADS) and urea (*S. salivarius* and *A. naeslundii)* by urease enzymes. These microbes act opposite to aciduric bacteria, leading to a decrease in the formation of biofilm. While maintaining an alkaline pH can help prevent tooth decay, excessively alkaline conditions in the oral cavity can also have negative consequences, such as promoting the growth of certain pathogenic bacteria or interfering with normal oral functions (Luo et al., 2024) .

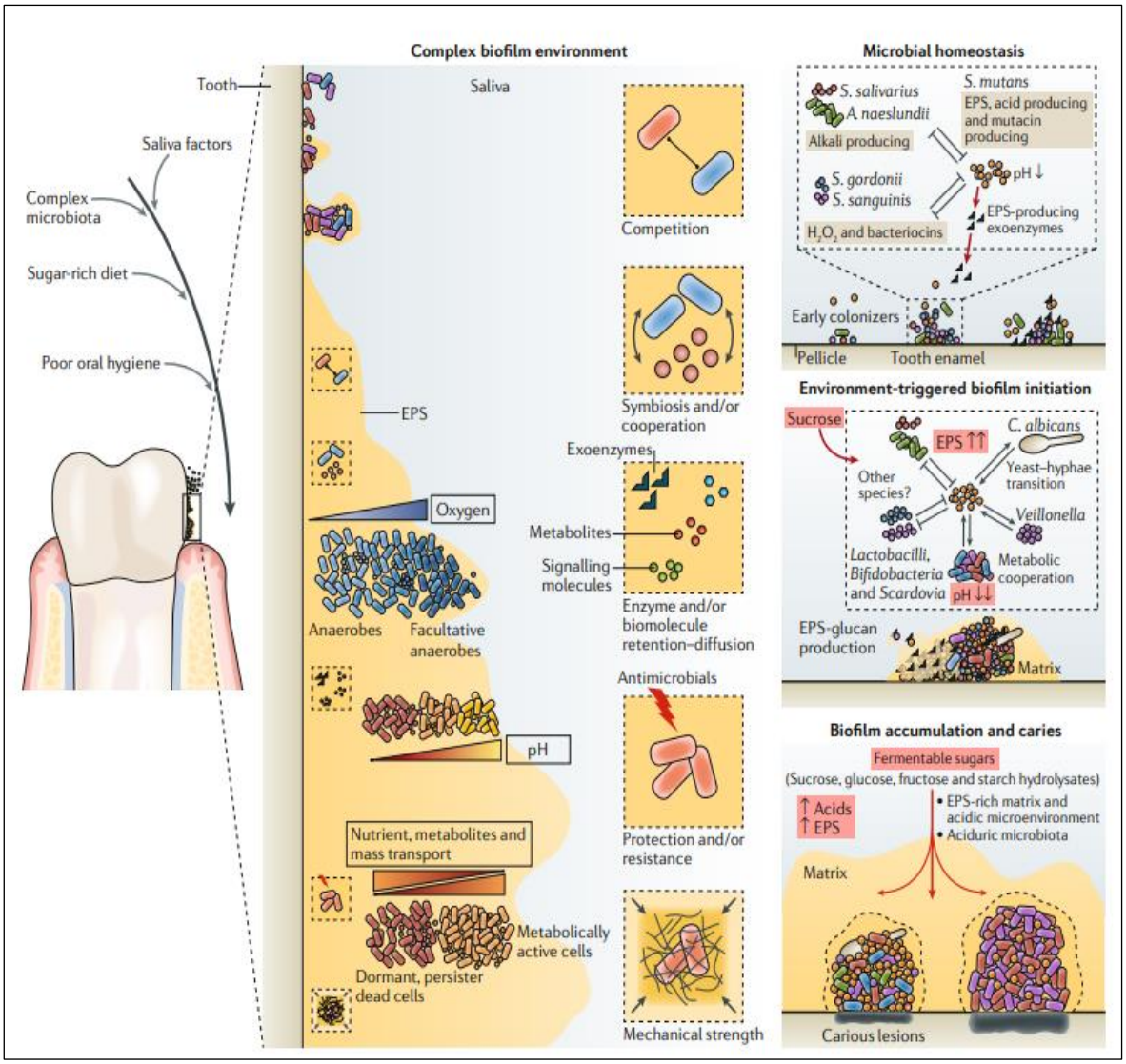

Fig 2. 1 Factors triggering pathogenesis of dental caries (Hajishengallis et al., 2018)

Many salivary proteins, such as proline-rich glycoproteins (PRPs), mucins, and immunoglobulins act as modulators of oral health (Guo & Shi, 2013) (Vacca Smith et al., 2007).

A similar finding was concluded by Chen and co-workers, They stated that mature biofilms are the complex association of polymers from host and bacteria mainly *S.mutans*. Mature biofilms contain polysaccharides, proteins, and DNA which act as a protective barrier to the various pharmacological agents used in the treatment of dental caries (Chen & Wang, 2011)

As a part of the defense mechanism by the body IgA antibody is produced in the salivary gland which binds specific antigens present in cariogenic bacteria. Activation of innate

immunity of the host results in further differentiation and maturation of B-cells which try to wipe them out of the body (Chen & Wang, 2011)

Another study states that the prevalence of the disease is dependent upon the dynamic and delicate balance between pathological and protective factors. Risk factors include aciduric, acidogenic, and cariogenic bacteria, hypo-salivation and frequent ingestion of fermentable carbohydrates, and poor oral hygiene (Table 2. 1). Among acidogenic bacteria are *S. mutans* and *lactobacillus*. Early detection of bacterial load can be helpful in the early selection of an anticaries agent. While the study says the exact pH at which carious lesions start to form cannot be estimated the critical value is thought to be between 5.5 to 5. Saliva on the other hand helps in protecting the teeth' enamel by its buffering capacity, presence of remineralizing calcium phosphate content, and presence of urea to raise the local pH. So, to prevent caries propagation protective factors like biological, therapeutic, and dietary factors are to be considered collectively to target the disease. Lifestyle changes like including fluoridated water and other fluoridated toiletries can be beneficial in limiting the progression of the disease (Maheswari, Raja, Kumar, & Seelan, 2015)

Gradual complex biological interactions of acidogenic bacteria, fermentable food, saliva, etc. in contrast to others their finding states that disease involves complex microbiota in the pathogenesis of the disease. The researcher concluded the progression of the disease is due to interaction between various determinants like substrate, host, and micro-organisms. The prominent ones are *S. mutans*, *Streptococcus sobrinus* and *lactobacilli*. Carious lesion development is not a continuous process rather is developed due to cyclic episodes of imbalance between demineralization and remineralization. Enamel demineralization does not involve inflammation as enamel does not contain blood vessels and nerve endings (Ramos et al., 2018)

Simon and associates (Simón-Soro & Mira, 2015) state that various DNA and RNA studies found that dental caries is a poly-microbial disease. The diversity within each lesion makes the finding complicated. But primarily different species of lactobacilli genera are involved mainly in all the lesions. Also, the presence of one type of bacteria influences the survival and adherence of the bacteria as stated (Hajishengallis et al., 2018). The diversity of microbiome consortia is such that the composition of various microbes is different in different stages of the disease and also different in different subjects. The concerned microbe is considered pathobionts as in normal conditions they are non-pathogenic but

when they find a critical modulator they become pathogenic and the progression of the disease starts. The risk factors for caries are mentioned below(Fallah, 2019)(J. D. B. Featherstone & Chaffee, 2018)

Table 2. 1 Factors responsible for dental caries

Pathological Factors	Dietary Factors	Physiological Factors	External protective factors
Acidogenic microbes, Acidouric microbes, Insoluble glucan production, Adhesion of extracellular polysaccharides to tooth pellicle, and High plaque on the teeth	Sugar intake, Frequent snacking, Carbonated beverages, and Recreational substances	Deep pits and fissures, Inadequate saliva flow, Exposed tooth roots, and Antibodies (Ig A, Ig G)	Brushing, dental flossing, fluoride mouth rinses, and toothpaste

2.2 Therapeutic classes explored till now

Depending upon the complex nature involving the etiology of the disease, its treatment also involves many different drugs belonging to various therapeutic classifications. As mentioned above the pathological factors involve the amalgamation of biological, microbial, physiological, socioeconomic, and dietary factors various formulations involving different targets to minimize carious lesions have been made (Table 2. 2).

2.2.1 Chemo-prophylactic agents

Chen and co-workers (Chen & Wang, 2011) give the idea of novel technologies for the treatment of dental caries. Chemoprophylactic agents have been used in the past as mouthwashes, toothpaste, gels, and varnishes to prevent dental caries occurrence. The antibiotics used were penicillin and vancomycin.

Among prophylactic agents, the major one is chlorhexidine (Chen & Wang, 2011) which is cationic and binds with a pellicle, mucus membrane, and hydroxyapatite. There it adheres and is retained for a longer period disrupting biofilm. However, retention for a longer period leads to staining on the tooth surface and calculus formation. As a solution to this chlorhexidine gluconate with an anionic anti-calculus agent was also given.

Triclosan (anti-microbial agent) rinses, toothpaste, and dentifrices were developed and found a promising candidate in the treatment of caries. But being low soluble in water, its emulsions along with various emulsifiers and surfactants were developed, also it shows less retention capacity as compared to chlorhexidine (Chen & Wang, 2011).

To increase the longer retention of triclosan, it was formulated with a polyvinyl methyl ether/maleic acid copolymer. This increases retention capacity and enhanced anti-plaque activity. To increase the solubility of this non-ionic anti-microbial drug mineral-binding micelles were developed and release the encapsulated drug in the vicinity of the tooth (Chen & Wang, 2011)

Naturally occurring antimicrobial agents are gaining attention as they have fewer side effects than synthetic ones. Such naturally occurring agents can inhibit GTFs activity in *S. mutans* culture, thus preventing plaque formation. So various mouth rinses and toothpaste are also available.

2.2.2 Antimicrobial peptides (AMP)

These are the primary or secondary proteins produced by the innate immunity of the body, which has amphipathic nature and is positively charged. They offer an advantage over antibiotics as they target the bacterial cell by interacting with surface components having a negative charge on them so they are least become ineffective due to the development of resistance in bacteria (Philip, Suneja, & Walsh, 2018). They have a more robust nature and are used as wide-spectrum agents including drug-resistant strains. But they are difficult to manufacture and have short half-lives. A compound called meta-phenylene ethynylene and a peptide derived from milk casein has been formulated for caries treatment. Recent advances made targeted peptide delivery possible by the use of adding a targeting domain to the peptide. The AMPs can also be modified to make pH specific to reduce secondary infections produced by killing unwanted microbes (Chen & Wang, 2011).

2.2.3 Vaccines

Antibodies are produced as adaptive immunity of the host against the pathogen. These vaccines are also explored in the treatment of dental caries. The suitable antigen is injected into local lymphoid tissues resulting in the migration of antigen-specific IgA antibody locally. The three main types of secretory IgAs that have been found are antigen I/II, GTFs, and glucan-binding proteins which are responsible for caries development. Results have shown that passive immunization of the host helps to prevent the colonization of the

causative bacteria. These antibodies competitively bind with the surface pellicle of the tooth thus preventing the adhesion of *S.mutans* to the tooth surface (Chen & Wang, 2011). Attachment of these antibodies to GTFs interferes synthesis of soluble and insoluble glucans thus preventing adhesion of the microbes to each other.

2.2.4 Probiotics and replacement therapy

These are live microorganisms that help in maintaining a balanced microbiota of the oral cavity. Studies from the past have shifted from the destruction of the microbial community to selectively inhibiting the pathogenic microorganisms. The destruction of the microbiota leads to unwanted side effects. Probiotics have seen a promising effect in preventing dental caries. The proposed mechanism could be competition for nutrition among bacteria, competition for the binding site to the host surface, production of anti-adhering components by probiotics, or release of antimicrobial peptides which leads to the destruction of the pathogenic microbes (Chen & Wang, 2011). Contrary to this study conducted by Philip *et al.,* 2018 got shreds of evidence that probiotics have potentially harmful effects on dental caries than benefits.

2.2.5 Sugar substitutes

Xylitol is a sugar alcohol (Polyol) having a sweet taste. As it cannot be consumed by the *S.mutans*, it has shown a strong anti-caries effect. As it does not affect the pH of the microenvironment, also it has a bacteriostatic effect on *S.mutans*. But studies till far shows that xylitol shows dose-dependent and frequency-dependent effect. Still, studies are to be conducted to justify the aforementioned statements (Chen & Wang, 2011) While the anti-cariogenic effect of xylitol is found to be effective against *S. mutans, S. saliviarius,* and *S. sanguis* (Saleem, Khan, Kazmi, & Afzal, 2019)

Above mentioned sugar substitutes are (polyol) formulated as chewing gums (Rethman et al., 2011). As they provide short contact of the xylitol with the tooth surface so difficult to maintain a prolonged effect using this technique (Chen & Wang, 2011).

2.2.6 Remineralizing approach

Fluoride salts can be commonly found in drinking water, toothpaste, and mouth rinses. Fluorides are traditionally known to have an anticaries effect. A membrane-controlled reservoir-type system is developed that controls the rate of fluoride release from the core through a gradient between the core and outer membrane(Chen & Wang, 2011).

2.2.7 Casein phospho-peptides

Milk, milk concentrates, and cheese are known to have a non-cariogenic effect. The main component for this is casein phosphoproteins. These are known to produce calcium and phosphate-rich matrix, which ultimately increases the remineralization of the teeth (Chen & Wang, 2011)

Besides these roles of various phytochemical is summarized in an article which states that polyphenols like catechins and cranberry juices, flavonoids found in grapefruit, flavones extracted from *Leguminosae* family, and alkaloids from various sources have been identified and analyzed for anti-caries effects (Kabra, 2012)

Table 2. 2 Therapeutic classes used till now

Sr. No.	Therapeutic class	Drugs
1	Antimicrobial peptides	Meta-phenylene ethynylene and a peptide derived from milk casein
2	Chemo-prophylactic agents	Penicillin and vancomycin, chlorhexidine, Triclosan
3	Vaccines	GTFs and glucan-binding proteins
4	Sugar substitutes	Xylitol, Sorbitol
5	Probiotics and Replacement Therapy	Probiotics or release of antimicrobial peptide
6	Remineralising approach	Fluoride, Dicalcium phosphate anhydrous
7	Casein phospho-peptides	Casein phosphoproteins present in milk

2.3 Novel formulations for dental caries

2.3.1 Tooth binding micelles (TBMs) of farnesol

It is an antimicrobial agent. Tooth-binding micelles are formed by pluronic copolymer (poly ethene oxide PEO and polypropylene oxide PPO) and increased adhesion capacity by attaching a bio-mineral binding moiety like alendronate. Fast adhesion of micelles to hydroxyapatite surface was seen and remarked antimicrobial activity of the formulation was observed (Chen & Wang, 2011)

Similarly, tooth-binding micelles were prepared using the drug triclosan which is known for its antibiotic activity. They used different binding moieties than alendronate, naming diphosphoserine peptide and pyrophosphate as they are more biocompatible and

biodegradable. These TBMs were prepared using Self micellization. TBMs have shown 60% retention capacity in the oral cavity and were able to retain there for 24 hrs. TBMs prepared using this manner has shown promising antiplaque effect (Chen et al., 2013).

2.3.2 Antimicrobial peptide (AMP) loaded in liquid crystals

Liquid crystalline system (LCs) was made using oleic acid, polyethylene, Carbopol® . and water or 0.5% polycarbophil was used as an aqueous phase in which polymers were to dispersed. Results have shown that after 24 hrs of treatment, drug retention has increased significantly after getting diluted with saliva than after 4 hrs ((Aida et al., 2018)

2.3.3 Dental molds

These are polymeric molds of lidocaine hydrochloride to treat dental caries. These are prepared using corn zein, carbopol, and gum karaya powder, by solvent evaporation technique. Sustained release drug patterns were observed for 24 hrs where amoxicillin released 50% and Lidocaine 98% of entrapped drug (Table 2. 3) (Ghosh, Roy, & Mukherjee, 2009)

2.3.4 Nano-hydroxyapitite dentifrices

This compound is known to have preventive, regenerative, and restorative activity. It is also the main part of bone structure and the mineral part of teeth. Studies reveal that the formulation has shown good anti-cariogenic effect by improving the remineralizing capacity of the teeth (Pepla, 2014)

2.3.5 Novel toothpaste

Calcium silicate and phosphate fluoride with dual-phase gel toothpaste were prepared and interproximal remineralization was observed. The study has shown that improved remineralization is achieved using novel toothpaste (Ramos et al., 2018)

2.3.6 Cationic liposomes

These are made as part of photodynamic therapy where aluminum chloride phthalocyanine is entrapped in the cationic liposomes. This drug is called photosensitizer. On application of the photosensitizers, light is irradiated. The said photosensitizer on light sensitization produces reactive species which kills the local bacteria. Due to the cationic nature of the liposomes, they adhere specifically to the anionic part of the bacterial cell wall components, targeting them to prevent dental caries (Longo et al., 2012)

2.3.7 Nanoparticles and Nanorods

Nanoparticles have been prepared by casein phosphopeptides and amorphous calcium phosphate. These nano-complexes have remineralizing capacity by mimicking the biomineralization process. A biocompatible nanoparticle is prepared initially in the field of nanotechnology by Bako and coworkers. 2-hydroxyethyl methacrylate (HEMA) and polyethyleneglycol dimethacrylate (PEGDMA) are used as polymers (Piñón-Segundo, Mendoza-Muñoz, & Quintanar-Guerrero, 2012)

These are also prepared using chlorhexidine digluconate and sodium hexametaphosphate. The prepared nanoparticles are negatively charged and adhere to the tooth surface for up to 50 days (Wood et al., 2015). Other formulations containing Silver, titanium dioxide, and silica nanoparticles are also prepared to check the efficacy of metals as antimicrobial agents. While silica and titanium dioxide have shown the least activity, silver nanoparticles have shown 25 fold decrease in the bacterial cell count than chlorhexidine alone (Besinis, De Peralta, & Handy, 2014)

Table 2. 3 List of novel formulations reported for dental caries

Sr. No.	Novel formulations	Drugs used	References
1	Liquid crystals	Antimicrobial peptide (AMP)	(Aida et al., 2018)
2	Nano-hydroxyapitite dentifrices	Hydroxyapatite	(Pepla, 2014)
3	Novel toothpaste	Calcium silicate and phosphate fluoride	(Ramos et al., 2018), (Renugalakshmi et al, 2011)
4	Tooth-binding micelles (TBMs)	Farnesol	(Chen & Wang, 2011)
5	Cationic liposomes	Aluminum chloride phthalocyanine (PDT)	(Longo et al., 2012)
6	Dental molds	Amoxicillin trihydrate and lidocaine hydrochloride	(Ghosh et al., 2009)
7	Nanoparticles and Nanorods	Casein phosphor-peptides and amorphous calcium phosphate	(Piñón-Segundo et al., 2012),(Renugalakshmi et al., 2011)

2.4 Marketed nano-formulations of dental caries: (Ramos et al., 2018)

A list of marketed nano-formulations reported in the literature for the treatment of dental caries is mentioned in table 2. 4.

Table 2. 4 List of nano-formulations reported for dental caries

Sr. No.	Applications	Material	Brand	Nano-formulation
1.	Restorations	Nano-composite resins	KetacTM Nano 3M ESPE	Zirconia/silica nanofillers and nanoclusters
2	Restorations	Nano-composite resins	Herculite XR Ultra, Kerr	Nanosilica
3	Restorations	Nano-composite resins	Tetric Evo cream,	SO2 spherical nanofillers
4	Cavity disinfectant	Mineral solution	NanoCare gold® DNTTM	Spherical silver nanoparticles (48 nm)

2.5 State of the science

Traditionally, dental caries treatment involves antibacterial and remineralizing agents. But the suggestive data on the prevalence and disease management of dental caries explains the insufficiency of current antibacterial and remineralization therapy. When the severity of the disease in terms of oral microbial imbalance progresses, a state of dysbiosis appears. Wherein, the existing therapies become insufficient to bring disease management, and improvement in current technologies is needed for achieving effective treatment.

Dental caries is a multifactorial disease and preventive measures which can limit the disease progression are considered to provide effective therapeutic management of disease. The restorative approach is another suggestive strategy as reparative therapy for disease management. A combination approach wherein the use of antibacterial agents along with restorative therapy could also be used to increase the effectiveness of therapy.

Two major limitations of the use of antibacterial therapy involve, creating a state of dysbiosis among oral microbiome and unwanted exposure of antibiotics to non-pathogenic microbes present in the oral cavity. These limitations increase the chances of drug resistance in oral pathogens. To overcome these challenges and so to maintain a healthy oral microenvironment, an alternative and cost-effective approach is required. This along with behavioral and lifestyle changes can be fruitful in minimizing the progression of the disease.

The literature review suggested that existing fluoride therapy is insufficient once the oral microbiome is already in a state of dysbiosis. Alternative preventive and reparative approaches to fluoride therapy are the use of Silver and fluoride, and L-Arg with fluoride are the formulations researched for a synergistic effect on each other (Fig 2. 2).

Various novel approaches to biofilm modification and remineralization therapy are in progress and should be the basis for researchers to explore the area.

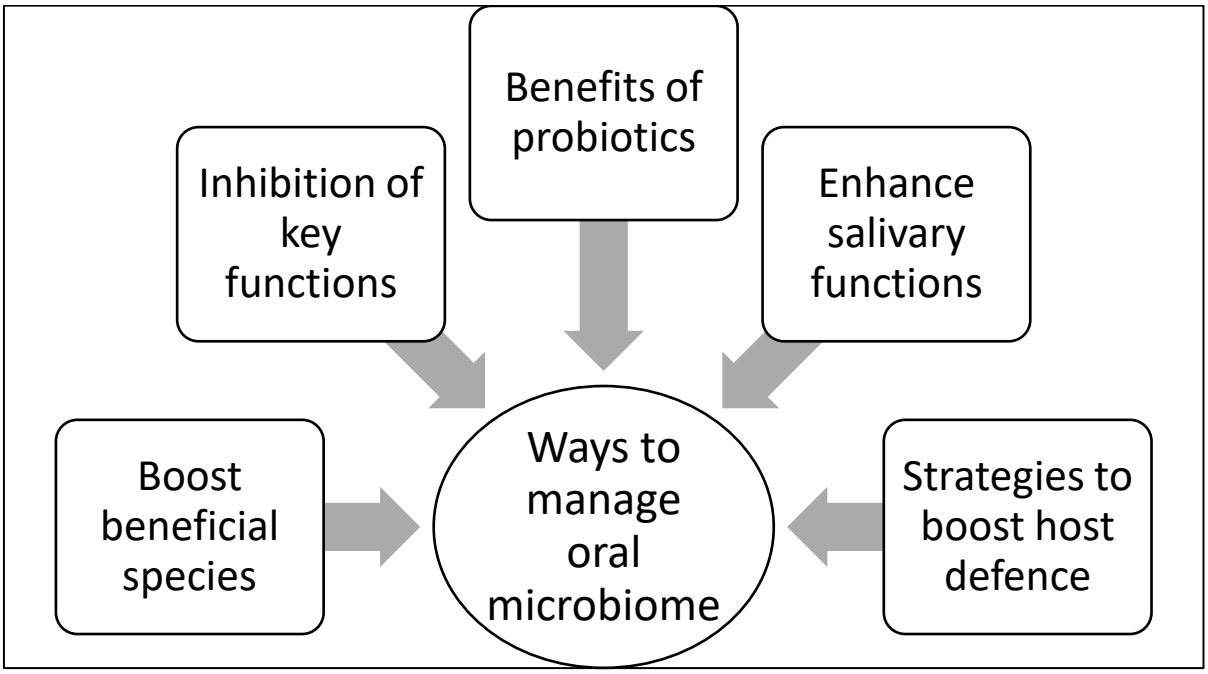

Fig 2. 2 Representation of different ways to manage the oral microbiome. (J. D. Featherstone, Fontana, & Wolff, 2018)

2.6 Selection of the drug

Current efforts are required to maintain a state of symbiosis of the microbiota of the buccal cavity(Scharnow, Solinski, & Wuest, 2019). To promote the growth of beneficial microbes instead of inhibiting the pathogenic microbes and to waive off the prevalence of drug resistance in the acidogenic microbes it is essentially a promising approach to rather choose an alternative to antimicrobial agents like choosing an antibiofilm or antiadhesive agents, GTFs inhibitors, using a substrate to promote the growth of beneficial microbe, etc. Among the above-mentioned, GTF inhibitors have the potential to regard as promising candidates to explore for caries management. From various herbal sources polyphenolic compounds, flavonoids, and hydroxy chalcone derivatives have shown selectivity towards GTFs (Table 2. 5)

Table 2. 5 Reported GTF inhibitors from the herbal origin (Roupe et al., 2006)

Sr. No.	Class	Structure	Compound	References
1	Hydroxychalcone derivatives	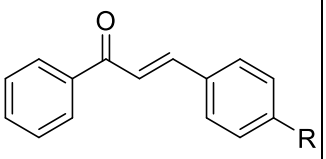	Apigenin (4',5,7-trihydroxy flavone, myricetin	(Nijampatnam, 2016)
2	Flavanoids	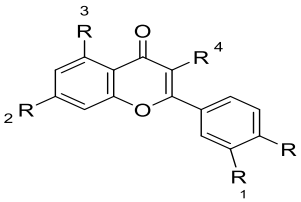	Pinocembrin, galangin, caffeic acid, and ferrulic acid	(Bozcuk Erdem & Ölmez, 2004)
3	Catechin based polypHenols	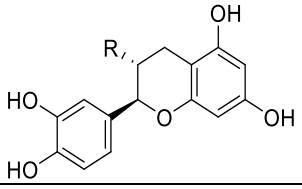	Crude oolong tea extract, Epigallo-catechin gallate	(Nakahara et al., 1993)(Xu, Zhou, & Wu, 2011)
4	Proanthocyanidin	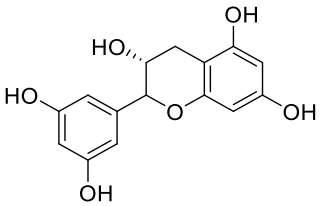	PAC-enriched extract	(Koo et al., 2010)
5	Stilbene derivatives	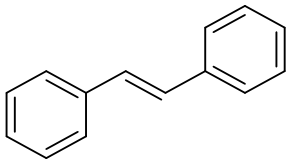	Trans-Resveratrol, Piceatannol and Gallic acid	(Osamudiamen et al., 2020)(Scharnow et al., 2019)
6	Marine alkaloid	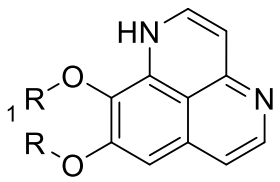	Mukaaluvamine derivatives	(Nijampatnam, Nadkarni, Wu, & Velu, 2014)
7	Alkaloidene lactam derivatives	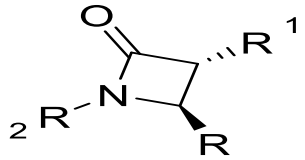	Synthetic analogs	(Pereira et al., 2014)

The above-mentioned drug is a novel therapeutic agent to be used as an anticaries agent. It has anti-biofilm properties which disrupt the biofilm formed by *S. mutans*, which is responsible for caries formation. Secondly, due to the development of drug resistance using an antibacterial agent, other favorable approaches to prevent caries are being explored. PIC

is a strong and selective antibiofilm agent and has an IC_{50} of 52 μM and acts by glucosyltransferase inhibition, to prevent caries formation(Nijampatnam et al., 2018).

2.7 Mechanism of action of anti-biofilm agents

Mechanism of action of Anti-biofilm agents	Dispersion of extracellular polysaccharides by enzyme
	Cleavage of peptidolycan
	Inhibition of quorum sensing among microbes
	Biofilm disassembly
	Disassembly of lipopolysaccharides
	Alteration of membrane permeability
	Inhibition of adhesion molecules
	Inhibition of GMP signaling
	Direct cytotoxicity

Fig 2. 3 Various mechanisms by which an anti-biofilm agent can inhibit the incidence of the disease (Roy, Tiwari, Donelli, & Tiwari, 2018)

2.8 Novel Anti-caries agent

Ideal therapeutics for dental caries as evaluated from the state of the science should selectively inhibit biofilms caused by *Streptococcus mutans*. As this approach will eradicate the onset of drug resistance among microbes present in oral microbiota. The selection of antibiofilm agent PIC along with L-Arg is a novel approach that could disrupt the microbial biofilm causing dental caries and promoting the growth of protective microbes in the oral microbiome. Both drugs in combination can prove synergistic in reducing the incidence of the disease.

2.8.1 PIC

PIC is a polyphenolic (stilbene derivative) obtained from the seeds of *Euphorbia lagascae, Polygonum cuspidatums, Passiflora edulis* (Passion Fruit). It was reported to have antioxidant and anti-inflammatory effects. Studies revealed that PIC has an anti-biofilm effect with a 52 μM IC_{50} value and more selectivity than its precursor resveratrol. PIC is

known to have glucosyltransferase inhibitory action thus preventing biofilm formation (Banik et al., 2020). Its viability does not get affected by PIC (Fig 2.3) (J. D. Featherstone et al., 2018) (Osamudiamen et al., 2020). Some physicochemical properties of PIC are mentioned in tabl 2. 6

Table 2. 6 Physicochemical properties of PIC (Roupe et al., 2006)

Property name	Property value
Structure	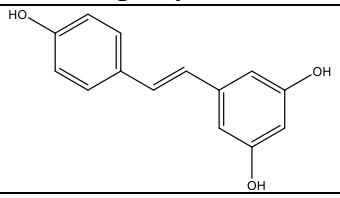
IUPAC name	4-[(*E*)-2-(3,5-dihydroxypHenyl) ethenyl]benzene-1,2-diol
Molecular Weight	244.24 g/mol
XLogP$_3$	2.9
Mass	244.073559 g/mol
LD$_{50}$	217 mg/kg
Molecular Formula	$C_{14}H_{12}O_4$
Synonyms	3-Hydroxyresveratol,3,5,3',4'-Tetrahydroxystilbene
Melting point	234°C-237°C
Boiling point	107°C-109°C
Density	1.5 g/cm^3
Solubility	DMSO (10 mg/ml), DMF, ethanol (10 mg/ml), methanol, acetone, ethyl acetate, and water (0.5 mg/ml)
pK value	9.17
U.V Analysis	323.5, 224.5
AUC$_{inf}$ (mg hr/ml)	8.48 ± 2.48
Vd (l/kg)	10.76 ± 2.88
Plasma half-life	4.23±1.25 hr
Urine half-life	19.88±5.66 hr
Dose	10 mg/kg
Metabolite	Glucuronidated metabolite
Bioavailability	50.7+/-15.0%
C$_{max}$	710+/-219 ng/ml
T$_{max}$	45-120 mins

2.8.2 L-Arg

L-Arg is a basic, semi-essential amino acid, which serves as food for carioprotective microbes of oral bacteria. They are known to consume L-Arg by the arginine deiminase system (ADS) which produces urea and ammonia that raises the pH of dental plaque, thus protecting the host from dental caries (Chakraborty & Burne, 2017). The report suggests that the presence of other commensal bacteria (*S. sanguinis)* in plaque provides competition to SM. These commensals are alkali-producing microbes and have proved beneficial in preventing caries by increasing the local pH(Chakraborty & Burne, 2017). L-Arg metabolism produces ammonia thus neutralizing biofilm pH. L-Arg also provides ecological benefits to oral microbiota to prevent caries (Roupe et al., 2006) Some general properties of L-Arg are mentioned in table 2. 7.

Table 2. 7 Physicochemical properties of L-Arg

Property name	Property value
Structure	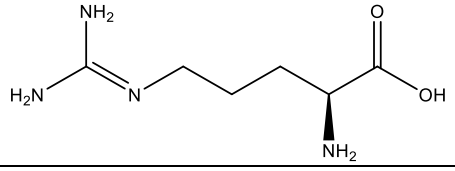
IUPAC name	(2*S*)-2-amino-5-(diaminomethylideneamino)pentanoic acid
Molecular Weight	174.2 g/mol
XLogP$_3$	-4.2
Solubility	Insoluble in ethyl ether, slightly soluble in ethanol
Molecular formula	$C_6H_{14}N_4O_2$
Melting point	244°C
pH	Strongly alkaline
pka	2.24 (at 0°C)
Lambda max (λ max)	207.5 nm

2.9 Liposomes in the treatment of biofilms

Literature review shows a variety of liposomes using triclosan drug has been explored to date to check its utility. Triclosan alone and in combination is also observed for antimicrobial activity (Table 2. 8) (Ramos et al., 2018).

Table 2. 8 Liposomes in the treatment of oral biofilms

Sr. No.	Formulation	Drug	Excipients	Organism
1	Liposome	Triclosan	dimyristoyl phosphatidylcholine, cholesterol; dimethyl dioctadecyl ammonium bromide (64:23:13)	*Streptococcus oralis, Streptococcus sanguis,*
2	Liposome	Triclosan-zinc combination	Dimethyl dioctadecyl ammonium bromide (4%-19%), dimyristoyl phosphatidylcholine, cholesterol	*S. oralis*
3	Liposome	Triclosan-zinc combination	Phosphatidylinositol, 1,2-dipalmitoyl-glycero-3-phosphocholine	*S. oralis*
4	Nanoemulsion	Cetylpyridinium chloride	Soybean oil, deionized water, Triton X-100	*S. mutans*

2.10 Method of preparation of flexi-liposomes

2.10.1 Composition of flexi-liposomes

Elastic vesicles are made up of a phospholipid backbone which forms around 90% of the composition and a non-ionic surfactant which acts as an edge activator to the formed vesicles (Table 2. 9). The solvent system is selected based on solubility criteria and buffer to provide hydration to the vesicles which causes them to form vesicles

Table 2. 9 Components of flexi-liposomes (Huang, 1969)

Sr. No.	Components	Purpose	Example
1.	Phospholipids	Vesicles forming component	Soya phosphatidylcholine, egg phosphatidylcholine,
2.	Edge activator	To impart flexibility	Sod. deoxycholate, Tween-80, Span-80, Span 60
3.	Alcohol	Solubilizing agent	Ethanol, methanol
4.	Buffering agent	hydration medium	Saline Phosphate buffer (pH 6.4), Water

2.10.1.1 Phospholipids

Phospholipids are the class of lipid which is the main structural component of the cell membrane. Phosphatidylcholine is widely used phospholipid for vesicles formation. Phosphatidylcholine has a combination of various chemical moieties depending upon the

carbon chain length and according to the fatty acid group attached they are named accordingly for example dipalmitoyl phosphatidyl choline (DPPC), dioleoyl phosphatidylcholine (DOPC), dilauroylphosphatidyl choline (DLPC) (Huang, 1969)

2.10.1.2 Edge activator

These are surface-active agents that tend to lower the surface tension. They tend to loosen the bridges between the outer surface and phospholipid bilayer which gives these vesicles flexibility to adjust for stress. Molecules that are greater than 500 Da normally do not cross the skin. The self-optimizing ability offered to liposomes is with the help of an edge activator. Edge activators are mainly non-ionic surfactants (because of their non-toxic nature) which offer local bilayer destabilization and flexibility when used in the right amount in the formulation (Cevc, 2003). Till now mainly used surfactants are sodium cholate, sodium deoxycholate, span 20, span 40, span 60, span 80, and tween 80 (Duangjit et al., 2014)

2.10.1.3 Hydration media

The purpose of hydration media is to re-suspend the lipidic film in media for vesicle formation. The temperature at which hydration is done is of particular importance since it has to be above the glass transition temperature (Tm) of the thin layer. Because the lipid which is to hydrate should be in a fluid state while hydration so it is better done on a rotary evaporator by controlling temperature (above 55ºC). Contact time with hydration media should also be controlled especially for high transition lipids because at elevated temperatures hydrolysis of lipids may occur. Most used hydration media includes distilled water and buffer solutions,

2.10.1.4 Solvent system

For homogenous mixing of the lipid system and surfactant, a solvent system is required. Generally, a chloroform-methanol mixture is widely used for making a clear solution of lipids for uniform dispersion. As an alternative cyclo-hexane or butanol can also be used in place of chloroform.

2.10.2 Method of preparation

Nano-vesicles are prepared similarly to liposomes, with a few modifications like sonication, extrusion or high-shear homogenization. The most widely used technique is thin-film hydration method using a rotary vacuum evaporator. This method forms elastic vesicles which are then sonicated to produce the required size of vesicles.

Other than this sonicated vesicle is extruded through a polycarbonate membrane to bring it to the required size.

2.10.3 Mechanism of skin penetration

Walve and co-workers (Walve, Bakliwal, Rane, & Pawar, 2011) explained the mechanism of penetration of nano-elastic vesicles through the stratum corneum of the skin. They called them self-optimized aggregates which can penetrate even pore sizes of less than 30nm. When present on one side of the stratum corneum, the driving force behind penetration is the naturally occurring transcutaneous gradient, or in other words, the mechanism behind skin penetration for these vesicles is xerophobia (tendency to avoid dry surroundings) (Cevc & Gebauer, 2003) These are concentration insensitive vesicles, to maintain its hydration integrity these are bound to move inside the skin by passing through the narrow pore of the skin by squeezing themselves. After passing through the pores, they can regain their original structure without loss of vesicle content (Fig 2.4).

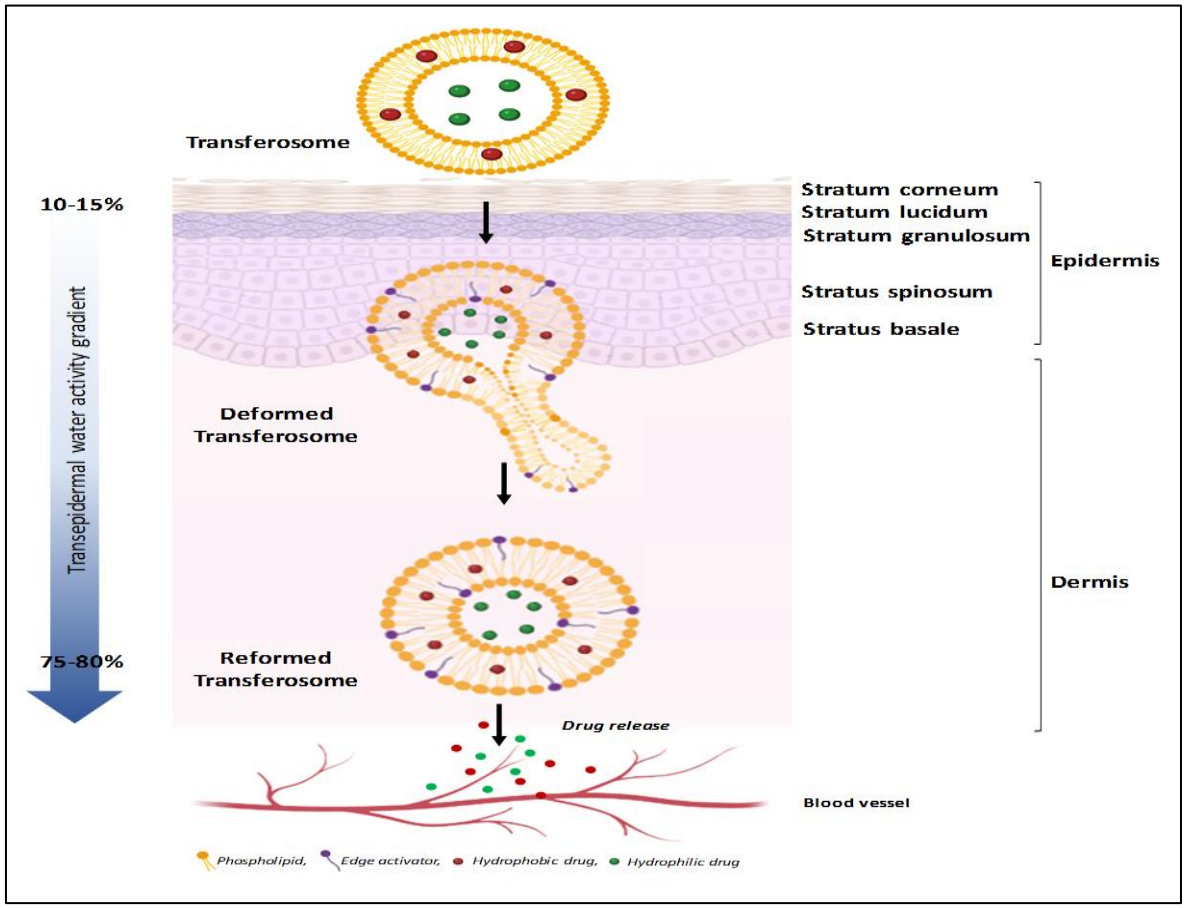

Fig 2. 4 Mechanism of penetration of flexi-liposomes

The penetration of vesicles is proportional to the pore density and inversely proportional to the elasticity of the membrane (Romero & Morilla, 2013)

2.10.4 Formulation variables

2.10.4.1 Concentration of surfactant

Studies conducted by (Gupta, Aggarwal, Singla, & Arora, 2012) revealed that the entrapment efficiency of the drug depends upon the surfactant concentration in the bilayer. The initial increase in surfactant concentration causes increase in entrapment efficiency but after the threshold, a further increase in surfactant concentration resulted in a decrease in the same. The reason predicted that at a certain concentration, surfactant gets incorporated in the Phospholipid bilayer resulting in better drug partitioning. At 20% surfactant concentration micelle formation of surfactant may start resulting in pore formation which completely converts the vesicle to mixed micelles. Mixed micelles have poor drug-carrying capacity and skin penetration.

2.10.4.2 Drug concentration

(Gupta et al., 2012) observed drug loading of vesicles also increases to a certain point till there is a higher amount of Phospholipid present in the bilayer. In their experiment, they increased the drug amount from 0.5% - 1.8% w/w, and vesicles were observed for maximum drug entrapment and crystal formation. It was observed at 1.6% concentration entrapment efficiency was the highest. Above this value, less entrapment and crystal formation was observed.

2.10.4.3 Cholesterol

Vesicles containing cholesterol in them are smaller in size than non-cholesterol vesicles as observed by. The reason proposed is that cholesterol may cause the bilayer to be more compact.

2.10.4.4 Effect of different surfactants

Various studies conducted on different surfactants showed that there is no significant difference in using different surfactants on vesicle formation

2.10.4.5 Zeta potential

Negative zeta potential will cause effective skin penetration of vesicles. Phospholipids have an isoelectric point at 6-7. At pH 7.4 they are bound to be more anionic. Surfactants and drug ions further contribute to skin penetration likewise. Hence negatively charged particles have better skin penetration.

2.10.4.6 Entrapment efficiency

(Mohammed, Weston, Coombes, Fitzgerald, & Perrie, 2004)and (Bernsdorff, Wolf, Winter, & Gratton, 1997) described the role of cholesterol and length of surfactant on entrapment efficiency. Cholesterol whether present or not doesn't affect entrapment efficiency. Lower the carbon chain length of the surfactant higher will be the entrapment of the drug.

2.10.4.7 Vesicle size

(Maheshwari et al., 2012) described that with an increase in the concentration of surfactant lowering of vesicle size occur up to 15 parts of surfactant concentration.

2.11 Evaluation models

2.11.1 In-situ model for photodynamic activity

Human dentine slabs were inserted intra-orally in 20 volunteers for 14 days. Daily 10 times exposure with 40% sucrose solution was given and CFU were observed (Lima et al., 2009)

2.11.2 Disc diffusion method

The prepared dental implants were cut and dipped into Phosphate buffer saline. 1 ml is withdrawn each time to check the content of the drug released over time. To check the antimicrobial study, implants of one suitable size were cut and incubated on the chocolate agar medium having SM colonies on them (Mastiholimath et al., 2006)

2.11.3 Biofilm model

Renzo and workers developed a model to study. In this model, the demineralization and remineralization of dental enamel was observed on bovine incisor teeth. These were treated with 2% formol solution for at least 30 days and a dental slab of teeth on an acrylic base was prepared. The enamel surface was polished and treated. 3 indentations spacing 100 µm were made on the enamel surface.

A culture medium having suitable medium was placed and incubated with SM containing 1% glucose, and 10% CO_2 at 37˚C. The media was replenished periodically to meet the demand for growing microbes. After the collection of biofilm,, the treatment can be done to evaluate the result of the anti-plaque activity (Ccahuana-Vásquez & Cury, 2010a)

2.11.4 Remineralizing pH cycling model

Dose-Response Test: The produced bovine incisor blocks were subjected to 8 full cycles of recurrent demineralization and remineralization in this model. There are 4 sets of 13 blocks

each made up of 52 blocks total. This tooth administers a negative control to one group and maintains it in distilled demineralized water (DDW). For the remaining three patients, three separate anti-caries treatments are administered by dilutions with content including 70, 140, and 280 g F/ml, respectively. For each cycle, the teeth were first washed with DDW, and kept in a demineralizing solution for 4 hrs. Finally, the teeth were removed and held in a remineralizing solution for 20 hrs. After four days, the solutions are changed and the cycle is repeated for eight days. The blocks remained in the remineralizing solution after the eighth cycle for an extra 24 hrs until the analyses. (Queiroz, Hara, Paes Leme, & Cury, 2008)

2.11.5 Caries lesion formation model

A preliminary investigation was done to create caries-like lesions on blocks of bovine enamel. From 8 to 64 hrs, 40 blocks were submerged in a demineralizing solution, and the amount of mineral loss was calculated. As soon as the surface microhardness of enamel blocks after 32 hrs is measured, caries-like underlying lesions are already present. Caries-like lesions are employed for additional analysis as part of a 32 hrs demineralization model that is applied to a subset of blocks.

Model Validation - Dose-Response Test. Test to Determine Dose-Response from a Model. The placement of 65 enamel blocks into 5 groups (n=13) was done at random. The aforementioned procedure (pH-cycling demineralizing model) was applied to four groups, with the fifth serving as a control. The blocks were kept in the demineralizing solution for 2 hrs and the remineralizing solution for 22 hrs both at 37 ℃. Blocks were then rinsed with DDW and subjected for 1 min to treatment. while being agitated three times a day at 9:00, 14:00, and 17:00 hr. The blocks were once again rinsed after the procedures. The de- and remineralizing solutions were swapped out for new ones on the fourth day. The evaluation of the enamel remineralization came after a further 4-day cycle. (Queiroz et al., 2008)

2.12 Clinical trials from 2010 to 2020

2.12.1 Resin infiltration technique with fluoride varnish

From 2013 to 2017, 6 to 12-year-old children under randomized control design were given treatment for 6 months to check the efficacy of resin infiltration technique over fluoride varnish (Giray et al., 2018).

2.12.2 Ozone in dental caries treatment

In a study from 2007 to 2009, The positive clinical effect of ozone by the remineralization of caries has been shown in vitro and in vivo. 394 subjects were selected for randomized controlled double treatment given for one year. Among 394 after-ozone treatment no progression was found to be in 278. And results say that ozone found promising results in clinical trials for dental caries treatment (Almaz & Sönmez, 2015).

3 Rationale

Currently, various therapeutic approaches are available in the market as preventive or reparative therapy for dental caries. Among them, the majority of agents belong to the antibacterial class like fluorides and antibiotics. These are formulated to be applied either topically in the form of toothpaste or given orally as systemic therapy. The prime mode of action involves a bacteriocidal or bacteriostatic effect on the pathogenic microorganism i.e. *Streptococcus mutans*.

Dental caries progresses as a result of biofilm accumulation on the teeth' surface. As the disease progresses, the co-play of exo-polysaccharides, glucosyltransferases, and Pathogenic microbe *streptococcus mutans* helps in the development of virulent bio-films. The biofilms are heterogeneous and available therapeutic interventions hold major drawbacks as they produce a state of dysbiosis by killing the causative pathogenic microbe along with non-pathogenic microbes. The lack of targetability offers unwanted drug exposure to all types of microbes, thus increasing the chances of drug resistance by oral microbiomes and rendering therapeutic failure in disease management.

The literature survey reflects the insufficiency of marketed formulations to achieve effective results in the treatment of dental caries. In India, Northern India shows 75% of the population is affected by the disease with southern, eastern, and western being at 48%, 59%, and 55% respectively(Janakiram et al., 2018). Around 10% of antibiotics used by dentists have a problem of developing drug resistance by a cariogenic microbe through mutation of antibiotic resistance gene (Bessa, Botelho, Machado, Alves, & Mendes, 2022).

As an alternative to this, a novel therapeutic combination of PIC and L-Arg is proposed and incorporated in flexi-liposomes to improve the targetability and reduce the incidence of drug resistance. PIC is an anti-biofilm agent obtained naturally from *Euphorbia lagascae.* It is known to disrupt the binding of insoluble glucans with microbes, hence preventing biofilm formation. L-Arg is a natural substrate for non-cariogenic microbes present in the oral cavity. It is reported to promote the growth of protective microbes orally and has been reported as carioprotective in nature

A combination of PIC and L-Arg promote the growth of beneficial microorganism in the oral cavity, which themselves offers competition to pathogenic microbes *S. mutans.* This offers an organic approach to maintaining a state of symbiosis in the oral microbiome, thus eliminating the chances of drug resistance (Fig 3. 1).

Loading of this combination in flexi-liposomes helps in carrying the drug across the diffusion limiting matrix, which is formed due to *S. mutans* biofilm. These vesicles have deformable character and thus can penetrate through a pore smaller than its diameter. These vesicles will penetrate the pores of biofilm and reach the vicinity of the tooth pellicle where the drug release causes biofilm disruption and L-Arg will promote the growth of carioprotective microbe and thus in combination can play a significant role in dental caries treatment.

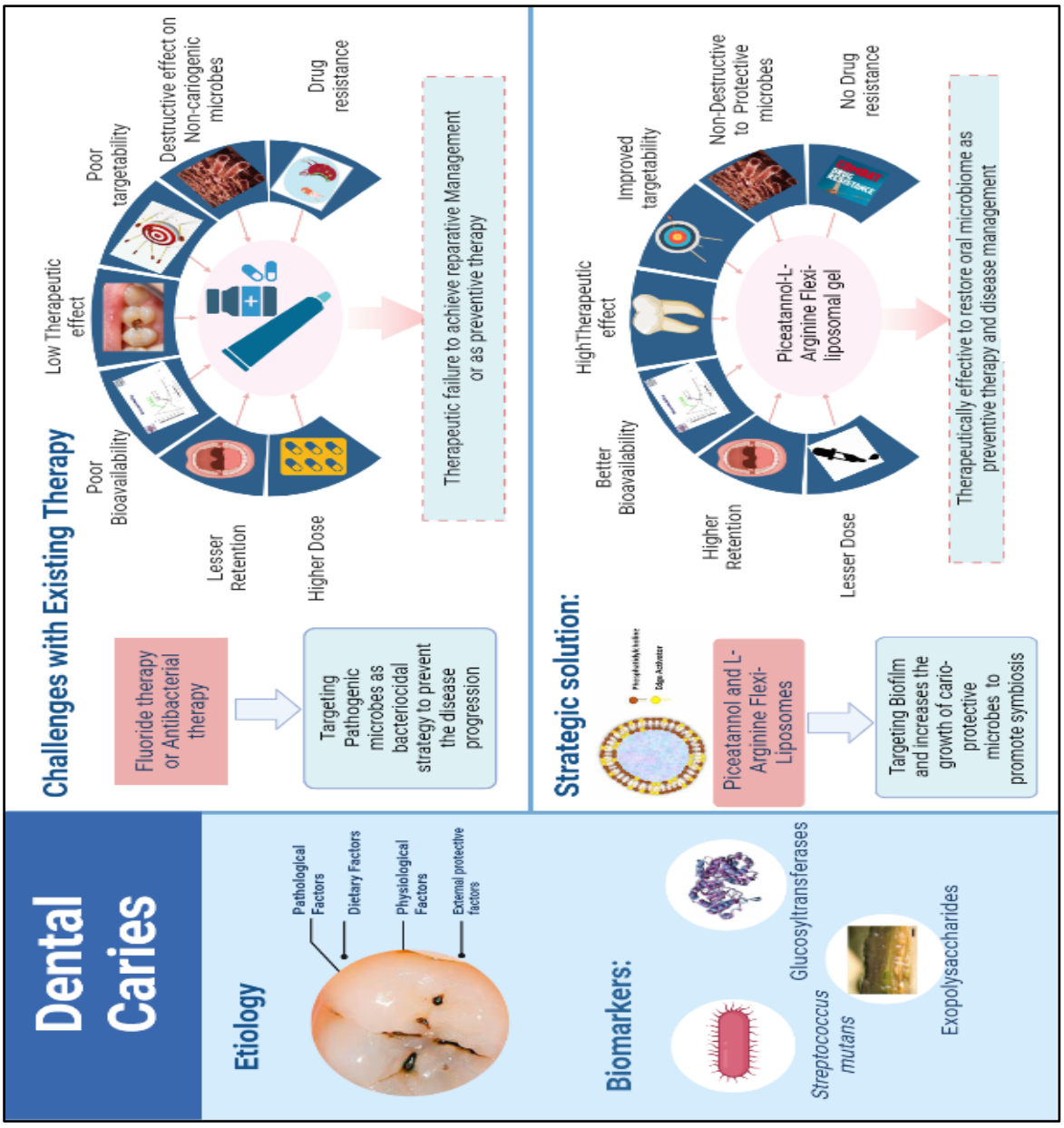

Fig 3. 1 Challenge of existing therapies vs solutions offered by optimized formulation

4 Aim and Objectives

4.1 Aim

Development and evaluation of Piceatannol-L-Arginine flexi-liposomes against microbial biofilms for the treatment of dental caries.

4.2 Objectives

- Preformulation studies on piceatannol, arginine and excipients
- Formulation and optimization of piceatannol arginine nano-elastic vesicles.
- Characterization of piceatannol arginine nano-elastic vesicles.
- Evaluation of the optimized formulation on salivary biofilms of human volunteers.

5 Experimental Work

5.1 Procurement of the drug

PIC was procured from TCI Chemicals (India) Pvt. Ltd. and L-Arg was procured from Avarice Industries (India).

5.2 Evaluation of general physical properties

A basic physical evaluation of the procured drugs was done for colour, texture, odour, state, and melting point.

5.2.1 Evaluation of organoleptic properties

PIC and L-Arg were evaluated on physical parameters e.g., colour, odour, lustre, and clarity.

5.2.2 Melting point determination

The purity of a solid can be identified by melting point determination. The melting point was analyzed by the melting point apparatus. PIC was crushed lightly to get more fine powder to fill the powder into the capillary with ease to determine the melting point. The capillary was then checked for any entrapped air. The apparatus was then turned on and was checked for an increase in temperature gradually and a range for melting point was observed. The same experiment was performed for L-Arg and the melting point temperature range was checked.

5.3 Evaluation of PIC and L-Arg using chemical test

5.3.1 Chemical test for PIC

PIC belongs to the chemical class of polyphenols so to identify the compound, tests for phenolic compounds were applied to check the chemical nature of the drug.

5.3.1.1 Ferric chloride test

The drug was added to the test tube to which 3-4 drops of ferric chloride solution is added and colour change was noted.

5.3.1.2 Lead acetate test

To a pinch of the drug, a few drops of 10 % w/v solution of lead acetate were added and the formation of precipitates was observed.

5.3.2 Chemical test for L-Arg

5.3.2.1 Biuret test

To the compound, a few drops of copper sulfate solution was added. To this, a few drops of ethanol and potassium hydroxide were added and color change was noted.

5.3.2.2 Ninhydrin test

To the drug in the test tube drops of ninhydrin reagent were added and warmed a little and observed for any change.

5.4 Fourier transform infrared spectral (FTIR) analysis of PIC and L-Arg

Qualitative analysis of PIC and L-Arg was conducted using FTIR. This was performed to check the molecular composition and structure of the chemical compounds when the spectrum is compared against a database of reference spectra. It is the graph between IR light % transmittance on the vertical axis and wavenumber on the horizontal axis. FTIR analysis was done using the Central Instrumentation Facility at LPU using Spectrum IR Software, model Spectrum TWO liTa, made in Liantrisant, UK.

5.4.1 FTIR for PIC

PerkinElmer FT-IR spectrometer was used for the spectra. The 1 mg of Sample was introduced in the analyzer. The FT-IR spectra were collected with 4 scan testing and ranging in 4000–450 cm^{-1} using the software Spectrum IR (Perkin Elmer Corporation, Lambda).

5.4.2 FTIR for L-Arg

PerkinElmer FT-IR spectrometer was used for the spectra. The 1 mg of Sample was introduced in the analyzer. The FT-IR spectra were collected with 4 scan testing and ranging from 4000–450 cm^{-1} using the software Spectrum IR (Perkin Elmer Corporation, Lambda).

5.5 Identification of drugs by UV-Visible spectroscopy

5.5.1 UV-Visible spectra of PIC

The stock solution of weighed amount of the procured drug was prepared in methanol to make 1000 µg/ml solution. Further dilutions were made with methanol to make 5 µg/ml of solution and scanned from 800 nm to 200 nm in a UV-Visible spectrophotometer to identify the drug.

5.5.1.1 Establishment of calibration plot of PIC

To conduct the *in vitro* analysis of the drug during dissolution studies, standard plots (in triplicate) for PIC were constructed in methanol.

5.5.1.2 Preparation of stock solution

The stock solution of weighed amount of the procured drug was prepared in methanol to make 1000 µg/ml solution.

5.5.1.3 Preparation of serial dilutions

Serial dilutions from the stock solution were then prepared in concentrations ranging from 1 µg/ml to 5 µg/ml in methanol. Absorbance was then taken at 326 nm using a UV-Visible spectrophotometer.

5.5.2 UV-Visible spectra of L-Arg

The stock solution of weighed amount of L-Arg was prepared in distilled water to make 1000 µg/ml solution. Further dilutions were made with distilled water to make 40 µg/ml of solution and scanned from 800 nm to 200 nm in a UV-Visible spectrophotometer to identify L-Arg.

5.5.2.1 Establishment of calibration plot of L-Arg

To conduct the *in-vitro* analysis of the drug during dissolution studies, standard plots (in triplicate) for L-Arg were constructed in distilled water.

5.5.2.2 Preparation of stock solution

The stock solution of weighed amount of L-Arg was prepared in distilled water to make 1000 µg/ml solution.

5.5.2.3 Preparation of serial dilutions

Serial solutions from the stock solution were then prepared in concentrations ranging from 80 µg/ml to 160 µg/ml in distilled water. Absorbance was then taken at 272 nm using a UV-Visible spectrophotometer.

5.6 HPLC For qualitative analysis of PIC and L-Arg

5.6.1 HPLC for qualitative analysis of PIC

5.6.1.1 Material and Methods

Analysis was performed on a high-performance liquid chromatographic system (Prominence, Shimadzu, Japan) having Shimadzu-RP C18 (250* 4.6 mm) column and LC 20 AD liquid pumps. 1-100 sample injection loop (SIL-20AC HT) equipped with PDA

detector (SPD-M20A). The temperature was maintained using a column oven CTO-10AS VP. Data integration was made with Lab solution version 6.87 SP1 software.

5.6.1.2 Sample preparation

2.5 mg of the PIC was dissolved in 10 ml of methanol. This concentration of the sample (0.25 mg/ml) is then used by the injector to inject the sample into the column.

5.6.1.3 Mobile phase preparation

The mobile phase for isocratic flow was prepared by using methanol: water in a 90:10 ratio. The mobile phase was kept at ambient temperature before starting the analysis. 45 minutes were given for the column to equilibrate and conditioned with the mobile phase before the start of the analysis. Manual purging was done to avoid any damage to the column due to pressure.

5.6.1.4 Procedure

The mobile phase was degassed and mixed in a ratio of 9:1 (Methanol: Water) and the column was preconditioned. The temperature of the system was kept at 30˚C with flow rate at 1ml/min. The sample was injected into 20 µl in the column. The total run time was kept for 25 min. The pressure inside the column was kept at 5400 psi and detection was performed at 324 nm and a chromatogram was recorded.

5.6.2 HPLC for qualitative analysis of L-Arg

5.6.2.1 Material and Methods

HPLC was performed on the Shimadzu apparatus equipped with a UV-Vis PDA detector at reverse phase column C-18.

5.6.2.2 Sample preparation

2.4 mg of the L-Arg was dissolved in 10 ml of methanol. This concentration of the sample (0.24 mg/ml) is then used by the injector to inject the sample into the column.

5.6.2.3 Mobile phase preparation

The mobile phase was prepared for isocratic flow by using 0.05 M potassium dihydrogen phosphate buffer of pH 2.6 and methanol in a 50:50 ratio. The mobile phase was kept at 45˚C before starting the analysis. 45 minutes were given for the column to equilibrate and conditioned with the mobile phase before the start of the analysis. Manual purging was done to avoid any damage to the column due to pressure.

5.6.2.4 Procedure

The mobile phase was degassed and mixed with the mobile phase and the column was preconditioned. The temperature of the system was kept at 45˚C with flow rate at 1 ml/min. The sample was injected in 50 µl in the column. The total run time was kept for 30 mins. The pressure inside the column was kept at 5400 psi at 215 nm and a chromatogram was recorded.

5.7 Drug-excipient compatibility studies

5.7.1 Physical compatibility

Physical compatibility of the selected excipients was performed with the drug of choice by mixing the excipients with PIC and L-Arg in a 1:1 ratio. and keeping it at room temperature (25˚C±2˚C)(Gorain et al., 2018). The mixture was identified for any physical change like caking, liquefaction, discoloration, or odor change for 21 days. The sample mixtures as described in the table 6.13 were prepared in triplicates and kept in petri dishes. One set of each sample mixture was kept in the room by covering the petri dish with aluminum foil having holes on it, simulating the open room conditions. The other set of the sample containing the same mixture was kept in the room by covering it with another petri dish, simulating the closed condition (Patel, Ahir, Patel, Manani, & Patel, 2015). All sample mixtures were identified for any physical change like caking, liquefaction, discoloration, or odor change for 21 days. Observations were taken on 0^{th} day, 2^{nd} day,4^{th} day, 7^{th} day, 15^{th} day, and 21^{st} day (Aminu et al., 2021).

5.7.2 Chemical compatibility

The chemical compatibility of a mixture is an indication of no chemical interaction taking place between various chemical entities. It can also be referred to as no new chemical compound being formed when the mixture of various chemical entities under study is mixed. FTIR and Differential scan calorimetry (DSC) methods were adopted to check any alteration in the functional group or formation or elimination of any peak in the DSC thermogram. The various combinations of drugs and excipients were made as described in the table 6.13. The FTIR analysis of drug PIC was done alone for the first 7 days alternatively to confirm any change in FTIR spectra. Chemical compatibility of the selected excipients was performed with the drug of choice by mixing the excipients with PIC and L-Arg in a 1:1 ratio. and keeping it at room temperature (25˚C±2˚C). The mixture was identified for any chemical change for 21 days. The sample mixtures were prepared in

triplicates as described in the table and kept in petri dishes. One set of each sample mixture was kept in the room by covering the petri dish with aluminum foil having holes on it, simulating the open room conditions. The other set of the samples containing the same mixture was kept in the room by covering it with another petri dish, simulating the closed condition (Patel et al., 2015). All sample mixtures were identified for any chemical change for 21 days. Observations were taken on the 0^{th} day, 2^{nd} day,4^{th} day, 7^{th} day, 15^{th} day, and 21^{st} day.

5.8 Method development and validation of an HPLC method for simultaneous estimation of PIC and L-Arg

5.8.1 Method development

Method development includes various parametric changes in the method to acquire system suitability and resolution of the peaks. Test trials using sample preparations with various solvents along with the use of mobile phases of different polarity were conducted. Various hits and trials led to the successful selection of method parameters which leads to the separation of two components. Analysis was performed on a high-performance liquid chromatographic system (Prominence, Shimadzu, Japan) having Shimadzu-RP C18 (250* 4.6 mm) column and LC 20 AD liquid pumps. 1-100 sample injection loop (SIL-20AC HT) equipped with PDA detector (SPD-M20A). The temperature was maintained using a column oven CTO-10AS VP. Data integration was made with lab solution version 6.87 SP1 software.

While selecting mobile phase different compositions such as methanol-water in various proportions, 0.05 M potassium dihydrogen phosphate buffer of pH 2.6 and methanol in 50:50 ratio and 0.1% orthophosphoric acid (in water): acetonitrile. pH and flow rate were used. Finally, 0.1% orthophosphoric acid (in water): acetonitrile (70:30) was used as a mobile phase based on observations. The wavelength for detection was chosen as 215 nm at a flow rate of 1 ml/min.

5.8.1.1 Experimental conditions

The separation was carried out on an RP-HPLC system with a PDA detector using RP C-18 Column. The mobile phase was kept in a 70:30 ratio of 0.1% orthophosphoric acid (in water) and acetonitrile respectively. The sample mixture was prepared in a 100:1 proportion of L-Arg and PIC in the mobile phase. The temperature is kept at 30˚C with a flow rate of 1ml/min and an injection volume of 10 microliters. The run time was kept for 12 mins and

separation was observed at RT 1.9 min and 7.6 min for L-Arg and PIC respectively. Detection of effluents was observed at 215 nm.

5.8.1.2 Procedure

The glassware was properly washed and rinsed with Milli-Q water to remove any contamination. The preparation of the mobile phase was carried out by dissolving 0.1 ml of orthophosphoric acid in Milli-Q water forming (0.1 % v/v). On the other side, acetonitrile was taken into the glass bottle and both the bottles were ultrasonicated for 10 min to degas any air bubbles. Both the bottles were fixed to the HPLC system and the system was set at 70:30 isocratic flow of mobile phase and purging was done before the start of the system. Meanwhile, L-Arg: PIC were weighed in the ratio of 100:1 and dissolved in the mobile phase making concentrations from 100 µg/ml to 600 µg/ml for L-Arg and 1 µg/ml to 6 µg/ml for PIC. The system parameters were set as described in section 4.8.1.1 and the validation was carried out.

5.8.1.3 Preparation of stock solution

The stock solution of PIC and L-Arg containing 10 µg/ml and 1000 µg/ml was prepared in mobile phase containing 0.1% orthophosphoric acid (in water): acetonitrile in 70:30 v/v ratio respectively. Further dilutions were made to produce the required concentrations.

5.8.1.4 Preparation of sample solution

Dilutions from the above stock solution were made to produce concentrations from 100 µg/ml to 600 µg/ml for L-Arg and 1 µg/ml to 6 µg/ml for PIC.

5.8.1.5 Development of calibration curve

To generate the calibration curve for PIC and L-Arg, withdrawing 1ml, 2ml, 3ml, 4ml, 5ml and 6ml aliquots from the stock solution and diluting them to 10 ml with the mobile phase produced concentrations of 100 µg/ml to 600 µg/ml for L-Arg and 1 µg/ml to 6 µg/ml for PIC, respectively. The sample's linearity was assessed at these concentrations. A small portion of the prepared sample 10 µl was added to the RP-HPLC. The elution operation was carried out as per section 4.8.1.2, and calibration was achieved by plotting the concentration against the matching peak area. Three repeats of this experiment were conducted, and the averaged data was collected.

5.8.2 Method validation

The created technique was approved in accordance with ICH Q2 (R1). Utilizing metrics for system appropriateness, the performance was assessed. Sample solutions were injected

through RP-HPLC six times in duplicate. Additionally, the peak purity index, peak resolution, and number of theoretical plates were measured.

5.8.2.1 Linearity and range

The calibration curve was developed using mean peak area of six concentrations taken in triplicate versus corresponding PIC and L-Arg concentrations. The regression of the equation was recorded.

5.8.2.2 Accuracy

It was created using an estimate of the total amount of pharmaceuticals recovered from the mobile phase. Different method concentrations (100:1 µg/ml) were prepared at the three levels. To achieve these concentrations, the stock solution was serially diluted to create the concentrations of 80:0.8 µg/ml, 100:1 µg/ml, and 120:1.2 µg/ml. Thus, the actual drug recovery was divided by the theoretical concentration, multiplied by 100, and the result was the percent absolute recovery. The data was recorded, and the study was conducted in three copies.

5.8.2.3 Precision

It makes the procedure repeatable and reproducible. Three samples of different concentrations were injected on the same day under identical test settings. The LQC, MQC, and HQC values were calculated on various days and by various analysts in order to assess the intermediate precision. The mean data was noted, and the relative standard deviation percentage was computed.

5.8.2.4 Robustness

This study was carried out by varying the flow rate at 0.8, 1.0, and 1.2 ml/min and different wavelengths 210 nm, 215 nm, and 220 nm (LoBrutto & Kazakevich, 2006) (European Medicines Agency ICH, 2005). Three replicates of sample concentration (300:3 µg/ml of L-Arg: PIC) and standard concentrations (300:3 µg/ml of L-Arg: PIC) and their effect on the peak area, recovery, and retention time were observed. The mean and relative standard deviation was calculated.

5.8.2.5 Solution stability studies

Solution stability is regarded as a parameter to assure the stability of the sample compound in the medium in which it is dissolved. It indicates the possibility of any degradation product or any other thing that decreases the effective concentration of the sample in the solution. Solution stability studies indicate the stability of the sample for 24 hrs. To test the

solution stability, one sample of known concentration having a mixture of two drugs was prepared and kept in an injection sampler at 4°C for 24 hrs. During this time at regular intervals, sample injection was applied to make a chromatogram at 2, 4, 6, 8, 12, 18, and 24 hrs. The % RSD and % recovery of the sample were calculated.

5.8.2.6 Estimation of LOD, LOQ, and system suitability

LOD and LOQ were determined using the following equations. The standard deviation (σ) of the Y-intercept of the regression line and slope was used (S) (Eqn 4. 1, 4. 2).

$$LOD = 3.3\ \sigma/S \quad \text{……. Eqn 5. 1}$$

$$LOQ = 10\ \sigma/S \quad \text{……..Eqn 5. 2}$$

5.9 Development of flexi-liposomes

5.9.1 Method of flexi-liposomes preparation

Vesicle formation was done by the established thin-film hydration method (Duong et al., 2021). In this method, soy lecithin and edge activator were accurately weighed (Nayak & Tippavajhala, 2021) (Sultana & Sailaja, 2015) (Aboud, Ali, El-Menshawe, & Elbary, 2016) (Garg et al., 2016) (Al-Mahallawi, Khowessah, & Shoukri, 2014) (El Zaafarany, Awad, Holayel, & Mortada, 2010) (Fernández-García et al., 2020) and transferred to 100 ml dried beaker. To the beaker added freshly distilled chloroform and methanol in an 80:20 ratio (30 ml) (Shaji & Lal, 2014) (Venkatesh et al., 2014) (Pahwa, Pal, Saroha, Waliyan, & Kumar, 2021). To the same beaker, 1 mg of PIC was added. The beaker was placed on a magnetic stirrer at 600 rpm for 15 mins with the magnetic bead in it. The clear solution of the above mixture thus formed was transferred to a clear R.B.F. This R.B.F was then attached to the rotatory vacuum evaporator (Bozzuto & Molinari, 2015) (Sultana & Sailaja, 2015). The vacuum evaporator was kept at 60°C (Ravalika & Sailaja, 2017) (G. P. Kumar & Rajeshwarrao, 2011) (Garg et al., 2016) at 100 rpm. Water circulation was turned on to allow condensation of the solvent to occur. Serial evaporation of solvent allows a thin layer to form. The R.B.F was allowed to rotate for 10 more mins to allow complete drying of the thin layer. After evaporation, the R.B.F was removed and covered with aluminum foil with pin holes in it and kept overnight in vaccum oven at 55˚C. After 24 hrs the R.B.F. was hydrated with 24 ml of hydration media containing 100 mg of L-Arg (Šturm & Ulrih, 2021) (Miranda et al., 2020) (Yang et al., 2016) (Kolderman et al., 2015) for one hour at 65˚C. Which is above the Tm of soy lecithin (60˚C). The hydrated vesicles were then transferred

to a beaker and then kept at room temperature for 2 hrs. After this, ultrasonication of vesicles were done to allow size reduction and size uniformity.

5.9.1.1 Preparation of hydration media

This was made by dissolving 28.80 gm of disodium hydrogen phosphate and 11.45 gm of potassium dihydrogen phosphate in enough water to make 1000 ml of a phosphate buffer with a pH of 6.8. 100 mg of L-Arg were mixed with 24 ml of the phosphate buffer previously described.

5.9.2 Screening of factors influencing flexi-liposomes

5.9.2.1 Selection of Edge activator

Screening of variables starts with the selection of a suitable EA. EAs has a strong effect on vesicle size, deformability of the vesicles, and entrapment efficiency of formed vesicles (Zeb et al., 2016). There are number of EAs that are used in the formulation of Flexi-liposomes e.g., of ionic surfactants like sodium deoxycholate and sodium cholate. These ionic surfactants offer a high degree of flexibility to the prepared vesicles as they impart a high degree of curvature. Also, they can produce vesicles of lower size ranges (Fernández-García et al., 2020). Another category of surfactants includes non-ionic surfactants for instance spans and tweens. These two are most extensively researched for imparting good flexibility to the vesicles. Span 20, Span, 40, Span 60, Tween 20, and Tween 80 are top on the list to be used as EAs (Akram et al., 2022). As a selection criterion, one EA from each surfactant category was selected i.e., Span 60 (sorbitan monostearate) and Sodium deoxycholate (ionic surfactants) were selected. Spans are chosen over tweens as a literature survey revealed spans show less hemolytic activity and hence are less toxic, less irritating, and have good gel transition temperature than tweens (Fernández-García et al., 2020). Apart from these properties, Tween are comparatively more hydrophilic than corresponding spans, and owing to their hydrophilicity (larger hydrophilic head), they usually need the addition of cholesterol in the preparation to reach to the suitable value of critical packing parameter (CPP) i.e. 0.5 to 1 to form vesicles (Junyaprasert, Singhsa, Suksiriworapong, & Chantasart, 2012) (Chacko, Ghate, Dsouza, & Lewis, 2020). When the attributes of various span 60 are compared with other spans it was found that span 60 has a good balance of saturated and unsaturated fatty acids in their composition, with suitable alkyl chain length to impart good radius of curvature to vesicles to become deformable. Among other non-ionic surfactants span 60 showed better deformability, entrapment efficiency, and stability of the formed vesicles than other spans and tweens. For

this reason, span 60 of HLB 4.7 was selected to screen against sodium deoxycholate HLB 16.

Span 60 (HLB 4.3) and sodium deoxycholate (HLB 16) were selected for screening. In the selection of these two for screening, entrapment efficiency was selected as a prime attribute for PIC and L-Arg. Four different combinations, as reviewed from the literature were made and checked for entrapment efficiency.

An essential stage in the rational preparation of vesicles is the selection of the most crucial factors (screening). As dependent variables, or Critical Quality Attributes, in this study, the vesicular size, polydispersity index (PDI), zeta potential, and entrapment efficiency (E.E.) were used. These are the most important since they directly affect the majority of Flexi-liposomes' final uses. DoE has been widely used in recent years for the analysis and improvement of vesicles and other vesicular carriers. Different designs can be used to cut down on the variables involved in preparation methods and, as a result, to reduce the number of tests while preserving important data.

Flexi-liposome characteristics (vesicle size, PDI, zeta potential, and E.E.) depend on their composition (Drug: lipid ratio, phospholipid concentration, and phospholipid: surfactant ratio), as well as on process variables used in their preparations, like temperature and rotary evaporator speed. Using the conventional method, the parameters were initially screened by changing one variable while keeping the others constant. The investigations showed that the amount of phospholipids and surfactants for optimization study utilizing response surface method (RSM), and more specifically a central composite design (CCD), plays an important role in the production of optimum formulations among various independent variables.

5.10 QbD-based formulation optimization studies

The impact of the amount of soy lecithin and the chosen EA on the characteristics of flexi-liposomes was investigated using CCD. The range for the aforementioned parameters was determined from the literature, and the soy lecithin and EA lower and upper ranges were chosen. Four axial points were chosen in the two-factor CCD design so that the distance, between any two axial points and the design's center is equal to 1.414. For L-Arg, the dosage was held constant at 100 mg, and for PIC, it was 1 mg (Table 5).

Table 5. 1 Experimental variables of CCD for flexi-liposomes

Variables			Design level	
Uncoded	**Coded**	**Units**	**Low**	**High**
Soy Lecithin	A	mg	75	95
SDC	B	mg	5	25

Using Design-Expert® software, version 11, the design matrix with thirteen runs and five replicates was created based on the above-coded parameters. The CCD matrix for each created formulation is shown in Table 5. 2, and each formulation's vesicle size, PDI, zeta potential, and PIC and L-Arg's efficiency as CQAs were also assessed.

Table 5. 2 Summary of all the flexi-liposomal formulations as per CCD

Run	Factor 1	Factor 2
	Soy Lecithin (mg)	**SDC (mg)**
1	85.00	15.00
2	85.00	15.00
3	75.00	25.00
4	95.00	5.00
5	85.00	15.00
6	95.00	25.00
7	85.00	15.00
8	85.00	15.00
9	85.00	29.14
10	75.00	5.00
11	85.00	0.86
12	99.14	15.00
13	70.86	15.00

The coefficients of polynomial equations were obtained using Design-Expert® software by applying multi-linear regression analysis (MLRA), which was then used to correlate the pre-existing CMAs and CQAs. P-value, R, and projected residual error sum of the square, among other model parameters, were examined. Additionally, 2D contour plots and 3D response surfaces were produced, and lastly, the best solution was found using numerical optimization with the goal of achieving a desire function value close to unity.

5.11 Optimized formulation and validation studies

Optimization of the formulation was done to find out the level of factors A and B, with various values for vesicle size in the range of 189.2 to 241.15 nm, zeta potential in the

range of -40 to -30 mV, PDI less than 0.5, and entrapment efficiency for L-Arg in range of 13 to 35 % and PIC in range of 18 to 70 %.

5.11.1 Vesicle size

This was analyzed from the Malvern Zeta sizer using the Differential Light Scattering technique at the Central Instrumentation Facility, LPU, Phagwara.

5.11.2 Zeta potential

Zeta potential was analyzed from Malvern Zeta sizer using the Differential Light Scattering technique at the Central Instrumentation Facility, LPU, Phagwara (Sultana & Sailaja, 2015)

5.11.3 Entrapment efficiency

The prepared formulations were evaluated for the amount of entrapped drug PIC and L-Arg in the vesicles. Sephadex-G25 mini-column gel filtration was the method used to separate the unentrapped drug from the formulation by passing through the gel column. The pure vesicles were recovered as filtrate. Vesicles then ruptured using 0.1 % Triton X and were observed under HPLC for peak areas (Garg et al., 2017).

5.11.4 Degree of deformability

To check deformability, the vesicles were run through a 100 nm polycarbonate membrane installed on an extruder to verify this. Size, elasticity, and deformability index of the vesicles were examined before and after extrusion. The vesicle size was examined. By dividing the size of the extruded vesicle by the size of the mesh that it passed through, elasticity was estimated. By dividing the vesicle size prior to and following extrusion, the deformability index was computed.

5.11.5 Drug loading calculation

The optimized formulation was calculated to check the drug loading of PIC in the optimized vesicles with equation 4. 3

$$Drug\ loading = \frac{Actual\ loading}{Theoretical\ loading} \times 100 \qquad \text{……. Eqn. 5. 3}$$

5.12 Preparation of secondary vehicle/gel

The optimized vesicles were added to the carbopol 934 gel to make them usable. 20 ml of hydrated vesicle dispersion was obtained and mixed with 10 % w/w Carbopol 934 hydrogel to create hydrophilic Carbopol gel. 3.3% of the gel's ultimate weight was made up of carbopol 934 hydrogel. To maintain the gel's neutral pH and clarity, triethanolamine was

added to it. Methylparaben and propylparaben were added as preservatives. The hydrogel's composition is presented in Table 5. 3.

Table 5. 3 Formation of optimized flexi-liposomal gel

Ingredients	Optimized flexi-liposomal gel
Optimized nano-vesicular suspension	20 ml of vesicular suspension
Carbopol 934	10 ml of 10 % w/v
Methyl paraben	0.2 % w/v
Propyl paraben	0.02 % w/v
Triethanolamine	q.s

5.12.1 Characterization of the flexi-liposomal gel

Hydrogel prepared from optimized vesicles was evaluated for flowability and homogeneity as per the following parameters (Singh et al., 2016).

5.12.1.1 Appearance

The prepared gel was visually checked for clarity, colour and grittiness. This test is crucial to evaluate the formulation's aesthetic merit. (Thakur, Jain, & Jain, 2018).

5.12.1.2 pH

A digital pH meter was used to determine the gel's pH. The suspension was prepared by dissolving 2 gm of gel in distilled water and making the volume upto 50 ml and the solution's pH was determined. (J. R. Kumar, 2018).

5.12.1.3 Viscosity

A digital brook field viscometer was used to measure the viscosity of the gel formulation that had been created. At room temperature, a suitable spindle was used to shear the samples at a rate of 100 rpm (Thakur et al., 2018).

5.13 *In-vitro* release studies of optimized flexi-liposomal gel

To carry out the release study, the dialysis bag method was adopted. This method is widely adopted for estimating the *in-vitro* release profile of liposomal formulations as it also provides good precision. The dialysis bag serves as a donor compartment wherein a known amount of drug is added and the sides of the dialysis bag were then sealed to prevent any drug leakage. In the receiver's compartment, phosphate buffer simulating *in-vivo* pH was added and maintained at 32°C. The rpm was kept at 80 and sink conditions were maintained as at the time of sample withdrawal equal aliquot of fresh phosphate was added. The

analysis of the sample was done using HPLC. The release study of optimized Flexi-liposomal gel was compared with a gel containing free drug solution as described below.

5.13.1 Preparation of gel containing a combination of L-Arg and PIC

10 % w/w and 0.1 % w/w solution of L-Arg and PIC together were prepared in 10 ml of distilled water. This drug solution was added to 5 ml of 10 % w/w Carbopol 934 gel. The resulting gel will be 3.3 % w/w approx. 5 ml of this gel was added to the donor compartment and release was checked under HPLC.

To check the release of Flexi-liposomal gel, 5 ml of the final optimized gel as mentioned earlier was taken in the dialysis bag and analyzed for release under HPLC.

5.13.2 Analysis of the release mechanism of optimized flexi-liposomal gel

Once the release study was done, the percentage cumulative drug release and various other parameters were calculated to fit into the mathematical models as mentioned below. The release mechanism is predicted from the r^2 value of the graphs which are formed as under. The closer the value of r^2 to 1 is a predictor of the release mechanism followed by the formulation (Table 5. 4) (Brahmankar et al., 2009).

5.13.2.1 Zero-order kinetics

Drug dissolution from pharmaceutical dosage form that does not follow dependency either on the concentration or any other factor follows this mechanism (Eqn 4. 4)

$$Q_t = Q_0 + K_0 t \qquad \text{.....Eqn 5. 4}$$

Q_t = Amount of drug at time t

Q_0 = Initial amount of drug in dosage form

K_0 = Zero-order release constant

A graphical representation of drug dissolved fraction vs. time will be linear. This indicates that the dosage form following this profile releases the same amount of drug per unit of time irrespective of the drug remaining in the formulation.

5.13.2.2 First-order kinetics

This model describes the rate process dependent upon one component of the reaction for instance release of the drug from the formulation is affected by the amount of drug remaining in the formulation (Eqn 4. 5).

$$\text{Log } C = \text{Log } C_0 + K_{t/2.303} \quad \text{……..Eqn 5. 5}$$

C_0 = Initial amount of drug in solution

K_0 = First order release constant

5.13.2.3 Higuchi model

Higuchi in 1963 provided the theoretical basis for defining drug release from inert matrices. Penetration of the elution media creates channels in the matrix through which diffusion takes place. The depletion zone gradually extends into the core of the matrix. A high tortuosity means an increase in effective diffusional path length (Eqn 4. 6). The porosity accounts for space availability for drug dissolution and increased porosity results in an increase in drug release.

$$Q_t = K_H\, t^{1/2} \quad \text{……..Eqn 5. 6}$$

Q_t = Amount of drug released at time t

K_H = Higuchi dissolution constant

Higuchi describes drug release as a diffusion process based on Fick's law of diffusion is time-dependent. Pharmaceutical transdermal systems and matrix tablets with water-soluble drugs follow this release model.

5.13.2.4 Korsmeyer peppas model

Korsmeyer et al., In 1983, developed a release model relating drug release exponentially to elapsed time (Eqn 4. 7).

$$F_t = at^n \quad \text{…Eqn 5. 7}$$

a = constant incorporating structural and geometrical characteristics of the drug dosage form.

n = release exponents indicative of the drug release mechanism and function of t.

Under some experimental situations, the anomalous behavior is predicted with (non-fiction) (Eqn 4. 8). In these cases, a more general equation can be used under

$$M_t/M_\infty = Kt_n \quad \text{.....Eqn 5. 8}$$

Ritger and Peppas employed this N value to describe various release processes, arriving at slab values for the Fick's diffusion of n = 0.5 and higher values of n between 0.5 and 1.0 or n = 1.0 for mass transfer based on a non-fiction model.

Table 5. 4 Interpretation of diffusion release mechanism

Release exponent (n)	Drug transport mechanism
n = 0.5	Fickian diffusion
0.5 > n >1.0	Anomalous transport
n = 1.0	Case 2 transport
n > 1.0	Super case 2 transport

5.13.2.5 Hixson-Crowell model

This model describes the systems that tend to change in surface area and diameter of the particle with time (Eqn 4. 9).

$Q_0^{1/3} - Qt^{1/3} = K_{HC}\, t$ ….Eqn 5. 9

Q_0 = Amount of drug released after 0^{th} time

Qt = Amount of drug released after time t

K_{HC} = Hixon Crowell rate constant

The plot made in cube root of drug % remaining in matrix vs. time.

5.14 Stability studies on the final formulation

The final optimized formulation was kept for stability testing for six months at accelerated conditions i.e. 25°C±2°C/60% RH ± 5% RH which are accelerated stability studies according to ICH guidelines Q1A(R2) (ICH Q1A(R2), 2003). The aged sample was sampled at 0-, 3- and 6-month frequency. The critical attributes of the drug product which can affect the quality, purity, and safety were checked. The samples were checked for vesicle size, zeta potential, entrapment efficiency, and drug release. It is then compared with the student's t-test and model-dependent analysis (F2 Value). The values were found to be significant if the p value was less than 0.05 and profiles of fresh drug products and aged drug products will be called similar if the F2 value was more than 50. The dissolution profiles were compared using a pairwise comparison method that is similarity factor (F2) as suggested by Flammer and Moore with MS Excel add-in DD solver (Zhang et al., 2010).

5.15 Cytocompatibility assay

To test the cytocompatibility, The developed formulation was diluted to make final concentration of 5.63µg/ml of PIC in distilled water and labeled as D_1 for simplicity. NIH3T3 fibroblast cells were cultured in a 25 cm^2 cell culture flask using Dulbecco's Modified Eagle's Medium (DMEM) supplemented with 10 % Fetal Bovine Serum (FBS) and 1 % Penicillin-Streptomycin antibiotic. The test was performed by studies performed by Fischer et al (Fischer, Li, Ahlemeyer, Krieglstein, & Kissel, 2003). Once the cells had reached 70% confluency, they were trypsinized using 0.25 % trypsin and 1 mM ethylenediamine tetraacetic acid (EDTA). The trypsinized cells were seeded at a density of 1×10^4 cells per well in a 96-well plate with a flat bottom, and then they were incubated for 24 hrs in a CO_2 incubator. Tricalcium phosphate (TCP) was taken as positive control.

Before the testing, the nanovesicles were sterilized using a UV light for 30 minutes. After replacing the day-old media from the 96 well plates with fresh DMEM media, 10 µL of diluted formulations were added at various concentrations, including D_1, $D_{1/2}$, $D_{1/10}$, $D_{1/100}$. For the next 24 hrs, the cytotoxic effects of the formulation were investigated. The 96-well plate's oral formulation-containing fluid was then removed, and the cells were then treated with a 0.5 mg/ml MTT solution in DMEM media without serum for the following 4 hrs to observe the production of formazan crystals. The MTT solution was withdrawn after 4 hrs of incubation, and 200 µl DMSO was then added to the well plate. To dissolve the developed formazan crystals in the cells, the plate was shaken for 30 minutes using a shaker. As a positive control, cells that had grown without the addition of the formulation were used. Using a plate reader, the absorbance of the dissolved formazan particles from the supernatant was evaluated at 570 nm (BioTek Gen5 Microplate reader). The cell viability was quantified in terms of percentage (%) by the Eqn 4. 10.

$$cell\ viability\ \% = \frac{sample\ absorbance}{Positive\ control\ absorbance} \times 100 \qquad \text{.....Eqn 5. 10}$$

5.16 Clinical investigations

To check the efficacy of the optimized formulation, clinical investigations were conducted to check the response. The human saliva model was used to conduct the study. The human saliva from healthy volunteers was pooled and observed for changes in salivary pH and biofilm formation (dental plaque) to check the effect of the formulation.

5.16.1 Sample collection procedure

5.16.1.1 Inclusion exclusion criteria (Eligibility criteria)

To determine the efficacy of the prepared optimized Flexi-liposomal gel (OFG) on healthy volunteers, investigations were conducted on unstimulated healthy human saliva. To collect the unstimulated human saliva eligibility criteria were established (Food and Drug Administration, 2020). These eligibility criteria determine who can participate in the study. This results in the enrolment of study populations that represent the broader population that can use approved products (Temple et al., 2018). As the OFG is a preventive care therapy, meant to provide a healthy microenvironment for the prevention of dental caries, healthy volunteers based on the following criteria were selected. The criteria were established to minimize heterogeneity ("noise"), which can mask a finding of the effect and generate data that are generalizable to a broader patient population. While In designing eligibility criteria, investigators, institutional and regulatory aspects were considered (National Institutes of Health, 2019).

5.16.1.1.1 Inclusion criteria

The Inclusion criteria specify the characteristics required for the selection of volunteers for saliva samples. The selection was made considering the capacity of OFG to maintain a healthy human oral microbiome.

- Participants should be able to read, complete, and sign the consent form.
- Participants should understand and answer the questionnaire.
- Volunteers should be disease-free, specifically concerning the salivary glands and oral mucosa.
- Participants should not have dry mouth or dry eye sensations.

5.16.1.1.2 Exclusion criteria

Considering the ethical and scientific considerations, exclusion criteria were established so that potential adverse impacts arising from co-morbidities and concomitant medications can be avoided. As general ethical considerations, children, adolescents, and pregnant and lactating women were not included in the clinical investigation. Therefore, a case-by-case basis inclusions/exclusions were made (Food and Drug Administration, 2020) (Bhattarai, Kim, & Chae, 2018).

- Participants who are under the age of 18.
- Participants who find the consent form difficult to read or comprehend.

• People who respond "yes" to the inquiry about dryness. These people are not eligible to take part in the study because they are thought to have xerostomia.

• Participants who express mouth or eye dryness.

• Patients who are sensitive to touch or have oral lesions.

• Oral dryness has been linked to individuals who use drugs often or acutely. Antihistamines, antipsychotics, and antidepressants are a few examples of them.

• Patients receiving radiotherapy (mostly for the treatment of head and neck cancer).

• People with chronic medical conditions are not under good control.

Some general considerations were observed to preclude the population from enrolment, Geographical location, consent issues, historical mistrust or common concerns, etc (Fig 4.1) (National Institutes of Health, 2019).

On the other hand, some strategies were developed to improve the enrolment of participants. For instance, participants were explained in detail about the study to ensure their transparency in how eligibility criteria were determined. These strategies further encouraged trial participation. Understanding the patient's psychology behind resistance to participate in the study was also minimized with the above strategy. The participant's consent was kept as a priority even when the participant choose not to participate in clinical trials. Surveys indicate that patients who say they are willing to participate in clinical research may decide not to enrol when faced with the decision to participate (Holbein, 2009). Fig 5. 1 explains the Inclusion/exclusion criteria format.

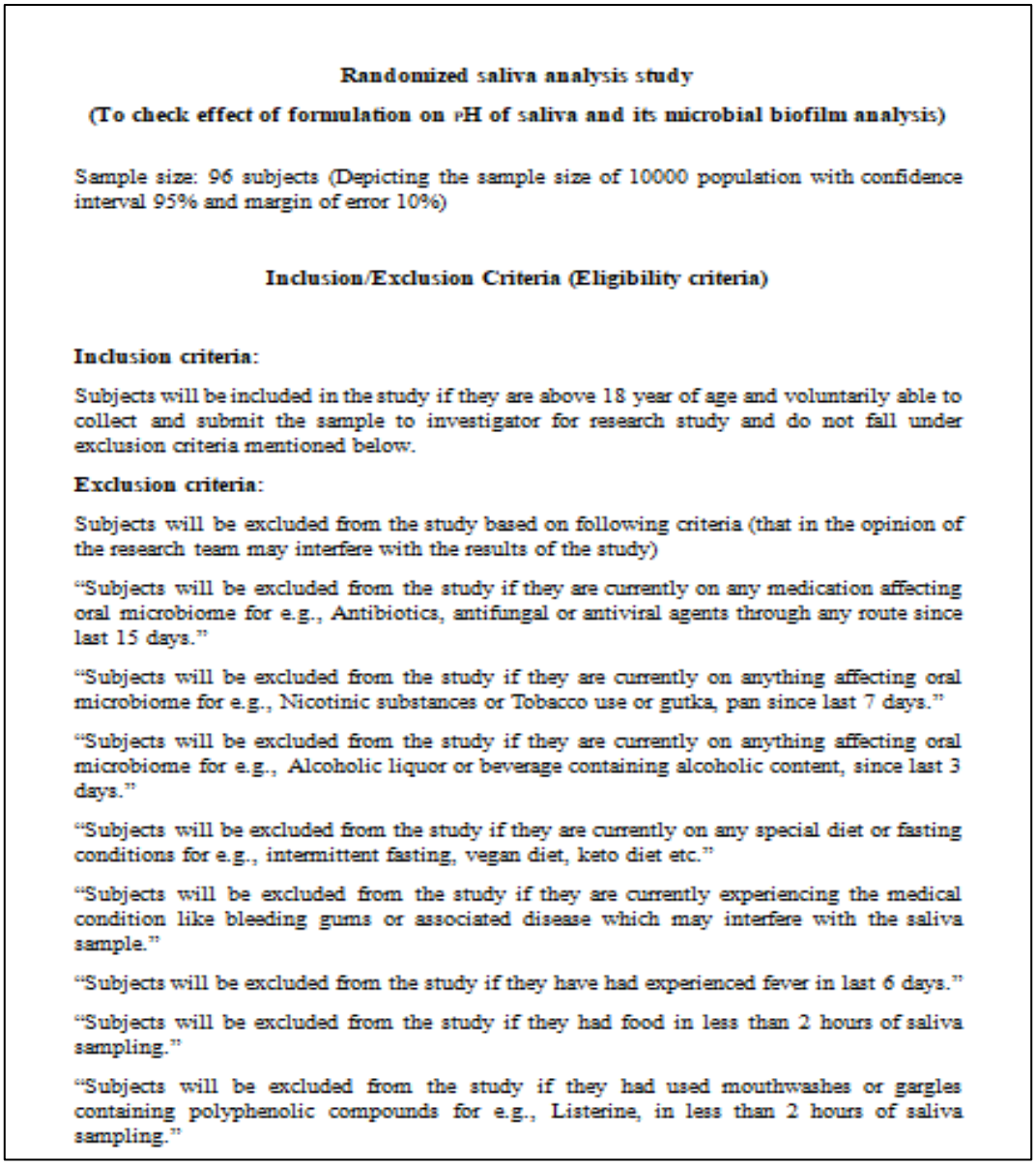

Randomized saliva analysis study

(To check effect of formulation on pH of saliva and its microbial biofilm analysis)

Sample size: 96 subjects (Depicting the sample size of 10000 population with confidence interval 95% and margin of error 10%)

Inclusion/Exclusion Criteria (Eligibility criteria)

Inclusion criteria:

Subjects will be included in the study if they are above 18 year of age and voluntarily able to collect and submit the sample to investigator for research study and do not fall under exclusion criteria mentioned below.

Exclusion criteria:

Subjects will be excluded from the study based on following criteria (that in the opinion of the research team may interfere with the results of the study)

"Subjects will be excluded from the study if they are currently on any medication affecting oral microbiome for e.g., Antibiotics, antifungal or antiviral agents through any route since last 15 days."

"Subjects will be excluded from the study if they are currently on anything affecting oral microbiome for e.g., Nicotinic substances or Tobacco use or gutka, pan since last 7 days."

"Subjects will be excluded from the study if they are currently on anything affecting oral microbiome for e.g., Alcoholic liquor or beverage containing alcoholic content, since last 3 days."

"Subjects will be excluded from the study if they are currently on any special diet or fasting conditions for e.g., intermittent fasting, vegan diet, keto diet etc."

"Subjects will be excluded from the study if they are currently experiencing the medical condition like bleeding gums or associated disease which may interfere with the saliva sample."

"Subjects will be excluded from the study if they have had experienced fever in last 6 days."

"Subjects will be excluded from the study if they had food in less than 2 hours of saliva sampling."

"Subjects will be excluded from the study if they had used mouthwashes or gargles containing polyphenolic compounds for e.g., Listerine, in less than 2 hours of saliva sampling."

Fig 5. 1 Inclusion/exclusion criteria for randomized saliva analysis

5.16.1.1.3 Questionnaire and consent form

To ensure compliance with the eligibility criteria, a suitable and coherent questionnaire was established. The questionnaire was provided to potential volunteers before filling out the consent form (Fig 5. 2, Fig 5. 3). The purpose of the questionnaire was to identify whether the volunteer will be included in the study or not. The questionnaire was also helpful to give better insight to the volunteers and thus act as a mean to provide more confidence in the volunteer participation and elimination risk of potential risks or health hazards.

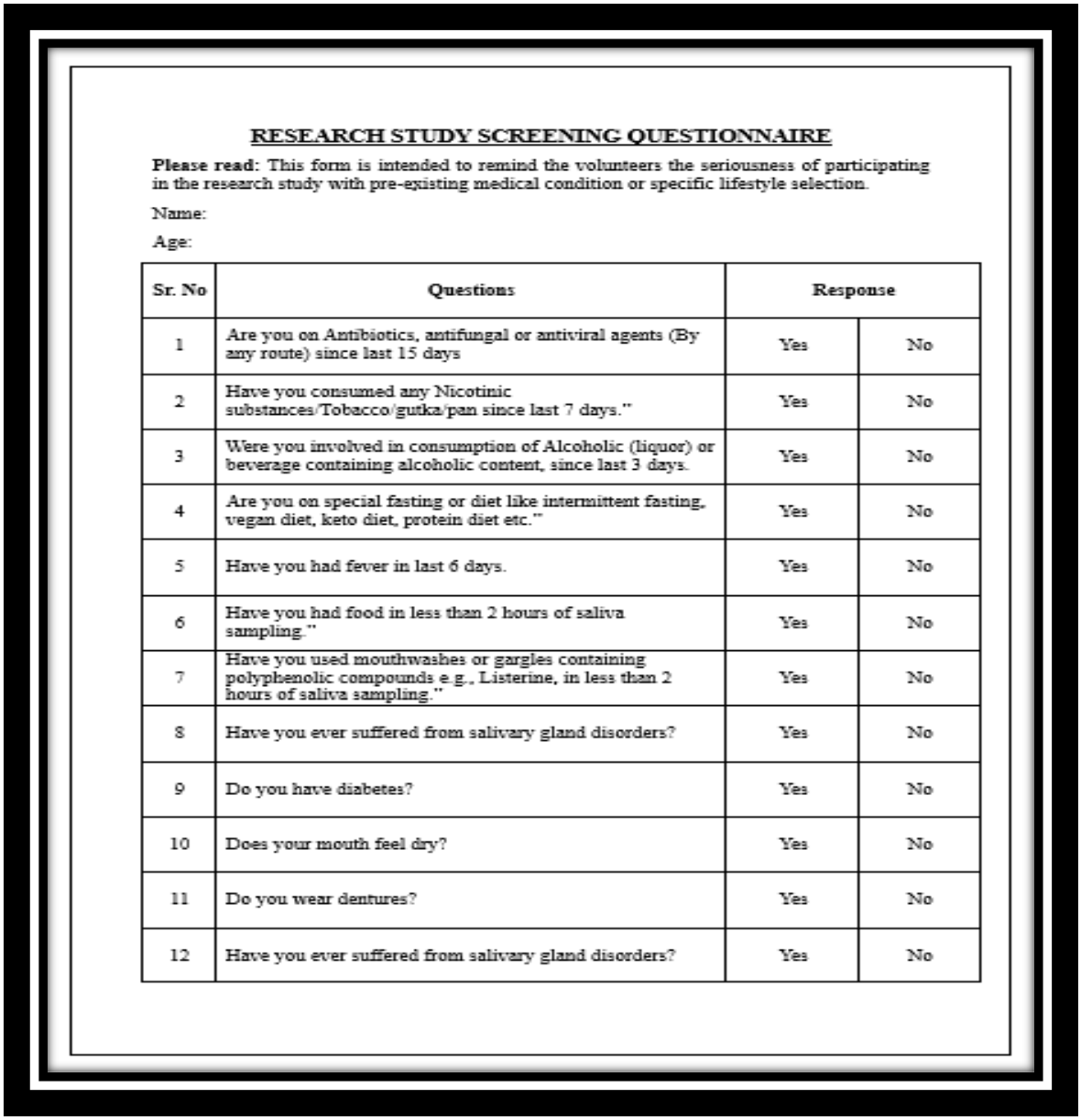

RESEARCH STUDY SCREENING QUESTIONNAIRE

Please read: This form is intended to remind the volunteers the seriousness of participating in the research study with pre-existing medical condition or specific lifestyle selection.

Name:

Age:

Sr. No	Questions	Response	
1	Are you on Antibiotics, antifungal or antiviral agents (By any route) since last 15 days	Yes	No
2	Have you consumed any Nicotinic substances/Tobacco/gutka/pan since last 7 days."	Yes	No
3	Were you involved in consumption of Alcoholic (liquor) or beverage containing alcoholic content, since last 3 days.	Yes	No
4	Are you on special fasting or diet like intermittent fasting, vegan diet, keto diet, protein diet etc."	Yes	No
5	Have you had fever in last 6 days.	Yes	No
6	Have you had food in less than 2 hours of saliva sampling."	Yes	No
7	Have you used mouthwashes or gargles containing polyphenolic compounds e.g., Listerine, in less than 2 hours of saliva sampling."	Yes	No
8	Have you ever suffered from salivary gland disorders?	Yes	No
9	Do you have diabetes?	Yes	No
10	Does your mouth feel dry?	Yes	No
11	Do you wear dentures?	Yes	No
12	Have you ever suffered from salivary gland disorders?	Yes	No

Fig 5. 2 Research study screening questionnaire

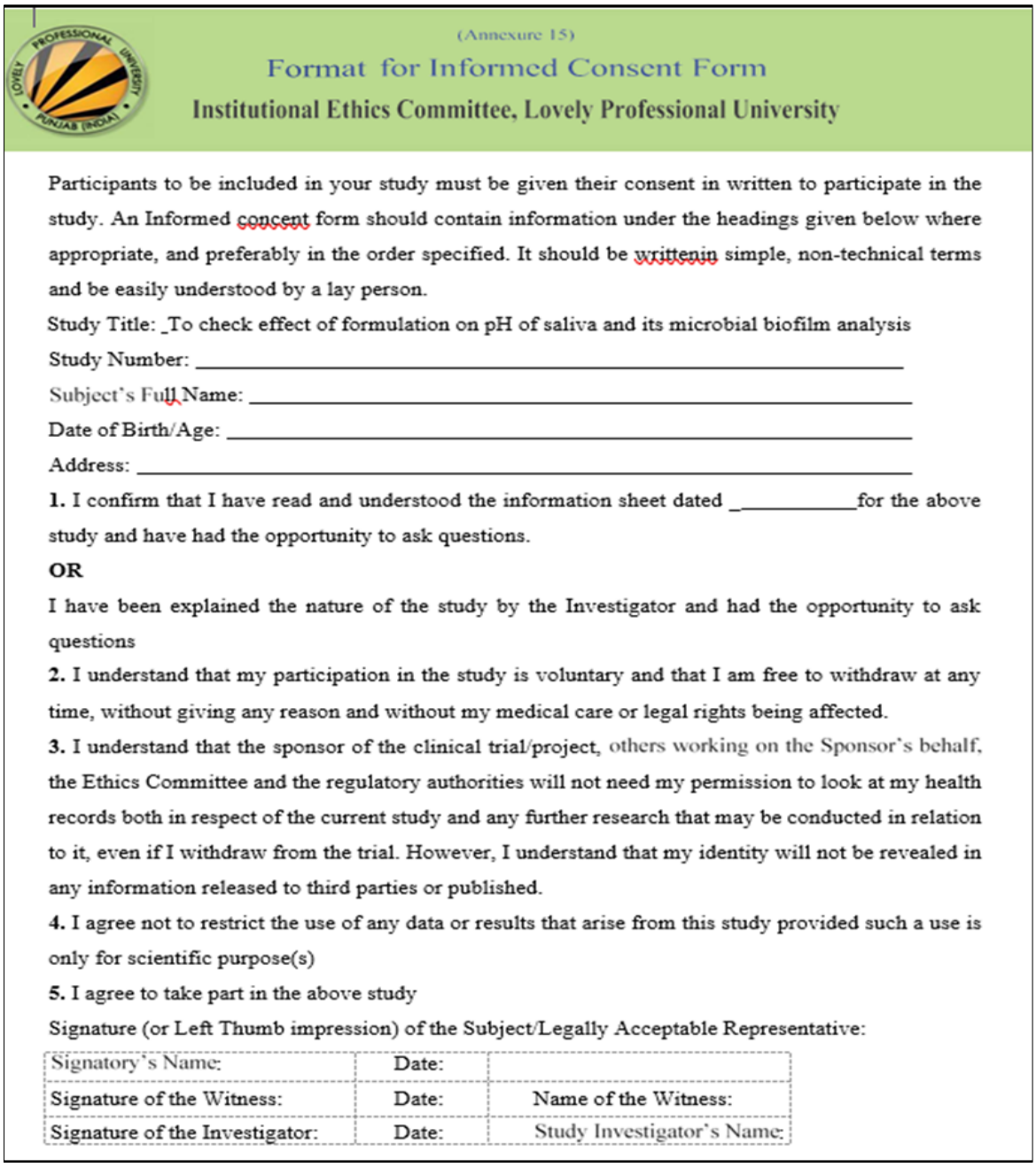

(Annexure 15)

Format for Informed Consent Form

Institutional Ethics Committee, Lovely Professional University

Participants to be included in your study must be given their consent in written to participate in the study. An Informed concent form should contain information under the headings given below where appropriate, and preferably in the order specified. It should be writtenin simple, non-technical terms and be easily understood by a lay person.

Study Title: _To check effect of formulation on pH of saliva and its microbial biofilm analysis

Study Number: _____

Subject's Full Name: _____

Date of Birth/Age: _____

Address: _____

1. I confirm that I have read and understood the information sheet dated _____for the above study and have had the opportunity to ask questions.

OR

I have been explained the nature of the study by the Investigator and had the opportunity to ask questions

2. I understand that my participation in the study is voluntary and that I am free to withdraw at any time, without giving any reason and without my medical care or legal rights being affected.

3. I understand that the sponsor of the clinical trial/project, others working on the Sponsor's behalf, the Ethics Committee and the regulatory authorities will not need my permission to look at my health records both in respect of the current study and any further research that may be conducted in relation to it, even if I withdraw from the trial. However, I understand that my identity will not be revealed in any information released to third parties or published.

4. I agree not to restrict the use of any data or results that arise from this study provided such a use is only for scientific purpose(s)

5. I agree to take part in the above study

Signature (or Left Thumb impression) of the Subject/Legally Acceptable Representative:

Signatory's Name:	Date:	
Signature of the Witness:	Date:	Name of the Witness:
Signature of the Investigator:	Date:	Study Investigator's Name:

Fig 5. 3 Informed consent form for sample-only studies

5.16.1.2 Study population selection

The study was approved by Institutional Ethics Committee, Lovely Professional University under approval number LPU/IEC-LPU/2023/01/36. It was conducted in the premises of Lovely Professional University, Department of Pharmaceutical Sciences, Phagwara, Punjab, India. The volunteers verbally explained the nature of the study and informed written consent was obtained (as per the Helsinki Declaration). The total number of volunteers selected for the population was calculated from the Qualitrics^{XM} software © 2023 version. The sample size was calculated by taking a population size of 100000 at a

95% confidence interval and a 10 % margin of error. The sample size comes out to be 96 volunteers. Hence, the sample saliva was collected from 96 healthy volunteers between the age of 18-40 years of age.

5.16.1.3 Saliva collection and pooling procedure

Nevertheless, the procedure for collecting saliva is less complicated and intrusive. To assure the biosafety features of the study, its use necessitated optimizing saliva collection and handling techniques. The technique for collecting samples includes selecting reliable volunteers, identifying the container, collecting samples in appropriate containers, and storing and transporting obtained samples to the designated processing locations. The draining method, spitting method, suction method, and swab method are typical techniques. The subsequent examination of saliva components may be impacted by the fact that samples taken by spitting include more bacteria than samples taken by drooling (Baliga, Muglikar, & Kale, 2013).

Food and drink were not allowed while collecting saliva. However, in some circumstances, eating should wait up to 30–1 hour before spitting. Before presenting a specimen, the person should thoroughly rinse their mouth with water. The subjects were instructed to remain silent, droop their heads, and allow their saliva to flow freely into their mouths. In sterile 10 ml beakers, saliva was collected. Containers ought to have a suitable identification number after sample collection (Bhattarai et al., 2018). (Bhattarai et al., 2018).

Saliva was collected in accordance with the World Health Organization/International Agency for Research on Cancer guideline "Common Minimal Technical Standards and Protocols." Subjects were instructed to only drink water while the saliva samples were being taken (Mendy, Caboux, Lawlor, Wright, & Wild, 2017). The test subjects were given bottled water to drink and instructed to thoroughly rinse their mouths. The patient was instructed to expectorate the collected saliva into the given sample container after the saliva had been allowed to build in the mouth for two minutes (Pittman, Decsi, Punyadeera, & Henry, 2023). The individual was instructed to spit out all of her saliva five minutes following this oral rinse. Additionally, the patients were instructed to avoid coughing while the saliva was being collected. Once each, the participants spat into the container. The salivary sample was taken between 9:00 and 11:00 AM in the morning. To stop the sample from degrading, the pH of the saliva was immediately tested.

5.16.2 Salivary pH analysis

5 ml of pooled saliva was taken in a sterilized beaker. To the saliva, 2 % of sucrose was added to each of the two beakers (sterilized at 121°C for 15 min in an autoclave). To one container the treatment was added to make a final concentration of 2.8 µg of PIC (making the final concentration of PIC at 0.563 µg/ml in saliva) while the other was kept blank and labeled as a positive control. The containers were kept in an incubator at 37 °C up to 24 hrs while covered with the container lid and regularly observed for pH measurements. The sample was taken as Blank and at 0 hrs, 4 hrs, and 24 hrs pH was measured (Lolayekar & Kadkhodayan, 2019) (Ccahuana-Vásquez & Cury, 2010b). Salivary pH was measured with the help of a single-electrode digital pH meter (Ali et al., 2012). The container was kept in an incubator at 37 °C for up to 24 hrs while covered with the container lid and regularly observed for pH measurements. The sample was termed as 'treatment' and at 0 hrs, 4 hrs, and 24 hrs pH was measured. With the use of a single-electrode digital pH meter, salivary pH was determined. With recently made pH 7 and pH 4 buffers, the pH meter was calibrated before use (Baliga et al., 2013). The electrode was washed with distilled water before being dipped into the sample. The electrode tip was once more gently rinsed with distilled water after the pH analysis, and it was then submerged in the distilled water. Every day, new preparations of the liquids and chemicals were made (Dodds, Roland, Edgar, & Thornhill, 2015).

5.16.2.1 Statistical analysis

The mean pH for all the two groups was calculated. The *p* values were calculated by student t-test (two samples assuming equal variance) was considered to check statistical significance at p value < 0.05 (Baliga et al., 2013).

5.16.3 Biofilm assay

In contrast to the various *in vitro* laboratory model biofilm systems which are either focused on single-species models or may to some extent focus on selective multi-species biofilms made on artificial media, ignore the complexity of inter-species interactions that is naturally present in the oral cavity. Secondly, such biofilms may offer microbial species which are metabolically and phenotypically way different than their normal state in flowing saliva. For this reason, the study was conducted on pooled human saliva wherein the saliva is taken as inoculum to represent real-world scenarios of multiple species along with their natural

habitat. The study was conducted as described by Kolderman et al. with some modifications(Kolderman et al., 2015).

5.16.3.1 Development of static microplate system

The pooled saliva was itself taken as an inoculum and nutrient source. 5 ml of pooled saliva was added to each one of the two sterilized petri dishes (sterilized at 121 °C for 15 min in an Autoclave). To the saliva, 2 % of sucrose was added as a nutrient source. To one petri dish, the treatment was added to make a final concentration of 2.8 µg of PIC (making the final dilution of PIC at 0.563 µg/ml in saliva) while the other was kept blank and labelled as a positive control. The Petri dishes were kept in an incubator at 37 °C for up to 24 hrs while covered with another Petri dish. At 0 hrs, 4 hrs, and 24 hrs time intervals the sample saliva was taken on a coverslip and airdried to fix the saliva on the cover slip. After complete drying of saliva on a cover slip and processed to observe under Field Emission Scanning Electron Microscopy. For each sample, elemental analysis was performed to identify the carbon content in the saliva sample (Kolderman et al., 2015) (Sharma et al., 2012).

5.16.3.1.1 FESEM analysis of samples

The sample for biofilm assay was observed for FESEM at the Central Instrumentation Facility, Lovely Professional University. The samples were observed at 0 hr, 4 hrs, and 24 hrs to check the effect of OFG on oral biofilms. The observations were taken and reported at the same resolutions and magnifications.

5.16.3.1.2 EDX analysis (EPS analysis)

From the SEM analysis, Elemental details w.r.t carbon content were identified at 10000x magnification. The observations were taken for that and statistically analyzed for the significance of the study.

6 RESULTS AND DISCUSSION

6.1 Procurement of the drug

The drug PIC was procured from TCI Chemicals (India) Pvt. Ltd. The drug was packed in an amber-coloured glass bottle with a plastic screw cap (sealed). The bottle was further bubble wrapped (Secondary packing material) and finally dispensed in cardboard (Tertiary Packing).

Instructions: Store in a cool place, Protect from the sunlight.

The L-Arg was procured from the Avarice industries. It was packed in a white plastic bottle with a seal (primary packing) and further sealed with plastic paper hermetically sealed (secondary packing).

Instructions: Store at room temperature.

6.2 Evaluation of general physical properties

6.2.1 Evaluation of organoleptic properties

The organoleptic characteristics of the PIC and L-Arg are mentioned in Table 6.1.

Table 6. 1 General properties of PIC and L-Arg

Sr. No.	Property	PIC	L-Arg
1	Colour	Tan orange to red crystals	White
2	Odour	Sharp astringent	Bland
3	Lustre	Shiny sharp powder	Dull
4	State	Solid	Solid

6.2.2 Melting Point Determination

The melting points of the PIC and L-Arg are mentioned in Table 6. 2.

Table 6. 2 Melting point of the PIC and L-Arg

Compound	Melting point (°C)		
	Mean	± S.D	% RSD
PIC	226.33	1.52	0.67
L-Arg	240.00	1.73	0.72

Results

The melting point was observed to be 226.33 and 240 ˚C for PIC and L-Arg, respectively.

6.3 Evaluation of PIC and L-Arg using chemical tests

6.3.1 Chemical test for PIC

Table 6. 3 Test for phenolic compounds

Sr. No.	Test	Inference	Result
1	Ferric chloride test	The blackish-brown colour appeared	Indicates the presence of polyphenolic compound
2	Lead acetate test	Light white precipitates	Indicates the presence of polyphenolic compound.

Results

The results obtained through chemical analysis (Table 6. 3) indicate the presence of phenolic compounds.

6.3.2 Chemical test for L-Arg

Table 6. 4 Test for amino acids

Sr. No.	Test	Inference	Result
1	Ninhydrin Test	The deep blue colour appeared	Indicates the presence of amino acids
2	Biuret's test	A dark pink colour appeared throughout the solution	Indicated presence of amino acids

Results

The results obtained through chemical analysis (Table 6. 4) indicate the presence of amino acids.

6.4 Fourier transform Infrared Spectral (FTIR) analysis of PIC and L-Arg

FTIR analysis was conducted as mentioned in section 4. 4 and the following are the findings.

6.4.1 FTIR for PIC

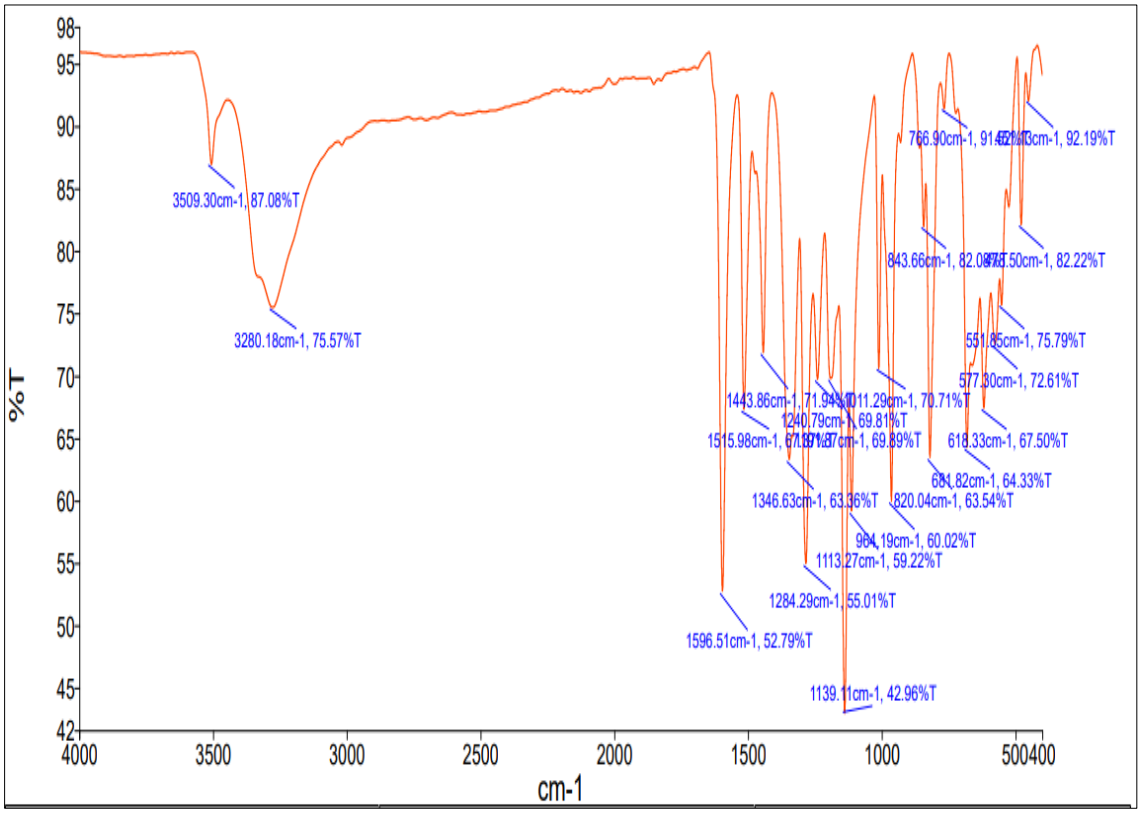

Fig 6. 1 FTIR spectra of PIC

6.4.1.1 Observations and findings

Table 6. 5 Scanning of FTIR spectra of PIC for observed peaks

Sr. No.	Wave number range (cm^{-1})	Functional Groups	Observed value (cm^{-1})	% Transmittance
1	3550-3200	Alcoholic/phenolic functional group	3509, 3280	87.08%, 75.50%
2	1600-1300	C-H bending	1596,1443	52.79%, 71.94%
3	1420-1330	-OH group	1347	63.36%
4	1310-1250	C-O stretching	1284	55.02%
5	1205-1124	C-O Stretching (Tertiary alcohol)	1139	42.97%
6	980-960	C=C Bending	964	60.02%

Table 6. 6 Comparison of procured PIC with reference spectra

PIC	Spectral Peaks (cm^{-1})									
Reference (Tashiro, Honzawa, & Sugihara, 2016)	3300	1600	1520	1445	1350	1280	1140	965	825	685
Test	3280	1596	1515	1443	1346	1284	1139	984	820	684

Results

FTIR spectrum of PIC gives information on functional groups present in the compound. Results revealed that the compound has maximum transmittance in the range of 3600-1000 cm^{-1} (Fig 6.1). The region between 3600-3200 cm^{-1} observed two characteristic peaks which are attributable to –OH groups (alcoholic and phenolic functional groups). Also, the peak in the region of 1300-1100 cm^{-1} is due to C-O stretching especially due to tertiary alcohol in the compound (Table 6.5). The compound has four hydroxyl groups joined to aromatic rings which give IR spectra in the region of 1205-1124 cm^{-1} as mentioned in Table 4.5. when compared with reference spectra (Table 6.6), The spectra show strong similarity in peaks as mentioned in the literature. This qualifies the drug as standard PIC.

6.4.2 FTIR for L-Arg

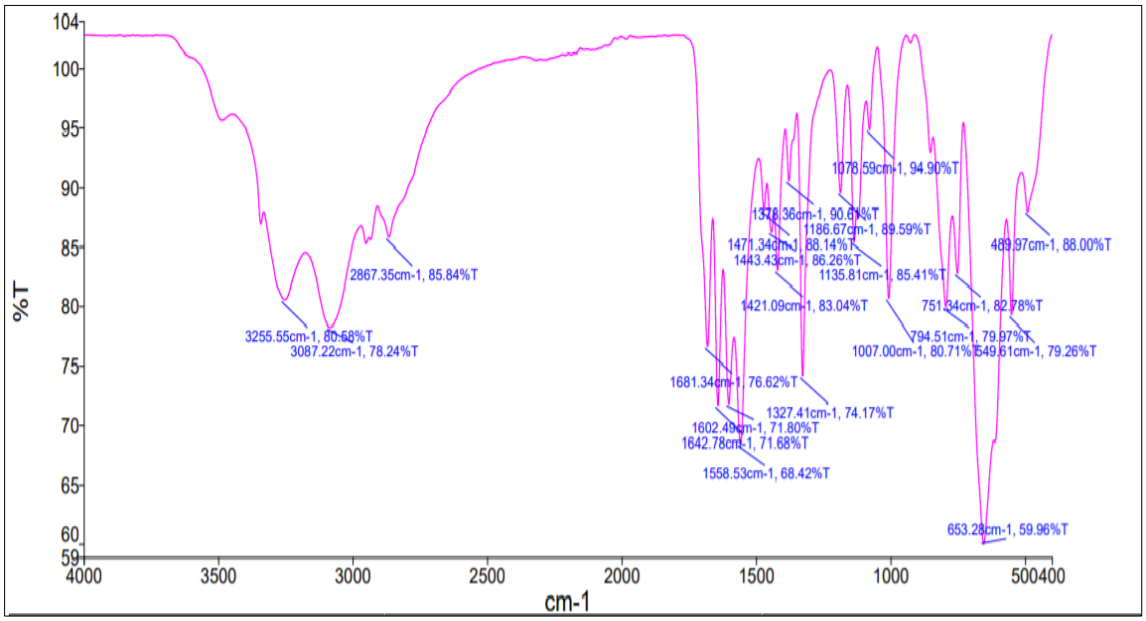

Fig 6. 2 FTIR spectrum of L-Arg

6.4.2.1 Observations and Findings

Table 6. 7 Scanning of FTIR Spectra of L-Arg for observed peaks

Sr. No.	Wave number range (cm^{-1})	Functional Groups	Observed value (cm^{-1})	% Transmittance
1	3300-3000	-COOH, -OH	3255, 3087	80.58, 78.24
2	3000-2800	N-H Stretching	2867	85.85
3	1690-1640	C=N stretching	1681,1642	76.62, 71.68
4	1580-1510	N-H bending	1558	68.42
5	1342-1266	C-N Stretching	1327	74.17
6	1200-1000	C-O Stretching	1007	80.71
7	800-550	C-H Bending	653	59.96

Table 6. 8 Comparison of procured L-Arg with reference spectra

L-Arg	Spectral peaks (cm^{-1})			
Reference(Ebrahiminezhad, Ghasemi, Rasoul-Amini, Barar, & Davaran, 2012)	3280	1614	1398	622
Test	3255	1602	1327	653

Results

The spectra obtained from FTIR analysis shows characteristic peaks depending upon functional groups present in the compound (Fig 6. 2). L-Arg is characterized based on a broader peak in the region of 3300-3000 cm-^{1} due to the carboxyl group (-COOH) present on the amino acid. Another characteristic peak was visible at 1558 cm^{-1} due to N-H stretching of the terminal amino group (-NH_2). The third characteristic peak was observed at 653 cm^{-1} attributed to strong C-H bending (Table 6.7). Observed FTIR spectra show a strong resemblance with the one mentioned in the literature which shows peaks at 3426 cm^{-1}, 3280 cm^{-1},1614 cm^{-1}, 1398 cm^{-1}, and 622 cm^{-1} (Table 6. 8). Hence the compound is identified as L-Arg.

6.5 Identification of drugs by UV-Visible spectroscopy

6.5.1 UV-Visible spectra of PIC

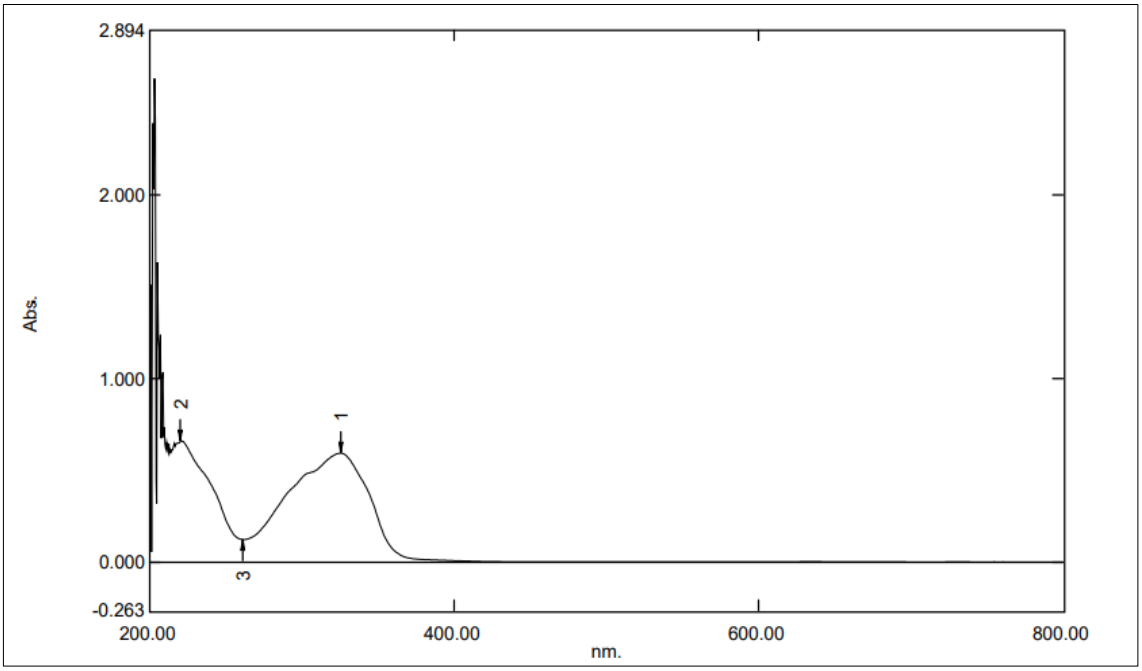

Fig 6. 3 UV spectra of PIC in methanol

Table 6. 9 Scanning of UV spectra of PIC in methanol

Sr. No.	Wavelength (nm)	Absorbance
1	324	0.5
2	220	0.6
3	261.5	0.123

Results

The procured drug revealed two characteristic peaks at 220 nm and 324 nm when dissolved in methanol (Fig 6. 3, Table 6. 9). When compared with reference spectra from the literature, two absorption maxima for PIC mentioned were 224 nm and 325 nm when dissolved in methanol. Thus, the procured drug is PIC.

6.5.1.1 Establishment of calibration plot of PIC

The values of absorbance of different concentrations of PIC from a stock solution in methanol are given in the following table 6. 10 and a standard plot is drawn Fig 6. 4.

Table 6. 10 Absorbance data for calibration curve of PIC in methanol

Conc. (µg/ml)	Absorbance		
	Mean	± S.D	% RSD
1	0.203	0.001	0.147
2	0.389	0.001	0.146

3	0.561	0.001	0.051
4	0.727	0.001	0.041
5	0.916	0.001	0.030

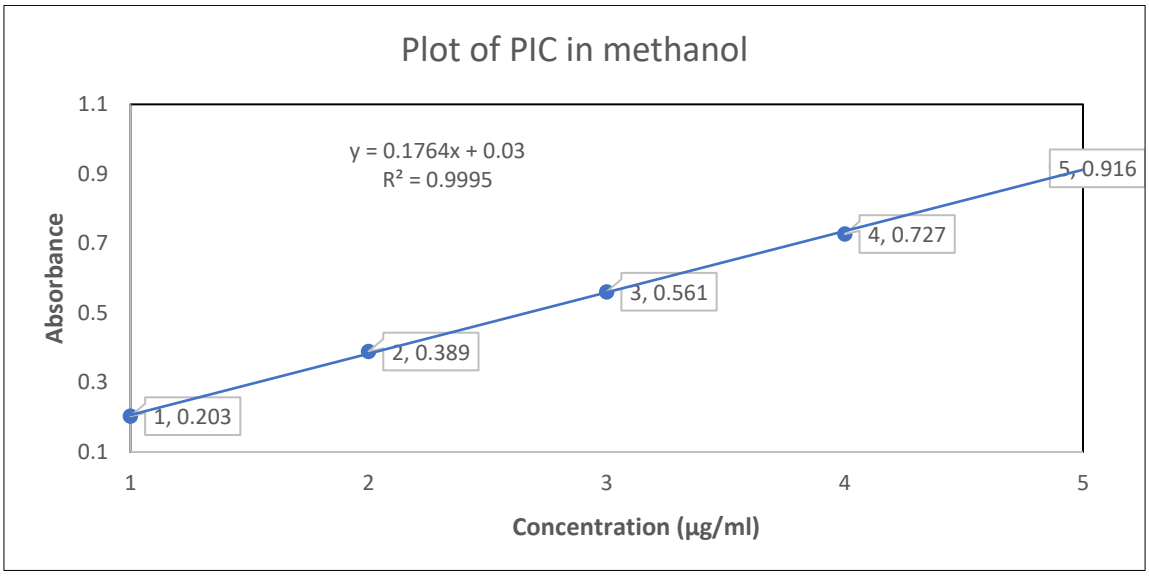

Fig 6. 4 Calibration plot of PIC in methanol at 324 nm

Results

The standard plot of PIC in methanol was found to be linear (Fig 6. 4) with an r^2 value of 0.9995, showing a proportional increase in absorbance with concentration from 1µg/ml to 5 µg/ml (Table 6. 10).

6.5.2 UV-Visible spectra of L-Arg

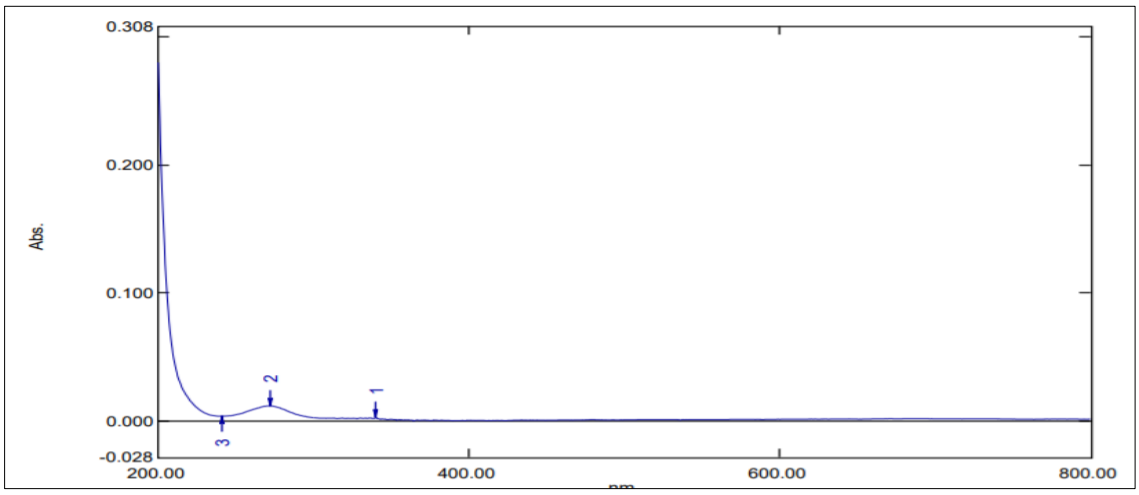

Fig 6. 5 UV spectra of L-Arg in distilled water.

Table 6. 11 Scanning of UV spectra of L-Arg in distilled water.

Sr. No.	Wavelength (nm)	Absorbance
1	340.5	0.003
2	272.5	0.012
3	241	0.004

Results

The solution of L-Arg was found to exhibit maximum absorption at 272.5 nm in distilled water (Fig 6. 5, Table 6. 11). Thus, the procured drug reflects similar absorption spectra when compared with the reference spectra.

6.5.2.1 Establishment of calibration plot of L-Arg

The values of absorbance of different concentrations of L-Arg from a stock solution in distilled water are given in the table 6. 12 and a standard plot is drawn (Fig 6. 6).

Table 6. 12 Absorbance data for calibration curve of L-Arg in distilled water

Conc (µg/ml)	Absorbance		
	Mean	±S.D	% RSD
80	0.15	0.001	0.76
100	0.17	0.001	0.33
120	0.18	0.001	0.53
140	0.21	0.001	0.47
160	0.23	0.001	0.42

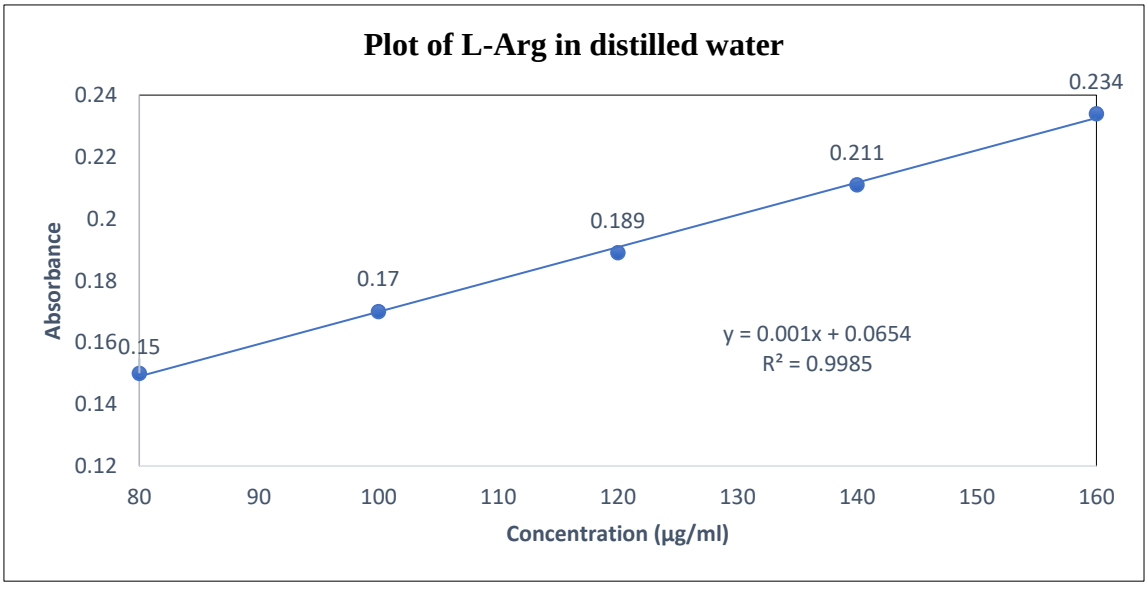

Fig 6. 6 Calibration plot of L-Arg in distilled water at 272 nm

Results

The standard plot of L-Arg in distilled water was found to be linear with an r^2 value of 0.998 (Fig 6. 6), showing a proportional increase in absorbance with concentration from 80 µg/ml to 160 µg/ml with % RSD value less than 2 (Table 6. 12).

6.6 HPLC for qualitative analysis of PIC and L-Arg

6.6.1 HPLC for qualitative analysis of PIC

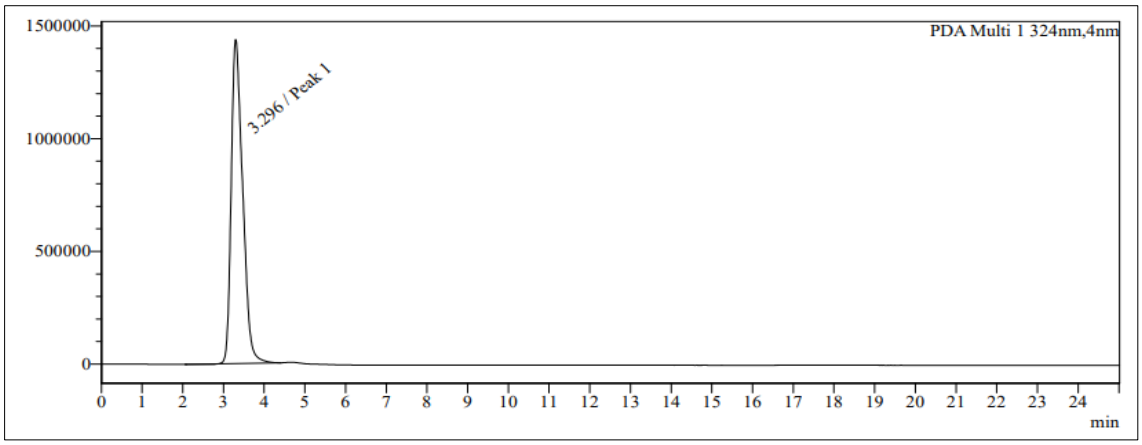

Fig 6. 7 HPLC chromatogram of PIC at 324 nm

Results

RP-HPLC was carried out and a single peak was detected with a retention time of 3.2 mins at 324 nm. Whereas the blank run does not show any peak throughout the UV range (Fig 6. 7). A single and sharp peak at absorbance maxima of PIC validates the presence of pure PIC in the procured sample. The method adopted for qualitative analysis was also found to be reliable and can be used for quantitative studies after method validation.

6.6.2 HPLC for qualitative analysis of L-Arg

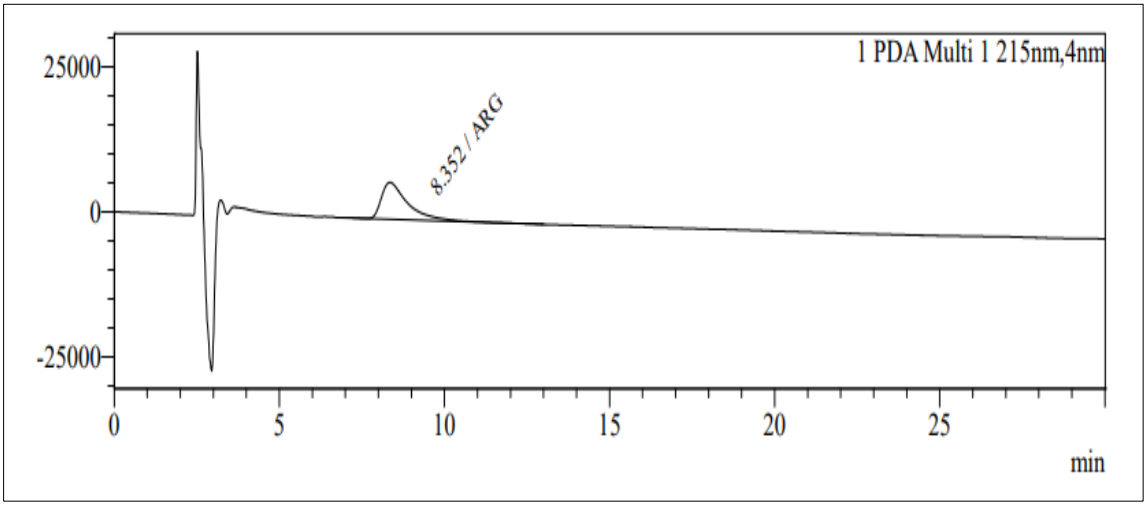

Fig 6. 8 HPLC chromatogram of L-Arg at 215 nm

Results

A single peak was detected with retention time 8.3 min at 215 nm (Fig 6. 8). A peak near absorbance maxima of L-Arg validates its presence in the sample. The method thus can be used to quantify the drug samples after method validation.

6.7 Drug-excipient compatibility studies

Drug excipient compatibility studies are an indicator of the inertness of various chemical excipients used in the formulation. These studies are an indicator of the physical and chemical stability of formulation ingredients in the most widely used combination. Compatibility studies during the preformulation phase of drug development help in selecting the most relevant excipients depending upon their inertness and unreactivity towards the pharmacological agents. Furthermore, these studies are an indicator of the most favourable possible combination in which the excipients can be used for formulating the formulation. In case of any physical or chemical change if observed during compatibility studies, the type of metabolite produced and its pathway can also be predicted. Drug excipient compatibility studies were conducted in PIC, L-Arg, Soy lecithin, Span 60/SDC and Carbopol by using various mixtures in 1:1 composition.

6.7.1 Physical compatibility

Following combinations were examined physically for any change in odour, discolouration, liquefaction, cake formation under room temperature and dim light conditions.

Table 6. 13 Compatibility study of drug and excipients used

Composition	Compatibility study observations (room temperature(25°C±2°C) and dim light)																							
	0th day				2nd day				4th day				7th day				15th day				21st day			
	without drug		with drug		without drug		with drug		without drug		with drug		without drug		with drug		without drug		with drug		without drug		with drug	
	OP	CL	OP	CL	OP	CL	OP	CL	OP	CL	OP	CL	OP	CL	OP	CL	OP	CL	OP	CL	OP	CL	OP	CL
PIC	NA	NA	*	*	NA	NA	*	*	NA	NA	*	*	NA	NA	*	*	NA	NA	*	*	NA	NA	*	*
L-Arg	NA	NA	*	*	NA	NA			NA	NA			NA	NA	*	*	NA	NA	*	*	NA	NA	*	*
PIC+ L-Arg	NA	NA	*	*	NA	NA	*	*	NA	NA	*	*	NA	NA	*	*	NA	NA	*	*	NA	NA	*	*
PIC + L-Arg + lecithin + SDC +carbopol	*	*	*	*	*	*	*	*	*	*	*	*	*	*	*	*	*	*	*	*	*	*	*	*
PIC + L-Arg + lecithin + span 60 +carbopol	*	*	*	*	*	*	*	*	*	*	*	*	*	*	*	*	*	*	*	*	*	*	*	*

* Combinations used FTIR analysis of samples to check chemical compatibility DSC sampling to check chemical incompatibility

Discussion

The physical compatibility study of PIC, L-Arg and various excipients was observed over 21 days at room temperature in dim light (no direct sunlight exposure) as given in the Table 6. 13. Signs of physical incompatibility were observed for any combination of drugs and excipients i.e., discoloration, lump formation, liquefaction etc. All the mixtures were free-flowing till the 21st day of the study. So, it was concluded that the drug and proposed excipients are compatible with each other.

6.7.2 Chemical compatibility

To check chemical incompatibility the samples were kept in triplicate as mentioned in Table 6.13 and FTIR analysis of PIC was done for the alternate day to assure any change in FTIR spectra of the drug. Sample from both open and closed Petri-dishes was taken and analyzed for FTIR spectra.

Table 6. 14 FTIR spectral peaks of PIC alone taken on 2nd, 4th and 7th day

Spectral peaks (cm^{-1})											
PIC	**Reference (Tashiro et al., 2016)**	**3300**	**1600**	**1520**	**1445**	**1350**	**1280**	**1140**	**965**	**825**	**685**
	Test	3280	1596	1515	1443	1346	1284	1139	984	820	684
Day 2	**Open**	3276	1595	1516	1444	1333	1284	1138	964	821	681
	Closed	3290	1594	1515	1444	1346	1286	1139	964	821	689
Day 4	**Open**	3280	1596	1516	1448	1346	1284	1138	964	819	680
	Closed	3279	1595	1515	1443	1346	1284	1138	963	819	680
Day 7	**Open**	3282	1595	1515	1443	1345	1283	1138	963	819	681
	Closed	3280	1596	1515	1443	1346	1284	1138	963	819	681

Discussion

FTIR spectra of PIC alone were observed for one week. Alternative spectral identification for 7 days taken from open and closed petri dishes were meant to assure no characteristic chemical change taking place when PIC was kept at room temperature in dim light. Spectral peaks confirmed that no functional group change or alteration has taken place in PIC (Table 6. 14, Fig 6. 9). So, it was concluded that PIC remains unchanged for 7 days when no direct sunlight is exposed to the drug.

6.7.2.1 FTIR spectra of PIC

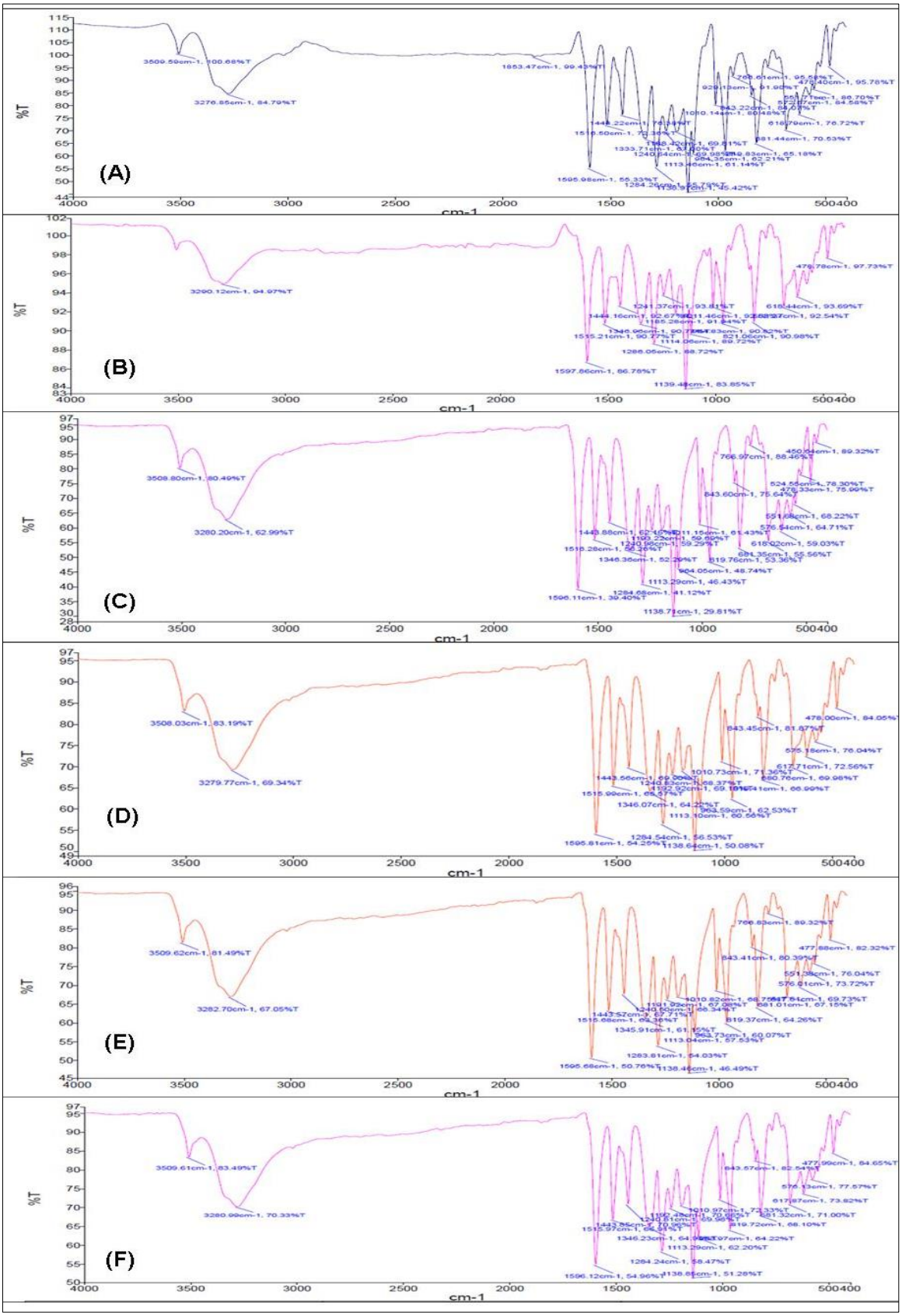

Fig 6. 9 FTIR spectra of PIC on various days (A, B) open and closed day 2, (C,D) open and closed day 4, (E,F) open and closed day 7.

6.7.2.2 DSC analysis of samples for chemical compatibility

6.7.2.2.1 Observations taken on day 7th

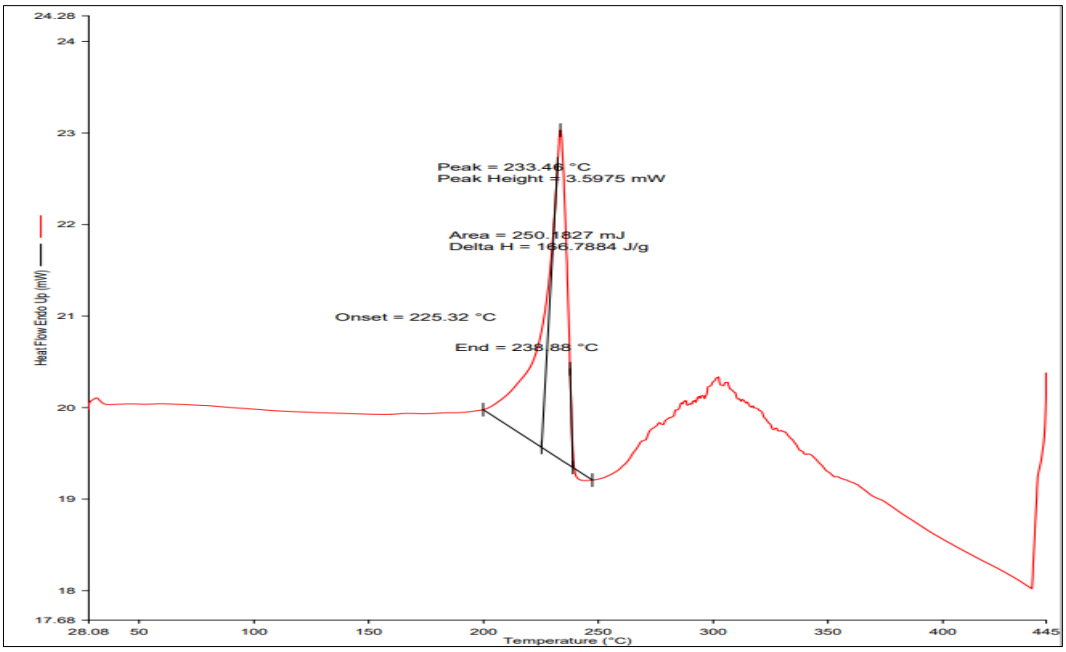

Fig 6. 10 DSC thermogram of PIC

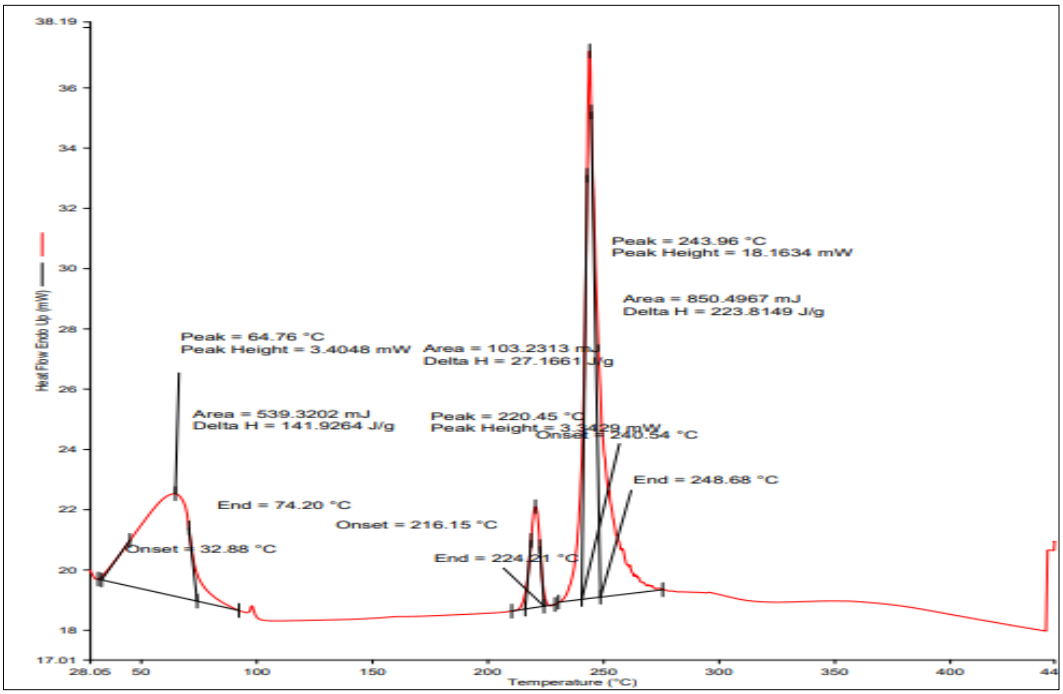

Fig 6. 11 DSC thermogram of L-Arg

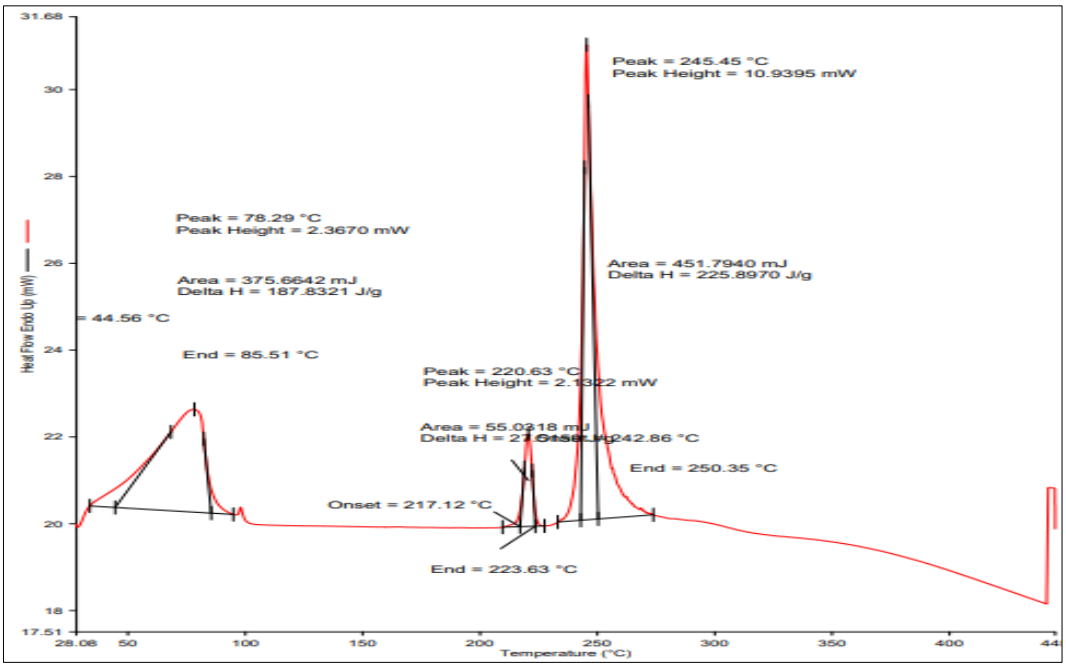

Fig 6. 12 DSC thermogram of PIC and L-Arg

6.7.2.3 Observations taken on day 21st

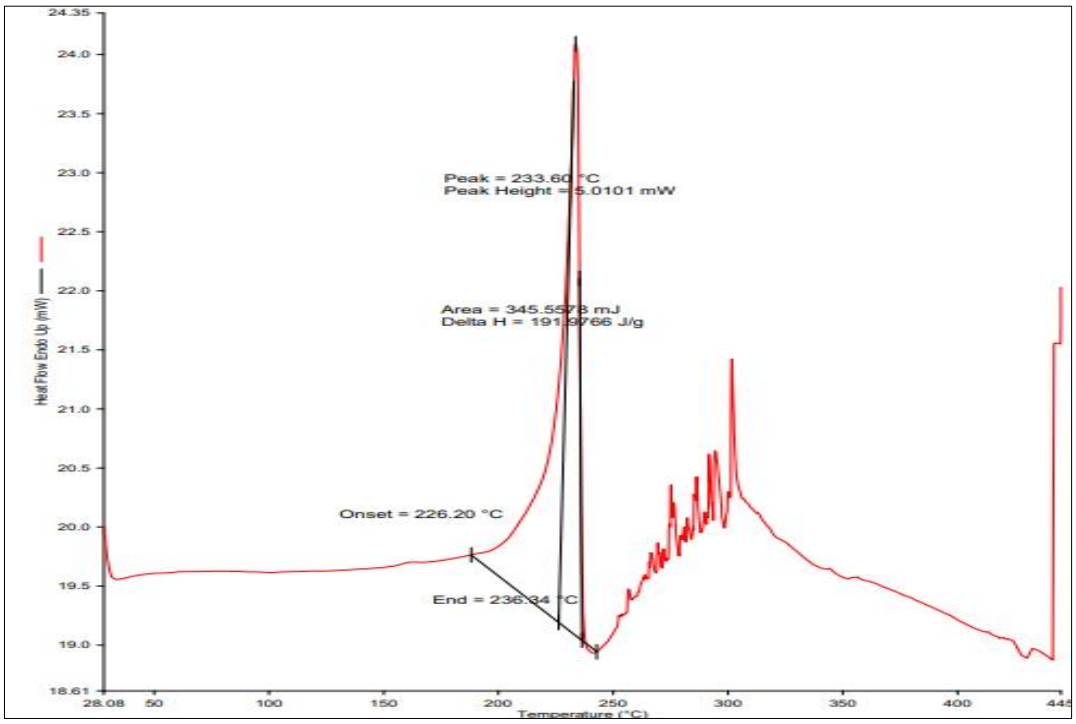

Fig 6. 13 DSC thermogram of PIC on 21st day

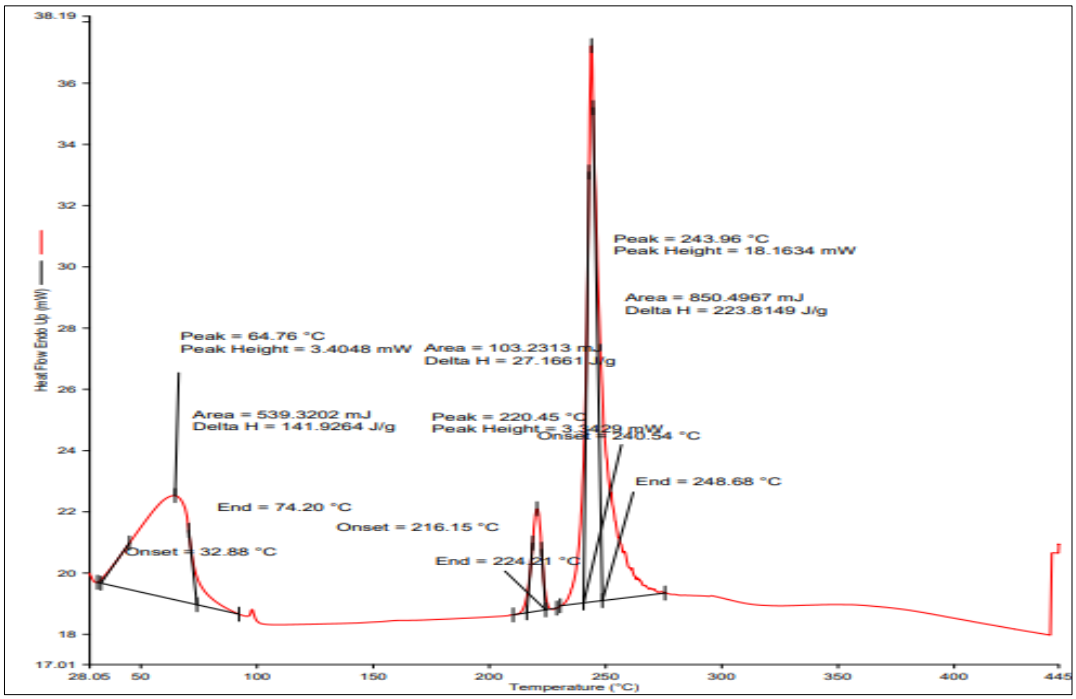

Fig 6. 14 DSC thermogram of L-Arg on 21st day

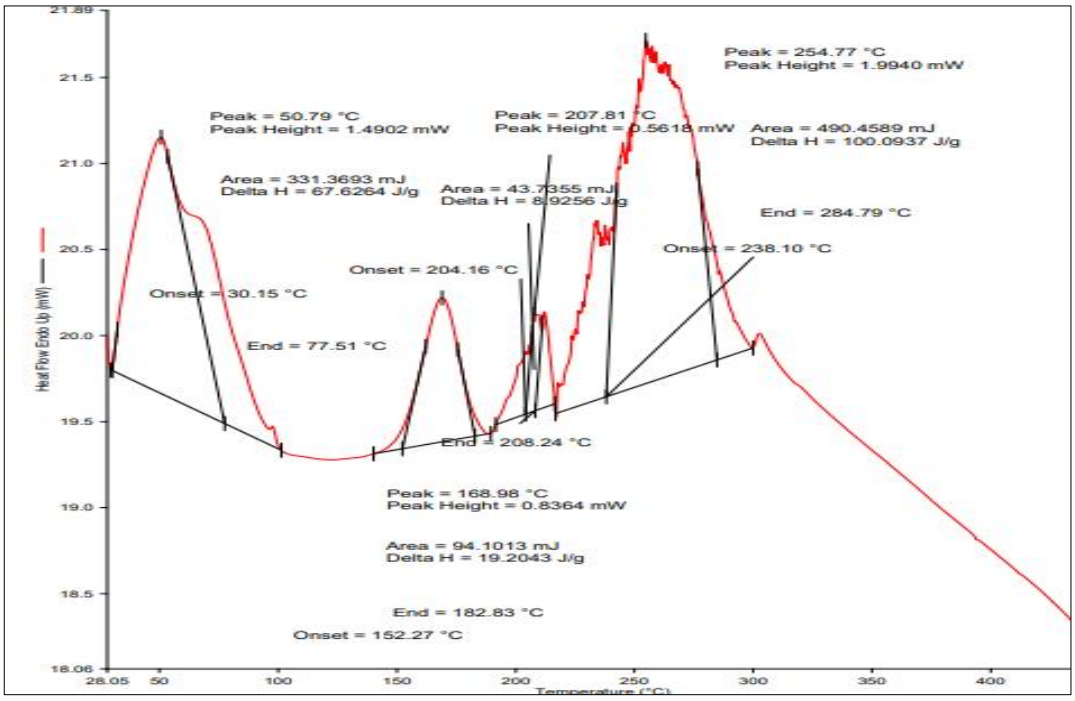

Fig 6. 15 DSC thermogram of PIC and L-Arg on 21st day

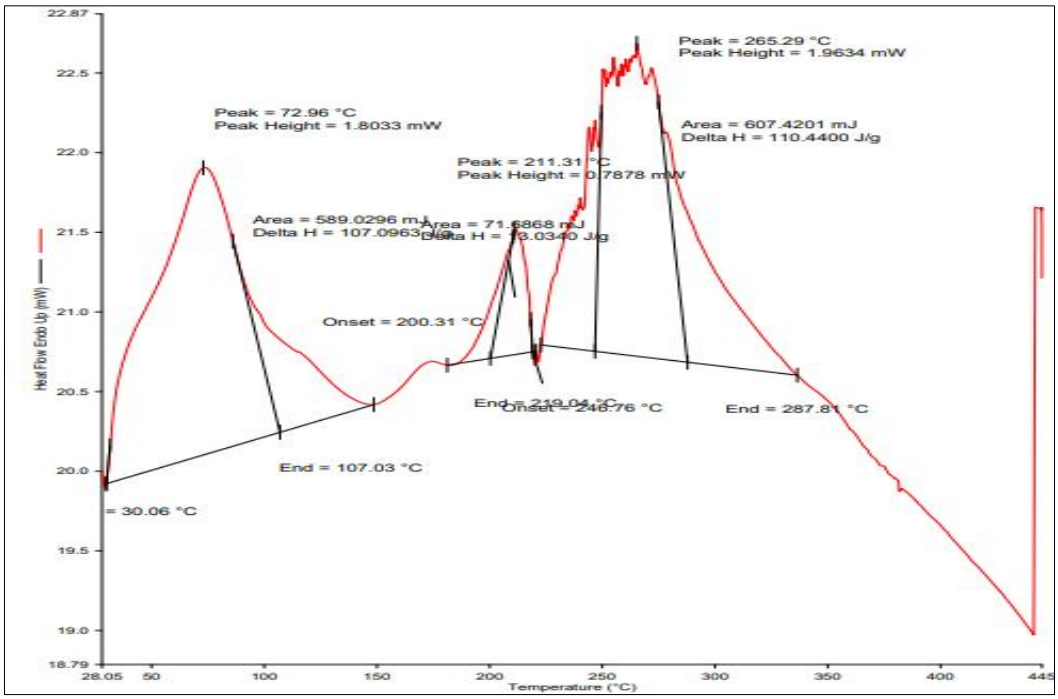

Fig 6. 16 DSC thermogram of all excipients with span 60 on 21st day

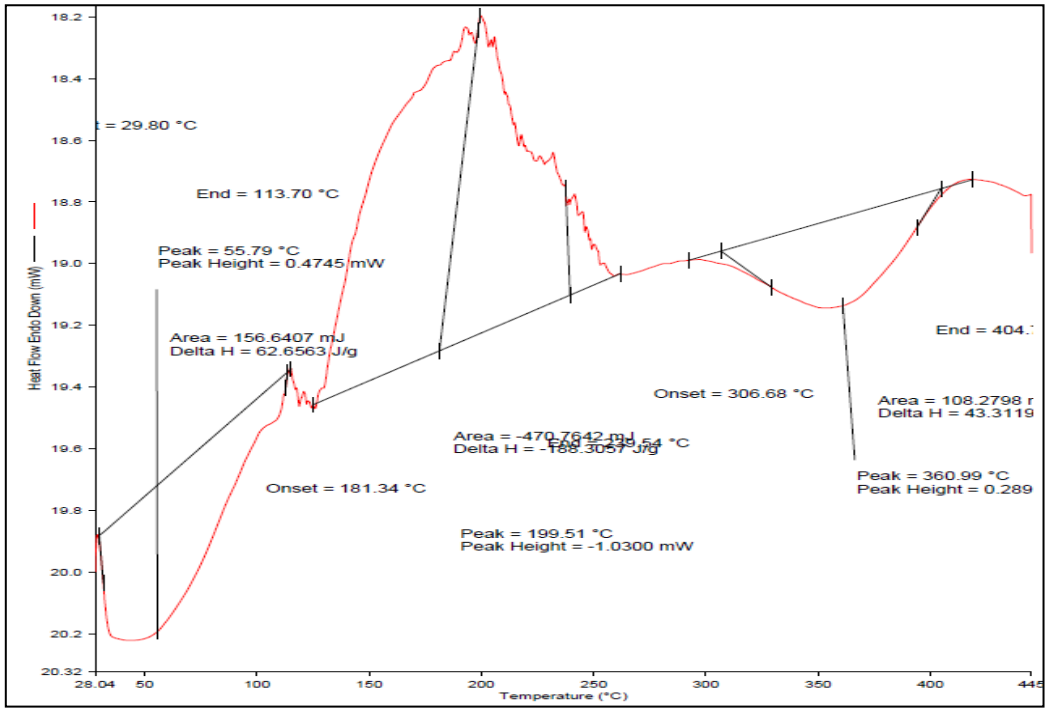

Fig 6. 17 DSC thermogram of all excipients with SDC on 21st day

Table 6. 15 Observations of day 21st

Combinations	Peak (°C)	Onset (°C)	End (°C)
PIC	233.6	226.2	236.34
L-Arg	64.76	32.88	74.2
	220.45	216.15	224.21
	243.96	240.54	248.68
PIC + L-Arg	50.79	30.15	77.15
	207.81	204	208
	254.77	238.1	284.79
Mixture (With SDC)	55.79	29.8	113.7
	199.51 (Exo)	121.16	259.61
	360.99	306.68	404
Mixture (Span 60)	72.96	30.06	107.03
	211.31	200.31	219.04
	265.89	246.76	287.81

Discussion

The compatibility study was conducted to check individual as well as combination stability of various chemical moieties. As a part of preformulation studies, the focus was to check no significant difference in physical or chemical character of any excipient or drug present in combination. Various combination mixtures were made in a 1:1 ratio at ambient room temperature and conditions. Triplicate samples of every combination were made and kept in a petri dish (Patel et al., 2015).

For the first 7 days, FTIR analysis on PIC alone was done and observed for any change in spectra. The results showed that (Table 6. 15) no spectral changes were observed for PIC in both open and closed conditions. This can be evaluated from the results that PIC is stable enough in open and closed conditions when kept at 25 °C±2 ˚C with ambient conditions under dim light.

For compatibility analysis, the 7th day DSC (Fig 6.10, 5.11, 5.12) and 21st day DSC (Fig 6.13, 5.14, 5.15) on various samples were done. On the 21st day, DSC analysis showed no chemical interaction between both PIC and L-Arg. The reference spectra of PIC shows peak at 225.9˚C and L-Arg shows at 101˚C and 241.7˚C (Park et al., 2020). The combination of PIC and L-Arg showed peaks at 50.79, 207.81 and 254.77 ˚C (Table 6. 15). This can be concluded that both L-Arg and PIC, in open condition does not interact with each other and are stable both chemically and physically.

The DSC thermogram of PIC and L-Arg in combination with soy lecithin, and carbopol with span 60 (Fig 6. 16) and SDC (Fig 6. 17) was observed. The reported endothermic peak observed for soy lecithin, Span 60 and Carbopol was reported to be 40, 58 and 250˚C (Sharma, Yusuf, & Pathak, 2014) (Hashim, El-Magd, El-Sheakh, Hamed, & El-Gawad, 2018) (Sharma et al., 2014) respectively. When all these excipients were kept individually with both L-Arg and PIC in a 1:1 ratio, the thermogram showed an endothermic peak at 40, 199, 290, and 420˚C. These peaks corresponds to Soy Lecithin (40˚C), L-Arg (50˚C), L-Arg (207˚C), PIC (233˚C), Carbopol (260˚C) and SDC (420˚C) respectively. For Span 60 mixture with all other excipients (Fig 6. 16, Table 6. 15), the endothermic peak was reported at 54.58˚C. DSC thermogram of a mixture of PIC, L-Arg and Span 60 showed peaks at 54.58˚C and 249.5˚C after the 21st day. Similar peaks were observed for span 60 and the wider peak around 249.5˚C represents PIC and L-Arg. DSC thermogram showed endothermic peaks at 248˚C which was expected to be due to all three chemical moieties. The mixture of all formulation ingredients containing sodium deoxycholate (SDC) as an Edge Activator is shown in Figure 1D. The thermogram showed two endothermic peaks at 55.79°C and 360°C corresponding to SDC (figure 1D). One broad exothermic peak starting from 121.16°C to 259.61°C was identified. Since many endothermic peaks were also expected in this region, that corresponds to PIC, L-Arg, Soy lecithin, and Carbopol, corresponding to 225, 241.7, 132, and 250°C respectively. One broader exothermic peak indicated more than one thermal process. As there was no significant change of (T_m) for any compound is observed, it is concluded that the excipients Soy lecithin, Span 60/SDC and Carbopol does not have any interaction with PIC and L-Arg and are compatible to formulate together.

6.8 Method development and validation of HPLC method for simultaneous estimation of PIC and L-Arg

6.8.1 Method development

Different compositions of mobile phase were used for the method development of HPLC. mobile phase such as methanol-water in various proportions and 0.1% orthophosphoric acid (in water): acetonitrile in different ratios were used. For all trials, other parameters such as pH, temperature and flow rate was kept the same. The initial run was kept for 35 mins with the isocratic flow for each trial. In trial 1, a combination 500:5 µg/ml (L-Arg: PIC) was made in methanol and the mobile phase was kept in 70:30 of methanol: water (Fig 6. 20). In trial 2, to improve the solubility of L-Arg instead of methanol the sample was prepared using water and methanol in a 1:9 ratio to make 500:5 µg/ml of L-Arg and PIC respectively. Trial 3, methanol:

water was kept at 50:50 for the mobile phase and the sample was prepared as trial 2 with the same concentrations. Trial 4 run was made using 0.1% orthophosphoric acid (in water): acetonitrile (9:1) and the sample was prepared in the mobile phase composition only. The final trial was made using 0.1% orthophosphoric acid (in water): acetonitrile (7:3) using same as sample preparation medium. The observations for each trial are given in Fig 6. 18

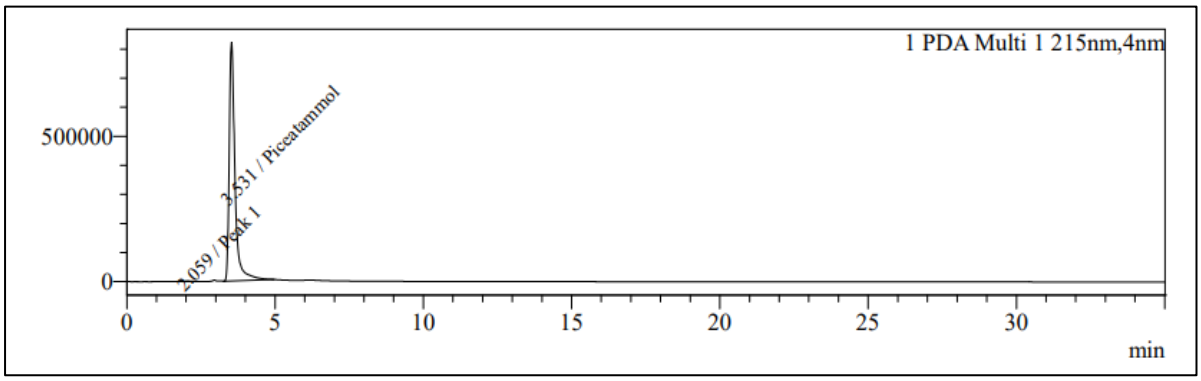

(A)

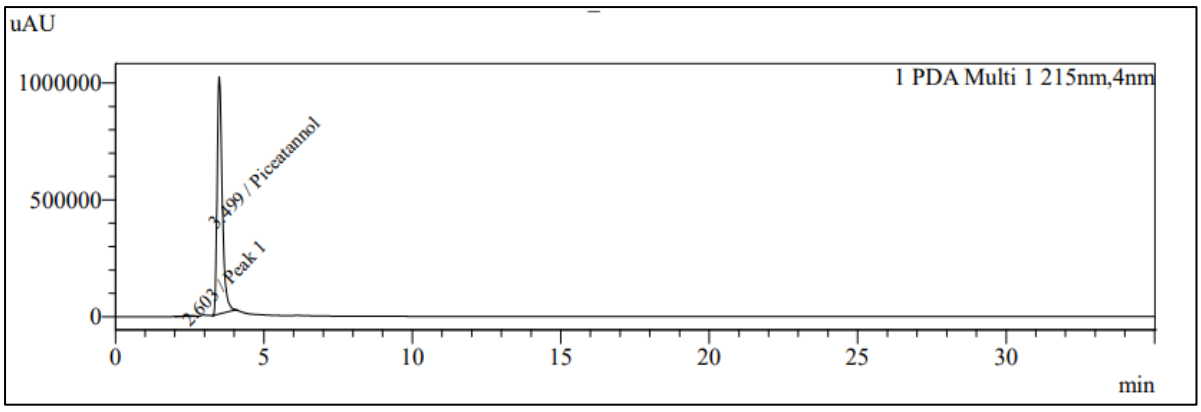

(B)

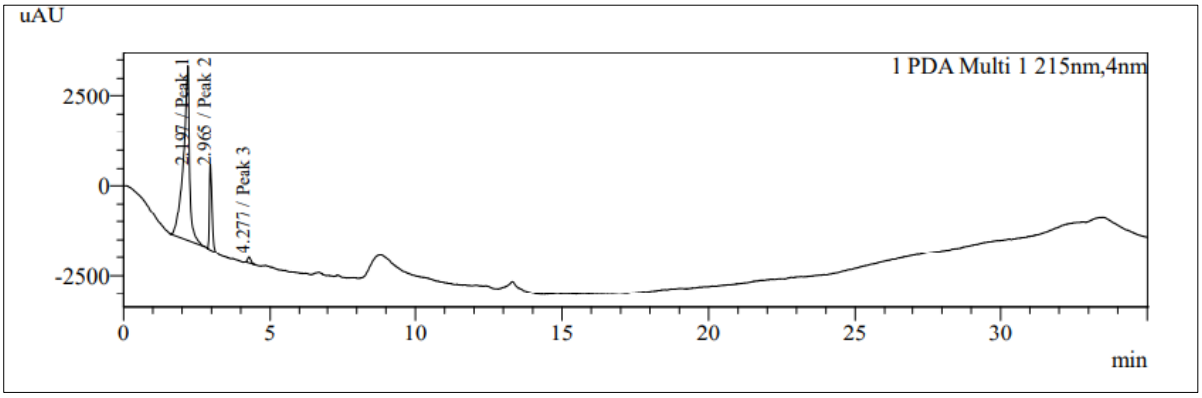

(C)

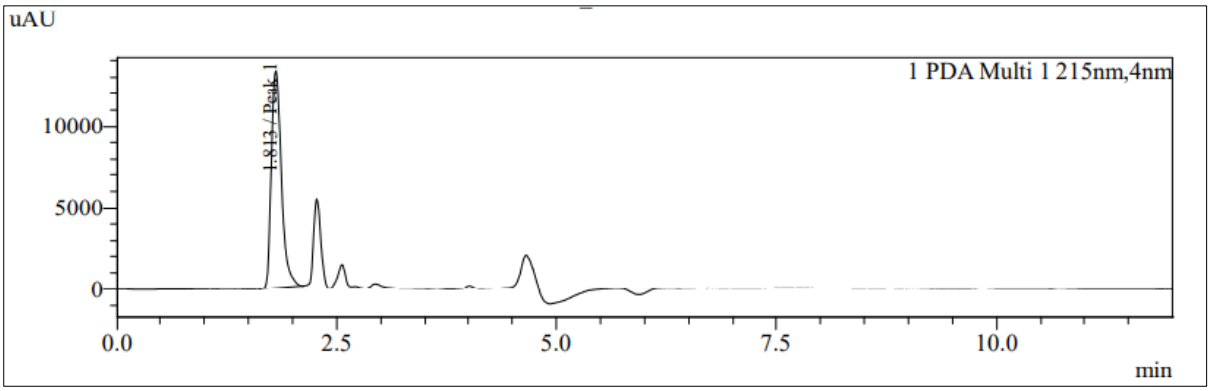

(D)

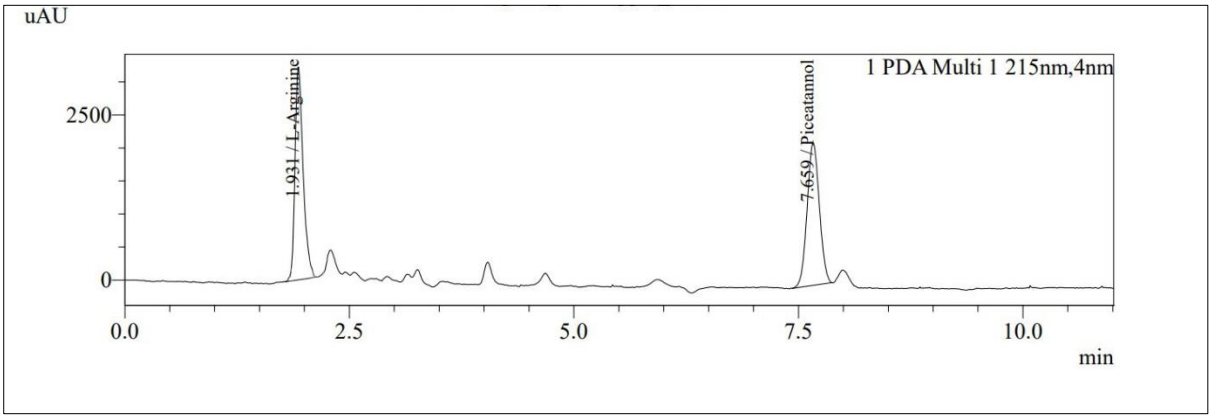

(E)

Fig 6. 18 (A) Mobile phase methanol:water (70:30), (B) Mobilephase methanol:water (70:30) with sample prepared in water:methanol (1:9), (C) Methanol:water (50:50), (D) Mobile phase 0.1% orthophosphoric acid (in water): acetonitrile (9:1), (E) Chromatogram of PIC and L-Arg in of 0.1% orthophosphoric acid (in water): acetonitrile (70:30).

Discussion

For simultaneous quantification of PIC and L-Arg, trials were started from using methanol: water (70:30 v/v) as mobile phase and preparing the sample in methanol. The chromatogram obtained thus does not show effective resolution as RT comes out to be 3.53 min for PIC and a very weak response of L-Arg at 2.059 min was seen. The low response of L-Arg was expected due to poor solubility in methanol, which is used as a solvent to prepare the sample to make 500 µg/ml of L-Arg. To improve the resolution and peak intensity, trial 2 was operated. In this, the drugs were dissolved in water and the final volume was made up using methanol, the ratio was fixed as (1:9) for water: methanol. The resolution of two peaks was further reduced as RT for PIC was 3.499 min and for L-Arg was 2.603 min, with no improvement in peak intensity of L-Arg. Trial 3 was conducted to improve the polarity of the mobile phase by increasing the

methanol: water composition to 50:50 v/v. The chromatogram thus obtained showed sufficient intensity of L-Arg but poor resolution and multiple peaks of PIC were observed on the chromatogram. As another trial, 0.1% orthophosphoric acid (in water): acetonitrile (9:1) opted as mobile phase, and as a trial to elute L-Arg only 500 µg/ml of L-Arg sample was prepared in 0.1% orthophosphoric acid (in water): acetonitrile (9:1). The intensity was improved drastically from 3500 uAU to 13000 uAU with RT at 1.813 min. To evaluate the separation of both L-Arg and PIC in combination, trial 5 was conducted using a mobile phase of 0.1% orthophosphoric acid (in water): acetonitrile (7:3) The sample was prepared using a mobile phase of the same composition and good resolution was observed with RT for PIC at 7.659 min and RT for L-Arg at 1.931 min. The peak intensity also comes out to be of sufficient. Therefore mobile phase consists of 70:30 of 0.1% orthophosphoric acid (in water): acetonitrile has been selected. The peaks of L-Arg and PIC are together shown in Fig 6. 18(E). The method was further validated according to ICH guidelines and found to have sufficient separation capacity to be used for the quantification of compounds in combination.

6.8.1.1 Development of calibration curve

6.8.1.1.1 Calibration plot of PIC

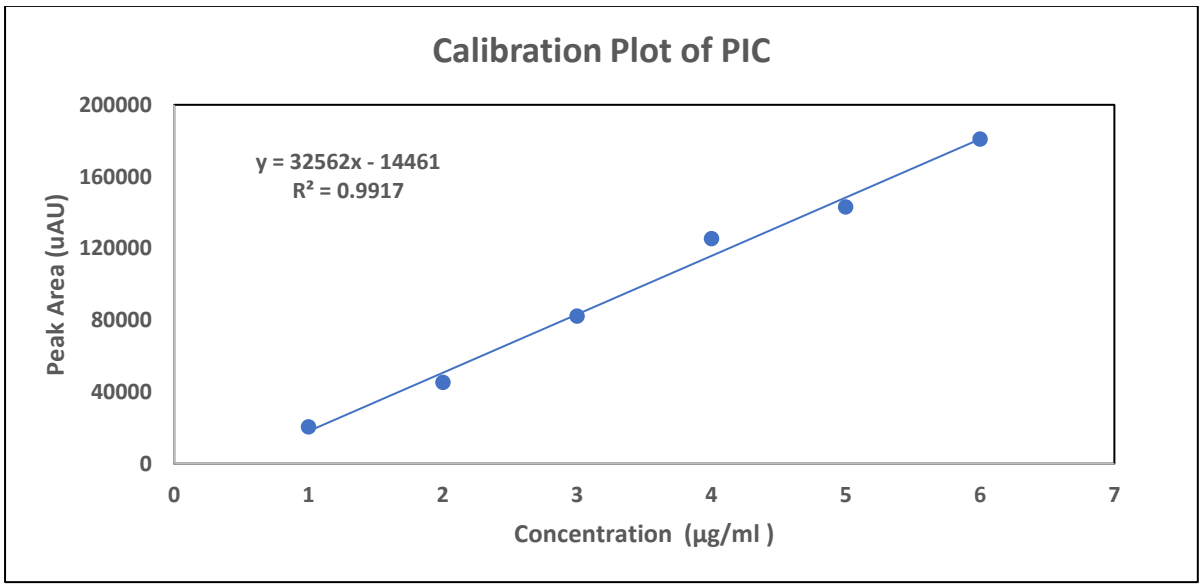

Fig 6. 19 Calibration plot of PIC

Table 6. 16 Data of calibration curve of PIC

PIC			
Conc. (µg/ml)	**Mean**	**± S.D**	**% RSD**
1	20384.67	90.13	0.44
2	45172.67	97.87	0.21
3	82126.67	43.98	0.05
4	125330.7	959.88	0.76
5	143112.3	28.21	0.01
6	180917.3	11.89	0.01

Results

The developed calibration plot shows a positive and good correlation of R^2 of 0.9917 (Fig 6. 19) for PIC. The % RSD also comes out to be less than 2 % (Table 6. 16).

6.8.1.1.2 Calibration plot of L-Arg

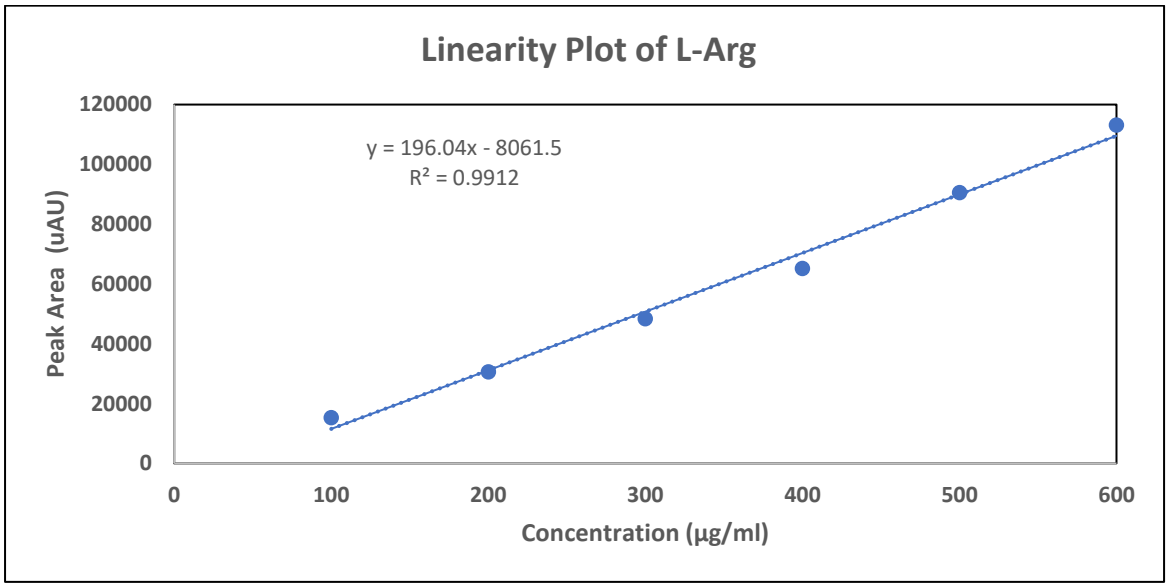

Fig 6. 20 Calibration plot of L-Arg

Table 6. 17 Data of calibration curve of L-Arg

L-Arg			
Conc. (µg/ml)	**Mean**	**± S.D**	**% RSD**
100	15295	69.30	0.45
200	30610.33	154.45	0.50
300	48421.33	164.39	0.33
400	65234.33	131.12	0.20
500	90551.33	81.09	0.08
600	113192.3	431.80	0.38

Results

The developed calibration plot shows a positive and good correlation of R^2 of 0.9912 (Fig 6. 20) of L-Arg. The % RSD also comes out to be less than 2 % (Table 6. 17).

6.8.2 Method validation

6.8.2.1 Linearity and range

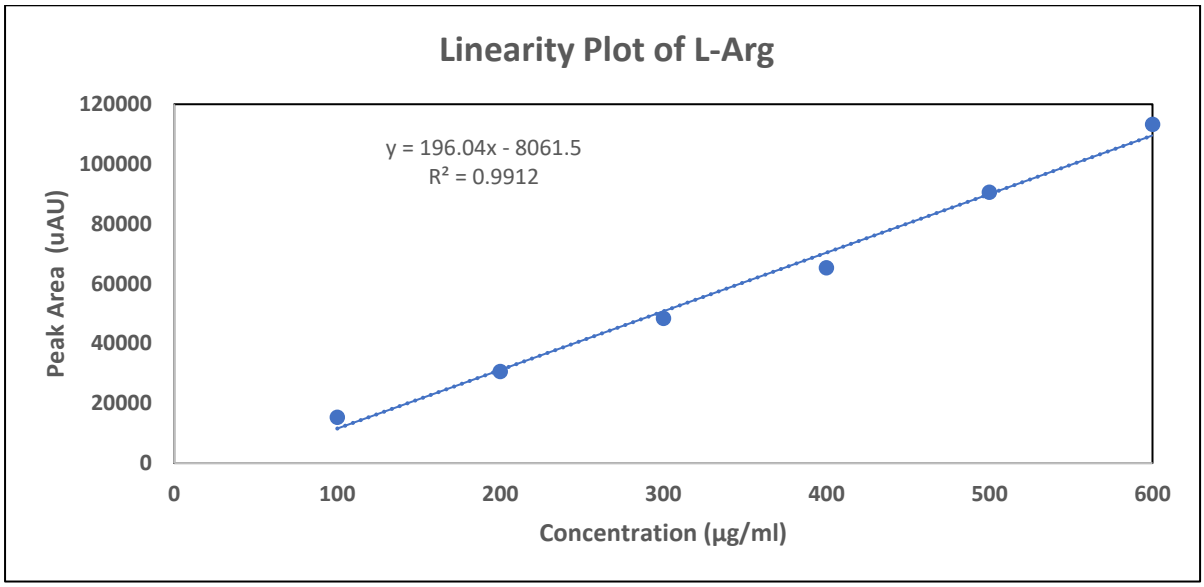

Fig 6. 21 Linearity plot of L-Arg

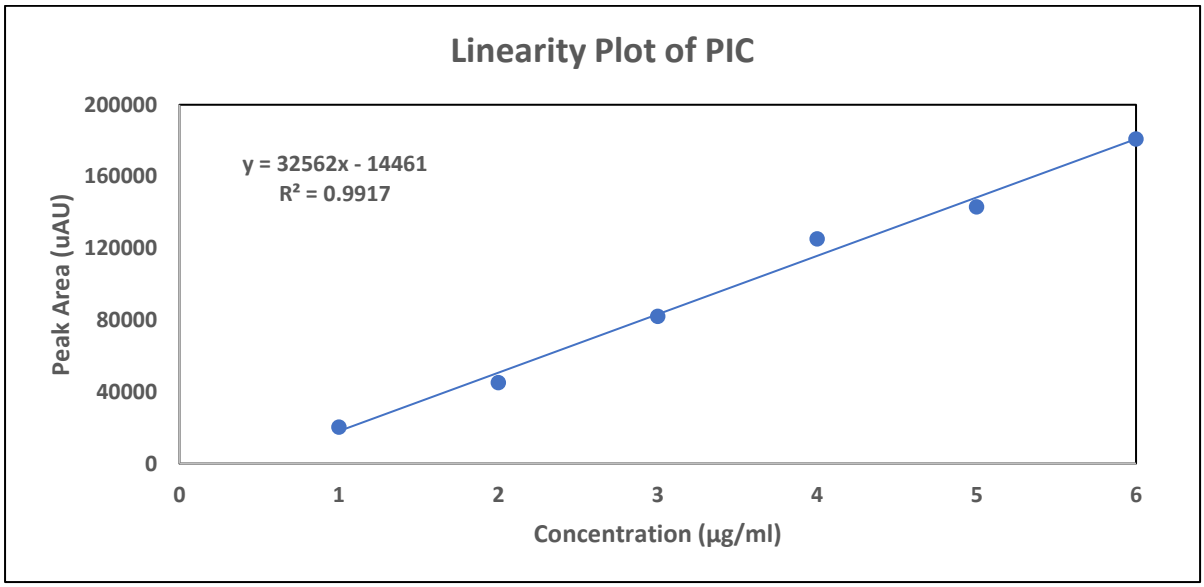

Fig 6. 22 Linearity plot of PIC

Table 6. 18 Data of linearity and range for L-Arg

L-Arg			
Conc. (µg/ml)	**Mean**	**± S.D**	**% RSD**
100	15295	69.30	0.45
200	30610.33	154.45	0.50
300	48421.33	164.39	0.33
400	65234.33	131.12	0.20
500	90551.33	81.09	0.08
600	113192.3	431.80	0.38

Table 6. 19 Data of linearity and range for PIC

PIC			
Conc. (µg/ml)	**Mean**	**±S.D**	**%RSD**
1	20384.67	90.13	0.44
2	45172.67	97.87	0.21
3	82126.67	43.98	0.05
4	125330.7	959.88	0.76
5	143112.3	28.21	0.01
6	180917.3	11.89	0.06

Results

Linearity plot of L-Arg from a range of 100 µg/ml to 600 µg/ml showed R^2 value 0.9912 (Fig 6. 21), which suggested changes in concentration results in a proportional change in the peak area. The % RSD comes out to be less than 2, thus the developed method validated for linearity of L-Arg (Table 6. 18).

Similarly, the linearity plot of PIC from range 1 µg/ml to 6 µg/ml showed an R^2 value of 0.9917 (Fig 6. 22), which suggested changes in concentration results in a proportional change in peak area for PIC. The % RSD comes out to be less than 2, thus the developed method validated for linearity of PIC (Table 6. 19).

6.8.2.2 Accuracy

Table 6. 20 Results of accuracy studies of L-Arg

Accuracy for L-Arg								
Level	**Conc. (µg/ml)**	**Mean Peak area**	**± S.D**	**% RSD**	**Mean Conc. (µg/ml)**	**± S.D**	**% RSD**	**% Recovery**
LQC	80	11279.33	3.51	0.03	98.65	0.01	0.01	123.32
MQC	100	15295	84.87	0.55	119.14	0.43	0.36	119.14
HQC	120	17421.67	124.50	0.71	129.98	0.63	0.48	108.32

Table 6. 21 Results of accuracy studies of PIC

Accuracy for PIC								
Level	**Conc. (µg/ml)**	**Mean Peak area**	**± S.D**	**% RSD**	**Mean Conc. (µg/ml)**	**± S.D**	**% RSD**	**% Recovery**
LQC	0.8	16400.67	240.32	1.46	0.94	0.007	0.77	118.46
MQC	1	20384.67	110.38	0.54	1.07	0.003	0.31	107.01
HQC	1.2	23880.33	70.81	0.29	1.17	0.002	0.18	98.12

Results

The accuracy of the proposed method was determined from the mean percentage recovery of the drug from LQC, MQC and HQC. The data revealed that ranging from 80, 100 and 120 µg/ml for L-Arg (Table 6. 20) and 0.8, 1 and 1.2 µg/ml for PIC (Table 6. 21). The % RSD was below 2%. This reflects the accuracy of the above method for simultaneous estimation of both L-Arg and PIC.

6.8.2.3 Precision

The precision was evaluated by calculating the percentage relative standard deviation of LQC, MQC and HQC at an interday, intraday and Interanalyst level under the same environmental conditions for L-Arg and PIC (Table 6. 22, Table 6. 23). The observed % RSD was less than 2 for all the concentrations. This indicates that the method developed was sufficiently precise.

6.8.2.4 Robustness

The robustness of the method was studied by varying flowrate (0.8, 1.0 and 1.2 ml/min) (Table 6. 24, Table 6. 25).and making observations at different wavelengths (210, 215 and 220 nm). The observed % RSD was found to be less than 2, indicating the method developed is robust and the responses were unaffected by these changes.

6.8.2.5 Solution stability

Solution stability studies indicate till 24 hours the prepared sample remained unaltered as the % recovery for L-Arg and PIC was come out to be 96.12 and 99.1 %, with % RSD less than 2 (Table 6. 26). Thus, the developed method shows sufficient solution stability after 24 hours also.

6.8.2.6 System suitability

The number of theoretical plates, peak purity, peak symmetry, height equivalent to theoretical plates, peak purity index, resolution, LOD and LOQ was measured. All the parameters were found to be within limits (Table 6. 27).

Table 6. 22 Result of precision studies for L-Arg

Intraday	Precision for L-Arg								
Interday		**Conc. (µg/ml)**	**Mean Area**	**± S.D**	**% RSD**	**Mean Conc. (µg/ml)**	**± S.D**	**% RSD**	**% Recovery**
Day 1	**LQC**	80.00	11279.33	3.51	0.03	98.65	0.017	0.018	123.32
	MQC	100.00	15295.00	84.87	0.55	119.14	0.432	0.363	119.14
	HQC	120.00	17421.67	124.50	0.71	129.98	0.635	0.488	108.32
Day 2	**LQC**	80.00	11289.00	68.78	0.60	98.70	0.350	0.355	123.38
	MQC	100.00	15443.00	253.20	1.63	119.89	1.291	1.077	119.89
	HQC	120.00	17281.33	65.43	0.37	129.27	0.333	0.258	107.72
Day 3	**LQC**	80.00	11694.33	278.86	2.38	100.77	1.422	1.411	125.96
	MQC	100.00	15496.00	290.56	1.87	120.16	1.482	1.233	120.16
	HQC	120.00	17460.67	145.51	0.83	130.18	0.742	0.570	108.49
Interanalyst									
Analyst 1	**LQC**	80.00	11279.33	3.51	0.03	98.65	0.017	0.018	123.32
	MQC	100.00	15295.00	84.87	0.55	119.14	0.432	0.363	119.14
	HQC	120.00	17421.67	124.50	0.71	129.98	0.635	0.488	108.32
Analyst 2	**LQC**	80.00	11272.33	64.73	0.57	98.62	0.330	0.334	123.27
	MQC	100.00	15453.33	270.49	1.75	119.94	1.379	1.150	119.94
	HQC	120.00	17268.00	66.09	0.38	129.20	0.337	0.260	107.67
Analyst 3	**LQC**	80.00	11724.33	289.31	2.46	100.92	1.475	1.462	126.15
	MQC	100.00	15517.33	326.58	2.10	120.27	1.665	1.385	120.27
	HQC	120.00	17449.67	197.39	1.13	130.13	1.006	0.773	108.44

Table 6. 23 Result of precision studies for PIC

Intraday	Precision for PIC								
Interday		**Conc. (µg/ml)**	**Mean Area**	**± S.D**	**% RSD**	**Mean Conc. (µg/ml)**	**± S.D**	**% RSD**	**% Recovery**
Day 1	**LQC**	0.80	16400.67	240.32	1.466	0.947	0.007	0.778	118.46
	MQC	1.00	20384.67	110.38	0.544	1.070	0.003	0.316	107.01
	HQC	1.20	23880.33	70.81	0.296	1.177	0.002	0.184	98.12
Day 2	**LQC**	0.80	16310.67	140.34	0.868	0.944	0.004	0.456	118.12
	MQC	1.00	20350.33	124.54	0.614	1.069	0.003	0.357	106.90
	HQC	1.20	23865.00	63.22	0.266	1.176	0.001	0.164	98.08
Day 3	**LQC**	0.80	16365.33	228.38	1.393	0.946	0.007	0.740	118.33
	MQC	1.00	20380.00	136.29	0.667	1.069	0.004	0.391	106.99
	HQC	1.20	23870.33	58.85	0.243	1.177	0.001	0.153	98.09
Interanalyst									
Analyst 1	**LQC**	0.80	16408.33	195.44	1.197	0.947	0.006	0.633	118.49
	MQC	1.00	20412.00	50.23	0.243	1.070	0.001	0.144	107.09
	HQC	1.20	23505.33	293.30	1.247	1.165	0.009	0.772	97.16
Analyst 2	**LQC**	0.80	16460.33	301.99	1.835	0.949	0.009	0.976	118.69
	MQC	1.00	20381.33	103.87	0.507	1.070	0.003	0.298	107.02
	HQC	1.20	23865.00	63.22	0.264	1.176	0.001	0.164	98.08
Analyst 3	**LQC**	0.80	16369.00	229.51	1.402	0.946	0.007	0.744	118.34
	MQC	1.00	20379.00	99.95	0.490	1.069	0.003	0.286	106.99
	HQC	1.20	23889.67	71.66	0.299	1.177	0.002	0.186	98.145

Table 6. 24 Results of robustness using various parameters for L-Arg

Robustness for L-Arg									
Variable	**Value**	**Conc. (µg/ml)**	**Mean Peak Area (uAU)**	**± S.D**	**% RSD**	**Mean Conc. (µg/ml)**	**± S.D**	**% RSD**	**Assay (%w/w)**
Flow rate (ml/min)	0.80	300.00	48421.33	164.39	0.34	288.12	0.84	0.29	96.04
	1.00	300.00	65234.33	131.13	0.20	287.44	0.22	0.08	95.81
	1.20	300.00	90551.33	81.10	0.09	287.48	0.01	0.00	95.83
Wavelength (nm)	210.00	300.00	90551.33	81.10	0.09	287.29	0.32	0.11	95.76
	215.00	300.00	90551.33	81.10	0.09	287.81	0.19	0.07	95.94
	220.00	300.00	90551.33	81.10	0.09	288.03	0.84	0.29	96.01

Table 6. 25 Results of robustness using various parameters for PIC

Robustness for PIC									
Variable	**Value**	**Conc. (µg/ml)**	**Mean Peak Area (uAU)**	**± S.D**	**% RSD**	**Mean Conc. (µg/ml)**	**± S.D**	**% RSD**	**Assay (%w/w)**
Flow rate (ml/min)	0.80	3.00	20384.67	90.13	0.44	2.97	0.00	0.04	98.90
	1.00	3.00	45172.67	97.88	0.22	2.97	0.00	0.05	98.90
	1.20	3.00	82126.67	43.99	0.05	2.97	0.00	0.05	98.88
Wavelength (nm)	210.00	3.00	125330.67	959.88	0.77	2.97	0.00	0.04	98.91
	215.00	3.00	82387.33	275.54	0.33	2.97	0.01	0.28	99.14
	220.00	3.00	82443.33	378.82	0.46	2.98	0.01	0.39	99.20

Table 6. 26 Results of solution stability testing

	Time (hrs)	0	2	4	6	8	12	18	24	Mean	± S.D	% RSD	% Recovery
L-Arg	**Area (uAU)**	48,217	48,217	48,572	48,240	48,517	48,911	48,827	48,263	48,470	264.18	0.55	96.12
	Conc (µg/ml)	287.07	287.08	288.89	287.19	288.61	290.62	290.19	287.31	288.37	1.35	0.47	
PIC	**Area(uAU)**	82,156	82,105	82,105	82,189	82,190	82,678	82,674	82,747	82,355	82356	0.33	99.11
	Conc (µg/ml)	2.97	2.97	2.97	2.97	2.97	2.98	2.98	2.99	2.97	0.01	0.26	

Table 6. 27 Results of system suitability

Parameters	L-Arg	PIC	Acceptance Criteria
Peak Purity	0.92	0.99	Close to 1
Theoretical Plates	2144	13288	>2000
Tailing factor	1.1	1.1	<1.5
Resolution	26.43		>20

Table 6. 28 LOD and LOQ

Value	L-Arg	PIC
LOD (µg/ml)	0.045	0.288
LOQ (µg/ml)	0.138	0.873

6.8.2.7 LOD and LOQ

The LOD and LOQ values for both L-Arg and PIC comes out to be 0.045, 0.288 and 0.138, 0.873 (µg/ml) respectively (Table 6. 28).

6.9 Development of flexi-liposomes

6.9.1 Screening of factors influencing flexi-liposomes

The preliminary screening studies revealed that among material attributes/ process parameters, the amount of soy lecithin and edge activator were highly influential on the studied Critical quality attributes (CQA) such as entrapment efficiency.

Table 6. 29 Effect of Edge activator (Span 60) on entrapment efficiency of flexi-liposomes

Formulation Code	Components				E.E. (%)	
	L-Arg (mg)	PIC (mg)	Soy lecithin (mg)	Span 60 (mg)	L-Arg	PIC
F1	100	1	75	25	8.93±1.67	2.47±1.41
F2	100	1	80	20	4.67±2.01	5.47±1.28
F3	100	1	85	15	10.15±1.72	21.1±2.09
F4	100	1	90	10	5.6±1.82	34.11±1.64

Table 6. 30 Effect of edge activator (SDC) on entrapment efficiency of flexi-liposomes

Formulation Code	Components				E.E. (%)	
	L-Arg (mg)	PIC (mg)	Soy lecithin (mg)	SDC (mg)	L-Arg	PIC
F1	100	1	75	25	28±1.45	39±1.92
F2	100	1	80	20	30±1.93	42±1.21
F3	100	1	85	15	33±2.03	57±1.62
F4	100	1	90	10	32±0.92	60±1.62

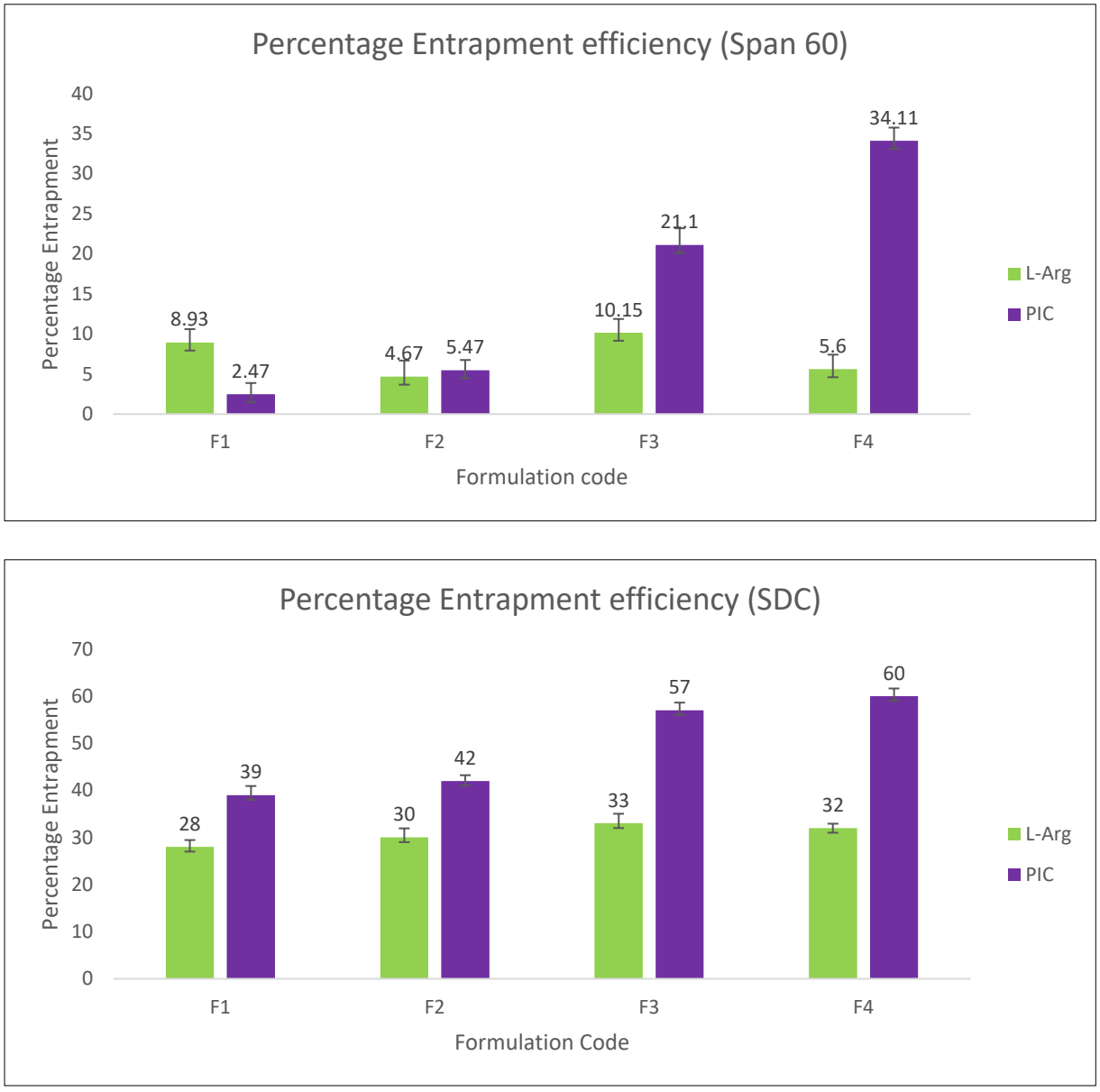

Fig 6. 23 Bar graph representing percentage entrapment of span 60 and SDC in various formulation combination

The other process parameters like temperature of the water bath or speed of the evaporator had only minor effect on the studied CQAs and hence, were kept constant for further studies.

In case of flexi-liposomes prepared from span 60 (Table 6. 29), the entrapment efficiency for L-Arg and PIC was found to be less as compared to when vesicles prepared with SDC (Table 6. 30). In case where span 60 was used, the maximum entrapment efficiency for L-Arg was found to be 10.15 % at 15 mg of surfactant concentration. The maximum entrapment efficiency of PIC was coming out to be 34.11 %. The reason can be predicted from the fact that span 60 has HLB value of 4.3, as the amount of span 60 in vesicle formation was increased from 15% to 25% entrapment of hydrophilic drug decreases. The reason could be low HLB of span 60 or increased pore formation in the vesicles is expected which can lead to leakage of hydrophillic drug.

As far as entrapment of PIC is concerned, being lipophilic drug, its entrapment is primarily affected by lipophilic component of the vesicles. So, increase in concentration of soy lecithin increases entrapment efficiency of PIC. The maximum was found to be 34.11 % when 90 mg of soy lecithin was used.

A similar trend was seen with the use of edge activator SDC with HLB value 16. Use of edge activator at 15 %, shows entrapment of 33 % and this value lowers as the concentration of edge activator increases from 15 % to 25 %. Significantly higher amount of entrapment efficiency with use of SDC can be attributed to the fact that it has higher HLB value.

The entrapment of PIC with the use of SDC as edge activator also seen to improve as compared to span 60 (Fig 6. 23).

Based upon the above observations, the SDC was selected as edge activator to optimize the flexi-liposomal formulation. The effect of process parameter was evaluated on the flexi-liposomes containing 85 mg soy lecithin and 15 mg of SDC (Table 6.31). The process variable such as temperature and speed of rotary evaporator did not have any significant effect on E.E. of both L-Arg and PIC.

Table 6. 31 Effect of process variables on entrapment efficiency of L-Arg and PIC

Components				Process Parameters		E.E. (%)	
L-Arg (mg)	PIC (mg)	Soy lecithin (mg)	SDC (mg)	Speed (RPM)	Temp. (°C)	L-Arg	PIC
100	1	85	15	80	55	33.17±1.92	56.3±1.92
100	1			80	60	33.23±1.23	56.5±1.27
100	1			100	55	33.19±0.92	57.3±1.23
100	1			100	60	33.58±1.26	57.4±1.25
100	1			120	55	33.24±2.01	57.1±1.36
100	1			120	60	33.19±1.92	57.2±0.91

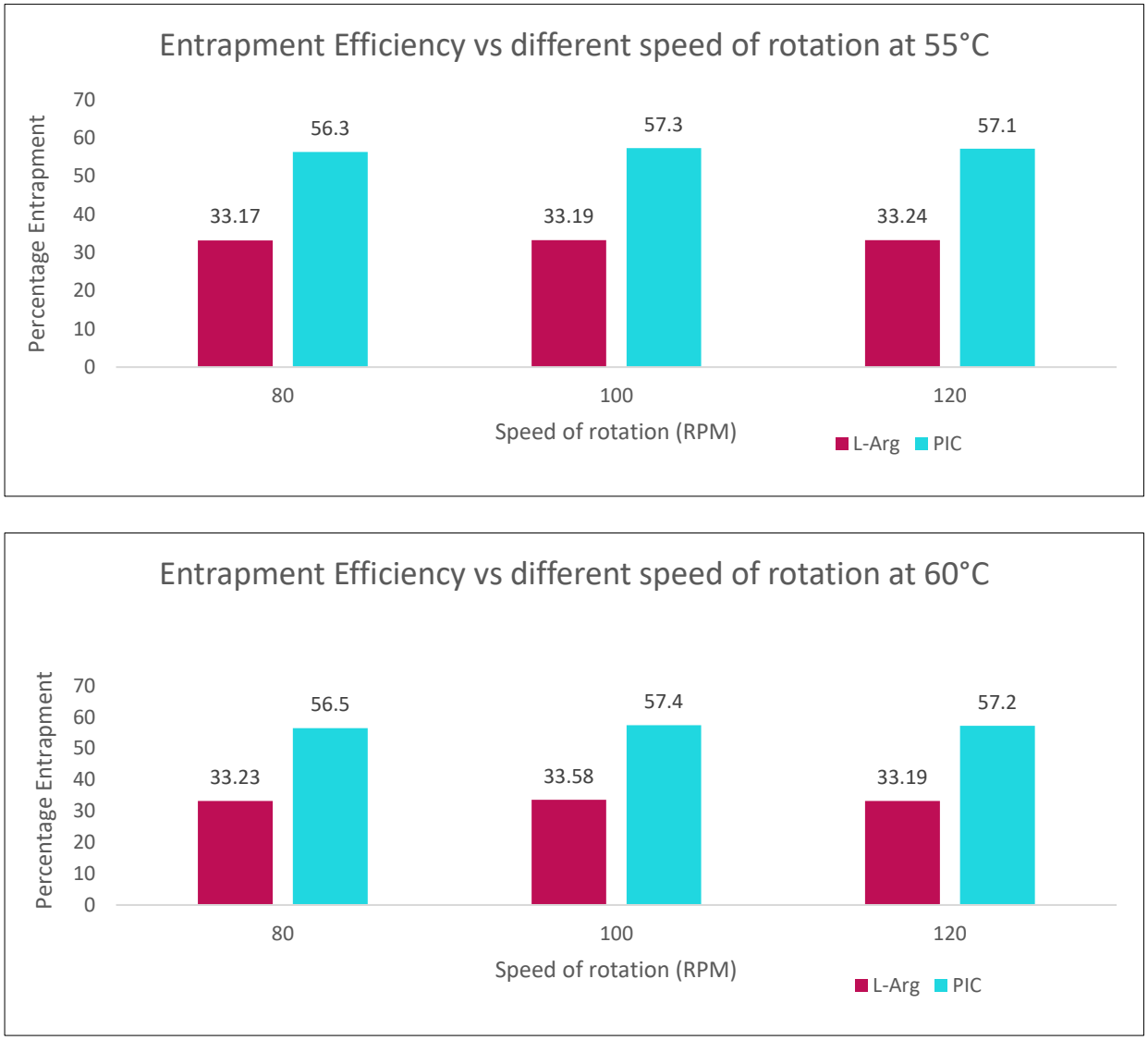

Fig 6. 24 Bar graph of percentage entrapment vs speed of rotation at two different temperatures.

The effects of process parameters like speed of rota-vapor and temperature of water bath were selected to optimize entrapment efficiency (Table 6. 31). These two were chosen to optimize the entrapment efficiency of formulation containing 85 mg of soy lecithin and 15 mg of SDC. These process parameters did not have any significant effect on E.E. on both L-Arg and PIC. Hence, in optimization study, the hydration of dried lipid film was done at 60 °C and speed of rotary evaporator was set at 100 RPM (Fig 6. 24).

6.10 QbD-based formulation optimization studies

The different flexi-liposomal formulations of both L-Arg and PIC in combination were prepared using variable amount of soy lecithin and SDC as suggested by DoE. The obtained responses were well modelled by quadratic function of independent variables (Table 6. 32).

Table 6. 32 Response of CQAs of SDC flexi-liposomes

Run	Factor 1	Factor 2	Response 1	Response 2	Response 3	Response 4	Response 5
	A: Soy Lecithin	B: SDC	Vesicle size	Zeta Potential	PDI	E.E. (L-Arg)	E.E. (PIC)
	mg	mg	nm	mV		%	%
1	85.00	15.00	198.13	-33.47	0.22	33.00	57.70
2	85.00	15.00	198.13	-33.47	0.22	33.00	57.70
3	75.00	25.00	205.80	-40.93	0.44	28.00	39.00
4	95.00	5.00	190.00	-38.93	0.44	23.00	65.00
5	85.00	15.00	198.13	-33.47	0.22	33.00	57.70
6	95.00	25.00	213.53	-14.10	0.18	27.00	45.30
7	85.00	15.00	198.13	-33.47	0.22	33.00	57.70
8	85.00	15.00	198.13	-33.47	0.22	33.00	57.70
9	85.00	29.14	212.60	-36.87	0.44	28.00	18.00
10	75.00	5.00	218.17	-41.10	0.16	27.00	63.00
11	85.00	0.86	189.20	-39.57	0.38	13.00	70.00
12	99.14	15.00	202.23	-37.83	0.21	35.00	59.00
13	70.86	15.00	241.15	-39.03	0.51	30.00	54.00

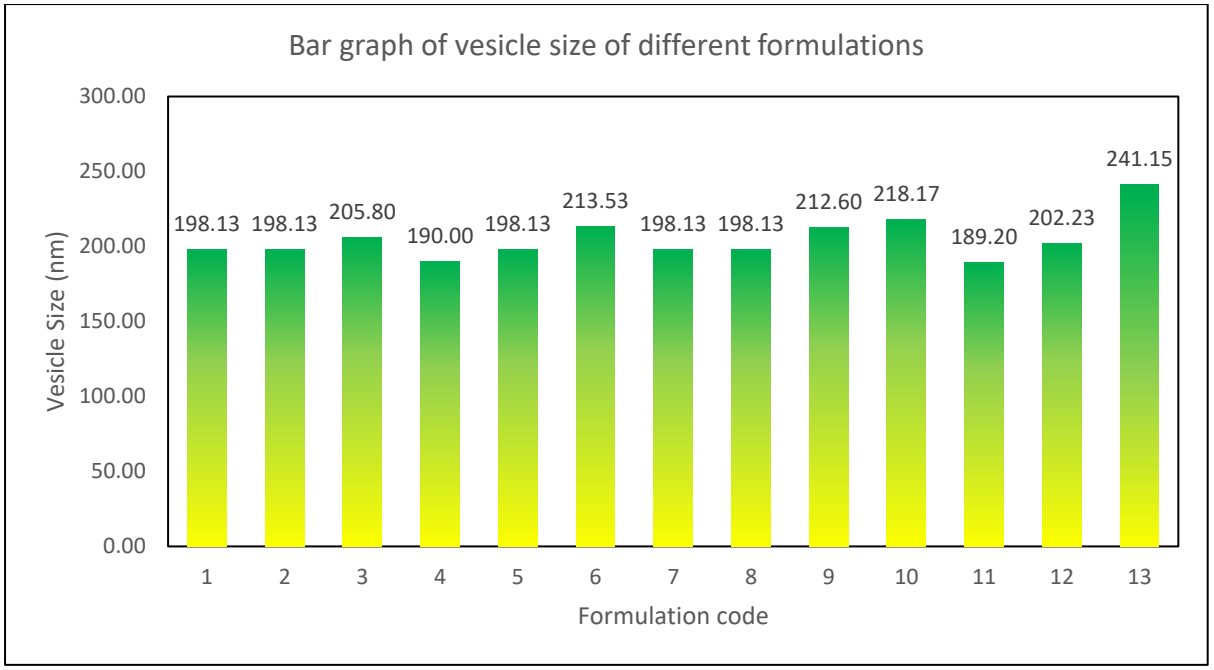

Fig 6. 25 Bar graph of vesicle size vs various formulations

The maximum vesicle size was 241.15 nm (run 13) and minimum was found to be 189.20 nm (run 11) (Fig 6. 25). It was observed that increase in surfactant concentration causes increase in vesicle size in general, which could be due to interdigitation developed due to presence of surfactant and as the surfactant is increased this causes fusion of smaller vesicles with each other, causing formation of bigger vesicles.

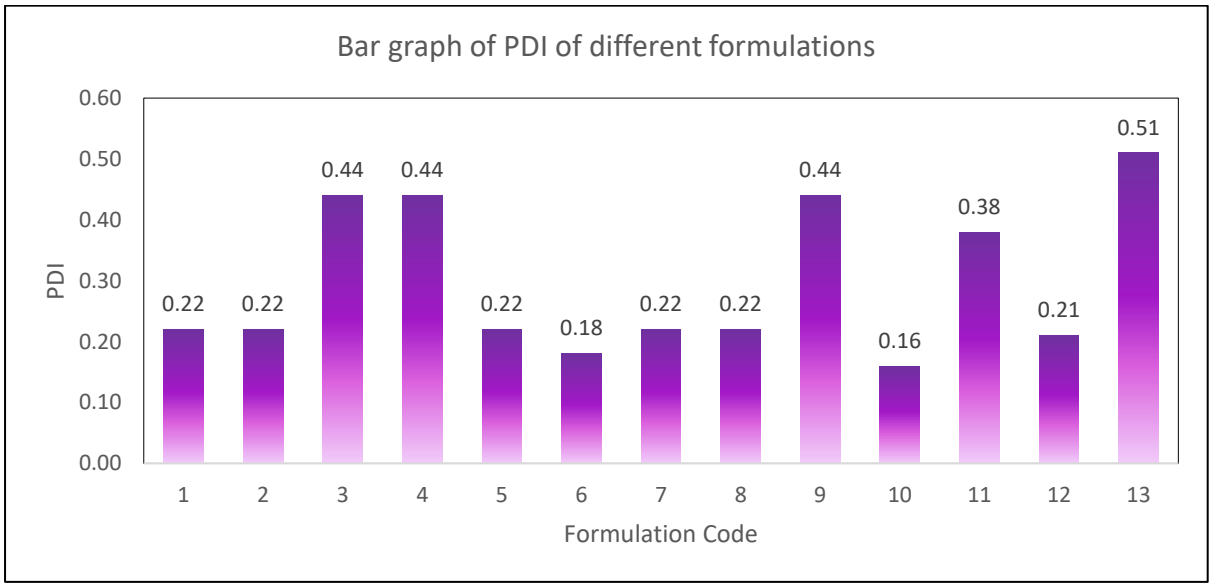

Fig 6. 26 Bar graph of PDI vs various formulations

The minimum PDI was observed as 0.16 (run 10) and maximum was found to be 0.51 (run 13) (Fig 6. 26). PDI describe distribution pattern of the particles. As in case of run 13, where wider

PDI was observed along with larger average particle size is observed, faster sedimentation is expected owing to instability. Whereas in case of run 10, PDI shows proximity of average particle diameter to its median diameter. Hence, indicates better chances of stability.

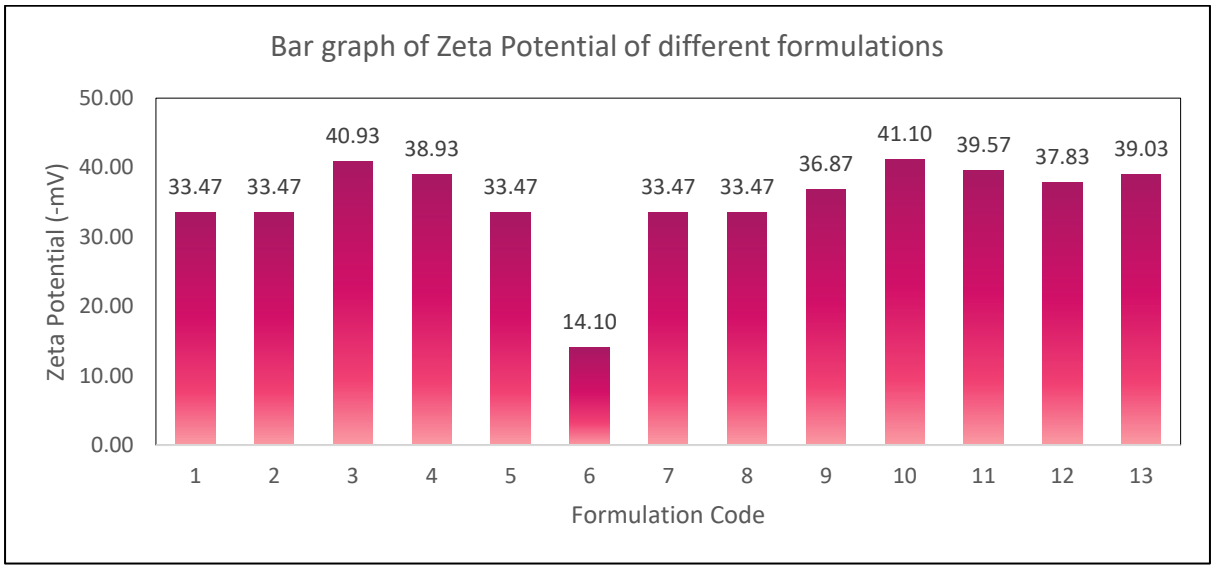

Fig 6. 27 Bar graph of zeta potential vs various formulations

The zeta potential was found to be -14.1 mV for run 6 and maximum found to be 41.1mV (Fig 6. 27). The entrapment efficiency for PIC was found to be maximum of 70% and minimum of 18 %. The entrapment efficiency of lipophilic drug is increases as the amount of hydrophilic surfactant is decreased. Presence of high amount of soy lecithin increases the entrapment efficiency of lipophilic drug proportionally. Whereas, in case of L-Arg maximum and minimum entrapment efficiency was found to be 35 % and 13% (Fig 6. 28). In case of entrapment of hydrophilic drug L-Arg the right balance of soy lecithin to surfactant is required, as high amount of surfactant may make the vesicles leaky. Thus optimum ratio of soy lecithin to surfactant ratio plays role in predicting the entrapment efficiency of L-Arg. The ratio of maximum to minimum for particle size, PDI. zeta potential, entrapment efficiency of L-Arg and PIC was found to be 1.27, 3.18, 2.91, 2.69 and 3.88 respectively. Since, these values were less than 10, power transformation was not required in case of both the formulations.

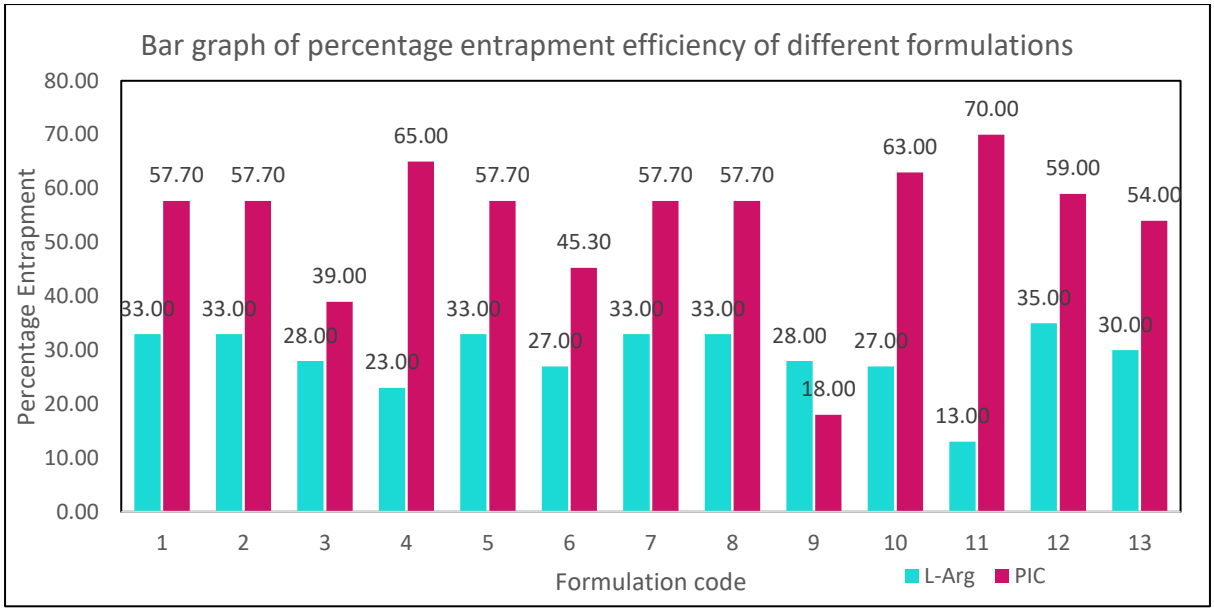

Fig 6. 28 Bar graph of percentage entrapment vs various formulations

The DoE tools, such as fit summary, sequential model sum of squares, lack of fit tests, and model summary statistics, were used to perform a statistical analysis of the model (Table 6. 33). The prob >F value of P <0.0001, the high R-Squared value, the low standard deviation, and the reduced predicted residual error sum of square (PRESS) value suggested using the quadratic model for all of the responses when analyzing. ANOVA was used to determine the significance and size of the effects of the key factors and their interaction (Table 6. 34). The F-Value was discovered to be 11.71, 5.30, 5.35, 10.06, and 22.20 for the replies of Y1, Y2, Y3, Y4, and Y5. The P-value was found to be <0.05, which indicates the model was significant.

Adequate precision measures the S/N ratio. The Adequate precision values for responses were found to be 11.77, 7.44, 7.41, 9.39 and 14.65 respectively. All values were found to be more than 4, indicating model adequacy and hence, has been used to investigate the design space. The difference between adjusted R^2 value and predicted R^2 value was found to be less than 2 for all responses. Model prob >F was less than 0.05, indicating adequacy of quadratic model.

Table 6. 33 Fit summary and ANOVA for vesicle size (Y_1), Zeta potential (Y_2), PDI (Y_3), E.E L-Arg (Y_4) and E.E-PIC (Y_5)

Fit summary															
Source	**Sequential p-value**					**Adjusted R^2**					**Predicted R^2**				
	Y_1	**Y_2**	**Y_3**	**Y_4**	**Y_5**	**Y_1**	**Y_2**	**Y_3**	**Y_4**	**Y_5**	**Y_1**	**Y_2**	**Y_3**	**Y_4**	**Y_5**
Linear	0.071	0.0925	0.5309	0.315	0.0002	0.293	0.2546	-0.0572	0.0476	0.7763	-0.1997	-0.3489	-0.7779	-0.5469	0.6217
2FI	0.131	0.0315	0.0235	0.81	0.7532	0.3988	0.5184	0.3556	-0.0511	0.7543	-0.0699	-0.2448	-0.137	-0.9716	0.5335
Quadratic	0.0065	0.7003	0.0517	0.0015	0.0189	0.8169	0.4407	0.6446	0.7905	0.8983	0.2403	-1.3202	-0.4743	0.1309	0.5781
Cubic	0.0098	0.0222	0.0659	< 0.0001	0.0056	0.9597	0.8294	0.8324	0.9993	0.9822	-0.0735	-3.5503	-3.4697	0.9809	0.5245

Sequential Model Sum of Squares [Type I]															
Source	**Sum of Squares**					**df**					**Mean Square**				
	Y_1	**Y_2**	**Y_3**	**Y_4**	**Y_5**	**Y_1**	**Y_2**	**Y_3**	**Y_4**	**Y_5**	**Y_1**	**Y_2**	**Y_3**	**Y_4**	**Y_5**
Mean vs Total	5.4456 E+05	15974.74	1.15	10875.08	37886.4	1	1	1	1	1	5.456 E+05	15974.74	1.15	10875.08	37886.4
Linear vs Mean	956.96	221.6	0.0218	86.43	1747.66	2	2	2	2	2	478.48	110.8	0.0109	43.21	873.83
2FI vs Linear	322.20	152.03	0.0729	2.25	4.62	1	1	1	1	1	322.20	152.03	0.0729	2.25	4.62
Quadratic vs 2FI	801.49	20.45	0.0506	279.05	268.41	2	2	2	2	2	400.75	10.22	0.0253	139.52	134.2
Cubic vs Quadratic	209.79	149.26	0.0252	51.07	111.49	2	2	2	2	2	104.89	74.63	0.0126	25.54	55.74
Residual	39.07	41.59	0.0128	0.125	15.96	5	5	5	5	5	7.81	8.32	0.0026	0.025	3.19
Total	5.480E+05	16559.67	1.33	11294	40034.54	13	13	13	13	13	42151.54	1273.82	0.1023	868.77	3079.58

Sequential Model Sum of Squares [Type I]										
Source	**F-value**					**p-value**				
	Y_1	**Y_2**	**Y_3**	**Y_4**	**Y_5**	**Y_1**	**Y_2**	**Y_3**	**Y_4**	**Y_5**
Mean vs Total										
Linear vs Mean	3.49	3.05	0.6751	1.3	21.82	0.0710	0.0925	0.5309	0.315	0.0002
2FI vs Linear	2.76	6.48	7.41	0.0613	0.1051	0.1310	0.0315	0.0235	0.81	0.7532
Quadratic vs 2FI	11.27	0.375	4.66	19.08	7.37	0.0065	0.7003	0.0517	0.0015	0.0189
Cubic vs Quadratic	13.42	8.97	4.92	1021.45	17.46	0.0098	0.0222	0.0659	< 0.0001	0.0056
Residual										
Total										

Lack of Fit Tests															
Source	**Sum of Squares**					**df**					**Mean Square**				
	Y_1	**Y_2**	**Y_3**	**Y_4**	**Y_5**	**Y_1**	**Y_2**	**Y_3**	**Y_4**	**Y_5**	**Y_1**	**Y_2**	**Y_3**	**Y_4**	**Y_5**
Linear	1372.55	363.33	0.1615	332.5	400.48	6	6	6	6	6	228.76	60.55	0.0269	55.42	66.75
2FI	1050.35	211.3	0.0886	330.25	395.85	5	5	5	5	5	210.07	42.26	0.0177	66.05	79.17
Quadratic	248.86	190.85	0.038	51.2	127.45	3	3	3	3	3	82.95	63.62	0.0127	17.07	42.48
Cubic	39.07	41.59	0.0128	0.125	15.96	1	1	1	1	1	39.07	41.59	0.0128	0.125	15.96
Pure Error	0	0	0	0	0	4	4	4	4	4	0	0	0	0	0

Model Summary Statistics															
Source	**Std. Dev.**					**R^2**					**Adjusted R^2**				
	Y_1	**Y_2**	**Y_3**	**Y_4**	**Y_5**	**Y_1**	**Y_2**	**Y_3**	**Y_4**	**Y_5**	**Y_1**	**Y_2**	**Y_3**	**Y_4**	**Y_5**
Linear	11.72	6.03	0.1271	5.77	6.33	0.4108	0.3789	0.119	0.2063	0.8136	0.293	0.2546	-0.0572	0.0476	0.7763
2FI	10.8	4.85	0.0992	6.06	6.63	0.5491	0.6388	0.5167	0.2117	0.8157	0.3988	0.5184	0.3556	-0.0511	0.7543
Quadratic	5.96	5.22	0.0737	2.7	4.27	0.8932	0.6737	0.7927	0.8778	0.9407	0.8169	0.4407	0.6446	0.7905	0.8983
Cubic	2.8	2.88	0.0506	0.1581	1.79	0.9832	0.9289	0.9302	0.9997	0.9926	0.9597	0.8294	0.8324	0.9993	0.9822

Model Summary Statistics										
Source	**Predicted R^2**					**PRESS**				
	Y_1	**Y_2**	**Y_3**	**Y_4**	**Y_5**	**Y_1**	**Y_2**	**Y_3**	**Y_4**	**Y_5**
Linear	-0.1997	-0.3489	-0.7779	-0.5469	0.6217	2794.79	789.01	0.3258	648.02	812.64
2FI	-0.0699	-0.2448	-0.137	-0.9716	0.5335	2492.31	728.12	0.2084	825.94	1002
Quadratic	0.2403	-1.3202	-0.4743	0.1309	0.5781	1769.66	1357.16	0.2702	364.07	906.29
Cubic	-0.0735	-3.5503	-3.4697	0.9809	0.5245	2500.66	2661.58	0.8192	8	1021.52

Table 6. 34 Summary of ANOVA of CCD for optimized formulation

*Indicates statistical significance at P<0.05.

Responses	Regression Parameters		Observed P-value*
	R^2	F_{cal}	
Vesicle Size	0.893	11.71	0.0027
Zeta Potential	0.6388	5.3	0.0222
PDI	0.7927	5.35	0.0242
%E.E.(L-Arg)	0.877	10.06	0.0043
%E.E.(PIC)	0.9407	22.2	0.0004

DoE software determined the final mathematical model in terms of coded factors (Y_1 to Y_5) as shown below. The positive sign in equation indicated the synergistic effect, whereas the negative sign indicates an antagonistic effect.

Y_1 (Vesicle Size) = + 198.13 - 9.44A + 5.53B + 8.98AB + 10.67A^2 + 0.2800B^2

Y_2 (Zeta potential) = -35.05 + 3.84A + 3.60B + 6.16AB

Y_3 (PDI) = + 0.2200 - 0.0505A + 0.0131B - 0.1350AB + 0.0500A^2 + 0.0750B^2

Y_4 (%E.E L-Arg) = + 33.00 + 0.2589A+ 3.28B + 0.7500AB - 0.3125A^2 - 6.3B^2

Y_5 (%E.E PIC) = +57.70 + 1.92A - 14.65B + 1.08AB + 0.1062A^2 -6.14B^2

In case of Y1, negative coefficient of A and positive coefficient of B indicated an increase in vesicle size at lower level of phospholipids and higher level of surfactant. This can be attributed to the fact that SDC has higher radius of curvature and incorporation of this into phospholipids will increases the interdigitations at the boundary which further increase particle size. Further at still higher concentrations of surfactant, fusion of vesicles may take place, which give rise to higher vesicle size. This is evident as run 11 having 99 % phospholipid content have the smallest particle size. Similar trend in seen in PDI, as the vesicle size increases, the dispersion becomes poor due to coalescence of the vesicles. In case of zeta potential, phospholipids and SDC both have positive coefficient, indicating increase in zeta potential with increase in amount of the both. Entrapment efficiency of L-Arg is altered positively with both the factors but effect of surfactant concentration is more evident than phospholipids. Whereas, in case of PIC increase in amount of phospholipids increase entrapment efficiency of PIC.

The perturbation plots were also plotted to understand the effect of factors on responses. The flat lines indicate no/minimal effect of factor on responses, whereas deep curvature indicates significant effect. As depicted in Fig 6. 31, Concentration of SDC has greater effect on PDI,

and entrapment efficiency of both L-Arg and PIC. Whereas, the number of phospholipids is greatly affecting the vesicles size than SDC.

In case of vesicle size, greater deviation from reference point is seen for factor A i.e. phospholipids. Which indicates that phospholipids have greater impact in determining the vesicle size as compared to SDC. whereas, perturbation plot for zeta potential indicates linear and predictable impact on stability of the vesicles (Fig 6. 29 (A, B)).

Plot for PDI signifies that both the factors show slight deviation from reference point. This indicates that, vesicle size distribution is affected both by the phospholipids and edge activator i.e., SDC. the deviation from reference point is opposite for both the factors as suggested by the equation, but factor B shows greater deviation as it has a factor of 0.0131 as compare to -0.0505 (Fig 6. 29 C).

The entrapment efficiency of L-Arg and PIC gets affected with the amount of SDC in the vesicles (Fig 6. 29 (D, E)). The only difference is that in case of L-Arg both the factors have similar effect but SDC has more impact in predicting the E.E. while E.E of PIC is altered conversely to each other with both the factors but factor B is more significant.

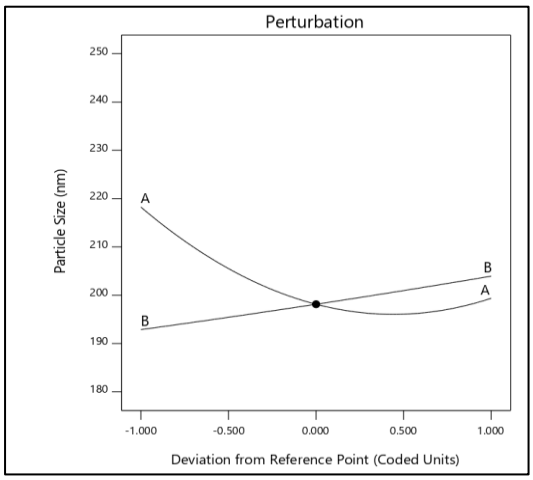

(A)

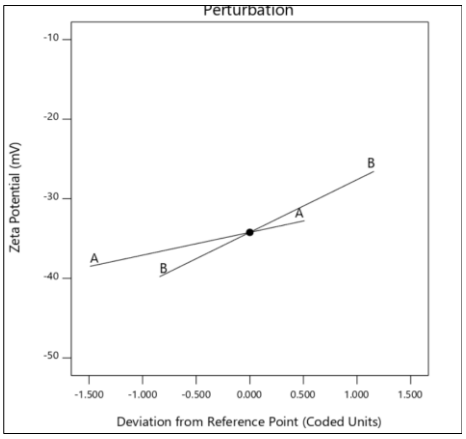

(B)

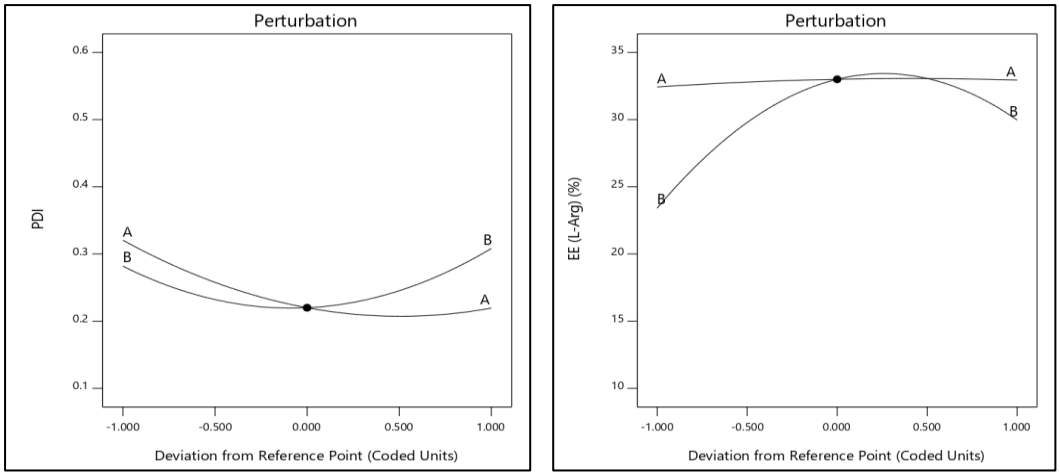

(C) (D)

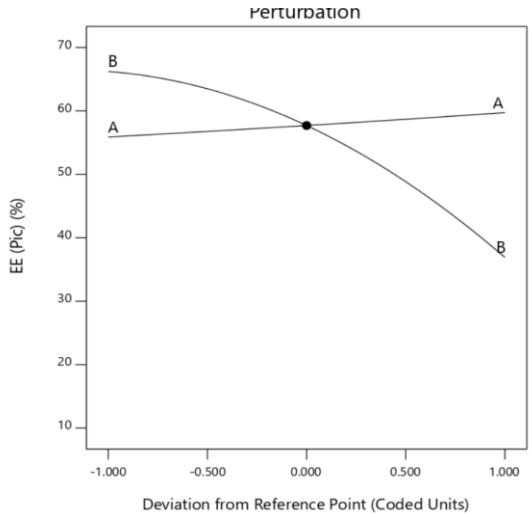

(E)

Fig 6. 29 Perturbation plot for vesicle size (A), zeta potential (B), PDI (C), entrapment efficiency of L-Arg (D), and entrapment efficiency of PIC (E) of optimized formulation.

The obtained polynomial equations helped in plotting 2D contour plots and 3D response surface plots and results were found in concordance with the obtained polynomial equations.

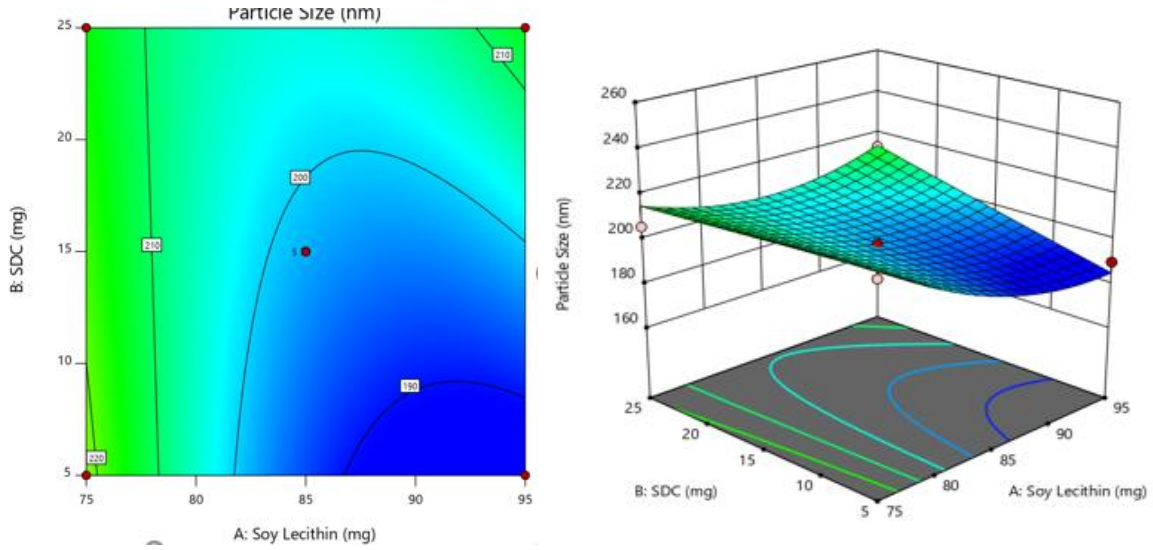

(A) (B)

Fig 6. 30 2D contour plot (A) and 3D response surface plots (B) for vesicle size

The effect on vesicles size is predominantly controlled by phospholipids than SDC (Fig 6. 30). At concentrations above 85 % of phospholipids, vesicle size is expected to decrease i.e. at higher phospholipids and at lower amount of edge activator. Interaction plot indicates, both factors play their role in vesicles size determination with low interaction of each other. Whereas, at soy lecithin concentration below 85 %, both factors show strong interplay of interactions to have impact on vesicle size.

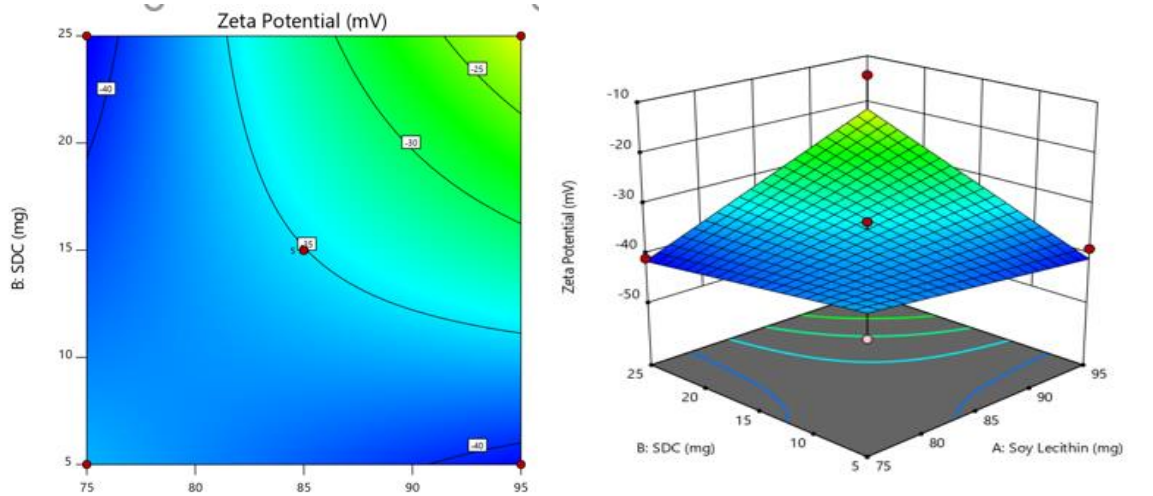

(A) (B)

Fig 6. 31 2D contour plot (A) and 3D response surface plots (B) for zeta potential

For zeta potential, both factors play the role to impart stability to the vesicles. Therefore, both the factors are important to impart stability to dispersion (Fig 6. 31).

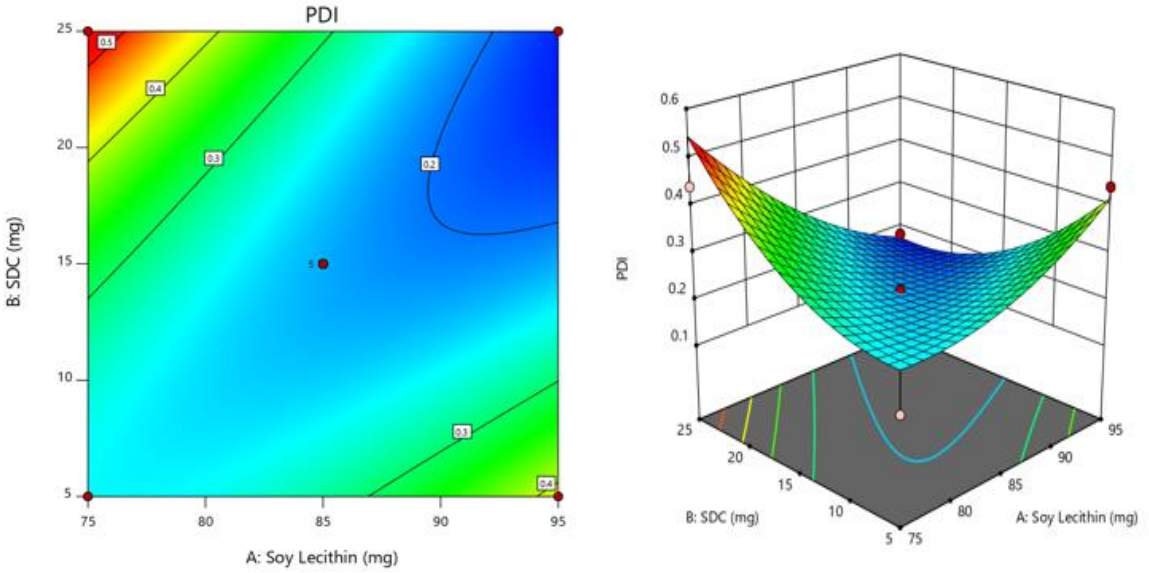

(A) (B)

Fig 6. 32 2D contour plot (A) and 3D response surface plots (B) for PDI

Like vesicle size, the impact of both the factors is seen on PDI (Fig 6. 32). The effect is more significant when the amount of phospholipids and edge activator is increased beyond 85 mg and 15 mg respectively. Although, the impact is less significant but similar when the concentrations of both the factors decreased linearly.

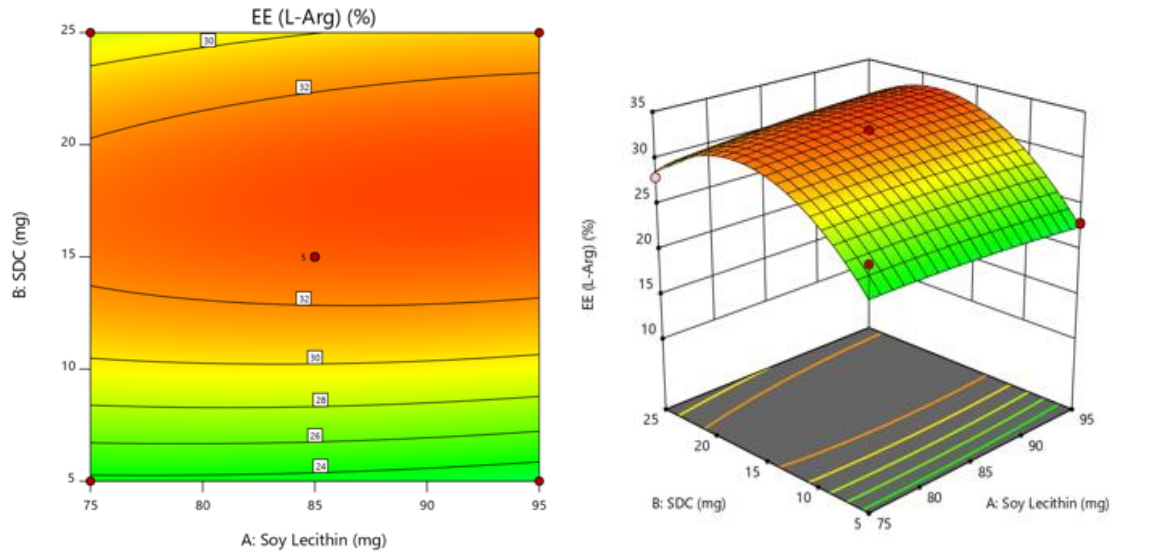

(A) (B)

Fig 6. 33 2D contour plot (A) and 3D response surface plots (B) for entrapment efficiency of L-Arg.

In case of E.E of L-Arg (Fig 6. 33), edge activator has greater impact than soy lecithin. In case of E.E. of PIC (Fig 6. 34), the impact of SDC is comparatively more but decreases drastically when the amount of SDC increases beyond 15 mg in the formulation.

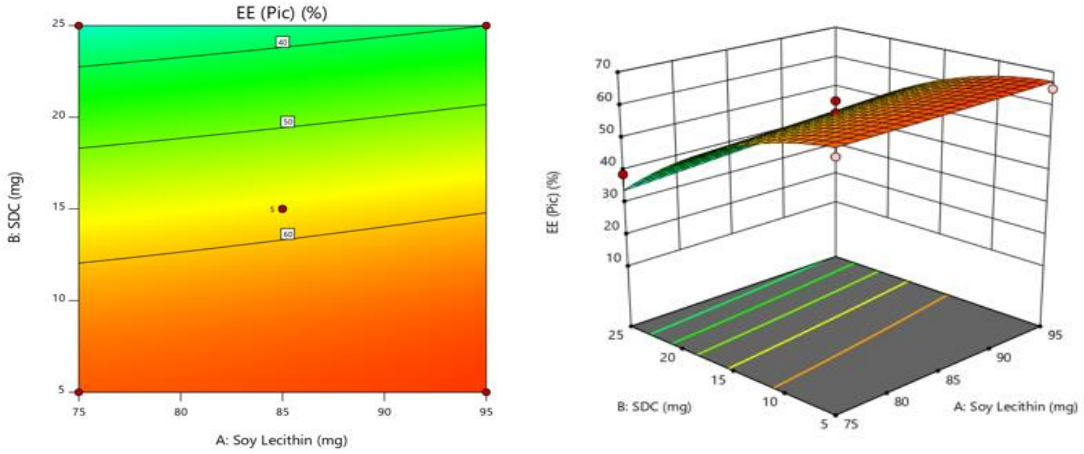

(A) (B)

Fig 6. 34 2D contour plot (A) and 3D response surface plots (B) for entrapment efficiency of PIC.

6.11 Optimized formulation and validation studies

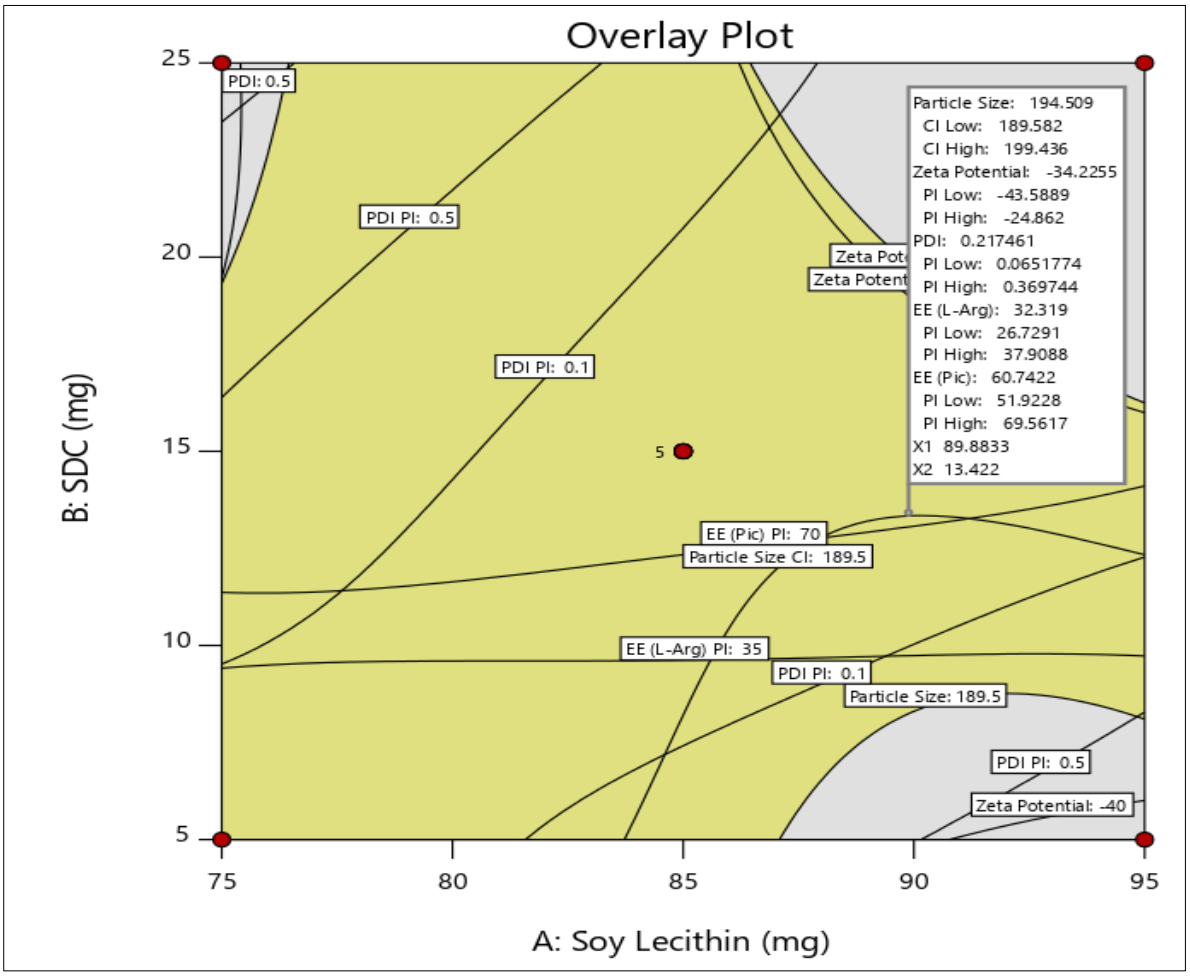

Fig 6. 35 Overlay plot indicating the location of optimized flexi-liposomal formulation

The optimised overlay plot was identified using DoE software (Fig 6. 35). The CCD model predicted particle size as 194.509 nm, zeta potential -34.22 Mv, PDI as 0.217, E.E for L-Arg as 32.3 % and for PIC as 60.74 %. By applying graphical optimisation model, the best fit optimum formulation was selected containing 89.8 mg soy lecithin and 13.42 mg of SDC. Figure 6. 35 depicts the optimised formulation in the overlay plot in demarcated optimal area. Comparison of the experimental and predicted responses along with the percentage error is listed in Table 6. 35. The percentage error ranged between -7.3 % and 8.35 %, i.e., well within ±10%. The data showed that most of the predicted values were close to the experimental values with correlation coefficient positive 0.6913. This indicated the excellent prognostic ability of the experimental design employed for the optimization of flexi-liposomal formulation of L-Arg and PIC.

6.11.1 Evaluation of vesicle size, zeta potential, PDI and entrapment efficiency

Table 6. 35 Validation of experimental results with predicted values and percentage error

Response	Predicted value	Average Experimental value	% Error
Vesicle size (nm)	194.5	194.7	0.10
Zeta potential (mV)	-34.22	-36.1	5.42
PDI	0.217	0.216	-0.46
% E.E (L-Arg)	32.3	35	8.35
% E.E (PIC)	60.74	56.3	-7.3

6.11.2 Degree of deformability of the optimized flexi-liposomal vesicles

Deformability index and elasticity were chosen to access the flexibility of vesicles. Table 6. 36 indicates the before and after vesicle size of optimised Flexi-liposomes. Ideal deformability index value is 1 as it indicates complete reformability of the vesicles after stress is induced. The Table 6. 36 indicates deformability index of optimised vesicles is 0.929 which indicates the vesicles have good reformability after passing through 100 nm polycarbonates membrane filter.

Table 6. 36 Observations of degree of deformability

Vesicle size before extrusion	Vesicle size after extrusion	Deformability Index	Elasticity
182.9±0.01	181.2±0.01	0.929	1.72

6.11.3 Drug loading in final formulation

The drug loading in optimized formulation was calculated as Table 6. 37.

Table 6. 37 Drug loading calculation

Formulation	Drug loading (% w/w)	References
Flexi-Liposomal suspension	56.3	(Wang et al., 2015) (Srisuwan & Baimark, 2014)
Flexi-Liposomal gel	0.02	(Vaghasiya, Kumar, & Sawant, 2013)

6.12 Preparation of secondary vehicle/gel

6.12.1 Characterization of the Optimised Flexi-liposomal Gel

The analysis of the optimized flexi-liposomal gel was prepared and evaluated for flowablity and homogeneity. The prepared hydrogel made from Carbopol gel was selected as base and showed sufficient clarity, neutral pH and viscosity as mentioned in the Table 6. 38.

Table 6. 38 Physicochemical evaluations of prepared optimized gel

Formulation	Appearance	pH	Viscosity (CPS)
Optimized Flexi-liposomal gel	Clear	7.8 ± 0.20	312800 ± 2437.5

6.13 *In vitro* release studies of optimized flexi-liposomal gel

Table 6. 39 *In vitro* release data of PIC and L-Arg solution incorporated in gel formulation

Sr. No.	Time (hrs)	% Release (L-Arg)	% Release (PIC)
1	0	0	0
2	0.25	48.4 ± 0.41	27 ± 0.61
3	0.5	59.2 ± 0.38	48 ± 0.34
4	1	74 ± 0.62	65 ± 0.72
5	2	89 ± 0.48	78 ± 0.72
6	3	97 ± 0.41	92 ± 0.41

Table 6. 40 *In vitro* release data of PIC and L-Arg from flexi-liposomal gel

Sr. No.	Time (hrs)	% Release (L-Arg)	% Release (PIC)
1	0	0	0
2	0.5	33.72 ± 0.09	28.47 ± 0.31
3	2	60.56 ± 0.18	47.28 ± 0.42
4	6	69.04 ± 0.25	61.67 ± 0.18
5	24	75.67 ± 0.07	82.70 ± 0.50
6	48	78.44 ± 0.41	86.19 ± 0.45

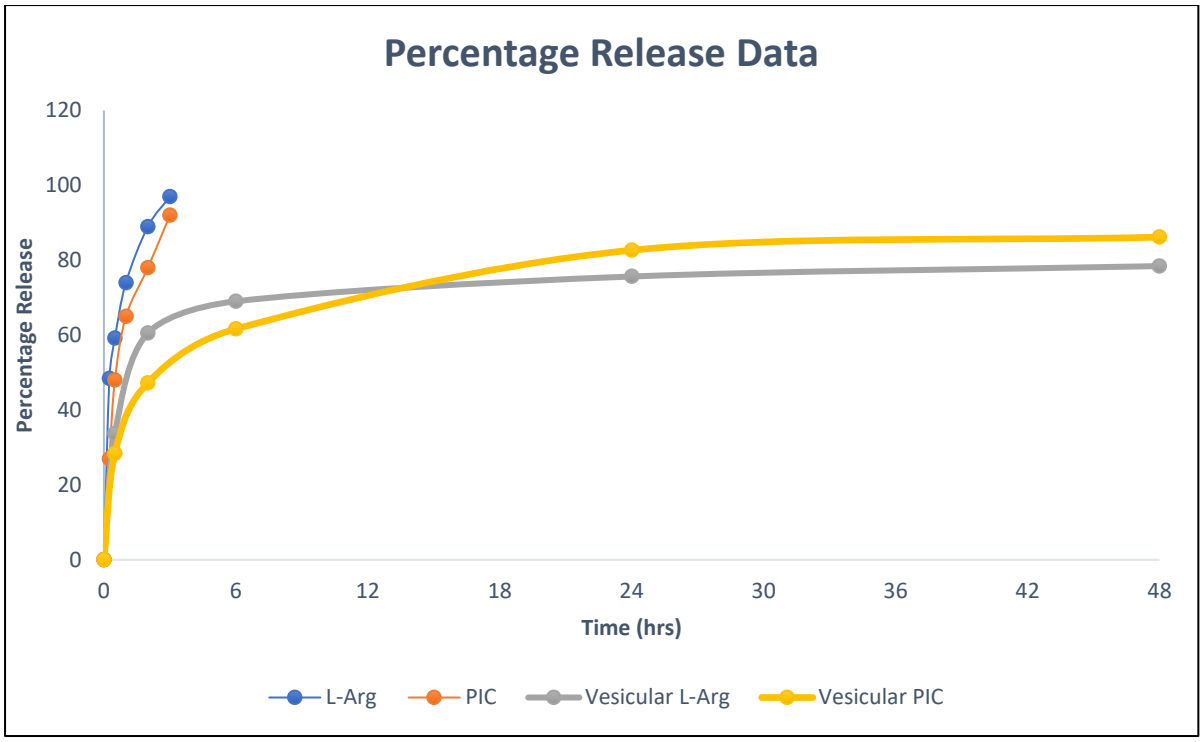

Fig 6. 36 Percentage release data of gel containing drug solutions and optimized flexi-liposomal gel

Table 6. 41 Time dependent drug release data

	Time taken (mins)			
	Gel containing PIC-L-Arg solution		Flexi-liposomes Gel	
	L-Arg	PIC	L-Arg	PIC
$DR_{25\%}$	<15	15	<30	<30
$DR_{50\%}$	15	30	120	120
$DR_{75\%}$	60	120	1440	1320
$DR_{100\%}$	180	180	>2880	>2880

Results

In vitro release data of optimized gel containing flexi-liposomes is compared with the combination of free drug solution in Carbopol gel. The results indicated that gel containing drug solution showed rapid release of the drug from donor to receiver compartment. As evident from the time dependent drug release data, it takes less than 15 mins for both L-Arg and PIC to release from the gel matrix and a maximum of 3 hours for both L-Arg and PIC to completely diffuse to the receiver's compartment (Table 6. 39). Whereas, in case of optimized flexi-liposomal gel (Table 6. 40), $DR_{25\%}$ was observed at almost 30 min of drug loading. $DR_{50\%}$ took 2 hrs for both L-Arg and PIC (Table 6. 41). Here after, a plateau release was observed extending upto 48 hrs, since initial dose. When compared with gel containing drug solution, it became conclusive that gel containing flexi-liposomes showed prolonged release, as it takes more than 2880 min for $DR_{100\%}$, which is almost 180 min for gel containing drug solution (Fig 6. 36).

6.13.1 Analysis of drug release mechanism

6.13.1.1 In vitro drug release data

Table 6. 42 *In vitro* drug release data of L-Arg

Sr. No	Time (hrs)	Log time	Square root of time	Cumulative % DR	Cumulative % drug remaining	log % drug remaining	Fraction DR	log fraction DR	Fraction drug remaining (Mt)	Initial Drug Conc (Mo)	(Mo)^1/3	(Mt)^1/3	(Mo)^1/3 - (Mt)^1/3
1	0.5	-0.30	0.71	33.72	66.28	1.82	0.34	-0.47	0.66	100	4.64	0.87	3.77
2	2	0.30	1.41	60.56	39.44	1.60	0.61	-0.22	0.39	100	4.64	0.73	3.91
3	6	0.78	2.45	69.04	30.96	1.49	0.69	-0.16	0.31	100	4.64	0.68	3.97
4	24	1.38	4.90	75.67	24.33	1.39	0.76	-0.12	0.24	100	4.64	0.62	4.02
5	48	1.68	6.93	78.44	21.56	1.33	0.78	-0.11	0.22	100	4.64	0.60	4.04

Table 6. 43 *In-vitro* drug release data of PIC

Sr. No.	Time (hrs)	Log time	Square root of time	Cumulative % DR	Cumulative % drug remaining	log % drug remaining	Fraction DR	log fraction DR	Fraction drug remaining (Mt)	Initial Drug Conc (Mo)	(Mo)^1/3	(Mt)^1/3	(Mo)^1/3 - (Mt)^1/3
1	0.5	-0.30	0.71	28.46	71.53	1.85	0.28	-0.55	0.72	100	4.64	0.89	3.75
2	2	0.30	1.41	47.27	52.72	1.72	0.47	-0.33	0.53	100	4.64	0.81	3.83
3	6	0.78	2.45	61.66	38.33	1.58	0.62	-0.21	0.38	100	4.64	0.73	3.92
4	24	1.38	4.90	82.69	17.30	1.24	0.83	-0.08	0.17	100	4.64	0.56	4.08
5	48	1.68	6.93	86.18	13.81	1.14	0.86	-0.06	0.14	100	4.64	0.52	4.12

6.13.1.1.1 Analysis of release mechanism of L-Arg from optimized gel:

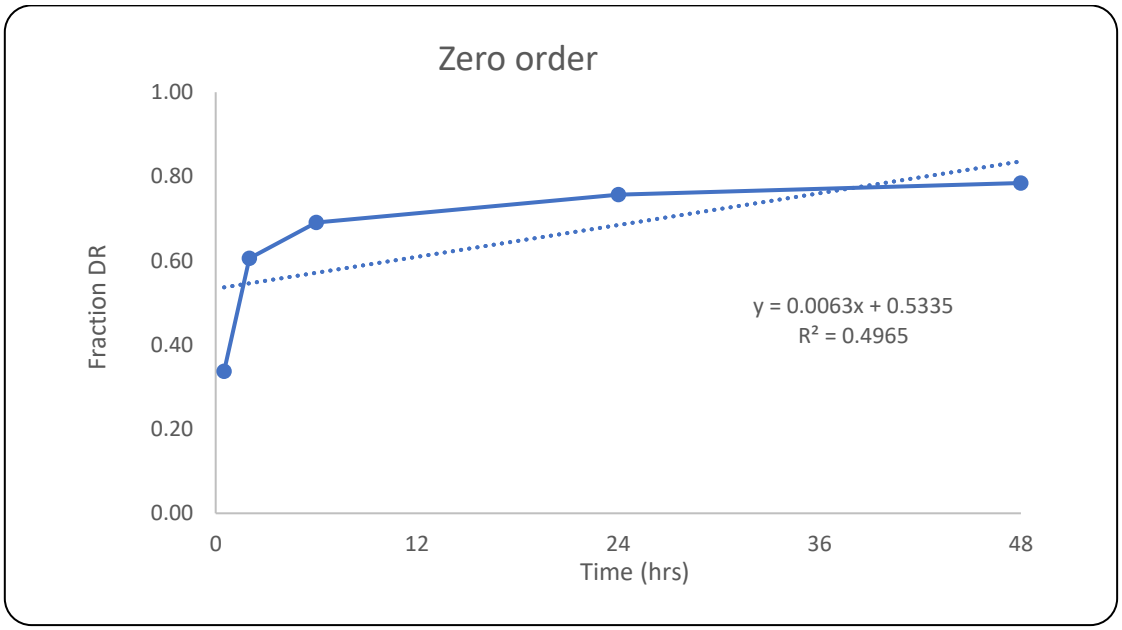

Fig 6. 37 Plot of fraction of drug remaining vs time (zero order)

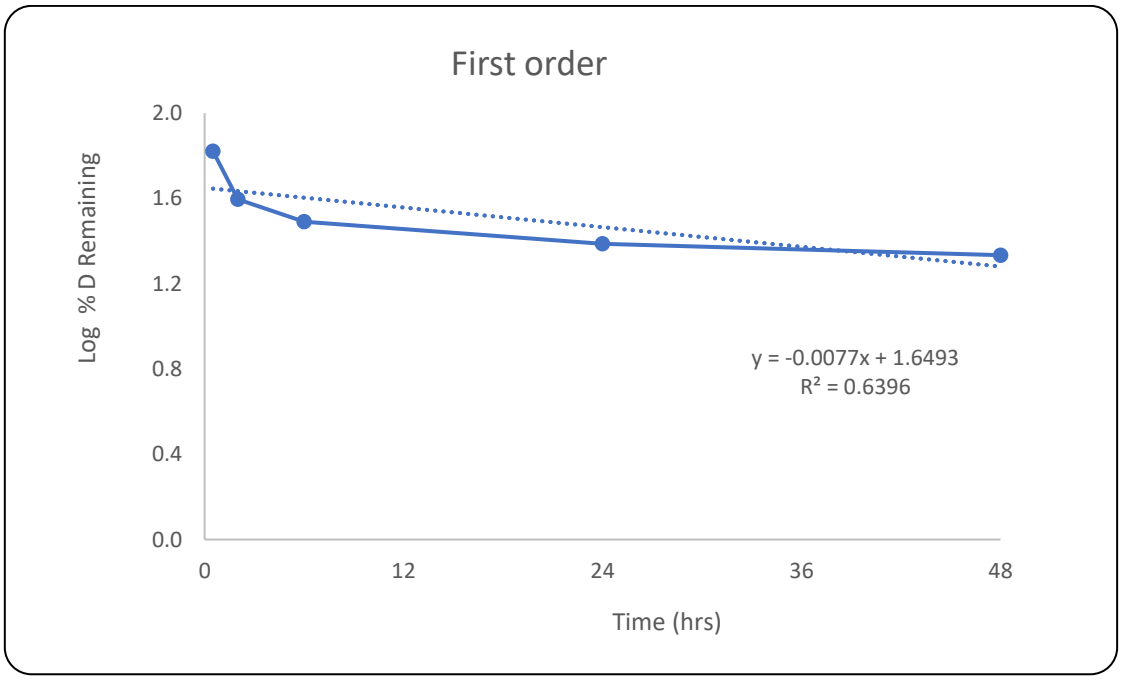

Fig 6. 38 Plot of log % drug remaining vs time (first order)

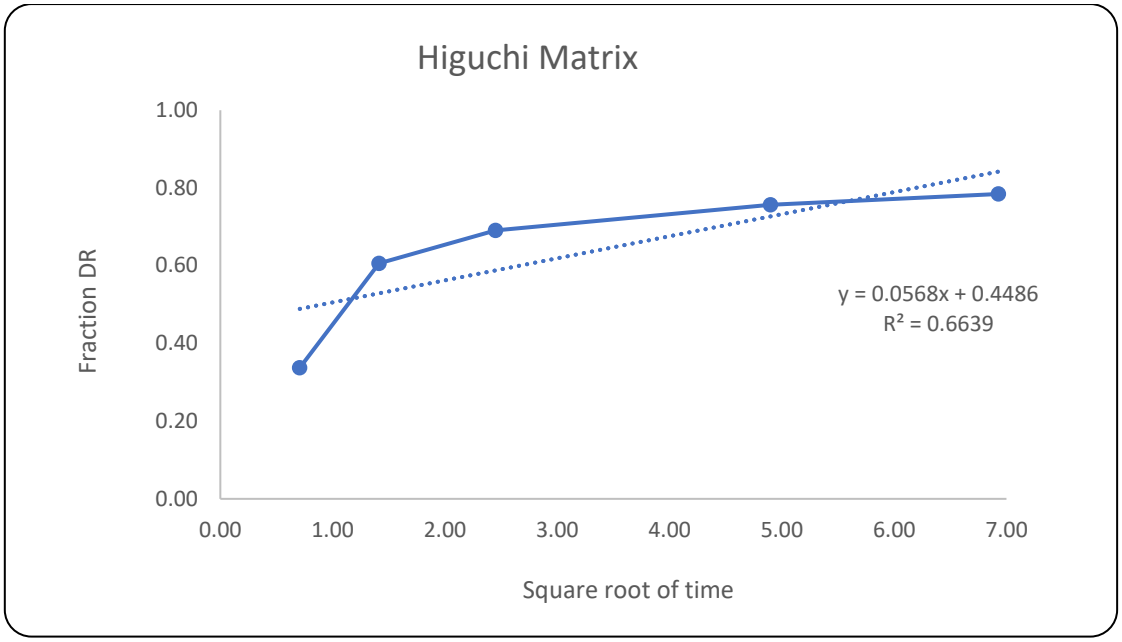

Fig 6. 39 Plot of fraction drug release vs square root of time (Higuchi model)

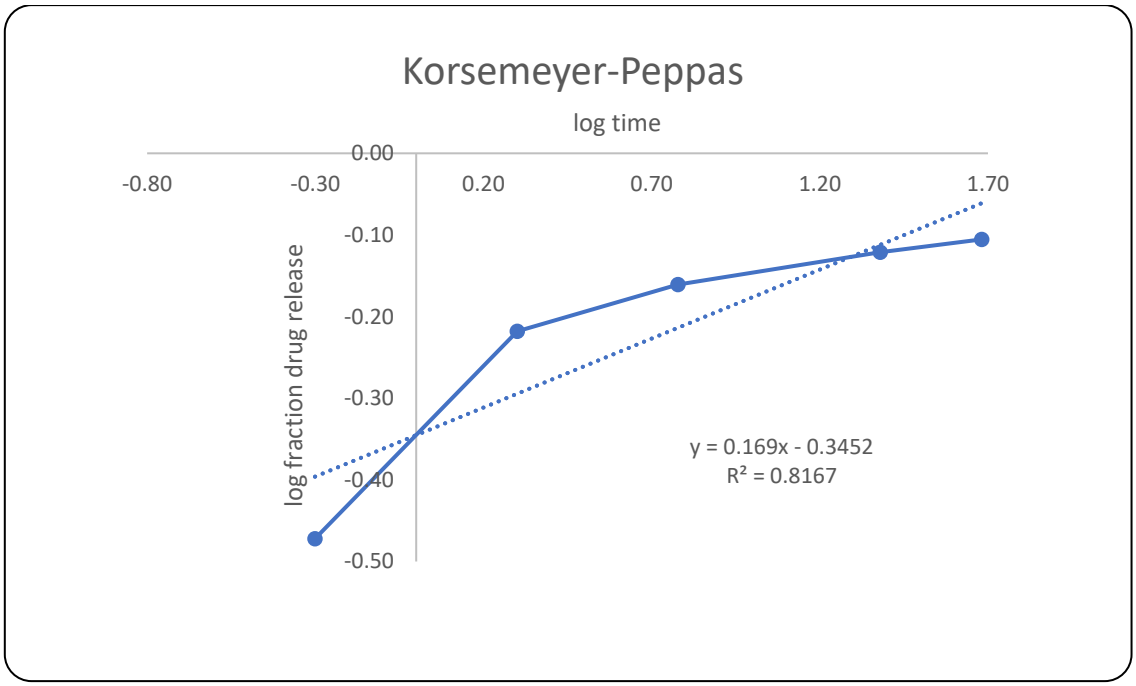

Fig 6. 40 Plot of log fraction drug release vs log time (Korsemeyer peppas model)

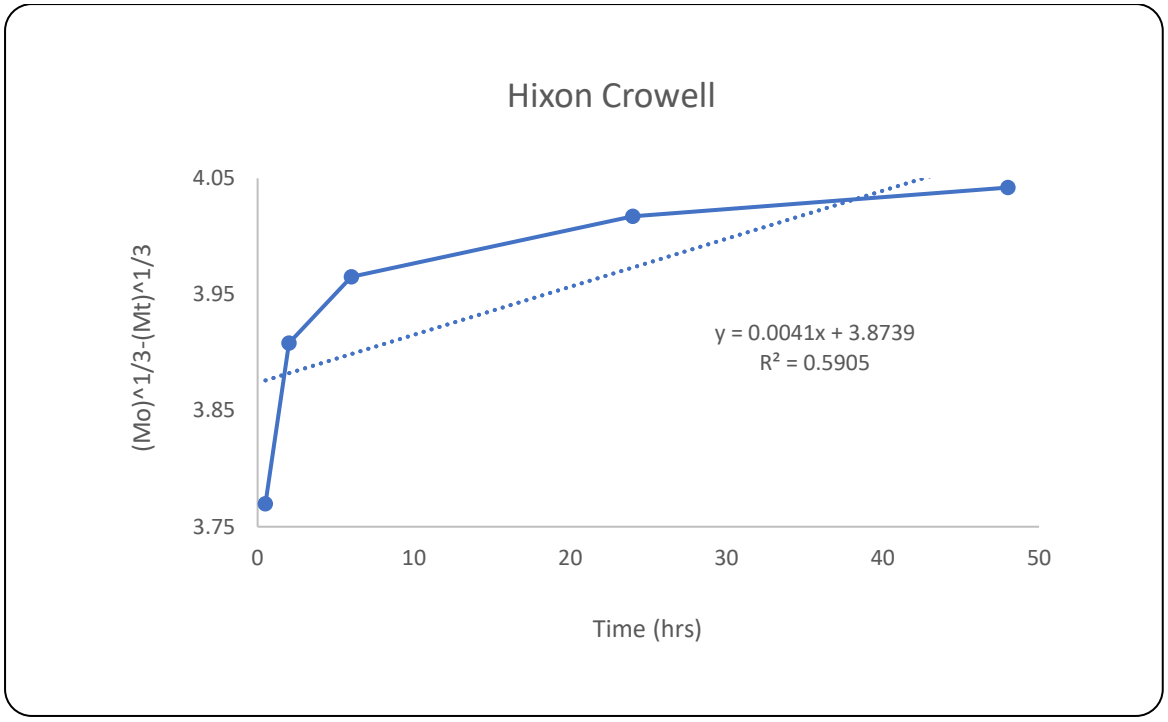

Fig 6. 41 Plot of Mo)^1/3-(Mt)^1/3 vs time (Hixon Crowell model)

6.13.1.1.2 Analysis of release mechanism of PIC from optimized gel

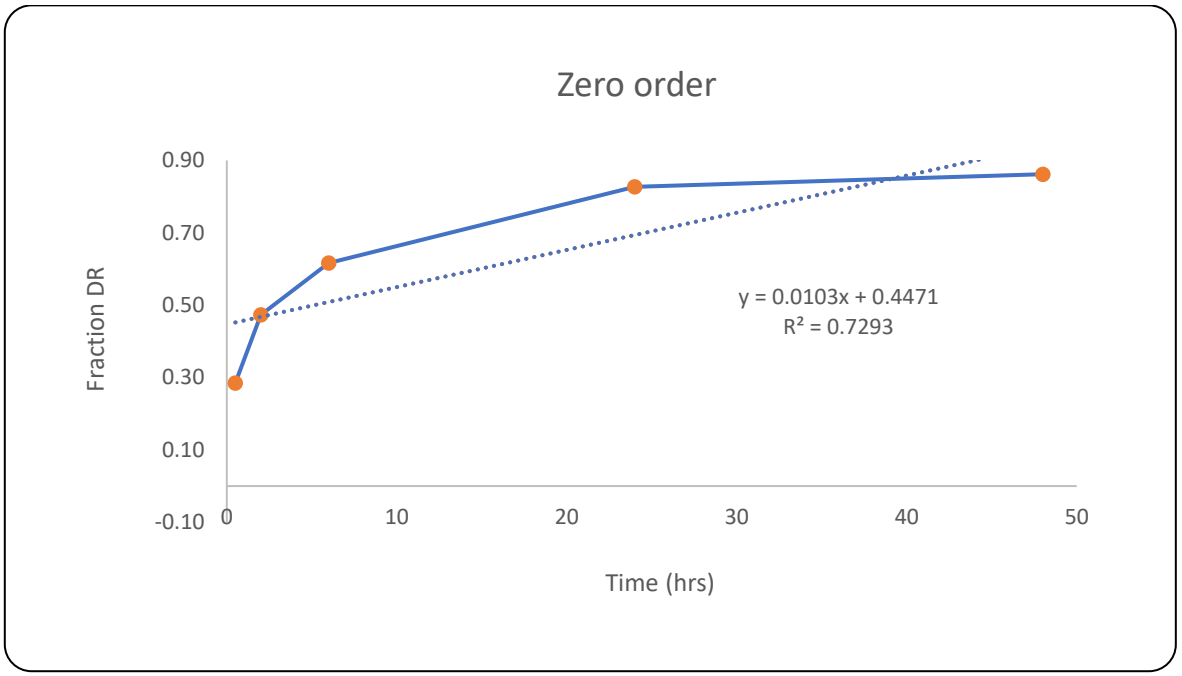

Fig 6. 42 Plot of fraction of drug remaining vs time (zero order)

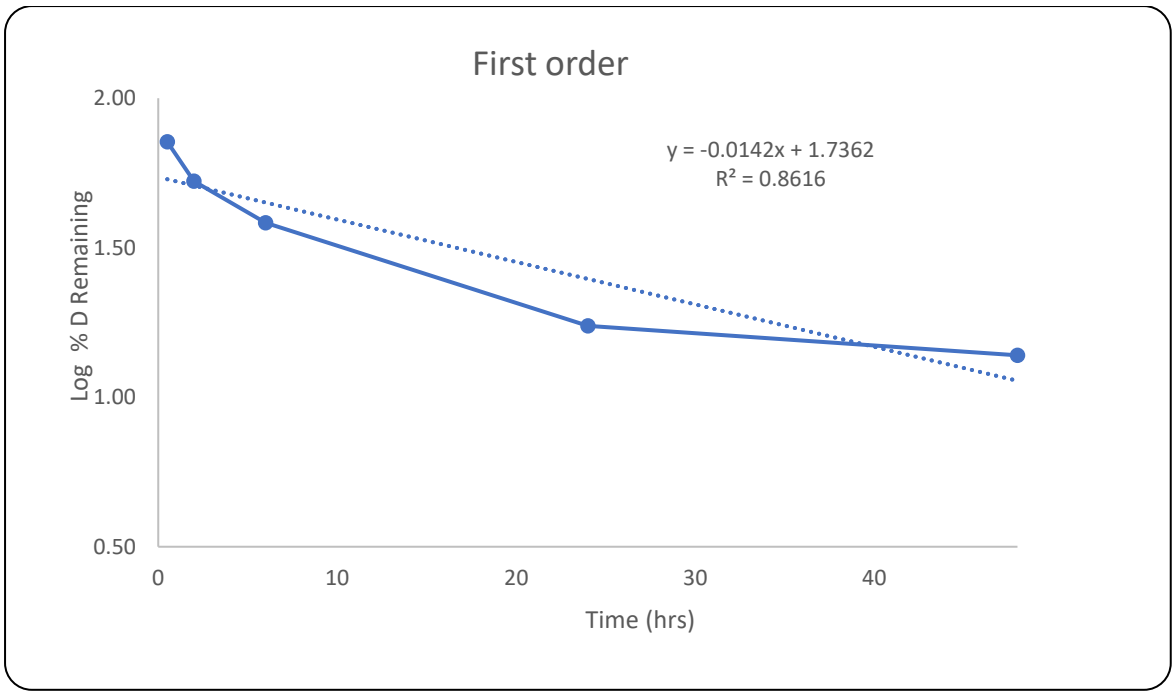

Fig 6. 43 Plot of log % drug remaining vs time (first order)

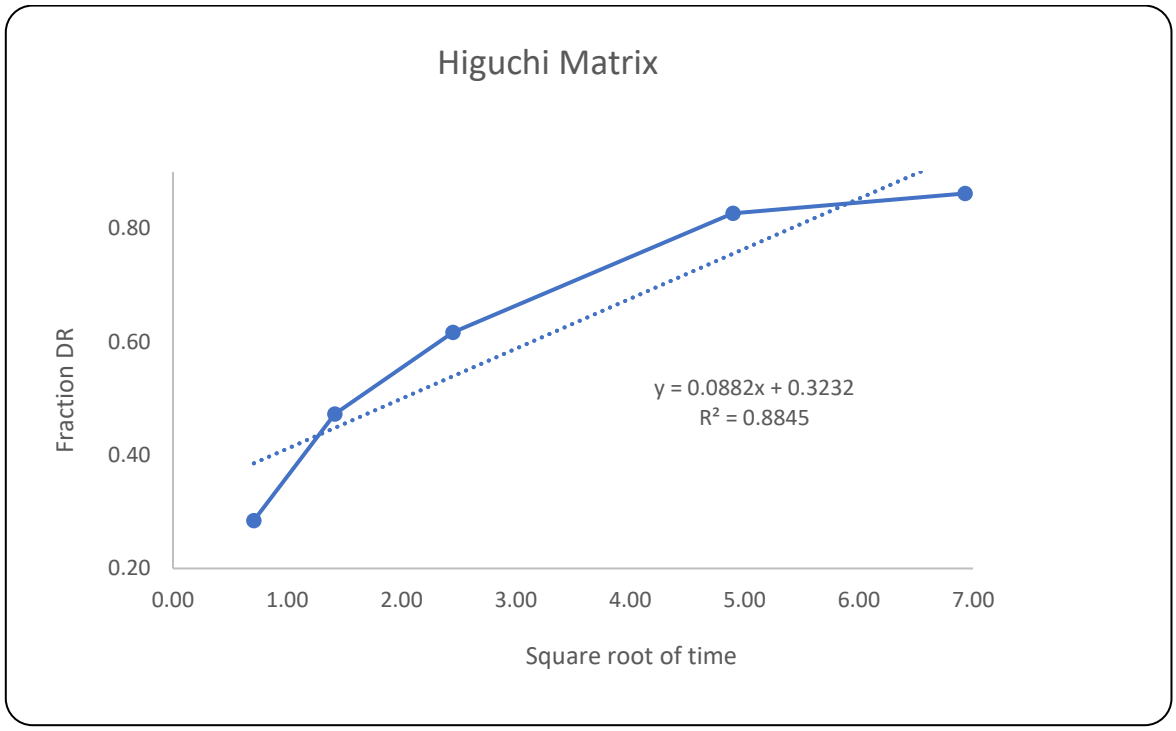

Fig 6. 44 Plot of fraction drug release vs square root of time (Higuchi model)

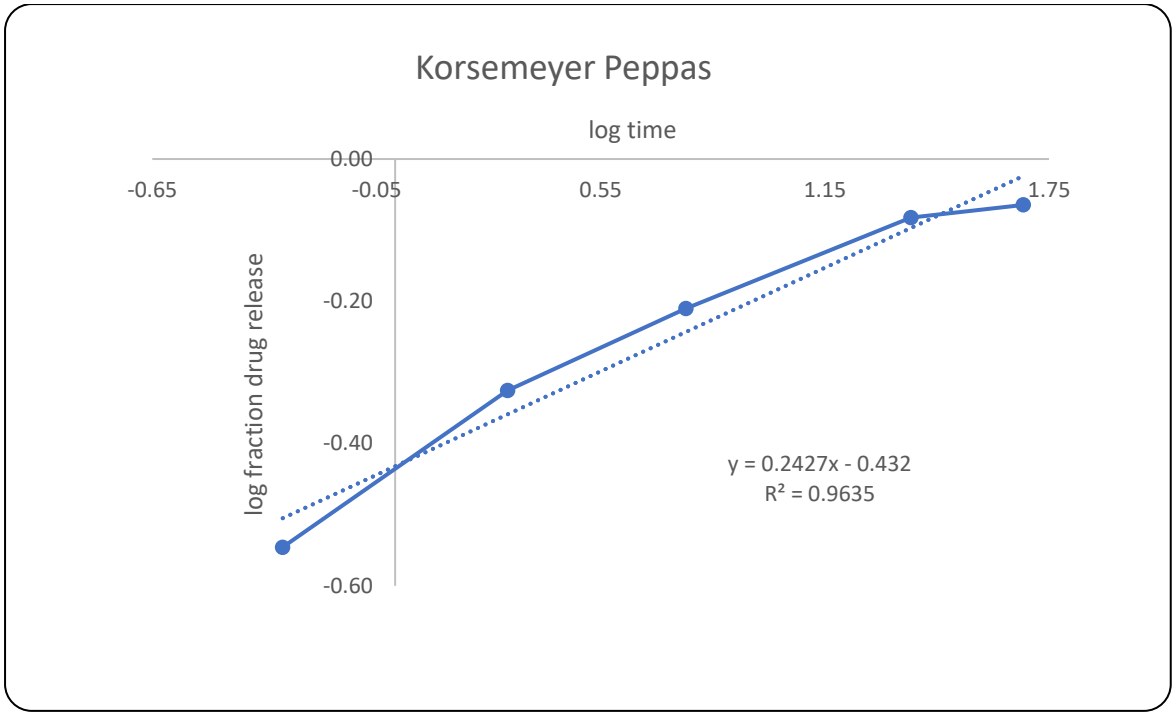

Fig 6. 45 Plot of log fraction drug release vs log time (Korsemeyer peppas model)

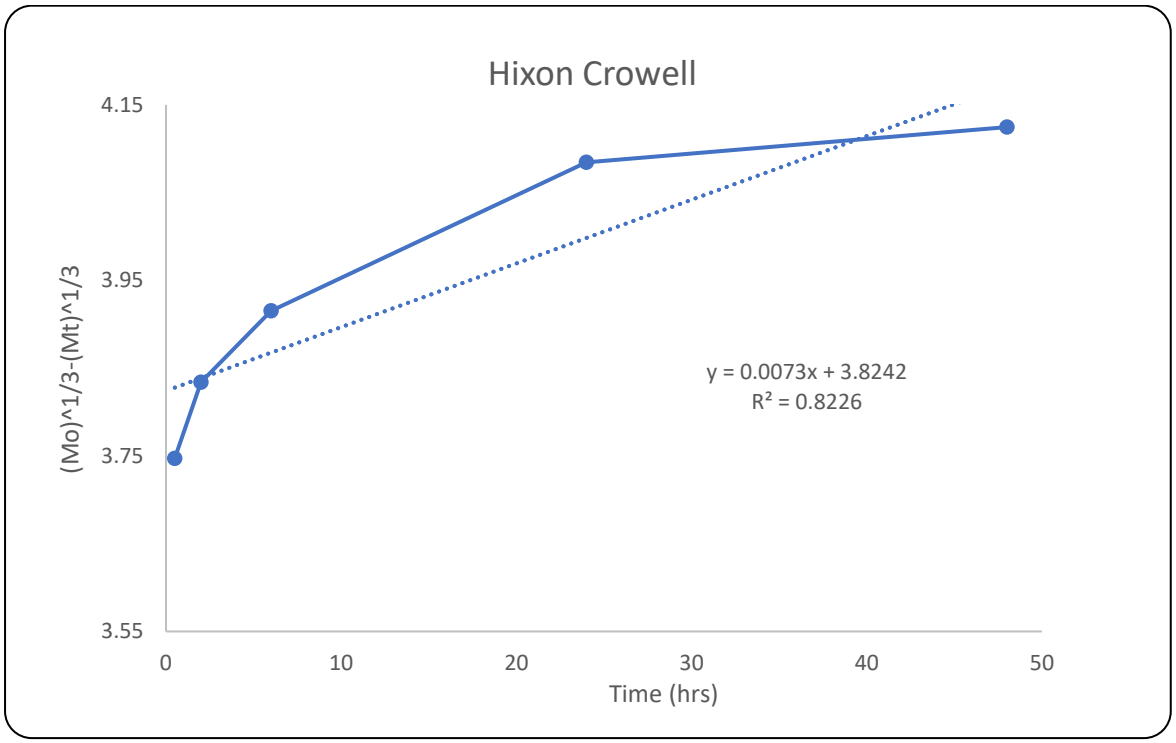

Fig 6. 46 Plot of Mo)^1/3-(Mt)^1/3 vs time (Hixon Crowell model)

Table 6. 44 Comparison of R^2 and slope of various models

OFG	Zero order		First order		Higuchi		Peppas		Hixon Crowell	
	R^2	Slope	R^2	Slope	R^2	Slope	R^2	Slope	R^2	Slope
L-Arg	0.496	0.006	0.639	0.007	0.663	0.056	0.816	0.169	0.59	0.004
PIC	0.729	0.01	0.861	-0.014	0.884	0.088	0.963	-0.241	0.822	0.007

Results

The release data was explored for the type of release mechanism of L-Arg (Table 6. 42) and PIC (Table 6. 43). Release kinetic study of optimized formulation was studies for different kinetic equations (Fig 6. 37 to Fig 6. 46). The best fit with higher correlation R^2 was found to be of Korsemayer-peppas model for PIC (Table 6. 44). Value of slope comes out to be 0.2427 which confirmed that release is fickian in nature.

6.14 Stability studies on final formulation

The results of the 3 month and 6 month stability studies are given in Table 6. 45 and Table 6. 46 respectively. The study showed slight changes in all formulation parameters like vesicle size, zeta potential, entrapment efficiency of L-Arg and PIC, when compared with fresh formulation. These changes are not significant as the p-value of 't'-test for these parameters at 3 months and 6 months duration was above 0.05 ($p>0.05$).

The 3 month stability data Table 6. 45 at 25°C±2°C/60% RH ± 5% RH showed p-value of 't'-test ($p>0.05$) The p-values of fresh gel formulation and at 3 months were found to be 0.12, 0.23, 0.23, 0.12 for vesicle size, zeta potential, entrapment efficiency for L-Arg and entrapment efficiency for PIC respectively.

The 6-month stability data Table 6. 46 at 25°C±2°C/60% RH ± 5% RH showed p-value of 't'-test ($p>0.05$) 0.42, 0.21, 0.10, 0.11 for vesicle size, zeta potential, entrapment efficiency for L-Arg and entrapment efficiency for PIC respectively.

Since in both the samples i.e. at 3 months and at 6 months p value comes out to be more than 0.05. It proves that the two formulations are statistically similar when kept at 25°C±2°C/60% RH ± 5% RH for up to 6 months.

The data for drug release was also compared statistically with model independence analysis (Table 6. 47, Fig 6. 47). The f2 (similarity value) for both fresh formulation and aged (at 6

months) was found to be 53.28 for PIC. As these values is comes out to be above 50, it indicated that the drug release profile of PIC after keeping at 25°C ± 2°C/60% RH ± 5% RH for 6 month showed similar release as that of the fresh formulation.

Table 6. 45 3-month stability study data

Sr.No.	Vesicle size (nm)			Zeta Potential (mV)			% E.E (L-Arg)			% E.E (PIC)		
	Fresh	3 months	p-Value	Fresh	3 months	p-Value	Fresh	3 months	p-Value	Fresh	3 months	p-Value
1	194.5	192		-36.4	-34.2		35	35		56.3	54.9	
2	193	196		-37.4	-36.4		39	38		58.7	57.4	
3	188	201	0.122	-37.6	-37.9	0.234	36	31.7	0.234	56.9	55.2	0.12
Mean	191.83	196.34		-37.13	-36.16		36.66	34.9		57.3	55.83333	
Std. Dev.	2.77	3.68		0.52	1.51		1.69	2.57		1.01	1.11	

Table 6. 46 6-month stability study data

Sr.No.	Vesicle size (nm)			Zeta Potential (mV)			% E.E (L-Arg)			% E.E (PIC)		
	Fresh	6 months	p-Value	Fresh	6 months	p-Value	Fresh	6 months	p-Value	Fresh	6 months	p-Value
1	194.5	190		-36.4	-37.2		35	33.5		56.3	54.9	
2	193	194		-37.4	-36.9		39	36.4		58.7	55.4	
3	188	190	0.422	-37.6	-35.9	0.218	36	31.2	0.100	56.9	57.2	0.108
Mean	191.83	191.33		-37.13	-36.66		36.66	33.7		57.3	55.83	
±S.D.	2.7788	1.88		0.52	0.55		1.69	2.12		1.01	0.98	

Table 6. 47 Mean cumulative percentage release data comparison for fresh formulation and aged (6 months)

Time (hrs)	Fresh formulation data		6 Month stability data	
	L-Arg	PIC	L-Arg	PIC
0	0	0	0	0
0.5	33.72 ± 0.15	27.93 ± 0.31	30.2 ± 0.46	23.61 ± 0.24
2	60.00 ± 0.24	45.78 ± 0.42	58.4 ± 0.12	37.65 ± 0.36
6	69.04 ± 0.39	60.68 ± 0.31	65.4 ± 0.77	53.4 ± 0.41
24	75.67 ± 0.41	81.99 ± 0.10	74.9 ± 0.44	70.5 ± 0.30
48	78.44 ± 0.29	87.24 ± 0.74	75.3 ± 0.17	77.5 ± 0.54

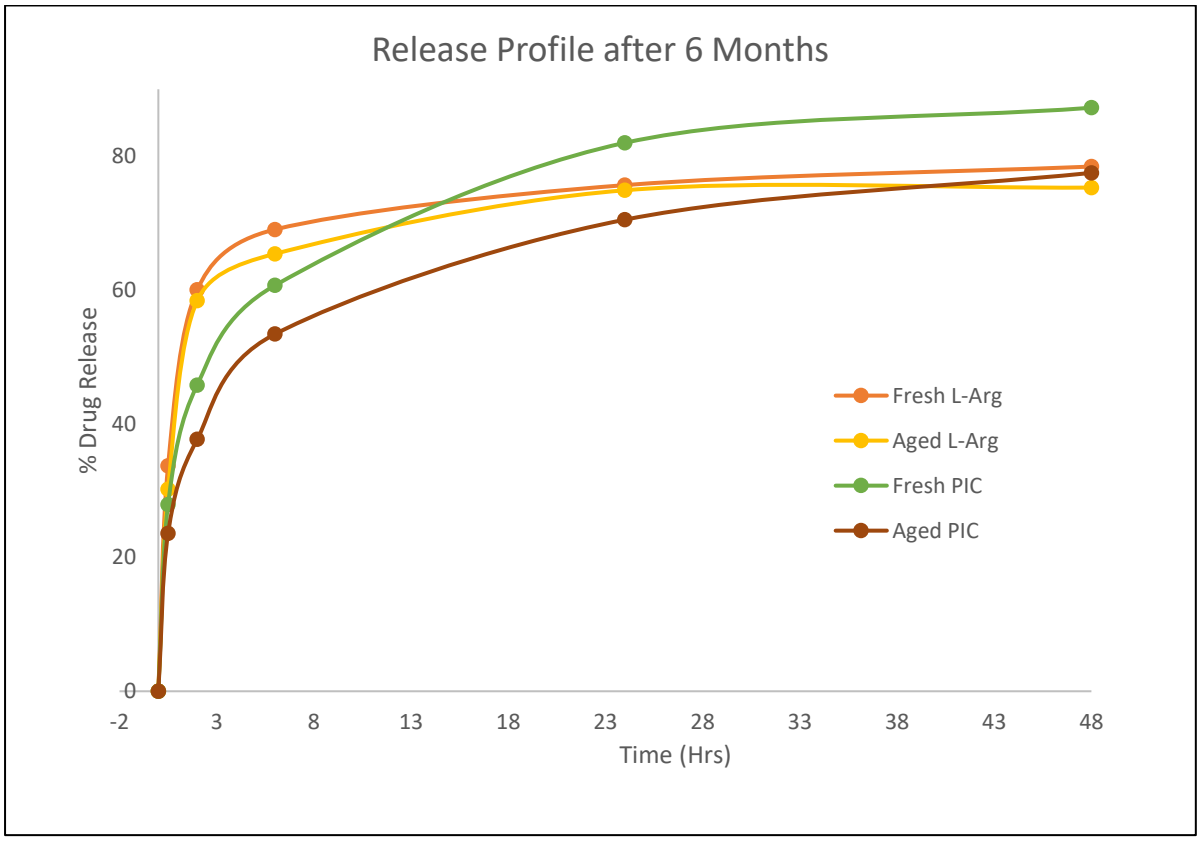

Fig 6. 47 Dissolution profile comparison of fresh formulation with 6 months old formulation after stability studies.

6.15 Cytocompatibility assay

The absorption of dissolved formazan crystals, which is directly related to the number of alive cells, was used to measure the cytocompatibility of the formulation. The sample test was contrasted with tissue culture plate growing cells that had not had any additional formulation added. Due to their ability to convert the tetrazolium dye MTT into purple formazan crystals,

only living cells exhibit metabolic activity. With consecutive dilutions (Table 6. 48), the final formulation demonstrated more than 80% cell vitality after 10× dilution (Fig 6. 48), which verifies the final formulations' cytocompatibility. The developed formulation showed a minor decline after diluting 2× in the percentage of cell viability.

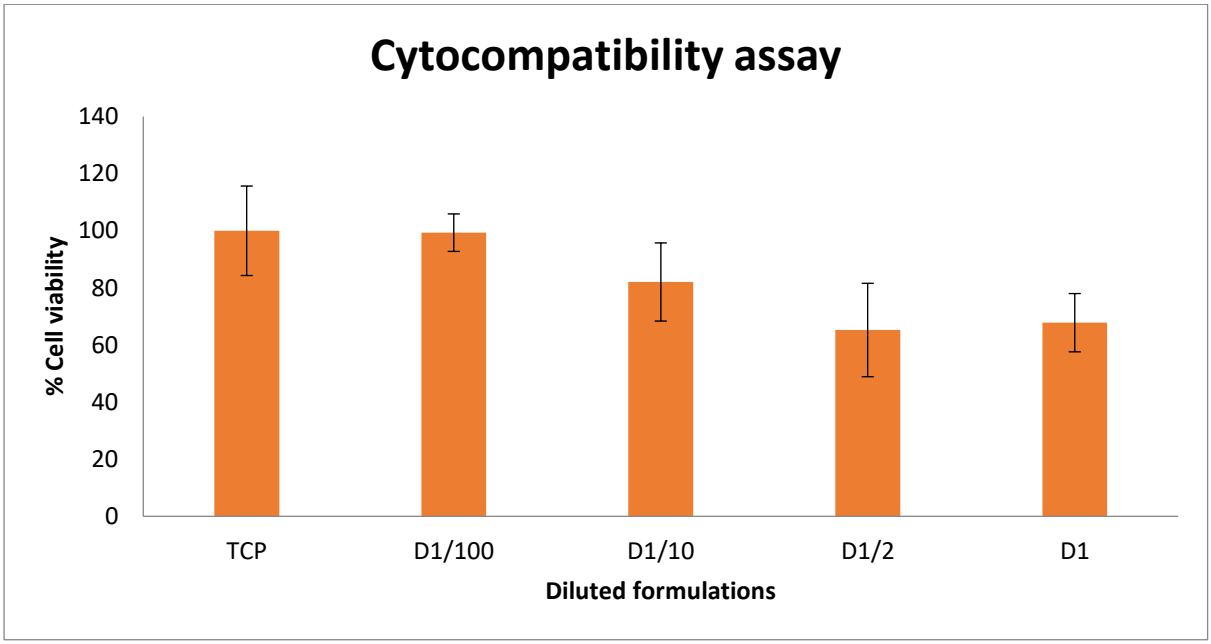

Fig: 6. 48 Effect of oral formulation on fibroblast cells by cytocompatibility assay

Table 6. 48 Cytocompatibility data of different formulations

Formulation code	Conc. of PIC (µg/ml)	Conc. of PIC (µM)	Log Conc. (µM)	% Viability
D_1	5.63	23.05	1.36	67.79
$D_{1/2}$	2.81	11.50	1.06	65.25
$D_{1/10}$	0.56	2.30	0.36	82.05
$D_{1/100}$	0.056	0.23	-0.63	99.32

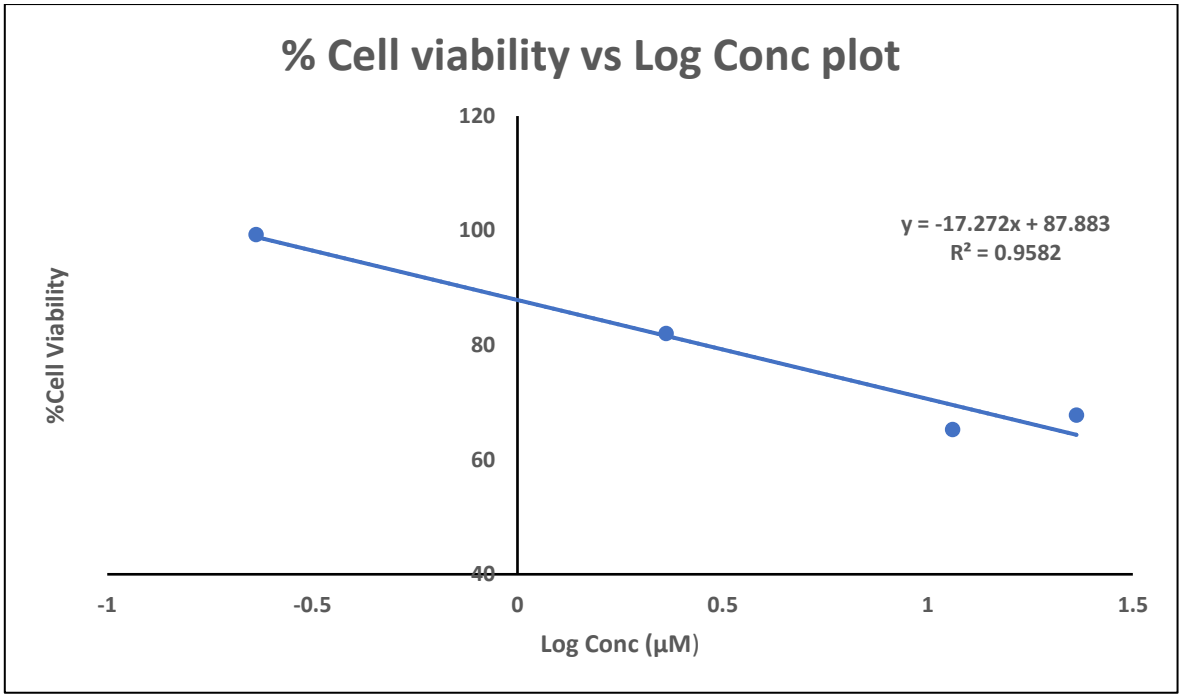

Fig: 6. 49 Percentage cell viability vs log conc. plot to check cell viability assay

Result

From the cell viability assay IC_{50} Value was calculated to be 15.488 µM of PIC (Fig 6. 49).

6.16 Clinical investigations

6.16.1 Salivary pH analysis

6.16.1.1 Salivary pH analysis (2 hrs study)

Table 6. 49 Salivary pH analysis data (2 hrs data)

Time (Min)	Saliva with 2% sugar solution					Saliva with 2% sugar solution and Treatment				
	Trial 1	Trial 2	Trial 3	Mean pH	± S.D.	Trial 1	Trial 2	Trial 3	Mean pH	± S.D.
0	7.8	7.6	7.6	7.67	0.09	7.8	7.6	7.6	7.67	0.09
5	6.5	6.8	6.9	6.73	0.17	7.8	7.6	7.7	7.70	0.08
10	6.2	6.4	6.2	6.27	0.09	7.58	7.4	7.3	7.43	0.12
30	5.8	5.8	5.4	5.67	0.19	7.4	6.9	7.1	7.13	0.21
60	5.2	5.4	5.4	5.33	0.09	7.21	6.4	6.3	6.64	0.41
75	5.1	5.2	5.2	5.17	0.05	6.86	6.2	6.3	6.45	0.29
90	5.1	5.2	5.2	5.17	0.05	6.52	5.9	6.1	6.17	0.26
120	5.1	5.2	5.1	5.13	0.05	6.26	5.7	5.9	5.95	0.23

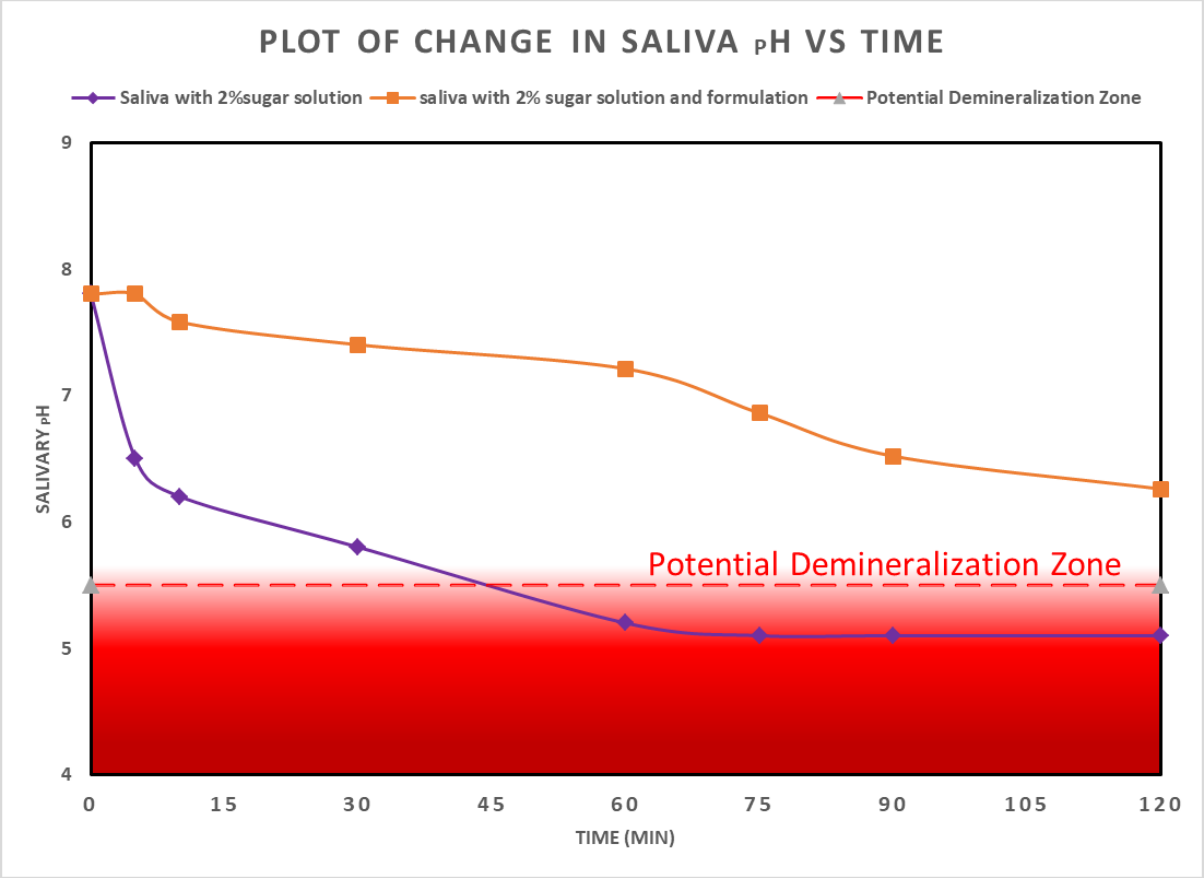

Fig 6. 50 Plot of saliva pH vs Time with and without formulation

6.16.1.2 Salivary pH analysis (24 hrs study)

Table 6. 50 Salivary pH analysis data (24 hrs data)

Time (Min)	Saliva with 2% sugar solution					Saliva with 2% sugar solution and Treatment				
	Trial 1	Trial 2	Trial 3	Mean pH	± S.D.	Trial 1	Trial 2	Trial 3	Mean pH	± S.D.
0	7.8	7.6	7.6	7.67	0.09	7.8	7.6	7.6	7.67	0.09
5	6.5	6.8	6.9	6.73	0.17	7.8	7.6	7.7	7.70	0.08
10	6.2	6.4	6.2	6.27	0.09	7.58	7.4	7.3	7.43	0.12
30	5.8	5.8	5.4	5.67	0.19	7.4	6.9	7.1	7.13	0.21
60	5.2	5.4	5.4	5.33	0.09	7.21	6.4	6.3	6.64	0.41
75	5.1	5.2	5.2	5.17	0.05	6.86	6.2	6.3	6.45	0.29
90	5.1	5.2	5.2	5.17	0.05	6.52	5.9	6.1	6.17	0.26
120	5.1	5.2	5.1	5.13	0.05	6.26	5.7	5.9	5.95	0.23
240	5.1	5.2	5.1	5.13	0.047	6.1	6.0	6.1	6.06	0.04
1440	4.7	4.9	4.8	4.80	0.081	5.6	5.8	5.8	5.70	0.09

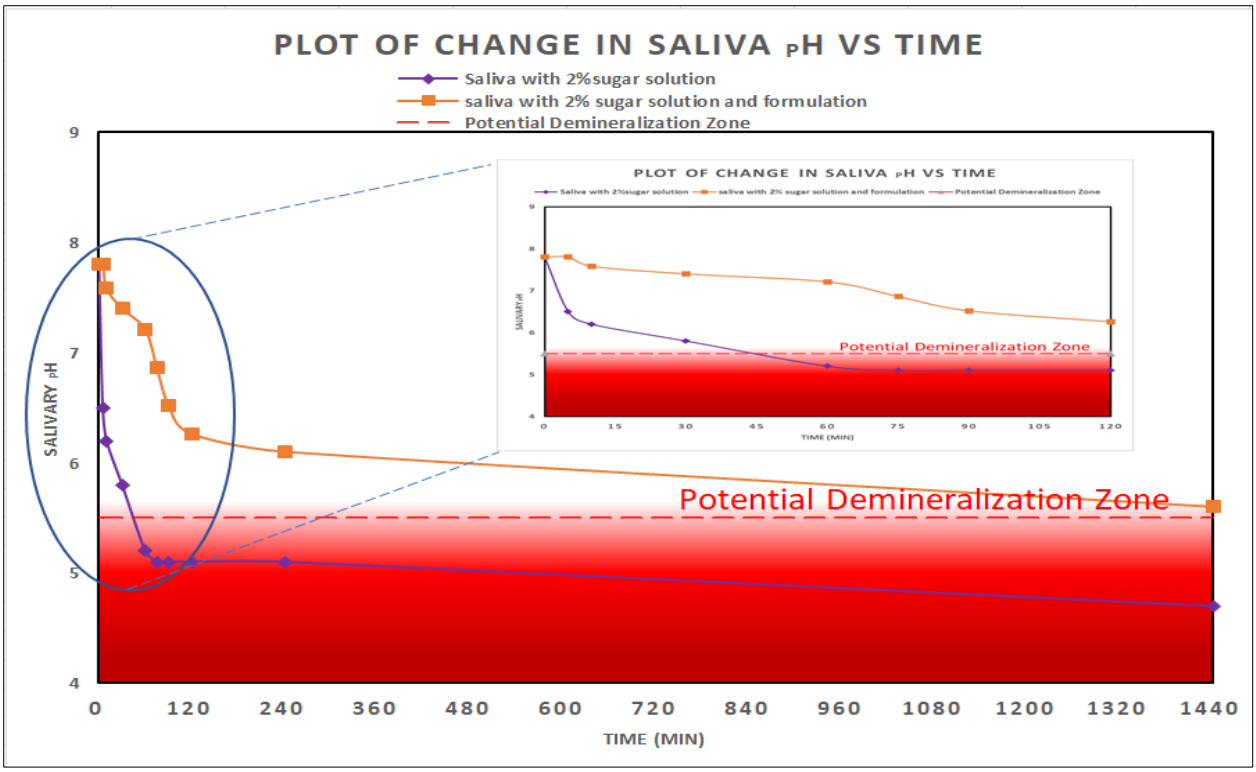

Fig 6. 51 Plot of saliva pH vs time with and without formulation (24 hrs)

Result

The results of the salivary pH analysis study were given in Table 6. 49 and Table 6. 50 for 2 hrs and 24 hrs respectively. The study showed the treatment group was able to maintain the pH of saliva above the potential demineralization zone for up to 24 hrs (Fig 6. 50 and Fig 6. 51). The change in pH of saliva between the control and treatment group was compared using student t-tests. These changes are significant as the p-value of the t-test for pH at 24 hrs was found to be 0.027 ($p<0.05$).

Since the sample's p-value comes out to be less than 0.05. It proves that the two groups are statistically different when treatment is provided to one group for up to 24 hrs.

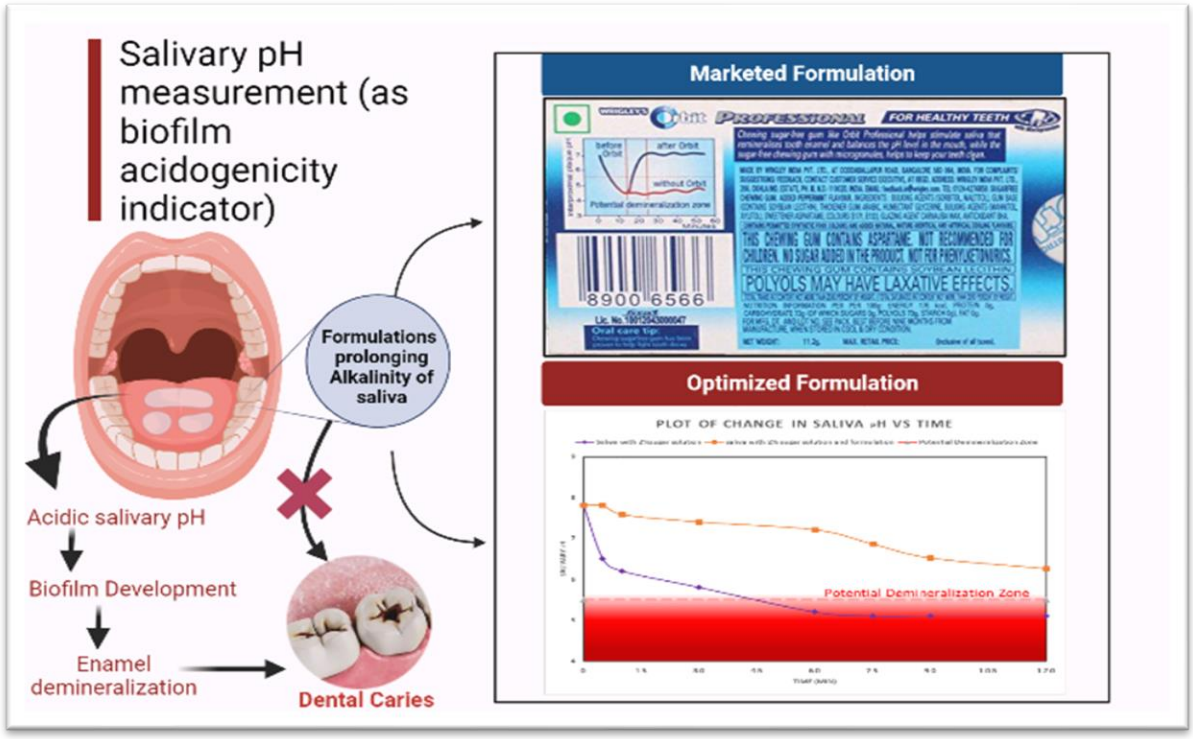

Fig 6. 52 Salivary pH as biofilm acidogenicity indicator

Discussion

Salivary pH has been identified as a potential biomarker in enamel demineralization, and strategies aimed at preventing a drop in salivary pH could have beneficial effects in decreasing the incidence of dental caries. (Harper et al., 2021). Studies suggested that acidic saliva or plaque pH renders it unsaturated with tooth minerals causing dissolution of the same from the enamel surface leading to dental caries. Rendering the salivary pH above 5.5 (potential demineralization threshold value) makes the saliva supersaturated with tooth minerals thus causing remineralization of enamel (Dodds et al., 2015). As, it was found that the treatment, was able to maintain the salivary pH above 5.5 for 24 hrs (*Information Sheet on pH of Home Oral Care Products*, n.d.). The potential of optimized formulation to control the drop in salivary pH could play a crucial role in managing enamel corrosion (Fig 6. 52).

6.16.2 Biofilm assay

6.16.2.1 FESEM analysis of samples

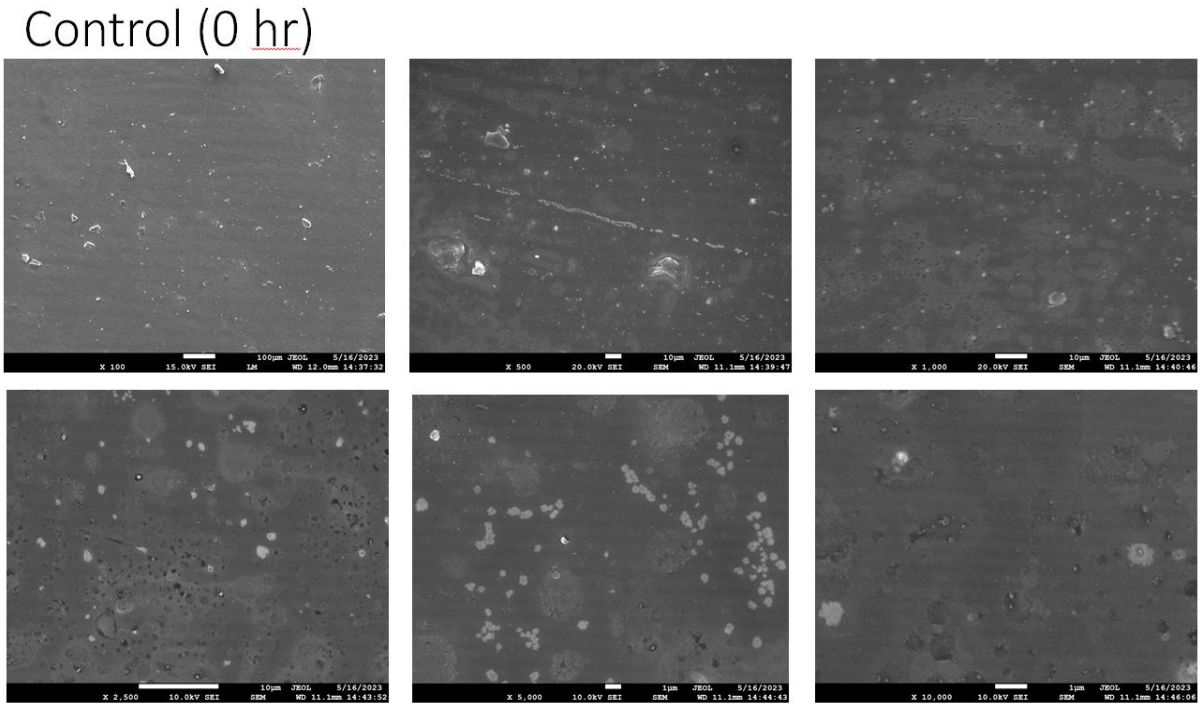

Fig 6. 53 SEM analysis of control saliva sample at time zero under various magnifications.

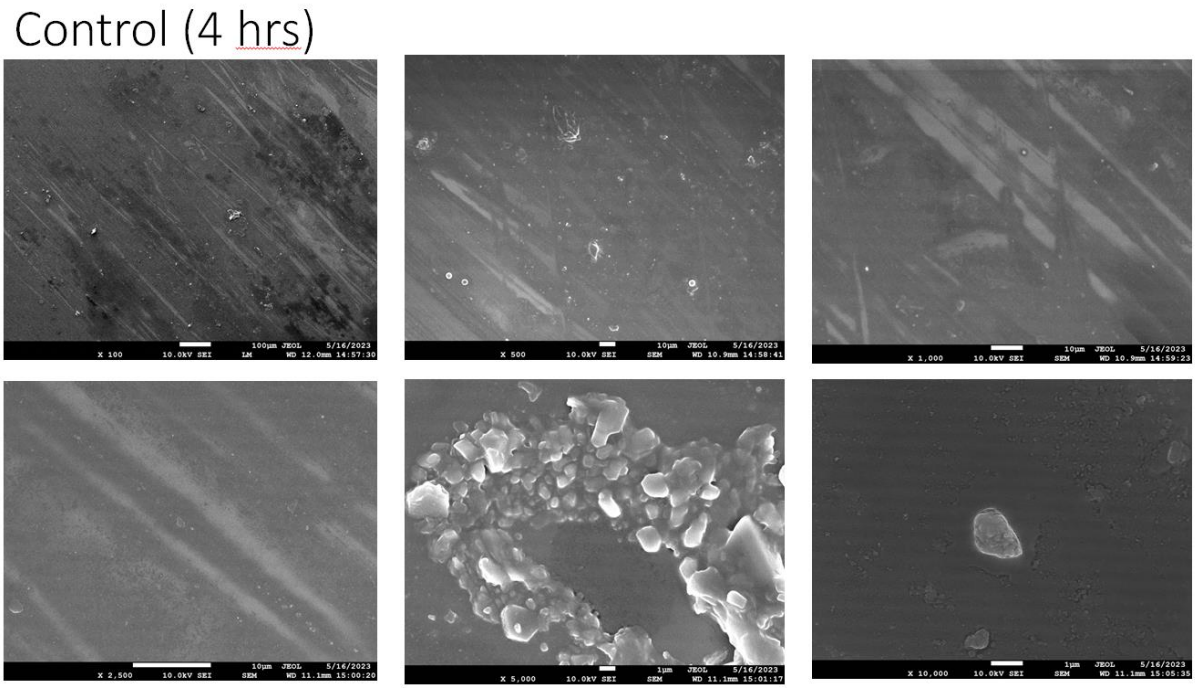

Fig 6. 54 SEM analysis of control saliva sample at 4 hrs under various magnifications.

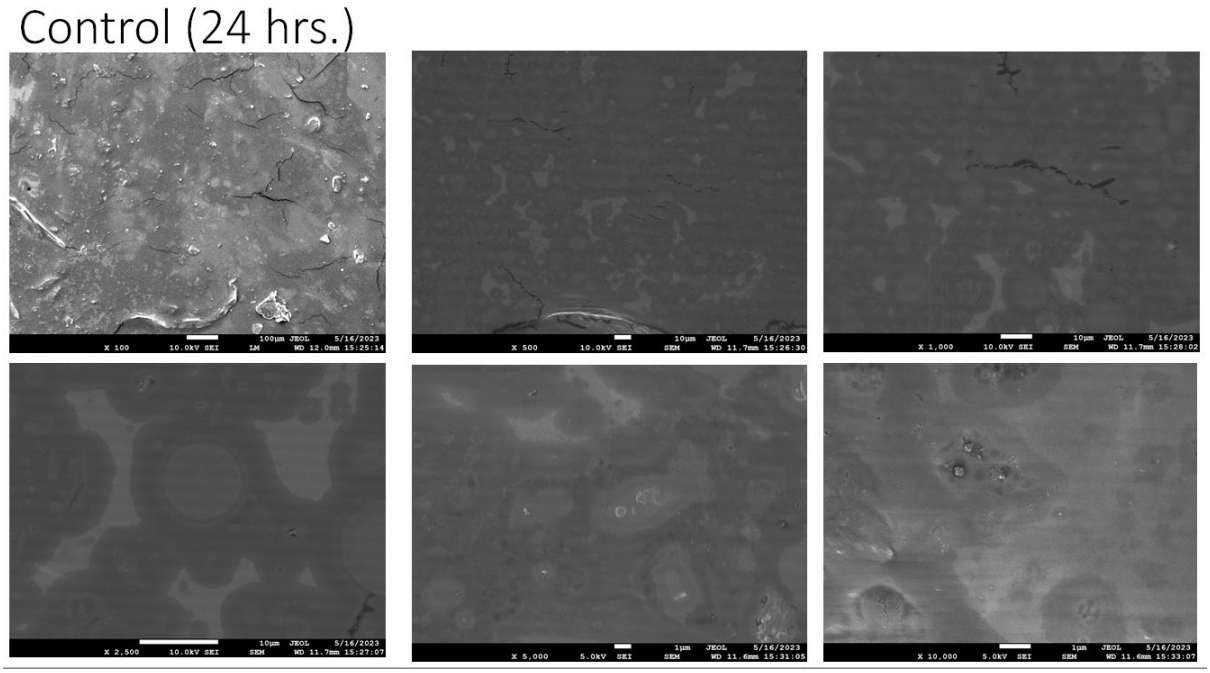

Fig 6. 55 SEM analysis of control saliva sample at 24 hrs under various magnifications.

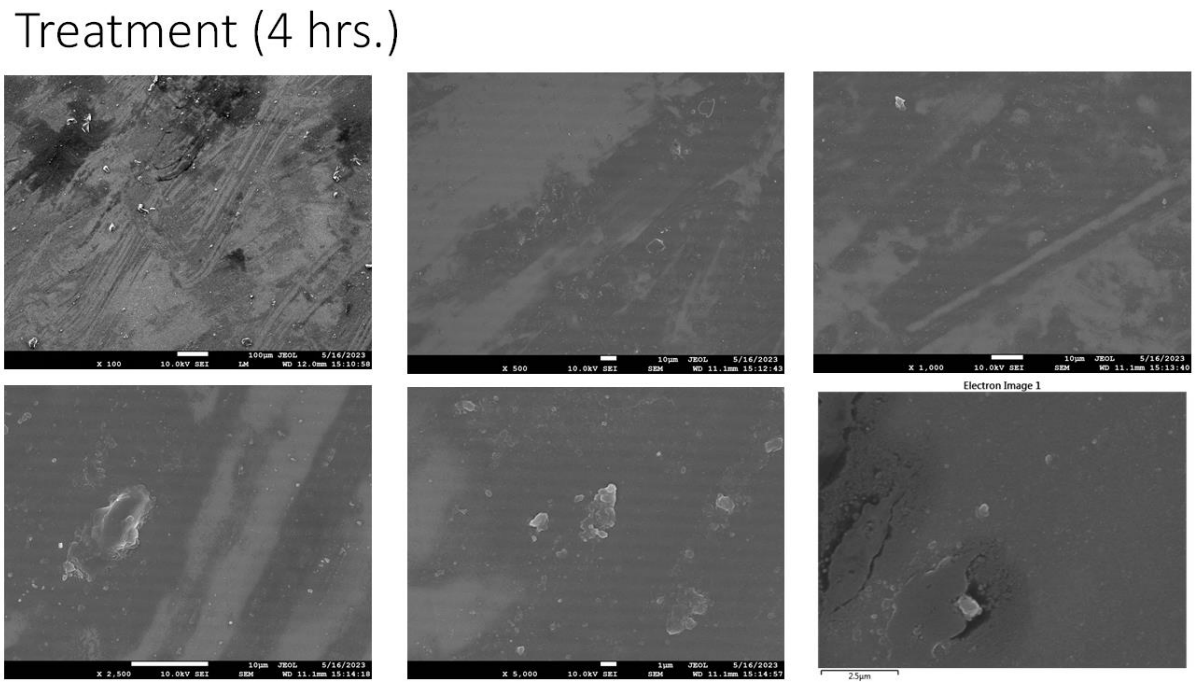

Fig 6. 56 SEM analysis of treated saliva sample at 4 hrs under various magnifications.

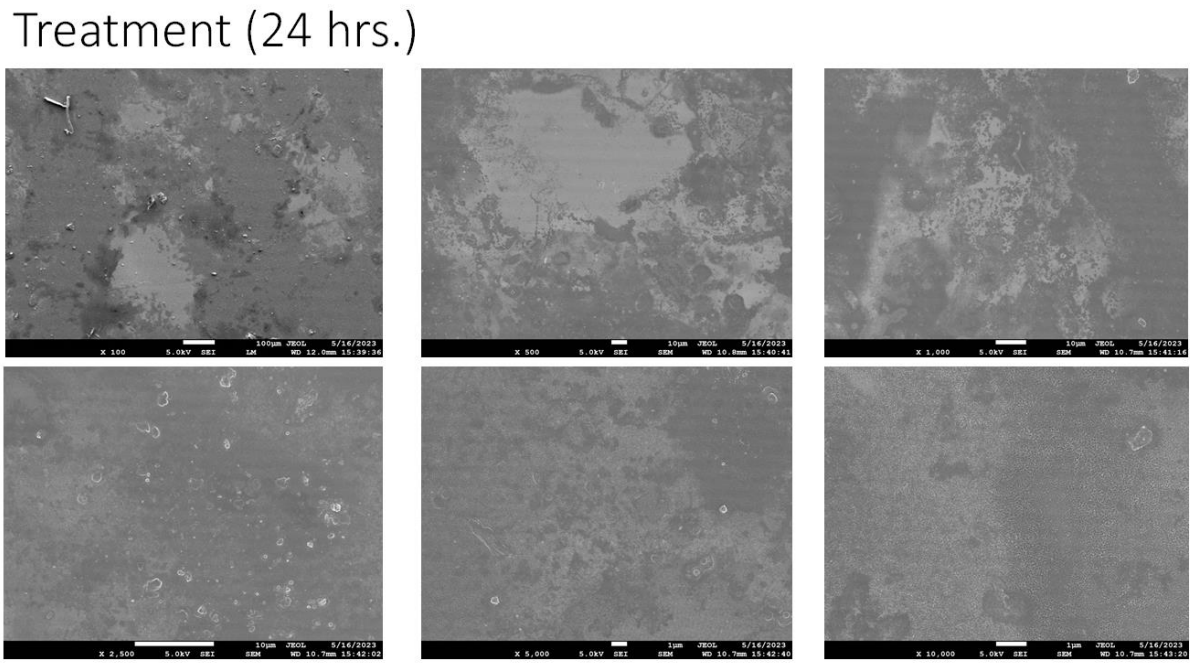

Fig 6. 57 SEM analysis of treated saliva sample at 24 hrs under various magnifications

Result

The FESEM analysis was conducted on six samples by drying them on the coverslip. The saliva was analyzed under FESEM (field emission scanning electron microscopy) at the Central instrumentation facility, Lovely Professional University, Phagwara. Each sample was Analysed at six different magnifications from 100X, 500X, 1000X, 2500X, 5000X, and 10000X. the observations are given in Fig 6. 53 to Fig 6. 57.

Discussion

From the FESEM analysis, the sample morphology and presence or absence of biofilm were observed. At 24 hrs, different microscopic images of positive control at various magnifications (from 500X to 10000X) showed the presence of concentrated colonies surrounded by a sheath or layer-like structure (Fig 6. 55). This can be considered as an indication of a biofilm in saliva. When FESEM images of the same magnifications for saliva with treatment were compared, no such matrix or sheath-like structure was observed. Instead, some discrete microbes were identified (Fig 6. 57). The absence of a sheath or layer around microbes in the treatment group, indicates the capacity of optimized formulation in decreasing the biofilm formation. As studies suggested, the absence of biofilm around microbes renders them less virulent and decreases the pathogenic potential of the microbes. The results from FESEM analysis were further confirmed through EDS analysis to check the carbon content in saliva after 24 hrs.

6.16.2.2 EDX analysis (EPS analysis)

Table 6. 51 Percent carbon content at various time points through EDX analysis

Time (hrs)	Control (% wt)		Treatment (% wt)	
	Mean	± S.D.	Mean	± S.D.
0	11.74	0.868	11.74	0.270
4	14.21	1.008	15.93	0.573
24	59.03	4.250	28.08	1.179

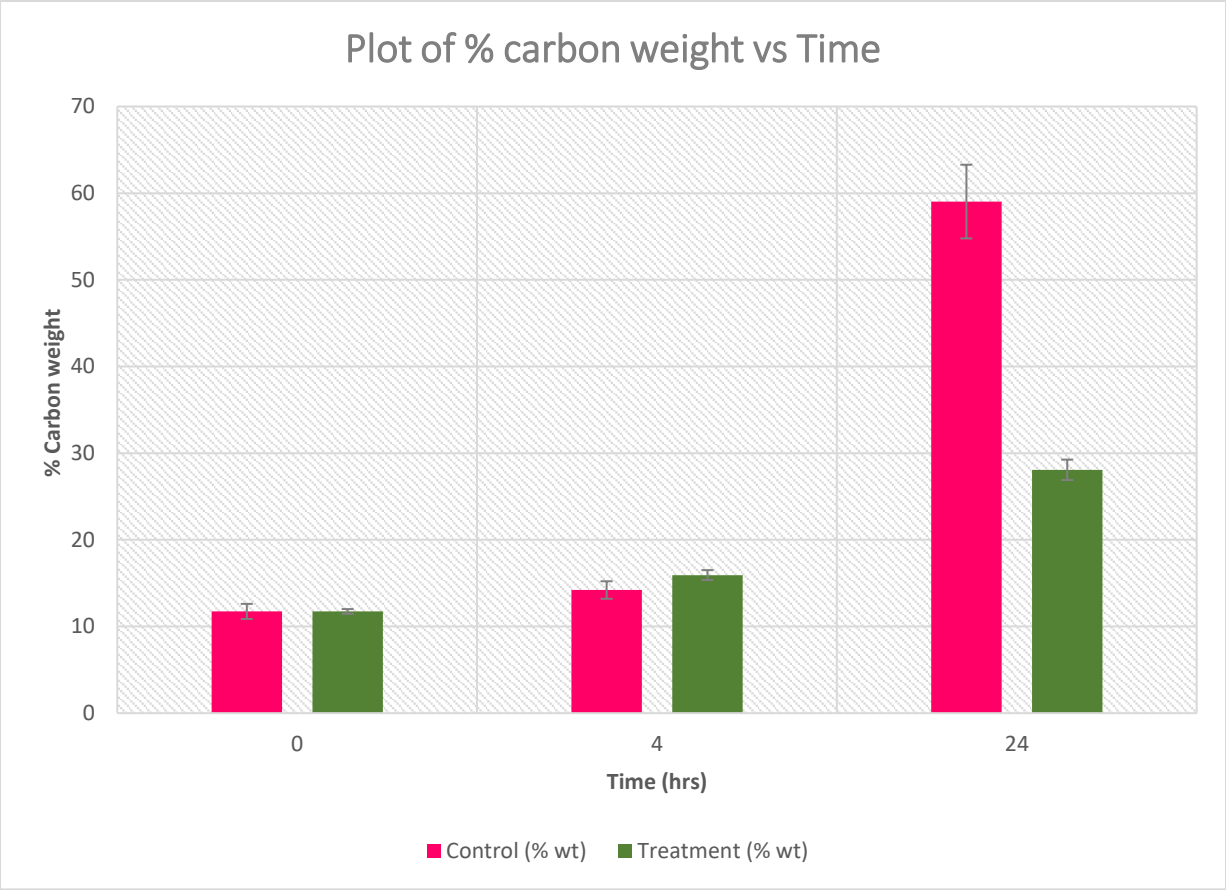

Fig 6. 58 Plot of percentage carbon weight vs time plot (24hrs)

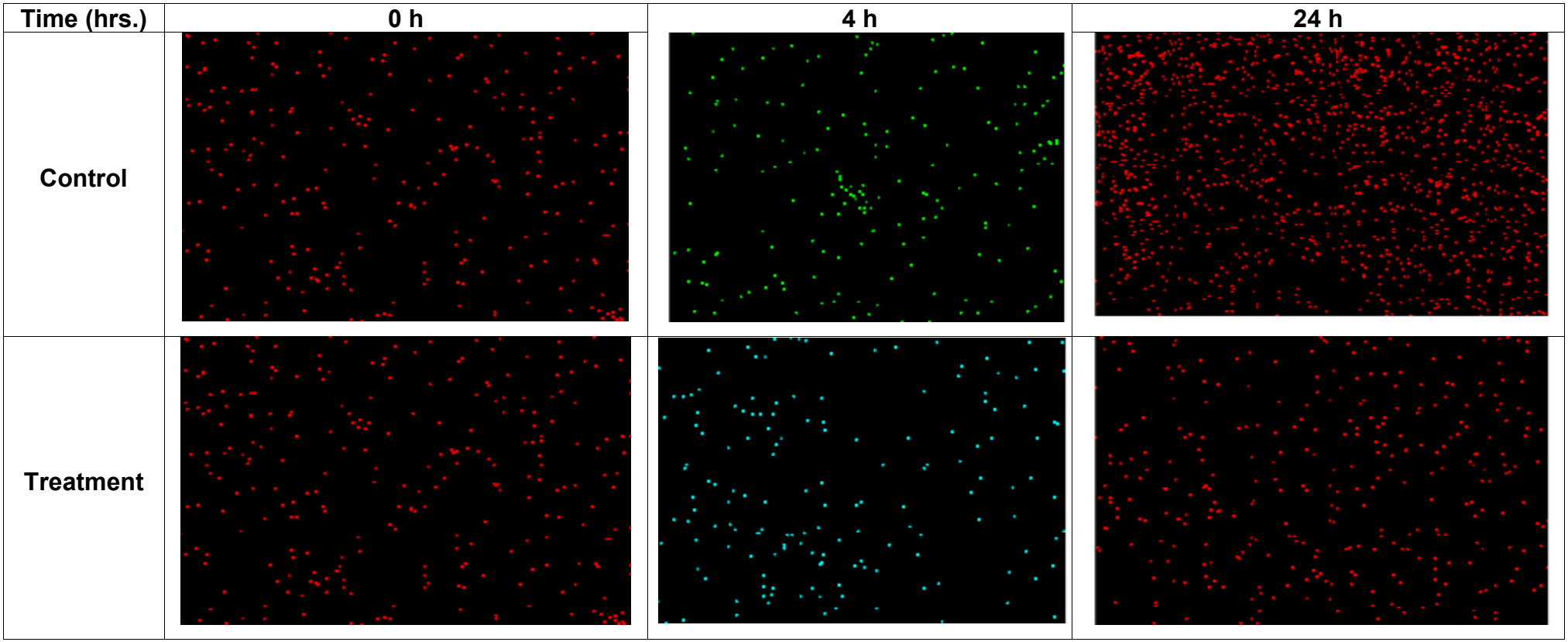

Fig 6. 59 EDX analysis of control and treatment groups at various time points

Results

The elemental analysis for the saliva sample was done to compare the presence of carbon content among various samples. The carbon content was identified relative to the oxygen content present in the sample. The results showed that carbon content in the controlled salivary sample kept on increasing from 11.74 to 59.03 % from 0 hrs to 24 hrs (Table 6. 51). which indicated that the microbial population kept on increasing when no treatment was given. On the other hand, the carbon content for treatment showed a significant reduced value at 24 hrs in contrast to control. At 24 hrs the treatment group showed a carbon content of 28.08 % (Fig 6. 58, Fig 6. 59). When a comparison is done at 4 hrs, no significant reduction is observed in the treatment group to the control group. This could be due to the slow release of API from the vesicles which at that point is unable to maintain a MIC to prevent microbial growth. Another possibility could be the presence of L-Arg, which act as a substrate for non-cariogenic microbes. When the student t-test was applied to both the treatment and control groups for 24 hours its p-value comes out to be 0.006 ($p<0.05$). Since the sample's p-value comes out to be less than 0.05. It proves that the two formulations are statistically different when treatment is provided for up to 24 hrs. 52.3 % reduction in carbon content in the treatment group was observed after 24 hrs when compared to the control. Hence it is evident that the optimized formulation can restrict exopolysaccharide production in salivary microbial colonies.

Discussion

The presence of carbon content is a strong indicator of exo-polysaccharides (EPS) present in between the microbes, which act as a matrix so that microbes can adhere to each other strongly and thus act as a medium to create biofilm. Exo-polysaccharides are primarily composed of insoluble glucans and fructans, which are produced by exo-enzyme (Glucosyltransferases) present in cariogenic microbes. Since exopolysaccharides are strong indicators of biofilm development, a reduction in their content indicates antibiofilm activity of optimized formulation. Hence, the anti-biofilm effect of the formulation is evident from the results. As, the formulation is preventive in nature, above model justifies its potential to control drop in pH to prevent caries development in saliva of healthy individual. This also confirmed that vesicles were stable enough to prevent the drop in pH of saliva after 24 hrs.

7 Summary and Conclusion

7.1 Summary

The development and evaluation of Flexi-liposomes started with the procurement of PIC and L-Arg. The procured PIC and L-Arg were identified using chemical tests, FTIR, UV-Visible spectroscopy and RP-HPLC. With FTIR, the spectra of procured PIC and L-Arg were mapped with reference spectra and they were concluded to be identical to the references.

UV-Visible spectra of PIC in methanol were established and two spectral peaks were identified at 325 and 220 nm. For L-Arg, UV-Visible spectra were obtained with distilled water and characteristic peaks were identified at 272.5 and 340.5 nm.

RP-HPLC was carried out to identify PIC and L-Arg individually. when 2.5 mg of the PIC was dissolved in 10 ml of methanol and the mobile phase was kept at a 90:10 ratio (methanol: water) at system temperature of 30˚C, sample injection volume was 20 µl and flow rate of 1 ml/min. The detection was performed at 324 nm and a chromatogram was recorded. A single peak was detected with a retention time of 3.2 mins at 324 nm for PIC. A single and sharp peak at absorbance maxima of PIC validated the presence of Pure PIC in the procured sample.

For L-Arg, 2.4 mg of the L-Arg was dissolved in 10 ml of methanol. The mobile phase was prepared for isocratic flow by using 0.05 M potassium dihydrogen phosphate buffer of pH 2.6 and methanol in a 50:50 ratio. The mobile phase was kept at 45˚C before starting the analysis. A single peak was detected with a retention time of 8 min at 215 nm. A peak near absorbance maxima of L-Arg validated the presence of L-Arg in the sample (Kaur, Vyas, & Verma, 2024)

Drug excipient compatibility studies were conducted to identify the physical and chemical stability of formulation ingredients. It was conducted on PIC, L-Arg, Soy lecithin, Span 60/S.D.C, and Carbopol by using various mixtures in 1:1 composition for 21 days at 25˚C±2˚C under dim light in both open dish and closed dish. FTIR analysis and DSC were conducted at various intervals to check any chemical incompatibility. DSC analysis suggested that after 21 days (in both open dish and closed dish) no chemical change in composition. This validated the physical and chemical inertness of excipients used in the formulation. Furthermore, these studies indicated that PIC, L-Arg, span 60, Carbopol, and soy lecithin were unreactive in a 1:1 combination. Similarly, no chemical change was identified with PIC, L-Arg, SDC, Carbopol, and soy lecithin in a 1:1 ratio at 25˚C±2˚C under dim light.

Simultaneous estimation of PIC and L-Arg using RP-HPLC was conducted. The new RP-HPLC method was developed and validated according to ICH guidelines. After various attempts, the final method was developed using a mobile phase of 0.1% OrthoPhosphoric Acid (in water): Acetonitrile (7:3). The sample was prepared with 0.5 mg/ml for both PIC and L-Arg in mobile phase (0.1% OrthoPhosphoric Acid (in water): Acetonitrile (7:3), and good resolution was observed with RT for PIC at 7.699 min and RT for L-Arg at 1.931 min. The method was further validated according to ICH guidelines and found to have sufficient separation capacity to be used for the quantification of compounds in combination.

As the use of Span 60 and SDC both qualify as stable Edge activator candidates to formulate vesicles, an initial study was conducted with four different concentrations of soy lecithin and Edge activator to check the entrapment efficiency of L-Arg and PIC. It was identified that for both L-Arg and PIC, vesicles fabricated with SDC showed better entrapment efficiency. The entrapment efficiency improved from 10 % to 33 % for L-Arg and 34 % to 60 % for PIC, when span 60 was replaced with SDC. Thus, SDC selected for further optimization. Various process parameters like the speed of rota-vapor and the temperature of the water bath were selected to optimize entrapment efficiency. These two were chosen to optimize the entrapment efficiency of the formulation containing 85 mg of soy lecithin and 15 mg of S.D.C. These process parameters were found to have no significant effect on E.E. of L-Arg and PIC. Hence, in the optimization study, the hydration of dried lipid film was done at 60°C, and the speed of the rotary evaporator was set at 100 RPM. Using the central composite design, two factors (Soy lecithin and SDC) at two levels (Soy lecithin from 75 to 90 mg and SDC from 10 to 25 mg) was carried out. Total 13 runs were conducted to check the response of 5 parameters i.e., vesicle size, PDI, zeta potential, E.E. of L-Arg and E.E. of PIC. The final overlay plot describes 89.88 mg of soy lecithin and 13.42 mg of SDC to have a probability of obtaining194.50 nm of vesicle size, -34.22 mV of zeta potential, 0.217 of PDI, 32.3 % E.E. of L-Arg and 60.7 % E.E. of PIC. When formulation was developed using above combination, the experimental and predicted responses along with the percentage error were found to range between -7.3 % and 8.35 %, i.e., well within ±10 %. This indicated the excellent prognostic ability of the experimental design employed for the optimization of flexi-liposomal formulation of L-Arg and PIC.

To prepare the optimized flexi-liposomal gel, 20 ml of optimized flexi-liposomal suspension was added to 10 ml of 10 % w/v of Carbopol 934. To this 0.2 % w/v methylparaben and 0.02 % w/v of propylparaben was added. The final gel formulation was evaluated for *in vitro* release studies conducted using the dialysis bag method. The release was found to be sustained up to

48 hrs. The L-Arg was found to release up to 78.44 % and PIC showed 86 % relaese after 48 hrs. The release data was explored for the type of release mechanism of drug PIC. The release kinetic study of optimized formulation was studied for different kinetic equations. The best fit with higher correlation R^2 was found to be of the Korsemayer-peppas model for PIC. The value of the slope comes out to be 0.2427 which confirmed that the release is fickian in nature.

Stability studies were conducted on optimized flexi-liposomal gel and were tested for 6 months at 25°C±2°C/60% RH ± 5% RH. The 6-month stability studies were evaluated for changes in release profile kinetics and other parameter used to optimize the formulation. The study showed slight changes in all formulation parameters like vesicle size, zeta potential, and entrapment efficiency of L-Arg and PIC when compared with the fresh formulation. These changes are not significant as the p-value of the t-test for these parameters at 3 months and 6 months duration was above 0.05 ($p>0.05$). The data for drug release was also compared statistically with model independence analysis. The f2 (similarity value) for both fresh formulation and aged (at 6 months) was found to be 53.28 for PIC. As these values come out to be above 50, it indicated that the drug release profile of PIC after keeping at 25°C ± 2°C/60% RH ± 5% RH for 6 months showed a similar release as that of the fresh formulation.

The optimized formulation was evaluated for cytocompatibility assay using MTT assay on fibroblast cells to evaluate the safety profile of the formulation. Various dilutions of optimized formulation were used and it was found that gel with a PIC concentration of 0.23051 µM showed 82.05 % cell viability. From the cell viability assay, IC_{50} Value was calculated to be 15.488 µM of PIC.

Clinical investigations were carried out on pooled human saliva of healthy volunteers of 18 to 40 years of age. The formulation was added to 5 ml of pooled saliva in a sterilized beaker. To the saliva, 2 % of sucrose was added and treatment was added (optimized gel) to make a final concentration of 2.8 µg of PIC and observed for any change in pH for up to 24 hrs. It was observed that the formulation was able to maintain the pH of saliva above the potential demineralization zone for up to 24 hrs. After 24 hrs, the salivary pH was found to be 5.7. The change in pH of saliva between the control and treatment groups was compared using student t-test. These changes were found to be significant as the p-value of the t-test for pH at 24 hrs was found to be 0.027 ($p<0.05$). Since the sample's p-value comes out to be less than 0.05. It proves that the two groups are statistically different when treatment is provided to one group for up to 24 hrs.

For evaluation of developed formulation on the microbial biofilms, the study was conducted on pooled human saliva, wherein, the saliva is taken as inoculum to represent factual and concrete scenarios of multiple species along with their natural habitat. To 5 ml of pooled saliva, 2 % of sucrose was added as a nutrient source, the treatment was added to make a final concentration of 2.8 µg of PIC. From the FESEM analysis, at 24 hrs, different microscopic images at various magnifications (from 500X to 10000X) showed the presence of concentrated colonies surrounded by a sheath or layer-like structure. This can be considered as an indication of the presence of a biofilm in the saliva sample in positive control. Whereas, for saliva samples with treatment no such matrix-like structure is visible. The absence of a sheath or layer around microbes in the treatment group indicates the capacity to act as anti-biofilm therapy. The elemental analysis for the saliva sample was done to compare the presence of carbon content among various samples. The carbon content in the controlled salivary sample kept on increasing from 11.74 to 59.03 % from 0 hrs to 24 hrs. whereas, At 24 hrs the treatment group showed a carbon content of 28.08 %. This indicated a 52.4 % (p-value (0.0205) reduction in carbon content in the treatment group. Hence it is evident that the optimized formulation can restrict exopolysaccharide production in salivary microbial colonies.

7.2 Conclusion

The work presented in this thesis successfully demonstrated the effectiveness of the developed formulation against microbial biofilms. The flexi-liposomes were able to offer sustained release of a medicament for up to 48 hrs. A selected safer dose, which showed 82.08 % cell viability in the MTT assay, was checked for its efficacy against salivary biofilms. The studies concluded that optimized formulated can show a 52.4 % (p-value 0.006) reduction in carbon content and treatment can slow down a drop in salivary pH for 24 hrs with a p-value of 0.027 when compared using the student t-test. As salivary pH and carbon content of microbial biofilm act as markers of dental demineralization and dental caries, the developed formulation can be proved efficacious in decreasing the incidence of dental caries at a safe dose.

8 Future Perspectives

- The present work can be extended to identify the effectiveness and safety of developed formulation on selective oral pathogens and the contribution of L-Arg and PIC individually on the growth of various pathogens.
- The formulation can be further explored to check extended-release gel for preventing the occurrence of dental caries in clinical settings.

9 References

Aboud, H. M., Ali, A. A., El-Menshawe, S. F., & Elbary, A. A. (2016). Nanotransfersomes of carvedilol for intranasal delivery: formulation, characterization and in vivo evaluation. *Drug Delivery*, *23*(7), 2471–2481. https://doi.org/10.3109/10717544.2015.1013587

Aida, K. L., Kreling, P. F., Caiaffa, K. S., Calixto, G. M. F., Chorilli, M., Spolidorio, D. M. P., … Duque, C. (2018). Antimicrobial peptide-loaded liquid crystalline precursor bioadhesive system for the prevention of dental caries. *International Journal of Nanomedicine*, *13*, 3081–3091. https://doi.org/10.2147/IJN.S155245

Akram, M. W., Jamshaid, H., Rehman, F. U., Zaeem, M., Khan, J. zeb, & Zeb, A. (2022). Transfersomes: a Revolutionary Nanosystem for Efficient Transdermal Drug Delivery. *AAPS PharmSciTech*, *23*(1). https://doi.org/10.1208/s12249-021-02166-9

Al-Mahallawi, A. M., Khowessah, O. M., & Shoukri, R. A. (2014). Nano-transfersomal ciprofloxacin loaded vesicles for non-invasive trans-tympanic ototopical delivery: In-vitro optimization, ex-vivo permeation studies, and in-vivo assessment. *International Journal of Pharmaceutics*, *472*(1–2), 304–314. https://doi.org/10.1016/j.ijpharm.2014.06.041

Ali, F., Sangwan, P. L., Koul, S., Pandey, A., Bani, S., Abdullah, S. T., … Khan, I. A. (2012). 4-epi-pimaric acid: A phytomolecule as a potent antibacterial and anti-biofilm agent for oral cavity pathogens. *European Journal of Clinical Microbiology and Infectious Diseases*, *31*(2), 149–159. https://doi.org/10.1007/s10096-011-1287-x

Almaz, M. E., & Sönmez, I. Ş. (2015). Ozone therapy in the management and prevention of caries. *Journal of the Formosan Medical Association = Taiwan Yi Zhi*, *114*(1), 3–11. https://doi.org/10.1016/j.jfma.2013.06.020

Aminu, N., Chan, S.-Y., Mumuni, M. A., Umar, N. M., Tanko, N., Zauro, S. A., … Toh, S.-M. (2021). Physicochemical compatibility studies of triclosan and flurbiprofen with excipients of pharmaceutical formulation using binary, ternary, and multi-combination approach. *Future Journal of Pharmaceutical Sciences*, *7*(1). https://doi.org/10.1186/s43094-021-00302-7

Baliga, S., Muglikar, S., & Kale, R. (2013). Salivary pH: A diagnostic biomarker. *Journal of Indian Society of Periodontology*, *17*(4), 461–465. https://doi.org/10.4103/0972-124X.118317

Banik, K., Ranaware, A. M., Harsha, C., Nitesh, T., Girisa, S., Deshpande, V., … Kunnumakkara, A. B. (2020). Piceatannol: A natural stilbene for the prevention and treatment of cancer. *Pharmacological Research*, *153*, 104635. https://doi.org/10.1016/j.phrs.2020.104635

Bernsdorff, C., Wolf, A., Winter, R., & Gratton, E. (1997). Effect of hydrostatic pressure on water penetration and rotational dynamics in phospholipid-cholesterol bilayers. *Biophysical Journal*. https://doi.org/10.1016/S0006-3495(97)78773-3

Besinis, A., De Peralta, T., & Handy, R. D. (2014). The antibacterial effects of silver, titanium dioxide and silica dioxide nanoparticles compared to the dental disinfectant chlorhexidine on Streptococcus mutans using a suite of bioassays. *Nanotoxicology*, *8*(1), 1–16. https://doi.org/10.3109/17435390.2012.742935

Bessa, L. J., Botelho, J., Machado, V., Alves, R., & Mendes, J. J. (2022). Managing Oral Health in the Context of Antimicrobial Resistance. *International Journal of Environmental Research and Public Health*, *19*(24). https://doi.org/10.3390/ijerph192416448

Bhattarai, K. R., Kim, H. R., & Chae, H. J. (2018). Compliance with saliva collection protocol in healthy volunteers: Strategies for managing risk and errors. *International Journal of Medical Sciences*, *15*(8), 823–831. https://doi.org/10.7150/ijms.25146

Bozcuk Erdem, G., & Ölmez, S. (2004). Inhibitory effect of Bursa propolis on dental caries formation in rats inoculated with Streptococcus sobrinus. *Turkish Journal of Zoology*, *28*(1), 29–36.

Bozzuto, G., & Molinari, A. (2015). Liposomes as nanomedical devices. *International Journal of Nanomedicine*, *10*, 975–999. https://doi.org/10.2147/IJN.S68861

Ccahuana-Vásquez, R. A., & Cury, J. A. (2010a). S. mutans biofilm model to evaluate antimicrobial substances and enamel demineralization. *Brazilian Oral Research*. https://doi.org/10.1590/S1806-83242010000200002

Ccahuana-Vásquez, R. A., & Cury, J. A. (2010b). S. mutans biofilm model to evaluate antimicrobial substances and enamel demineralization. *Brazilian Oral Research*, *24*(2), 135–141. https://doi.org/10.1590/S1806-83242010000200002

Cevc, G. (2003). Transdermal drug delivery of insulin with ultradeformable carriers. *Clinical Pharmacokinetics*, *42*(5), 461–474. https://doi.org/10.2165/00003088-200342050-00004

Cevc, G., & Gebauer, D. (2003). Hydration-driven transport of deformable lipid vesicles through fine pores and the skin barrier. *Biophysical Journal*. https://doi.org/10.1016/S0006-3495(03)74917-0

Chacko, I. A., Ghate, V. M., Dsouza, L., & Lewis, S. A. (2020). Lipid vesicles: A versatile drug delivery platform for dermal and transdermal applications. *Colloids and Surfaces B: Biointerfaces*, *195*, 111262. https://doi.org/10.1016/j.colsurfb.2020.111262

Chakraborty, B., & Burne, R. A. (2017). *crossm Effects of Arginine on Streptococcus*. *2017*(15), 1–13.

Chen, F., Jia, Z., Rice, K. C., Reinhardt, R. A., Bayles, K. W., & Wang, D. (2013). The development of dentotropic micelles with biodegradable tooth-binding moieties. *Pharmaceutical Research*. https://doi.org/10.1007/s11095-013-1105-5

Chen, F., & Wang, D. (2011). Caries : a Patent Survey. *Expert Opin Ther Pat.*, *20*(5), 681–694. https://doi.org/10.1517/13543771003720491.Novel

Dodds, M., Roland, S., Edgar, M., & Thornhill, M. (2015). Saliva A review of its role in maintaining oral health and preventing dental disease. *BDJ Team*, *2*(1–8), 1–3. https://doi.org/10.1038/bdjteam.2015.123

Duangjit, S., Obata, Y., Sano, H., Onuki, Y., Opanasopit, P., Ngawhirunpat, T., … Takayama, K. (2014). Comparative study of novel ultradeformable liposomes: Menthosomes, transfersomes and liposomes for enhancing skin permeation of meloxicam. *Biological and Pharmaceutical Bulletin*, *37*(2), 239–247. https://doi.org/10.1248/bpb.b13-00576

Duong, T. T., Isomäki, A., Paaver, U., Laidmäe, I., Tõnisoo, A., Yen, T. T. H., … Pham, T. M. H. (2021). Nanoformulation and evaluation of oral berberine-loaded liposomes. *Molecules*, *26*(9), 1–18. https://doi.org/10.3390/molecules26092591

Ebrahiminezhad, A., Ghasemi, Y., Rasoul-Amini, S., Barar, J., & Davaran, S. (2012). Impact of amino-acid coating on the synthesis and characteristics of iron-oxide nanoparticles (IONs). *Bulletin of the Korean Chemical Society*, *33*(12), 3957–3962. https://doi.org/10.5012/bkcs.2012.33.12.3957

El Zaafarany, G. M., Awad, G. A. S., Holayel, S. M., & Mortada, N. D. (2010). Role of edge activators and surface charge in developing ultradeformable vesicles with enhanced skin delivery. *International Journal of Pharmaceutics*, *397*(1–2), 164–172.

https://doi.org/10.1016/j.ijpharm.2010.06.034

European Medicines Agency ICH. (2005). "Q2 (R1): Validation of analytical procedures: text and methodology." *International Conference on Harmonization*, *2*(June 1995), 1–15.

Fallah, N. (2019). CAMBRA: A Comprehensive Caries Management Guide for Dental Professionals. *Cda*, (July), 1–44.

Featherstone, J. D. B., & Chaffee, B. W. (2018). The Evidence for Caries Management by Risk Assessment (CAMBRA®). *Advances in Dental Research*, *29*(1), 9–14. https://doi.org/10.1177/0022034517736500

Featherstone, J. D., Fontana, M., & Wolff, M. (2018). Novel Anticaries and Remineralization Agents: Future Research Needs. *Journal of Dental Research*, *97*(2), 125–127. https://doi.org/10.1177/0022034517746371

Fernández-García, R., Lalatsa, A., Statts, L., Bolás-Fernández, F., Ballesteros, M. P., & Serrano, D. R. (2020). Transferosomes as nanocarriers for drugs across the skin: Quality by design from lab to industrial scale. *International Journal of Pharmaceutics*, *573*, 118817. https://doi.org/10.1016/j.ijpharm.2019.118817

Fischer, D., Li, Y., Ahlemeyer, B., Krieglstein, J., & Kissel, T. (2003). In vitro cytotoxicity testing of polycations: influence of polymer structure on cell viability and hemolysis. *Biomaterials*, *24*(7), 1121–1131. https://doi.org/10.1016/s0142-9612(02)00445-3

Food and Drug Administration. (2020). *Enhancing the Diversity of Clinical Trial Populations — Eligibility Criteria, Enrollment Practices, and Trial Designs Guidance for Industry*. (November), November.

Garg, V., Singh, H., Bhatia, A., Raza, K., Singh, S. K., Singh, B., & Beg, S. (2017). Systematic Development of Transethosomal Gel System of Piroxicam: Formulation Optimization, In Vitro Evaluation, and Ex Vivo Assessment. *AAPS PharmSciTech*, *18*(1), 58–71. https://doi.org/10.1208/s12249-016-0489-z

Garg, V., Singh, H., Bimbrawh, S., Singh, S. K., Gulati, M., Vaidya, Y., & Kaur, P. (2016). Ethosomes and Transfersomes: Principles, Perspectives and Practices. *Current Drug Delivery*, *14*(5), 613–633. https://doi.org/10.2174/1567201813666160520114436

Ghosh, S., Roy, G., & Mukherjee, B. (2009). Dental mold: A novel formulation to treat common dental disorders. *AAPS PharmSciTech*, *10*(2), 692–702.

https://doi.org/10.1208/s12249-009-9255-9

Giray, F., Durhan, M. A., Haznedaroglu, E., Durmus, B., Kalyoncu, I. O., & Tanboga, I. (2018). Resin infiltration technique and fluoride varnish on white spot lesions in children: Preliminary findings of a randomized clinical trial. *Nigerian Journal of Clinical Practice*. https://doi.org/10.4103/njcp.njcp_209_18

Gorain, B., Choudhury, H., Pandey, M., Madheswaran, T., Kesharwani, P., & Tekade, R. K. (2018). Drug-Excipient Interaction and Incompatibilities. In *Dosage Form Design Parameters* (Vol. 2). https://doi.org/10.1016/B978-0-12-814421-3.00011-7

Guo, L., & Shi, W. (2013). Salivary biomarkers for caries risk assessment. *Journal of the California Dental Association*, *41*(2), 107–118.

Gupta, A., Aggarwal, G., Singla, S., & Arora, R. (2012). Transfersomes: A novel vesicular carrier for enhanced transdermal delivery of sertraline: Development, characterization, and performance evaluation. *Scientia Pharmaceutica*. https://doi.org/10.3797/scipharm.1208-02

Hajishengallis, E., Parsaei, Y., Klein, M. I., Koo, H., Paulista, U. E., & Paulo, S. (2018). *HHS Public Access*. *32*(1), 24–34. https://doi.org/10.1111/omi.12152.Advances

Harper, R. A., Shelton, R. M., James, J. D., Salvati, E., Besnard, C., Korsunsky, A. M., & Landini, G. (2021). Acid-induced demineralisation of human enamel as a function of time and pH observed using X-ray and polarised light imaging. *Acta Biomaterialia*, *120*, 240–248. https://doi.org/10.1016/j.actbio.2020.04.045

Hashim, I. I. A., El-Magd, N. F. A., El-Sheakh, A. R., Hamed, M. F., & El-Gawad, A. E. G. H. A. (2018). Pivotal role of acitretin nanovesicular gel for effective treatment of psoriasis: Ex vivo–in vivo evaluation study. *International Journal of Nanomedicine*, *13*, 1059–1079. https://doi.org/10.2147/IJN.S156412

Hiremath, A., Murugaboopathy, V., Ankola, A. V., Hebbal, M., Mohandoss, S., & Pastay, P. (2016). Prevalence of dental caries among primary school children of India - A cross-sectional study. *Journal of Clinical and Diagnostic Research*, *10*(10), ZC47–ZC50. https://doi.org/10.7860/JCDR/2016/22474.8642

Holbein, M. E. B. (2009). Understanding FDA regulatory requirements for investigational new drug applications for sponsor-investigators. *Journal of Investigative Medicine*, *57*(6),

688–694. https://doi.org/10.2310/JIM.0b013e3181afdb26

Huang, C. H. (1969). Phosphatidylcholine vesicles. Formation and physical characteristics. *Biochemistry*, *8*(1), 344–352.

ICH Q1A(R2). (2003). International Conference on Harmonization (ICH). Guidance for industry: Q1A(R2) STABILITY TESTING OF NEW DRUG SUBSTANCES AND PRODUCTS. *Ich Harmonised Tripartite Guideline*, *4*(February), 24.

Information Sheet on pH of Home Oral Care Products. (n.d.).

Ingle, N. A., Dubey, H. V., Kaur, N., & Gupta, R. (2014). Prevalence of dental caries among school children of Bharatpur city, India. *Journal of International Society of Preventive and Community Dentistry*, *4*(1), 52–55. https://doi.org/10.4103/2231-0762.131267

Janakiram, C., Antony, B., Joseph, J., & Ramanarayanan, V. (2018). Prevalence of dental caries in India among the WHO index age groups: A meta-analysis. *Journal of Clinical and Diagnostic Research*, *12*(8), ZE08-ZE13. https://doi.org/10.7860/JCDR/2018/32669.11956

Junyaprasert, V. B., Singhsa, P., Suksiriworapong, J., & Chantasart, D. (2012). Physicochemical properties and skin permeation of Span 60/Tween 60 niosomes of ellagic acid. *International Journal of Pharmaceutics*, *423*(2), 303–311. https://doi.org/10.1016/j.ijpharm.2011.11.032

Kabra. (2012). Medicinal Plants for Treating Dental Caries. *Asian Journal of Oral Health & Allied Sciences*, *2*(1), 12–16. Retrieved from http://www.sdclucknow.com/doc_file_uploads/3.pdf

Kaur, P., Verma, S., Tomar, B., Vyas, M., Kakoty, V., Saha, P., & Kc, S. (2023). Exploring Applications of Flexible Vesicular Systems as Transdermal Drug Delivery. *Current Drug Delivery*. https://doi.org/10.2174/1567201821666230830125253

Kaur, P., Vyas, M., & Verma, S. (2022). Dental Caries: A Review on Etiology, Therapeutic Approaches, Novel Formulations, and Marketed Preparations. *ECS Transactions*, *107*(1), 8035. https://doi.org/10.1149/10701.8035ecst

Kaur, P., Vyas, M., & Verma, S. (2024). Challenges and Strategies to develop RP-HPLC Method of L-Arginine with Polyphenolic compounds. *Research Journal of Pharmacy and Technology*, 115–119. https://doi.org/10.52711/0974-360X.2024.00018

Kolderman, E., Bettampadi, D., Samarian, D., Dowd, S. E., Foxman, B., Jakubovics, N. S., & Rickard, A. H. (2015a). L-arginine destabilizes oral multi-species biofilm communities developed in human saliva. *PLoS ONE*, *10*(5). https://doi.org/10.1371/journal.pone.0121835

Kolderman, E., Bettampadi, D., Samarian, D., Dowd, S. E., Foxman, B., Jakubovics, N. S., & Rickard, A. H. (2015b). L-arginine destabilizes oral multi-species biofilm communities developed in human saliva. *PLoS ONE*, *10*(5), 1–18. https://doi.org/10.1371/journal.pone.0121835

Koo, H., Duarte, S., Murata, R. M., Scott-Anne, K., Gregoire, S., Watson, G. E., … Vorsa, N. (2010). Influence of cranberry proanthocyanidins on formation of biofilms by streptococcus mutans on saliva-coated apatitic surface and on dental caries development in vivo. *Caries Research*, *44*(2), 116–126. https://doi.org/10.1159/000296306

Kumar, G. P., & Rajeshwarrao, P. (2011). Nonionic surfactant vesicular systems for effective drug delivery—an overview. *Acta Pharmaceutica Sinica B*, *1*(4), 208–219. https://doi.org/10.1016/j.apsb.2011.09.002

Kumar, J. R. (2018). Formulation and characterization of liposomal gel with povidone-iodine for wound healing activity by using box-behnken design. *Journal of Pharmaceutical Sciences and Research*, *10*(12), 3359–3364.

Lima, J. P. M., Sampaio De Melo, M. A., Borges, F. M. C., Teixeira, A. H., Steiner-Oliveira, C., Nobre Dos Santos, M., … Zanin, I. C. J. (2009). Evaluation of the antimicrobial effect of photodynamic antimicrobial therapy in an in situ model of dentine caries. *European Journal of Oral Sciences*, *117*(5), 568–574. https://doi.org/10.1111/j.1600-0722.2009.00662.x

Lolayekar, N. V, & Kadkhodayan, S. S. (2019). Estimation of salivary pH and viability of Streptococcus mutans on chewing of Tulsi leaves in children. *Journal of the Indian Society of Pedodontics and Preventive Dentistry*, *37*(1), 87–91. https://doi.org/10.4103/JISPPD.JISPPD_91_17

Longo, J. P. F., Leal, S. C., Simioni, A. R., De Fátima Menezes Almeida-Santos, M., Tedesco, A. C., & Azevedo, R. B. (2012). Photodynamic therapy disinfection of carious tissue mediated by aluminum-chloride-phthalocyanine entrapped in cationic liposomes: An in vitro and clinical study. *Lasers in Medical Science*. https://doi.org/10.1007/s10103-011-

0962-6

Luo, S.-C., Wei, S.-M., Luo, X.-T., Yang, Q.-Q., Wong, K.-H., Cheung, P. C. K., & Zhang, B.-B. (2024). How probiotics, prebiotics, synbiotics, and postbiotics prevent dental caries: an oral microbiota perspective. *Npj Biofilms and Microbiomes*, *10*(1), 14. https://doi.org/10.1038/s41522-024-00488-7

Maheshwari, R. G. S., Tekade, R. K., Sharma, A. P., Darwhekar, G., Tyagi, A., Patel, P. R., & Jaina, D. K. (2012). Ethosomes and ultradeformable liposomes for transdermal delivery of clotrimazole: A comparative assessment. *Saudi Pharm J*, *20*(2), 161–170.

Maheswari, S. U., Raja, J., Kumar, A., & Seelan, R. G. (2015). Caries management by risk assessment: A review on current strategies for caries prevention and management. *Journal of Pharmacy and Bioallied Sciences*, *7*(6), S320–S324. https://doi.org/10.4103/0975-7406.163436

Mastiholimath, V., Dandagi, P., Gadad, A., Patil, M., Manvi, F., & Chandur, V. (2006). Formulation and evaluation of ornidazole dental implants for periodontitis. *Indian Journal of Pharmaceutical Sciences*. https://doi.org/10.4103/0250-474X.22967

Mathur, V. P., & Dhillon, J. K. (2018). Dental Caries: A Disease Which Needs Attention. *Indian Journal of Pediatrics*, *85*(3), 202–206. https://doi.org/10.1007/s12098-017-2381-6

Mendy, M., Caboux, E., Lawlor, R. T., Wright, J., & Wild, C. P. (2017). *No Title*. Lyon (FR).

Miranda, M. L., Silva, B. N. S., Salomão, K. B., de Oliveira, A. B., Gabbai-Armelin, P. R., & Brighenti, F. L. (2020). Effect of arginine on microorganisms involved in dental caries: a systematic literature review of in vitro studies. *Biofouling*, *36*(6), 696–709. https://doi.org/10.1080/08927014.2020.1802587

Mohammed, A. R., Weston, N., Coombes, A. G. A., Fitzgerald, M., & Perrie, Y. (2004). Liposome formulation of poorly water soluble drugs: Optimisation of drug loading and ESEM analysis of stability. *International Journal of Pharmaceutics*. https://doi.org/10.1016/j.ijpharm.2004.07.010

Nakahara, K., Kawabata, S., Ono, H., Ogura, K., Tanaka, T., Ooshima, T., & Hamada, S. (1993). Inhibitory effect of oolong tea polyphenols on glucosyltransferases of mutans streptococci. *Applied and Environmental Microbiology*, *59*(4), 968–973.

https://doi.org/10.1128/aem.59.4.968-973.1993

National Institutes of Health. (2019). *Guidelines for the Review of Inclusion on the Basis of Sex / Gender , Race , Ethnicity , and Age in Clinical Research Scientific Review Group (SRG) Responsibilities*. (March), 1–8. Retrieved from https://grants.nih.gov/grants/funding/women_min/guidelines.htm.

Nayak, D., & Tippavajhala, V. K. (2021). A comprehensive review on preparation, evaluation and applications of deformable liposomes. *Iranian Journal of Pharmaceutical Research*, *20*(1), 186–205. https://doi.org/10.22037/ijpr.2020.112878.13997

Nijampatnam, B., Nadkarni, D., Wu, H., & Velu, S. (2014). Antibacterial and Antibiofilm Activities of Makaluvamine Analogs. *Microorganisms*, *2*(3), 128–139. https://doi.org/10.3390/microorganisms2030128

Nijampatnam, B., Zhang, H., Cai, X., Michalek, S. M., Wu, H., & Velu, S. E. (2018). Inhibition of Streptococcus mutans Biofilms by the Natural Stilbene Piceatannol Through the Inhibition of Glucosyltransferases. *ACS Omega*, *3*(7), 8378–8385. https://doi.org/10.1021/acsomega.8b00367

Osamudiamen, P. M., Oluremi, B. B., Oderinlo, O. O., & Aiyelaagbe, O. O. (2020). Trans-resveratrol, piceatannol and gallic acid: Potent polyphenols isolated from Mezoneuron benthamianum effective as anticaries, antioxidant and cytotoxic agents. *Scientific African*, *7*, e00244. https://doi.org/10.1016/j.sciaf.2019.e00244

Pahwa, R., Pal, S., Saroha, K., Waliyan, P., & Kumar, M. (2021). Transferosomes: Unique vesicular carriers for effective transdermal delivery. *Journal of Applied Pharmaceutical Science*, *11*(5), 1–8. https://doi.org/10.7324/JAPS.2021.110501

Park, H., Jin Seo, H., Hong, S. hyeon, Ha, E. S., Lee, S., Kim, J. S., … Hwang, S. J. (2020). Characterization and therapeutic efficacy evaluation of glimepiride and L-arginine co-amorphous formulation prepared by supercritical antisolvent process: Influence of molar ratio and preparation methods. *International Journal of Pharmaceutics*, *581*(February), 119232. https://doi.org/10.1016/j.ijpharm.2020.119232

Patel, P., Ahir, K., Patel, V., Manani, L., & Patel, C. (2015). Drug-Excipient compatibility studies : First step for dosage form development. *The Pharma Innovation Journal*, *4*(5), 14–20. Retrieved from

http://www.thepharmajournal.com/archives/2015/vol4issue5/PartA/4-4-9.pdf

Pepla, E. (2014). Nano-hydroxyapatite and its applications in preventive, restorative and regenerative dentistry: a review of literature. *Annali Di Stomatologia*, 108–114. https://doi.org/10.11138/ads/2014.5.3.108

Pereira, U. A., Barbosa, L. C. A., Maltha, C. R. A., Demuner, A. J., Masood, M. A., & Pimenta, A. L. (2014). γ-Alkylidene-γ-lactones and isobutylpyrrol-2(5H)-ones analogues to rubrolides as inhibitors of biofilm formation by Gram-positive and Gram-negative bacteria. *Bioorganic and Medicinal Chemistry Letters*, *24*(4), 1052–1056. https://doi.org/10.1016/j.bmcl.2014.01.023

Philip, N., Suneja, B., & Walsh, L. J. (2018). Ecological Approaches to Dental Caries Prevention: Paradigm Shift or Shibboleth? *Caries Research*, *52*(1–2), 153–165. https://doi.org/10.1159/000484985

Piñón-Segundo, E., Mendoza-Muñoz, N., & Quintanar-Guerrero, D. (2012). Nanoparticles as Dental Drug-Delivery Systems. *Nanobiomaterials in Clinical Dentistry*, 475–495. https://doi.org/10.1016/B978-1-4557-3127-5.00023-4

Pittman, T. W., Decsi, D. B., Punyadeera, C., & Henry, C. S. (2023). *Theranostics Saliva-based microfluidic point-of-care diagnostic*. *13*(3). https://doi.org/10.7150/thno.78872

Pitts, N. B., Zero, D. T., Marsh, P. D., Ekstrand, K., Weintraub, J. A., Ramos-Gomez, F., … Ismail, A. (2017). Dental caries. *Nature Reviews Disease Primers*, *3*(May). https://doi.org/10.1038/nrdp.2017.30

Queiroz, C. S., Hara, A. T., Paes Leme, A. F., & Cury, J. A. (2008). pH-Cycling models to evaluate the effect of low fluoride dentifrice on enamel De- and remineralization. *Brazilian Dental Journal*. https://doi.org/10.1590/S0103-64402008000100004

Ramos, S., Bento, P., Silva, D., Spósito, L., Toledo, L. G. De, Rodero, C. F., … Santos, D. (2018). *Nanotechnology-based drug delivery systems for control of microbial biofilms : a review*. 1179–1213.

Ravalika, V., & Sailaja, A. K. (2017). Formulation and evaluation of etoricoxib niosomes by thin film hydration technique and ether injection method. *Nano Biomedicine and Engineering*, *9*(3), 242–248. https://doi.org/10.5101/nbe.v9i3.p242-248

Renugalakshmi, A., Vinothkumar, T. S., & Kandaswamy, D. (2011). *Nanodrug Delivery*

Systems in Dentistry : A Review on Current Status and Future Perspectives. 586–594.

Rethman, M. P., Beitrán-Aguilar, E. D., Billings, R. J., Burne, R. A., Clark, M., Donly, K. J., … Meyer, D. M. (2011). Nonfluoride caries-preventive agents: Executive summary of evidence-based clinical recommendations. *Journal of the American Dental Association*, *142*(9), 1065–1071. https://doi.org/10.14219/jada.archive.2011.0329

Romero, E. L., & Morilla, M. J. (2013). Highly deformable and highly fluid vesicles as potential drug delivery systems: Theoretical and practical considerations. *International Journal of Nanomedicine*. https://doi.org/10.2147/IJN.S33048

Roupe, K. A., Yáñez, J. A., Teng, X. W., & Davies, N. M. (2006). Pharmacokinetics of selected stilbenes: rhapontigenin, piceatannol and pinosylvin in rats. *Journal of Pharmacy and Pharmacology*, *58*(11), 1443–1450. https://doi.org/10.1211/jpp.58.11.0004

Roy, R., Tiwari, M., Donelli, G., & Tiwari, V. (2018). Strategies for combating bacterial biofilms: A focus on anti-biofilm agents and their mechanisms of action. *Virulence*, *9*(1), 522–554. https://doi.org/10.1080/21505594.2017.1313372

Rukavina, Z., & Vanić, Ž. (2016). Current trends in development of liposomes for targeting bacterial biofilms. *Pharmaceutics*, *8*(2). https://doi.org/10.3390/pharmaceutics8020018

Saleem, S., Khan, R., Kazmi, I., & Afzal, M. (2019). Medicinal plants in the treatment of arthritis. *Plant and Human Health: Pharmacology and Therapeutic Uses*, *3*(January 2012), 101–137. https://doi.org/10.1007/978-3-030-04408-4_6

Scharnow, A. M., Solinski, A. E., & Wuest, W. M. (2019). Targeting S. mutans biofilms: a perspective on preventing dental caries. *MedChemComm*, *10*(7), 1057–1067. https://doi.org/10.1039/C9MD00015A

Shaji, J., & Lal, M. (2014). For enhanced transdermal delivery of COX-2 inhibitors. *Int J Pharm Pharm Sci*, *6*(1), 464–477.

Shanmugam, K. T., Masthan, K. M. K., Balachander, N., Jimson, S., & Sarangarajan, R. (2013). Dental caries vaccine- A possible option? *Journal of Clinical and Diagnostic Research*, *7*(6), 1250–1253. https://doi.org/10.7860/JCDR/2013/5246.3053

Sharma, V., Yusuf, M., & Pathak, K. (2014). Nanovesicles for transdermal delivery of felodipine: Development, characterization, and pharmacokinetics. *International Journal of Pharmaceutical Investigation*, *4*(3), 119. https://doi.org/10.4103/2230-973x.138342

Simón-Soro, A., & Mira, A. (2015). Solving the etiology of dental caries. *Trends in Microbiology*, *23*(2), 76–82. https://doi.org/10.1016/j.tim.2014.10.010

Singh, S., Vardhan, H., Kotla, N. G., Maddiboyina, B., Sharma, D., & Webster, T. J. (2016). The role of surfactants in the formulation of elastic liposomal gels containing a synthetic opioid analgesic. *International Journal of Nanomedicine*, *11*, 1475–1482. https://doi.org/10.2147/IJN.S100253

Srisuwan, Y., & Baimark, Y. (2014). Biodegradable poly(D,L-lactide)/lipid blend microparticles prepared by oil-in-water emulsion method for controlled release drug delivery. *Oriental Journal of Chemistry*, *30*(1), 63–69. https://doi.org/10.13005/ojc/300108

Šturm, L., & Ulrih, N. P. (2021). Basic methods for preparation of liposomes and studying their interactions with different compounds, with the emphasis on polyphenols. *International Journal of Molecular Sciences*, *22*(12). https://doi.org/10.3390/ijms22126547

Sultana, S. S., & Sailaja, A. K. (2015). Formulation and evaluation of diclofenac sodium transferosomes using different surfactants by thin film hydration method. *Der Pharmacia Lettre*, *7*(11), 43–53.

Tashiro, T., Honzawa, S., & Sugihara, T. (2016). Synthesis of Piceatannol, an Oxygenated Analog of Resveratrol. *Natural Product Communications*, *11*(7), 997–1000. https://doi.org/10.1177/1934578x1601100732

Temple, R. J., Crews, D. C., Vasisht, K., Goodrich, K., Bernard, M. A., Nelson, R., … Sridhara, R. (2018). Evaluating inclusion and exclusion criteria in clinical trials. *The National Press Club*, (July), 204. Retrieved from www.fda.gov

Thakur, N., Jain, P., & Jain, V. (2018). Formulation Development and Evaluation of Transferosomal Gel. *Journal of Drug Delivery and Therapeutics*, *8*(5), 168–177. https://doi.org/10.22270/jddt.v8i5.1826

Turner, M. R. (2016). 乳鼠心肌提取 HHS Public Access. *Physiology & Behavior*, *176*(1), 139–148. https://doi.org/10.1016/j.physbeh.2017.03.040

Vacca Smith, A. M., Scott-Anne, K. M., Whelehan, M. T., Berkowitz, R. J., Feng, C., & Bowen, W. H. (2007). Salivary glucosyltransferase B as a possible marker for caries activity. *Caries Research*, *41*(6), 445–450. https://doi.org/10.1159/000107930

Vaghasiya, H., Kumar, A., & Sawant, K. (2013). Development of solid lipid nanoparticles based controlled release system for topical delivery of terbinafine hydrochloride. *European Journal of Pharmaceutical Sciences*, *49*(2), 311–322. https://doi.org/10.1016/j.ejps.2013.03.013

Veiga, N., Aires, D., Douglas, F., Pereira, M., Vaz, A., Rama, L., … Veiga, N. (2016). Scient Open Access Exploring the World of Science Dental Caries: A Review. *J Dent Oral Health*, *2*(5), 2–4. Retrieved from www.scientonline.org

Venkatesh, D. N., Kalyani, K., Tulasi, K., Priyanka, V. S., Ali, S. K. A., & Kiran, H. C. (2014). in Pharmaceutical and Nano Sciences TRANSFERSOMES : A NOVEL TECHNIQUE FOR TRANSDERMAL DRUG DELIVERY. *I Nternational J Ournal of P Harmacy & L Ife S Ciences*, *3*(4), 266–276.

Walve, J. R., Bakliwal, S. R., Rane, B. R., & Pawar, S. P. (2011). Transferosomes: A Surrogate Carrier For Transdermal Drug Delivery System. *IJABPT*, *2*, 204–213.

Wang, C., Li, B., Niu, W., Hong, S., Saif, B., Wang, S., … Shuang, S. (2015). β-Cyclodextrin modified graphene oxide-magnetic nanocomposite for targeted delivery and pH-sensitive release of stereoisomeric anti-cancer drugs. *RSC Advances*, *5*(108), 89299–89308. https://doi.org/10.1039/c5ra13082d

WHO. (2022). Global oral health status report. In *Dental Abstracts* (Vol. 57).

Wood, N. J., Jenkinson, H. F., Davis, S. A., Mann, S., O'Sullivan, D. J., & Barbour, M. E. (2015). Chlorhexidine hexametaphosphate nanoparticles as a novel antimicrobial coating for dental implants. *Journal of Materials Science: Materials in Medicine*. https://doi.org/10.1007/s10856-015-5532-1

Xu, X., Zhou, X. D., & Wu, C. D. (2011). The tea catechin epigallocatechin gallate suppresses cariogenic virulence factors of Streptococcus mutans. *Antimicrobial Agents and Chemotherapy*, *55*(3), 1229–1236. https://doi.org/10.1128/AAC.01016-10

Yang, H., Bi, Y., Shang, X., Wang, M., Linden, S. B., Li, Y., … Wei, H. (2016). Antibiofilm activities of a novel chimeolysin against Streptococcus mutans under physiological and cariogenic conditions. *Antimicrobial Agents and Chemotherapy*, *60*(12), 7436–7443. https://doi.org/10.1128/AAC.01872-16

Zeb, A., Qureshi, O. S., Kim, H. S., Cha, J. H., Kim, H. S., & Kim, J. K. (2016). Improved skin

permeation of methotrexate via nanosized ultradeformable liposomes. *International Journal of Nanomedicine*, *11*, 3813–3824. https://doi.org/10.2147/IJN.S109565

Zhang, Y., Huo, M., Zhou, J., Zou, A., Li, W., Yao, C., & Xie, S. (2010). DDSolver: An add-in program for modeling and comparison of drug dissolution profiles. *AAPS Journal*, *12*(3), 263–271. https://doi.org/10.1208/s12248-010-9185-1

ANNEXURE

Certificate No. 225333

LOVELY PROFESSIONAL UNIVERSITY
Transforming Education Transforming India

RAFAS

Certificate of Participation

This is to certify that **Ms. Palwinder Kaur**

of **Lovely Professional University**

has given poster presentation on **In-vivo and In-vitro formulation evaluation models for Dental Caries: An up-to-date review**

in the International Conference on "Recent Advances in Fundamental and Applied Sciences" (RAFAS 2021) held on June 25-26, 2021, organized by School of Chemical Engineering and Physical Sciences, Lovely Faculty of Technology and Sciences, Lovely Professional University, Punjab.

Date of Issue : 15-07-2021
Place of Issue: Phagwara (India)

Prepared by
(Administrative Officer-Records)

Organizing Secretary
(RAFAS 2021)

Convener
(RAFAS 2021

CUDC 2021

CHITKARA UNIVERSITY

CERTIFICATE
OF PARTICIPATION

This is to certify that

Ms. Palwinder kaur

from

Lovely Professional University

attended and presented a paper entitled

Dental Caries: A Review On Etiology, Therapeutic Approaches, Novel Formulations And Marketed Preparations For Dental Caries

Under Track - *Pharmaceutical Sciences*
in Chitkara University Doctoral Consortium (CUDC-2021)
held in virtual mode on November 12-13, 2021

DR. ARCHANA MANTRI
Vice Chancellor
Chitkara University, Punjab

DR. AMIT MITTAL
Dean- Doctoral Research Centre
Chitkara Business School
Chitkara University, Punjab

DR. PANKAJ KUMAR
Dean, PhD Programme
Chitkara University, Punjab

DIVISION OF RESEARCH AND DEVELOPMENT

[Under the Aegis of Lovely Professional University, Jalandhar-Delhi G.T. Road, Phagwara (Punjab)]

Certificate No.240189

Certificate of Participation

This is to certify that **Ms. Palwinder Kaur** of **Lovely Professional University, Phagwara, Punjab, India** has presented paper on **Development of Topical Formulation of Lycopene Nano-Elastic Vesicles to Combat Oxidative Stress** in the **International Conference on Materials for Emerging Technologies (ICMET-21)** held on February 18-19, 2022, organized by Department of Research Impact and Outcome, Division of Research and Development, Lovely Professional University, Punjab.

Date of Issue: 16-03-2022
Place: Phagwara (Punjab), India

Prepared by
(Administrative Officer-Records)

Dr. Vipul Srivastava
Convener
(ICMET-21)

Dr. Manish Vyas
Organizing Secretary
(ICMET-21)

Dr. Chander Prakash
Co-Chairperson
(ICMET-21)

Dental Caries: A Review on Etiology, Therapeutic Approaches, Novel Formulations, and Marketed Preparations

Palwinder Kaur[1], Manish Vyas[1] and Surajpal Verma[2]

ECS Transactions, Volume 107, Number 1

Citation Palwinder Kaur *et al* 2022 *ECS Trans.* **107** 8035

DOI 10.1149/10701.8035ecst

[1] Lovely Professional University

[2] Delhi Pharmaceutical Sciences and Research University

Abstract

Demineralization of dental enamel (dental caries) are widely prevalent throughout the world. According to the Global Oral Health Data Bank, this prevalence varies from 49% to 83% across different countries. Dental caries are a polyfactorial disease that still needs major pharmaceutical interventions to alleviate its prevalence. This paper delineates the latest understanding of pathological and protective factors associated with caries development. Based on the current knowledge of etiological factors, many therapeutic classes have been traversed since the past to decrease the severity of the disease. This includes drugs of herbal origin and synthetic molecules. On active ingredients, the latest pharmaceutical technologies have been applied to formulate novel drug delivery systems to accentuate the impact of drug delivery to combat the prevalence of the disease. A few of these novel formulations have been also been marketed. The present article explicates current etiological understanding on dental caries, therapeutic classes explored until now along with herbal classes and compounds, novel therapeutic systems, and marketed preparations used in dental formulations and future strategies to develop the efficient formulation.

In-vivo and in-vitro formulation evaluation models for dental caries: An up-to-date review

Palwinder Kaur; Manish Vyas; Surajpal Verma

+ Author & Article Information

AIP Conf. Proc. 2800, 020295 (2023)

https://doi.org/10.1063/5.0162907

Many formulations are being developed for the treatment of dental caries to cease its progression. Excessive demineralization of dental enamel leads to caries progression. To evaluate the efficiency of prepared formulations, various parameters are evaluated which represents their effectiveness to bring about caries progression. To measure parameters like surface hardness, mineral loss, Exopolysaccharide production, microbial activity, and tooth scanning, different evaluation models are used proposed and accepted by the tooth industry. This article explains various in-vitro as well as ex-vivo models used for the evaluation of formulations meant for dental caries. Models like the Disc diffusion method, various biofilm models, and $_{p}$H cycling models are explained along with their procedure and parameters which measure the effectiveness of formulation like Surface micro-hardness, Transverse microradiography, Micro-Computed Tomography (CT) analysis. Many Such models are also used as bio-waivers to in-vivo study as they explain their suitability in IVIVC.

REVIEW ARTICLE

Exploring Applications of Flexible Vesicular Systems as Transdermal Drug Delivery

Palwinder Kaur[1], Surajpal Verma[2], Bhupendra Tomar[3], Manish Vyas[1,*], Violina Kakoty[1], Paramita Saha[3] and Sarathlal KC[4]

[1]*School of Pharmaceutical Sciences, Lovely Professional University, Phagwara, Punjab-144401, India;* [2]*School of Pharmaceutical Sciences, Delhi Pharmaceutical Sciences and Research University, Delhi-110017, India;* [3]*College of Pharmacy, Teerthankar Mahaveer University, Moradabad, 244001-India;* [4]*Department of Pharmacy, Birla Institute of Technology and Science, Pilani, Rajasthan-333031, India*

ARTICLEHISTORY

Received: April 13, 2023
Revised: June 13, 2023
Accepted: July 19, 2023

DOI:
??????????

Abstract: Deformable lipidic-nano carriers are a category of advanced liposomal formulations. Deformable lipidic-nano carriers have a specific character to transform by rearranging the lipidic backbone to squeeze themself through a pore opening ten times smaller than their diameter when exposed to a variable condition like hydration gradient as these have potentially been used as a non-invasive delivery system to transdermally migrate various therapeutic agents for over three decades. Despite their vast application in transdermal drug delivery system, non-uniformity to express their chemical nature still exist and authors use various terms synonymously and interchangeably with each other.

The present study delineates the terminologies used to express different derived deformable vesicular carriers to harmonize the terminological use. It also includes the effectiveness of deformable nanocarriers like Transferosomes, Ethosomes, Menthosomes, Invasomes, and Glycerosomes in skin conditions like basal cell carcinoma, fungal and viral infections, and hyperpigmentation disorders, along with others.

Various review and research articles were selected from the 'Pubmed' database. The keywords like Transferosomes, Flexi-vesicular system, ultra-deformable vesicles, and nano-vesicular systems were used to extract the data.

The data was reviewed and compiled to categorically classify different flexible vesicular systems. The composition of the different vesicular systems is identified and a report of various pathological conditions where the use of flexible lipid nanocarrier systems was implemented is compiled. The review also offers suggestive approaches where the applicability of these systems can be explored further.

Keywords: Transdermal delivery, Flexible carrier systems, Skin diseases, viral infections, fungal infections.

1. INTRODUCTION

Liposomes were first identified in the 1960s by a British pathologist Dr Alec. D. Bangham, as a phospholipid vesicular system that delivers the drug to the target site. The historic milestone in the development of the said nano-vesicular system was laid down by Gregory Gregoriadis (*G. Gregoriadis*) in the 1970s, who justified the improved targetability to achieve an improved therapeutic index and limit the unwanted exposure of the drug to the body. Further publications by *G. Gregoriadis* led to the unceasing development of liposomes bringing them to clinical applications [1]. The *in-vivo* fate of liposomes along with the lysosomal localization of the developed liposomes was also explained. Further modifications like the insertion of adjuvants like protein antigens or enzymes or the addition of cholesterol in the lipid bilayer to alter the physical properties of vesicles like clearance rate and vesicle phospholipid composition were also done [2].

Liposomes are composed of phospholipid (PL) molecules, wherein PL undergoes self-aggregation on hydration, forming sandwiched bi-layered vesicular moieties of nanometer range of 10-200 nm diameter, hence called nanocarriers [3]. PL are amphiphilic molecules, having a hydrophilic head, made up of a phosphate group joined with molecules like serine, choline, *etc*. The hydrophobic tail part of PL is composed of two fatty acid chains joined to the hydrophilic phosphate group through a glycerol molecule [4]. Upon hydration, these PL molecules self-aggregate in a manner to minimize the hydrophobic effect from the long alkyl chain, thus making two layers of PL sandwiched in a manner ex-

*Address correspondence to this author at the School of Pharmaceutical Sciences, Lovely Professional University, Phagwara, Punjab-144401, India; E-mail: vymanish@gmail.com

1567-2018/XX $65.00+.00

Challenges and Strategies to develop RP-HPLC Method of L-Arginine with Polyphenolic compounds

Palwinder Kaur[1], Manish Vyas[1], Surajpal Verma[2]

[1]School of Pharmaceutical Sciences, Lovely Professional University, Phagwara, Punjab - 144401, India.

[2]School of Pharmaceutical Sciences, Delhi Pharmaceutical Sciences and Research University, Delhi -110017, India.

*Corresponding Author E-mail: **vymanish@gmail.com**, **surajpal_1982@yahoo.co.in**

ABSTRACT:

While developing a method of RP-HPLC for a new compound or combination of drugs simultaneously, many challenges are faced by the researcher pertaining to effective elution and sufficient resolution of a mixture of compounds. Many factors come into the picture, which reflects the ultimate elution of chemical compounds. Factors like the physicochemical properties of chemical compounds, the chemical nature of the mobile phase, instrumental factors, and experimental conditions play crucial roles in RP-HPLC method development. This research article discusses the challenges faced while developing a method of L-Arg along with polyphenolic compounds. Both the compounds have contrasting solubility profiles as L-Arg is soluble in water but PIC is soluble in organic solvents. Strategies were used to develop RP-HPLC of this combination with mobile phases like acetonitrile, orthophosphoric acid, methanol, and potassium dihydrogen phosphate buffer of pH 2.6. The present article provides an insightful approach to develop a new RP-HPLC method for a combination of compounds having related physicochemical characteristics.

KEYWORDS: RP-HPLC, Method development, L-Arginine, Strategies for RP-HPLC, Polyphenolic compounds.

INTRODUCTION:

The chromatographic technique was first discovered by Russian botanist Mikhail Tsvet[1], in 1901, and has today become an indispensable tool in all the areas wherein the separation of individual chemical components is concerned. The scope of High-performance liquid chromatography (HPLC) has gained popularity in the areas of forensics, marine technology, drug discovery, toxicology food safety, and many other[2]. Chromatography relies on a simple technique of physical separation of mixture components when passed through two phases having different polarities. One phase is a stationary (immobile)phase and the other is the mobile phase, the mobile phase is percolated over the stationary phase to bring about the separation of components in the stationary phase.

During the course, the mixture component undergoes various sorption and desorption events between mobile and immobile phases, and depending upon relevant affinity, the components of the mixture move across the stationary phase. The difference in physicochemical properties of mixture components will give different strengths of interactions between both the phases. Due to a characteristic differential transport phenomenon, the components get separated solitarily on the stationary phase[3]. Further advances in research and technology have catalyzed refined hybrid chromatographic methods like gas chromatography-mass spectroscopy (GC-MS), Micellar electrokinetic chromatography, and chromatography using chiral stationary phases for the separation of enantiomers[4,5]. The reverse-phase high-performance liquid chromatography (RP-HPLC) contains a hydrophobic stationary phase and the polar mobile phase (but not specific to), wherein the mixture components get distributed depending upon the affinity between the two phases. Normally, the least hydrophobic component elutes first and the most hydrophobic interacts strongly with the hydrophobic stationary surface[6,7]. The scope of HPLC also includes the establishment of a validated method that could explain the stability of the chemical compound under test individually or in a dosage form according to ICH guidelines[8].

Scope of L-Arginine in medicines:

L-Arginine (L-Arg) ((2*S*)-2-amino-5-(diamino methylidene amino) pentanoic acid), is semi- essential amino acid. Due to its role in nitric oxide generation in the body, it is used as a drug to reduce Blood pressure. A meta-analysis of L-Arginine reports that it reduces systolic and diastolic blood pressure in hypertensive patients, but only diastolic pressure was reduced in pregnant patients[9]. It also has pro-angiogenic properties[10]. L-Arginine serves as a precursor for the synthesis of polyamines, proline, glutamate, creatine, agmatine, and urea[11,12], it has been researched for its role in renal failure[13] reduction in erectile dysfunction was also reported when L-Arg alone is given for 3 months[14,15], and inhibition of gastric hyperacidity[16]. It is an essential component of the urea cycle. including neurotransmission, vasorelaxation, cytotoxicity, and immunity[17].

As the role of L-Arg applications as nutraceuticals and as supplements is well-known. As it has been researched for a variety of ailments, alone or in combination with main drug therapy, its combinations with various other pharmaceutical agents are also expected to increase in the future. It is recently being researched as the agent to reduce blood pressure (vasodilator) in combination with cancer therapy. Polyphenolic compounds like resveratrol and its precursor piceatannol are known to have anticancer activity. The combination of L-Arg with polyphenolic compounds is emerging as a new area of interest. These polyphenolic compounds are lipophilic. A combination of L-Arg with polyphenolic compounds for the treatment of cancer can be considered to have sufficient potential to alleviate high blood pressure associated with cancer chemotherapy.

Various parametric considerations for RP-HPLC Method development:

While developing the HPLC method for analysis, quantification, or purification of chemical components, physicochemical attributes of the chemical compounds, process variables, and instrumental variables are taken into account[18] (Table 1).

Table 1: Various Non-continuous attributes to consider while developing the HPLC method.

Physicochemical attributes	Electric charge, Polarity, Log K, PH, Dipole moment, H-Bond capacity, Molecular weight and size, Solubility, Volatility, Stability and Toxicity.
Process / instrumental variables	Buffer, flow rate, column length, Temperature, pressure, mobile phase, sample preparation technique

While developing a method for a chemical moiety the first and foremost character to observe is the effect of pH of the mobile phase on the ionization of the compound. Another technique to develop the RP-HPLC method involves the use of Quality by Design (QbD) approach which is done using the software. This exercise needs a complete literature survey to enter parameters into software to extract a computer-generated combination on which the experiment is conducted to check the reliability of the predicted combination[19]. Since many pharmaceutical compounds are ionizable, they tend to have different polarity, surface charge, and log D values at different pH[20]. To predict the behavior of ionizable compounds, one must understand the concept of pK_a, Isoelectric point, and pH. The ionization of the compound due to the mobile phase and pH determines the ultimate retention and selectivity[21,22]. This behavior can be explained by the Handerson hasselbalch equation.